

# **Effect of cannabinoid receptor ligands on microglial cell functions**

**Dr SAMIA HASSAN**

**MBBCH, MPil**



**School of Biomedical**

**The University of Nottingham**

**Nottingham**

**UK**

**Thesis submitted to the University of Nottingham for the**

**Degree of Doctor of Philosophy**

**2013**

## **Declaration**

I hereby declare that the data published in this thesis are the result of my own work carried out under supervision of Professor David Kendall and Dr. Steve Alexander at the University of Nottingham, UK. This thesis has been completed exclusively by myself and has not previously been submitted for any other degree or qualification.

SAMIA HASSAN

## Publications

Part of the results discussed in this thesis was presented in the following meeting:

**Hassan Samia**, Professor Kendall D & Alexander S (June, 2010) Role of the GPR55 receptor in microglial cell. Third Conference for Libyan students, Sheffield Hallam University, Sheffield (UK), poster

**Hassan Samia**, Professor Kendall D & Alexander S (December, 2010) Role of the GPR55 receptor in microglial cell. Poster Proceedings of the British Pharmacological Society at; <http://www.pA2online.org/abstracts/Vol8Issue1abst116P.pdf>

**Hassan Samia**, Khalil El-deeb, David Chatterton, Liaque Latif, Alexander Stephen and Kendall David (2011) Cannabidiol inhibits inducible nitric oxide synthase (INOS) via inhibition of P38 MAPK and NF-KB in microglial cells. Murray Edwards College, Cambridge James Black Meeting - Biologics for the New Millennium, Poster, 2011. Proceedings of the British Pharmacological Society at; <http://www.pA2online.org/abstracts/Vol9Issue2abst008P.pdf>

**Hassan Samia**, Kendall DA & Alexander S (2012) Cannabidiol enhances microglial phagocytosis via TRPV2 activation. 2012 Proceedings of the British Pharmacological Society at; <http://www.pA2online.org/abstracts/Vol10Issue4abst088P.pdf>.

**Hassan Samia**, Khalil El-deeb, David Chatterton, Liaque Latif, Alexander Stephen and Kendall David. Cannabidiol inhibits inducible nitric oxide synthase (INOS) via inhibition of P38 MAPK and NF-KB in microglial cells. Paper in preparation.

**Hassan Samia**, Kendall D & Alexander S. Cannabidiol enhances microglial phagocytosis via TRPV2 activation. Paper in press.

## ABSTRACT

**Background:** Microglial cells can be regarded as the macrophages of the central nervous system. Their activation has protective functions in the destruction of pathogens, removal of debris and release of neurotrophic factors, but excessive activation can exacerbate the effects of inflammation contributing to neurodegenerative conditions such as Alzheimers disease. The cannabinoids have a variety of anti-inflammatory properties and the main aim of this project is to determine the role of cannabinoids in modulation of microglial cell function using *in vitro* approaches, and to investigate the molecular mechanisms underlying such modulation.

**Methods:** BV-2 murine microglial and primary murine microglial cells were activated using bacterial lipopolysaccharide (LPS). Nitric oxide (NO) was determined with a Griess assay. Western blotting was used to measure the expression of NFκB p65, Iκβ $\alpha$ , inducible nitric oxide synthase (iNOS), COX-2, and total and phosphorylated forms of the MAP kinases, p38, JNK1/2 and ERK1/2; blots were analysed with an Odyssey imaging system (Li-Cor Bioscience), Expression of GPR55 mRNA was determined by RT-PCR. Phagocytosis was assessed in BV-2, HAPI and primary murine microglial cells and in RAW 264.7 monocyte/macrophages using fluorescent latex beads and the cells viewed by confocal microscopy. Fluorescent bead accumulation was quantified on consecutive image and rate phagocytic was calculated by normalizing the number of beads to the number of cells in each field.

Western blotting was used to measure the expression of the receptor channels TRPV2 and TRPV1 and AKT. Immunocytochemistry was used to investigate the translocation of TRPV2, and the involvement of MLC11, PLC $\gamma$ 2, PKC $\alpha$ ,  $\epsilon$  in phagocytosis. Fura-2-based Ca<sup>2+</sup> imaging of microglia was undertaken and migration was assessed using a novel "Compass" device.

**Result:** BV-2 cells did not express CB1 or CB2 receptor mRNA; however, the cannabinoid receptor agonist CP55-940, the CB1 antagonist AM251 and the non-psychoactive cannabinoid cannabidiol (CBD) all at 10 $\mu$ M produced significant inhibitions of lipopolysaccharide (LPS; 100ng/ml)-stimulated nitric oxide (NO) formation. The putative GPR55 receptor agonists VSN16R and O1916 (were without effect, as was the endogenous GPR55 agonist

lysophosphatidylinositol (LPI). A number of other cannabinoid receptor agonists and antagonists and the phytocannabinoids (CBG, CBDV, THCV, CBDA and CBGA (Pertwee, 2008) (all 10  $\mu$ M) were without.

Cannabidiol inhibited LPS-enhancement of both iNOS and COX-2 expression. LPS significantly induced phosphorylation of the MAP kinases ERK 1/2, p38 and JNK and CBD inhibited both LPS-induced p38 and JNK phosphorylation but was without effect on phosphorylation of ERK1/2. The p38 inhibitor SB203580 (10  $\mu$ M) also significantly reduced iNOS expression after 24 hours of LPS stimulation. LPS increased NF-KB p65 expression and this was significantly attenuated by CBD. LPS also stimulated NF-KB p65 translocation to the nucleus whereas CBD inhibited the effect.

CBD-induced phagocytosis of BSA latex beads was similarly induced in HAPI, RAW264.7 and primary murine microglial cells. Inhibitors of Rho kinase (Y27632) and PI (3)kinase (wortmannin) inhibited basal but not CBD-enhanced phagocytosis. CBD increased intracellular calcium in BV-2 cells and the TRP channel blocker ruthenium red reversed CBD-induced phagocytosis.

CBD increased expression of TRPV2 protein and mRNA and caused a translocation to the cell membrane. This was abolished in presence of cycloheximide and PI3K inhibitor. Other cannabinoids and phytocannabinoids (CBG, CBDV, THCV, CBDA and CBGA) were without effect. CBD also increased BV-2 cell migration.

**Conclusion:** The data presented demonstrate that CBD, despite inhibiting NO formation, mediated by reduction of NF-k $\beta$  P38 MAPK, JNK and ROS activity, enhances microglial migration and phagocytosis.

The mechanism of action appears to involve TRPV2 channel activation accompanied by increased protein synthesis and translocation to the cell membrane. Therefore, CBD might be developed as a useful treatment for neurodegenerative disease.

## **Acknowledgments**

Firstly I would like to express my gratitude towards the Libyan government for funding my PhD study. Without its support this PhD thesis would not have been completed.

I would also like to express appreciation for all of the people that helped me in so many ways during this project. Thank you all for helpful suggestions and important advice on all technical matters during this work. A special thank goes to Liaque Latif, Paul Millins and Dr. Michael Garle. Most importantly, my keen appreciation goes to Emma King for great patience for AMU problem solving and Dr Andrew Bennett for help and guidance for RT-PCR.

Finally, I owe my deepest gratitude to my supervisors, Professor Dave Kendall and Steve Alexander for inspiration and encouragement when they were required. Especially, many thanks to Professor Dave Kendall who was the supervisor I could have only wished for, giving me enough freedom to explore on my own but at the same time always being there for me supporting me with his guidance and advice.

And the last is my family; my dad, mum, my husband who had supported me, has believed in me and have been there for me and my kids for being.

## Table of Contents

DECLARATION .....	II
ABSTRACT .....	IV
ACKNOWLEDGEMENTS .....	VI
TABLE OF CONTENTS .....	VII
LIST OF FIGURES.....	XIV
ABBREVIATIONS .....	XXII

### CHAPTER ONE

1. General introduction .....	1
1.1 Origin of the microglia .....	1
1.2 Microglial functions and cytotoxicity.....	1
1.2.1 Microglia migration .....	7
1.3 Mechanisms of microglial activation .....	10
1.3.1 Microglial effector molecules .....	13
1.4 Microglial receptors .....	15
1.5 Cannabinoid signalling system .....	17
1.5.1 CB1/CB2 receptors .....	17
1.5.2 Non-CB1/CB2 receptors.....	20
1.5.2.1 GPR55 receptor .....	21
1.5.2.2 PPARs receptors .....	23
1.5.2.3 Transient receptor potential channels .....	24
1.6 Cannabinoid receptor ligands .....	25
1.6.1 General information .....	25
1.6.2 Classical cannabinoids .....	26
1.6.2.1 Cannabidiol (CBD) .....	26
1.6.3 Non classical cannabinoids.....	30
1.6.4 Aminoalkylindoles (hybrid cannabinoids) .....	31
1.6.5 Eicosanoids.....	31
1.6.6 Diarylpyrazoles .....	31
1.7 Allosteric modulators .....	32

1.8 Endogenous cannabinoids.....	32
1.9 Cannabinoids and Neuroinflammation .....	36
1.10 Models used in microglial function.....	40
1.10.1 Primary microglial cells.....	40
1.10.2 BV-2 cells .....	40
1.10.3 HAPI cells .....	41
1.11 Aim and Objectives .....	41
CHAPTER TWO	
The effect of cannabinoids on Nitric Oxide signalling in microglial cells	
2. 1 Introduction.....	43
2.2 The aim .....	47
2.3 Material and Methods .....	47
2.3.1 Reagents .....	47
2.3.2 Cell culture conditions .....	49
2.3.2.1 Cell counts .....	49
2.3.2.2 BV-2 cell line .....	49
2.3.2.3 HAPI cell line .....	49
2.3.2.4 Primary mouse microglial cultures .....	50
2.3.3 Nitric oxide (NO) assay .....	51
2.3.4 Cell viability .....	53
2.3.5 Intracellular Ca <sup>2+</sup> using the Flexstation .....	53
2.3.6 Immunoblotting .....	54
2.3.6.1 Whole Cell Protein Extraction .....	54
2.3.6.2 Cytoplasmic and Nuclear Protein Extraction .....	55
2.3.6.3 Gell electrophoresis.....	56
2.3.6.3.1 Antibodies used .....	57
2.3.7 Immunocytochemistry .....	57
2.3.7.1 Antibodies used .....	58
2.3.8 Dichlorofluorescein (DCF) assay .....	59

2.3.9 Antioxidant effect of CBD.....	59
2.3.10 RT-PCR.....	59
2.3.10.1 RNA extraction .....	60
2.3.10.2 Complementary DNA (cDNA) synthesis .....	60
2.3.10.3 Designing the Primers and Probe .....	61
2.3.10.4 Taqman Real-Time PCR .....	61
2.3.11 [ <sup>35</sup> S]-GTPγS binding assay.. ..	62
2.3.11.1 Reagents .....	62
2.3.11.2 Brain membranes.....	62
2.3.11.3 [ <sup>35</sup> S]-GTPγS assay .....	63
2.3.12 Statistical analysis... ..	64
2.4 Results.....	65
2.4.1 Characterization of LPS-evoked nitric oxide production in BV-2 .....	65
2.4.1.1 The influence of LPS concentration, time, serum and minocycline .....	65
2.4.1.2 The influence of calcium ions .....	67
2.4.1.2.1 intracellular Ca <sup>2+</sup> [Ca <sup>2+</sup> ] <sub>i</sub> in microglial activation .....	69
2.4.1.3 The involvement of inducible NOS .....	70
2.4.2 The effect of cannabinoid ligands on LPS-evoked nitric oxide production in BV2 cells .....	71
2.4.2.1 Endocannabinoids and related compounds .....	71
2.4.2.2 Cannabinoid receptor ligands .....	72
2.4.2.3 Phytocannabinoids .....	76
2.4.2.4 GPR55 .....	78
2.4.2.5 GPR18 and abn-CBD .....	81
2.4.2.6 TRPV channels .....	85
2.4.2.7 PPARs receptors .....	83

2.4.3 Characterization of CBD effects on LPS-evoked nitric oxide production in BV2 cells .....	84
2.4.3.1 Effect on Cell viability .....	84
2.4.3.2 Reactive oxygen species .....	86
2.4.3.3 cannabinoid receptor antagonists .....	87
2.4.3.4 Other receptors .....	88
2.4.3.4.1 (5-HT) receptors .....	88
2.4.3.4.2 Adenosine receptors .....	89
2.4.3.4.3 Purinergic receptors .....	90
2.4.3.5 The effect of pertussis toxin on CBD mechanism of action .....	91
2.4.3.6 Kinases .....	92
2.4.4 Characterization of CBD effects on LPS-evoked changes in inflammatory markers .....	95
2.4.4.1 iNOS expression .....	95
2.4.4.2 Reactive Oxygen Species (ROS).....	99
2.4.4.3 COX-2 expression .....	101
2.4.4.4 MAPK activation .....	102
2.4.4.5 NFkB/IkB alpha expression .....	108
2.4.5 Molecular investigation of BV2 cells .....	113
2.4.5.1 GTP gamma S binding .....	113
2.4.5.1.1 Optimization of assay method.....	113
2.4.5.1.2 The effect of saponin in GTPγS binding assays .....	114
2.4.5.1.3 Effects of cannabinoids ligands on [ <sup>35</sup> S] GTPγS .....	115
2.4.5.2 GPR55 and cannabinoids receptors expression .....	116
2.4.5.2.1 Cannabinoid receptors expression in BV-2 cells .....	116
2.4.5.2.2 Express GPR55 receptors in BV-2.....	117
2.5. Discussion .....	118
2.6. Conclusion.....	131
2.6. 1 Summary of the results.....	132

## CHAPTER THREE

### The effect of cannabinoids on Phagocytosis in microglial cells

3.1 Introduction.....	133
3.2 Aim of this study .....	136
3.3 Methods .....	136
3.3.1 Materials .....	136
3.3.2 Cell culture conditions .....	137
3.3.2.1 Murine microglial (BV-2) cell line .....	137
3.3.2.2 HAPI cell line.....	138
3.3.2.3 Macrophage like cells (RWA-264.7) .....	138
3.3.2.4 Primary mouse microglial cultures .....	138
3.3.3 Cell counts.....	138
3.3.4 Assessment of cell membrane integrity .....	138
3.3.5 Assessment of phagocytosis.....	139
3.3.5.1 Phagocyte assay .....	139
3.3.5.1.1 Fluorescent BSA latex beads.....	139
3.3.5.1.2 Non-fluorescent latex beads .....	141
3.3.6 Migration .....	141
3.3.7 Western blotting.....	142
3.3.7.1 Whole Cell Protein Extraction.....	142
3.3.7.2 Membrane fractionation .....	142
3.3.7.3 Gel electrophoresis .....	143
3.3.7.3.1 The primary antibodies used .....	144
3.3.8 Immunocytochemistry.....	144
3.3.8.1 The primary antibodies used .....	146
3.3.9 Reverse transcription polymerase chain reaction (RT-PCR) .....	146
3.3.9.1 RNA extraction .....	146
3.3.9.2 mRNA Preparation .....	147
3.3.9.3 Complementary DNA (cDNA) synthesis.....	147

3.3.9.4 Designing the Primer and Probe .....	147
3.3.9.5 Taqman Real-Time PCR .....	148
3.3.10 Fura-2 AM Ca <sup>2+</sup> imaging .....	149
3.3.11 Statistical analysis .....	149
3.4 Results.....	150
3.4.1 Phagocytic response after non- fluorescent latex beads exposure .	150
3.4.2 Fluorescent BSA latex beads .....	151
3.4.2.1 Optimization of protocol .....	151
3.4.2.2 The role of the cytoskeleton in phagocytosis .....	153
3.4.2.3 The role of mitochondria in phagocytosis .....	154
3.4.2.4 The role of myosin II in BV-2 phagocytosis .....	155
3.4.2.5 Expression of CD11b in microglial cells .....	155
3.4.2.6 The role of phospholipase C <sub>2</sub> (PLC <sub>2</sub> ) in BV-2 phagocytosis .....	157
3.4.2.7 The role of protein kinase C (PKC) in BV-2 phagocytosis .....	158
3.4.2.7.1 PKC $\alpha$ .....	158
3.4.2.7.2 PKC $\epsilon$ .....	159
3.4.2.8 The role of P2Y or P2X receptors in phagocytosis .....	160
3.4.2.9 The role of pro-inflammatory mediators in BV-2 phagocytosis ..	161
3.4.2.10 The role of anti-inflammatory drugs on BV-2 phagocytosis .....	163
3.4.2.11 Effects of cannabinoids and endocannabinoids on microglial and macrophage phagocytosis .....	163
3.4.2.12 Role of GPR18 and Abn-CBD receptors in CBD induced phagocytosis .....	167
3.4.2.13 The effect of pertussis toxin on CBD-induced phagocytosis.....	168
3.4.2.14 The roles of PI3K, Rho/Rock kinase and p38 MAPK in CBD-enhancement of phagocytosis.....	169
3.4.2.15 The role of ROS in CBD induced phagocytosis.....	172
3.4.2.16 The role of intracellular calcium [Ca <sup>2+</sup> ] <sub>i</sub> in microglial phagocytosis .....	172

3.4.2.17 Effect of CBD on ATP calcium increase in BV-2 cells.....	173
3.4.2.18 The role of transient receptor potential (TRP) channels in CBD- enhancement of phagocytosis .....	174
3.4.2.19 Expression of TRPV2 in BV-2 cells. ....	176
3.4.2.19.1 Effect of CBD on TRPV2 expression.....	176
3.4.2.19.2 The effect of latex bead phagocytosis on translocation of TRPV2 .....	177
3.4.2.19.3 Effect of serum on translocation of TRPV2 in BV-2.....	177
3.4.2.19.4 Expression of TRPV2 in Primary murine microglial cells .....	179
3.4.2.20 Effect of CBD on TRPV2 protein expression in BV-2 .....	179
3.4.2.21 The role of a protein synthesis inhibitor (cycloheximide) on CBD-enhanced phagocytosis.....	182
3.4.2.22 TRPV2 receptor message .....	183
3.4.2.23 Vanilloid receptor (TRPV1) protein expression in BV-2 .....	183
3.4.2.24 The role of AKT in CBD-mediated phagocytosis .....	185
3.4.3 Migration .....	187
3.4.3.1 Effect of UDP on cell migration in RAW 264.7 cells .....	187
3.4.3.2 Effect of CBD on BV2 cell migration .....	188
3.5 Discussion .....	190
3.5.1 Characterization of microglial phagocytosis.....	190
3.5.2 Regulation of phagocytosis .....	192
3.5.3 Migration of microglial cells.....	201
3.6 Conclusion.....	201
3.6 The summary of chapter .....	203
CHAPTER FOUR	
4 Overview .....	204
4.1 Future directions and Points to Consider .....	212
4.2 Conclusion.....	213
REFERENCE .....	214

## List of Figures

### CHAPTER ONE

Figure 1.1: Diagrammatic representations of the stages of microglia cell during activation.....	6
Figure 1.2: Diagrammatic representation of the LPS/TLR4 signalling LPS recognition is assisted by LBP and CD14, and is mediated by TLR4/MD-2 receptor complex .....	12
Figure 1.3: structures of phytocannabinoids CBD and THC .....	27
Figure 1.4: structures of HU-210, CP55,940, JWH015 and AM251 .....	28
Figure 1.5: Main pathways of synthesis and degradation of the endocannabinoids anandamide and 2-arachidonoylglycerol (2-AG) .....	35

### CHAPTER TWO

Figure 2.1: Sodium nitrite standard curve in BV-2 cell media.....	52
Figure 2.2: (A) Effect of LPS on NO production in BV-2 (concentration). (B) Effect of LPS on NO formation in BV-2 cells (by time) .....	66
Figure 2.3: (A) Effects of a selective microglial inhibitor, minocycline, on LPS-mediated NO release in the BV-2 cell line. (B) Effect of fetal bovine serum (FBS) and ethanol (01%) on LPS-induced NO production in BV-2 cells. ....	67
Figure 2.4: Effect of BAPTA-AM on LPS-induced NO formation .....	68
Figure 2.5: Effect of ionomycin-induced elevation of the basal $Ca^{2+}$ on NO formation .....	69
Figure 2.6: (A) Effect of LPS on $[Ca^{2+}]_i$ in BV-2. (B) Effect of ATP (100 $\mu$ M) on $[Ca^{2+}]_i$ in BV-2 cells .....	70
Figure 2.7: (A) Effect of 1400W an iNOS inhibitor on LPS-induced NO production in BV-2 cells. (B) Effect of Dexamethasone (DEX) on LPS-induced NO production in BV-2 cells. ....	71



Figure 2.29: Effect of apocynin a NADPH oxidase inhibitor on CBD-mediated NO inhibition LPS-induced in BV-2 .....	86
Figure 2.30: Effect of CB1/CB2 antagonist treatment on CBD-mediated NO inhibition LPS-induced in BV-2.....	87
Figure 2.31: Effect of WAY100635 (a 5-HT antagonist) on CBD-inhibited NO formation induced by LPS .....	88
Figure 2.32: Effect of xanthine amine carboxylic congener (XAC) adenosine antagonist (A1, A2B and A2A) on CBD-inhibited NO formation induced by LPS .....	89
Figure 2.33: Effect of different concentrations of ATP on NO production in BV-2 cells. BV-2 cells .....	90
Figure 2.34: Effect of UDP-glucose on NO production in BV-2 cells .....	91
Figure 2.35: Effect of PTX treatment on CBD-mediated NO inhibition LPS-induced NO in BV-2 .....	92
Figure 2.36: (A) Effect of P38 inhibitor (SB203580) treatment and (B) MEK1 (ERK 1/2) inhibitor (U0126) on CBD-mediated NO inhibition LPS-induced in BV-2 .....	93
Figure 2.37: Effect of PI3K inhibitor (wortmannin) treatment on CBD-mediated NO inhibition LPS-induced in BV-2.....	94
Figure 2.38: Effect of Rho/ROCK inhibitor (Y27632, 10 $\mu$ M) treatment on CBD-mediated NO inhibition LPS-induced in BV-2. ....	94
Figure 2.39: Western blot and histogram show increase in the expression of the ratio of iNOS expression and GAPDH in whole cell lysates of BV-2 .....	96
Figure 2.40: Western and histogram show the effect of apocynin on the ratio of iNOS expression and GAPDH levels in whole cell lysates of BV-2 cells .....	97

Figure 2.41: Western and histogram show the effect of MAPKs on the ratio of iNOS expression and GAPDH levels in whole cell lysates of BV-2 cells .....	98
Figure 2.42: Immunocytochemistry shows the effect of CBD on iNOS expression induced by LPS in BV-2 and mouse primary microglial cells .....	99
Figure 2.43: Histograms show the effect of LPS on ROS formation in BV-2 by DCF assay .....	100
Figure 2.44: DCF assay showed the effect of CBD on LPS-induced ROS in BV-2.....	101
Figure 2.45: Western blot is of COX-2 phosphorylation and GAPDH in whole cell lysates of BV-2 at 24 hours .....	102
Figure 2.46: Western blot of phospho-P38/P38 expression in whole cells lysates of BV-2. ....	104
Figure 2.47: Western blot and histogram show increase the ratio of phospho-P38 to total P38 expression in whole cells lysates at 30 and 60 mins .....	105
Figure 2.48: Western blot and histogram show the increase the ratio of phospho ERK 1/2 to total ERK 1/2 expression in whole cell lysates by LPS.....	105
Figure 2.49: Western blot show the effect of CBD and LPI ERK 1/2 expression in whole cell lysates of BV-2 .....	107
Figure 2.50: Western blot shows the effect of LPS and CBD on JNK 1/2 expression in whole cell extracts of BV-2 cells .....	108
Figure 2.51: Immunocytochemistry; Inhibition of LPS-induced NF-KB by CBD in BV-2 cells .....	110

Figure 2.52: Western blot and histogram show increase of phaspho-NF-KB and the ratio of phosphor-NF-KB to total NF-KB expression of nuclear lysates of BV-2 cells (protein 5µg) at 1hour by LPS and inhabited by CBD .....	111
Figure 2.53: Western blot is of NF-KB and phospho- NF-KB expression in whole lysis of BV-2 (protein 20µg) at 24 hours .....	112
Figure 2.54: Western blot is of IKBa and phospho- IKBa expression of cytoplasmic lysates of BV-2 (protein 20µg). .....	112
Figure 2.55: Western blot is of IKBa and phospho- IKBa expression of cytoplasmic lysates (protein 20µg) of BV-2 at 24 hours .....	113
Figure 2.56: HU210 (10 µM)-induced [ <sup>35</sup> S] GTPγS binding with increasing GDP concentration .....	114
Figure 2.57: HU-210 (10 µM)-induced [ <sup>35</sup> S]-GTPγS binding to rat brain membranes with increasing saponin concentrations...	115
Figure 2.58: Effects of cannabinoids on [ <sup>35</sup> S]-GTPγS binding in rat brain membranes .....	116
Figure 2.59: mRNA expression levels of GPR55 receptor by RT-PCR in mouse and BV-2 .....	117
Figure 2.60: Effect of CBD on GPR55 expression in BV2 cells by immunofluorescent staining .....	118
Figure 2.61: The summary graph shows the mechanism of inhabitation of LPS induced NO. ....	132
CHAPTER THREE	
Figure 3.1: "Compass" cell migration assay device .....	142
Figure 3.2: Phagocytosis of non-fluorescent latex beads assessed using an inverted microscope .....	150
Figure 3.3: images of phagocytic cells in BV-2 cells and primary mouse primary microglia. BV-2 cells. ....	151

Figure 3.4: The effect of BSA latex bead concentration on phagocytic activity in BV-2 cells. ....	152
Figure 3.5: The effect of incubation time on phagocytosis in BV2 cells ...	152
Figure 3.6: The effect of temperature and ethanol on phagocytosis in BV-2 cells .....	153
Figure 3.7: The effect of the cytochalasin D (a cytoskeleton inhibitor), oligomycin (a mitochondrial ATPase inhibitor) and FCCP (a mitochondrial uncoupler) on phagocytosis in BV-2 cells.....	154
Figure 3.8: The role of myosin light chain II protein on phagocytosis by immunocytochemistry .....	155
Figure 3.9: Confocal images showing expression of CD11b receptor in immunocytochemical analysis in BV-2 cells.....	156
Figure 3.10: confocal images showing expression of PLC $\gamma$ <sub>2</sub> protein immunocytochemical analysis of BV-2 cells.....	158
Figure 3.11: Expression of PKC $\alpha$ protein in by immunocytochemical analysis .....	159
Figure 3.12: Expression of PKC- $\epsilon$ protein in BV-2 by immunocytochemical analysis. ....	166
Figure 3.13: Effect of UDP and ATP (10 $\mu$ M) on phagocytosis in BV-2 cells.....	161
Figure 3.14: Effect of 1400W (selective iNOS inhibitor 1400W), interferon and LPS on phagocytosis in BV-2 cells .....	162
Figure 3.15: Effect of the microglial inhibitor minocycline and dexamethasone on phagocytosis in BV-2 cells.....	163
Figure 3.16: The effect of cannabinoids and endocannabinoids on phagocytosis in BV-2 .....	164
Figure 3.17: Effects of phytocannabinoids (10 $\mu$ M) on phagocytosis in BV-2 cells.....	165

Figure 3.18: The effect of phytocannabinoids on phagocytosis in primary mouse microglial .....	165
Figure 3.19: The effect of CBD on phagocytosis in RWA 264.7 cells. ....	166
Figure 3.20: The effect of CBD on phagocytosis in HAPI cells.....	167
Figure 3.21: Effect of N-arachidonylglycine (NAGLY; GPR18 agonist), O-1918 (an abn- CBD antagonist) on phagocytosis in BV-2 cells.....	168
Figure 3.22: The effect of pertussis toxin (PTX) on CBD-induced phagocytosis in BV-2 cells .....	169
Figure 3.23: The effect of Y27632 (a Rho/ROCK signalling inhibitor) on phagocytosis in BV-2 cells .....	170
Figure 3.24: The effect of SB203580 (a P38 inhibitor) on CBD induced phagocytosis in BV-2 .....	171
Figure 3.25: The effect of wortmannin on CBD induced phagocytosis in BV-2cells.....	171
Figure 3.26: The effect of apocynin on CBD induced phagocytosis in BV-2 cells.....	172
Figure 3.27: The effects of BAPT-AM (an intracellular Ca <sup>2+</sup> chelator) on CBD-induced phagocytosis in BV-2 .....	173
Figure 3.28: Effect of CBD on intracellular calcium in BV-2 by fura-2 ratiometric calcium imaging.....	174
Figure 3.29: The effect of ruthenium red on CBD induced phagocytosis in BV-2 cells.....	175
Figure 3.30: The effects of SKF96365 (SK) on CBD induced phagocytosis in BV-2 cells. ....	176
Figure 3.31: Colocalization of TRPV2 in BV-2 by immunocytochemical analysis. ....	178
Figure 3.32: Effect of CBD on colocalization of TRPV2 in primary mouse microglial cells by immunocytochemical analysis .....	179

Figure 3.33: Effect of CBD on TRPV2 protein of whole lysis cells and membrane in BV-2. ....	180
Figure 3.34: Effect of MAPK inhibitors (a Rho and PI3K) and non selective TRPVs inhibitor on CBD 10 $\mu$ M caused TRPV2 activation at 1 hour in whole lysis of BV-2 .....	181
Figure 3.35: The effect of cycloheximide (CHX) on phagocytosis in BV-2 cells .....	182
Figure 3.36: TRPV2 expression in BV-2 cells and the effect of CBD on activation of TRPV2 by RT-PCR. ....	183
Figure 3.37: Effect of CBD on TRPV1 protein of whole lysis cells in BV-2. ....	184
Figure 3.38: Expression of TRPV1 protein in BV-2 cells by immunocytochemical analysis .....	185
Figure 3.39: Effect of CBD on AKT protein in BV-2 cells. ....	186
Figure 3.40: Effect of CBD on P-AKT protein in BV-2 by immunocytochemical analysis. ....	187
Figure 3.41: Cell migration induced by UDP (10 $\mu$ M) in RAW 264.7.....	188
Figure 3.42: Histogram shows BV-2 cell migration induced by CBD .....	188
Figure 3.43: BV-2 cell migration induced by CBD .....	189
Figure 3.44: The graph represents the effect of CBD in enhancement of phagocytosis by increasing intracellular calcium and increases the expression of TRPV2.....	203

## Abbreviations

40X	lens magnification
2-AG,	2-arachidonoylglycerol
2-APB	2-aminoethoxydiphenyl borate
5-HT <sub>1A</sub>	serotonergic receptor 1A
Δ9-THC	delta-9-tetrahydrocannabinol
1400W	iNOS inhibitor
A <sub>2a</sub>	Adenosine receptor 2A
Aβ	amyloid β
abn-CBD	abnormal cannabidiol
ACEA	arachidonyl-2'chloroethylamide
ACPA	arachidonylcyclo-propylamide
AD	Alzheimer' disease
ADP	Adenosine Diphosphate
AEA	ethanolamine and arachidonic acid
AIDS	Acquired immunodeficiency syndrome
ALS	amyotrophic lateral sclerosis
ANOVA	analysis of variance
AP-1	activator protein-1
ATP	Adenosine triphosphate
BAPTA-AM	1,2-bis(o-Aminophenoxy)ethane- N,N,N',N'-tetraacetic acid
BBB	blood brain barrier
BDNF	Brain Derived Neurotrophic Factor
BK B2	bradykinin type 2 receptors
BSA	Bovine serum albumin
BV-2 cells	murine microglial cell
[Ca <sup>2+</sup> ] <sub>i</sub>	intracellular calcium

cAMP	cyclic adenosine monophosphate
CB	cannabinoid receptor
CB1	cannabinoid receptor 1
CB2	cannabinoid receptor 2
CBD	cannabidiol
CBDA	cannabidiol acid
CBG	cannabigerol
CBGV	cannabigerovarin
CBN	cannabinol
CBDVA	cannabidivarin acid
CBDV	cannabidivarin
CBNV	cannabinovarin
CCR(s)	chemokine receptors
CD	cluster of differentiation
cDNA	complementary DNA
CHX	cycloheximide a protein synthesis inhibitor
CNS	central nervous system
COX2	Cyclooxygenase 2
CPZ	capsazepine
CR3	complement receptor 3
CSF-1	colony stimulating factor-1
Cyclic AMP	Cyclic adenosine monophosphate
DAG	diacylglycerol
DAP12	DNAX activation protein of 12 kDa
DAPI	4,6-diamidino-2-phenylindole
DCF	Dichlorofluorescein
DEX	dexamethasone
DRG	rat dorsal root ganglion

DMEM	Dulbecco's modified Eagle's medium
DMSO	dimethyl sulfoxide
Ds	Dopamine receptors
EAE	experimental autoimmune encephalitis
EDTA	ethylenediaminetetraacetic acid
eNOS	endothelial NOS
ER	endoplasmic reticulum
ERK1/2	extracellular-signal-regulated kinases
FAAH	fatty acid amide hydrolase
FBS	fetal bovine serum
FCCP	Carbonyl cyanide 4 (trifluoromethoxy)phenylhydrazine
Fc $\gamma$ -RI	Fc gamma receptors
FITC	fluorescein isothiocyanate
GABA	gamma-amino butyric acid
GAE	granulomatous amoebic encephalitis
G $\beta\gamma$	G protein $\beta\gamma$ subunit
GDP	guanosine diphosphate
GPCR	G protein-coupled receptors
GPR18	G protein-coupled receptor 18
GPR55	G protein-coupled receptor55
GR	glucocorticoid receptor
GTP	guanosine triphosphate
GTP $\gamma$ S	Guanosine 5'-[ $\gamma$ -thio]- triphosphate
GSK	GPR55 ligands from GlaxoSmithKline
HAPI	Highly aggressive proliferating cell
HBSS	Hank's Buffered Salt Solution
HEK	human embryonic kidney
HIVE	human immunodeficiency virus encephalitis

HPLC water	high-performance liquid chromatography water
H2O2	hydrogen peroxide
HSV	herpes simplex viruses
HU210	(6aR)- <i>trans</i> -3-(1,1-dimethylheptyl) 6a,7,10,10a-tetrahydro-1-hydroxy- 6,6-dimethyl-6H-dibenzo [ <i>b,d</i> ] pyran- 9-methanol
Iba-1	Ionized calcium-binding adaptor molecule 1
IFN- $\gamma$	interferon gamma
I $\kappa$ B	inhibitor kappa B- $\alpha$
IL-	interleukin-
iNOS	inducible nitric oxide synthase
IP3	inositol triphosphate
IP-10	inducible protein-10
IRAK4	IL-1 receptor (IL-1R) - associated kinase 4
ITAM	immunoreceptor tyrosines-based activation motif
JNK	c-Jun NH2 -terminal kinase
LBP	LPS binding protein
LPI	Lysophosphatidylinositol
LPS	lipopolysaccharide
MAPK	mitogen-activated protein kinases
MCP-1	monocyte chemoattractant protein-1
M-CSF	macrophage-colony stimulating factors
MEA	myristoylethanolamine
MD-2	myeloid differentiation 2 receptor
MGL	monoacylglycerol lipase
MHC II	histocompatibility complex II
MHibA	Modified Hibernate A media
MIP-1	macrophage inflammatory protein-1
MLCII	myosin light chain II

MMP-3	matrix metalloproteinase-3
mRNA	messenger ribonucleic acid
MR	mineralocorticoid receptors
MS	Multiple Sclerosis
MyD88	myeloid differentiation primary-response gene 88
NAAA	N-acylethanolamine-hydrolyzing acid amidase
NADPH	nicotinamide adenine dinucleotide phosphate
NAGLY	N-arachidonoylglycine
NFκB	nuclear factor for kappa light chain in B cells
NFTs	neurofibrillary tangles
NGF	nerve growth factor
NK	natural killer
NO	nitric oxide
NR	Neutral Red
Nrf2	nuclear factor-erythroid 2
OEA	N-oleoylethanolamine
P2	purinoceptor
PAA	<i>N</i> -palmitoyl ethanolamine-preferring acid amidase
PAMPs	pathogen-associated molecular patterns
PBS	Phosphate Buffered Saline
PD	Parkinson's disease
PEA	palmitylethanolamide
PGE2	prostaglandin E2
PI	phosphatidylinositol
PI3K	phosphatidylinositol 3-kinase
PKCa	protein kinase Ca
PKCε	protein kinase ε
PLC	phospholipase C
PLD	phospholipase D

PRRs	pattern recognition receptors
PPARs	peroxisome proliferator-activated receptors
PTX	pertussis toxin
P <sub>2</sub> X and P <sub>2</sub> Y	purinergic receptors
Rac GTPase	Rac-type Rho guanosine triphosphatases
RANTLS	regulated upon activation normal T cell expressed/ secreted
RGA	recombinase gene activator protein
RNS	reactive nitrogen species
ROI	Reactive oxygen intermediates
ROCK	Rho A-associated kinase
ROD	relative optical density
ROS	Reactive oxygen species
RR	Ruthenium red
RT-PCR	Reverse transcription-polymerase chain reaction
SAPK	stress-activated protein kinase
SDS	sodium dodecyl sulphate
SDS-PAGE	SDS-polyacrylamide gel electrophoresis
SEA	N-stearoyl-ethanolamine
RWA-264.7	macrophage like cells
SEA	stearoyl-ethanolamine
SK	SKF96365
SNP	Sodium nitroprusside
SR1	SR141716A, CB1 selective antagonist
SR2	SR144528, CB2 selective antagonist
STAT	Signal transducers and activator of transcription
TGF	transforming growth factor
THCA	tetrahydrocannabinol acid

THCV	tetrahydrocannabivarin
TLR-	Toll-like receptor family
TNF- $\alpha$	tumor necrosis factor-alpha
tPA	tissue plasminogen activator
TREM2	triggering receptor expressed on myeloid cells-2
TRAF6	tumour necrosis factor receptor associated factor 6
TRAF6	tumour necrosis factor receptor associated factor 6
TREM2	Triggering receptor expressed by myeloid cells-2
TRPV-1	transient receptor potential vanilloid receptor1
TRPV-2	transient receptor potential vanilloid-2
VIP	intestinal polypeptide
VIR	virodhamine
VPAC1	VIP/pituitary adenylate cyclise activating peptide
Win55212-2	( <i>R</i> )-(+)-[2,3-dihydro-5-methyl-3-(4-Morpholinyl methyl)pyrrolo [1,2,3- <i>de</i> ]1,4benzoxazin-6-yl]-1-naphthalenyl methanone mesylate
XAC	xanthine amine carboxylic congener

## **1 General introduction**

### **1.1 Origin of the microglia**

Excluding the vasculature, the central nervous system (CNS) is populated by two main types of cells; neurons and glial cells. Glial cells include astrocytes, oligodendrocytes and microglia, with the microglia forming 10% of the total glial cell population (Perry, 1998). They were first described by Nissl in 1899 and were named Stäbchenzellen (rod cells), due to their rod-shaped nuclei, and they were classified as reactive neuroglia.

De Rio-Hortega (1932) later recognised that microglia were distinct from other glia and neurons (Pivneva, 2008). The origin of microglia is controversial; they might be derived from (1) neuroectoderm, (2) vascular adventitia (3) an intrinsic population of hematopoietic stem cells resident within the nervous system, (4) peripheral mesodermal/mesenchymal or (5) from circulating blood monocytes. It has also been suggested that the microglia originate from myeloid cells that enter the brain during early life before the blood brain barrier develops (Chan *et al.*, 2007). These parenchymal cells originate from the same monocyte lineage as other tissue macrophages (Facchinetti *et al.*, 2003; Rock *et al.*, 2004; Vilhardt, 2005).

### **1.2 Microglial functions and cytotoxicity**

The main function of the immune system is to protect the host, including the central nervous system (CNS) against infection by pathogens (Owens and Babcock, 2002). The immune system's

essential function, including both the innate and adaptive immune systems, is to protect the body through layered defenses of increasing specificity from infection. Pathogens, such as viruses and bacteria, are prevented from invading the organism first by physical barriers; however, if pathogens overcome these barriers, a non-specific but immediate, short-term response will be provided by the innate immune system. This is usually started by identification of the pathogen by pattern recognition receptors, or when injured, damaged or stressed cells release alarm signals (Litman *et al.*, 2005).

A third layer of defense, the adaptive immune system, becomes active if the innate response is overcome allowing for antigen-specific, stronger immune responses as well as immunological memory, where each pathogen is remembered. This response requires the identification of specific "non-self" antigens during a process called antigen presentation (Becher *et al.*, 2000). The immune system's effector mechanisms include antibodies and other immunity-related molecules (Hickey *et al.*, 1991). Under physiological circumstances, only activated T-lymphocytes are able to pass the BBB and get into the brain (Hickey *et al.*, 1991). They depart the brain if they do not encounter antigen presentation (Finsen *et al.*, 1991). In situations of acute or chronic brain damage or disease, activated leukocytes can enter the brain in large numbers even when the BBB is not opened (Brown 2001). The processes underlying this effect are still not clear. Next to blood-derived activated leukocytes, the brain-resident astrocytes, and microglia are also present at the site of brain injury but only the microglial cells possess complete competence for immunological functions (Gehrmann *et al.* 1995).

In the central nervous system, microglia play a major role in the inflammatory process (Nakamura, 2002). Microglia not only share surface molecules with peripheral macrophages but are also capable of antigen presentation, phagocytosis and secretion of cytokines, chemokines and cytotoxins (Nakajima *et al.*, 2001; Town *et al.*, 2005).

Microglial cells can be divided into three types according to their activation status: resting microglia, activated microglia and amoeboid phagocytic microglia (Cabral *et al.*, 2008). In the CNS, ramified resting microglia constitute 5-20% of the neuroglial population, are more prevalent in grey matter than in white matter and they adopt their morphology and expression of cell surface antigens according to their microenvironment (Kim and de Vellis, 2005).

Microglial cells with ramified morphology and sparse expression of molecules associated with macrophage function are found in healthy nervous tissue and have been associated with a resting phenotype. Resting microglia are not, however, inactive but are characterized by a lack of endocytic and phagocytic activity and low expression of the leukocyte common antigen CD45 (David and Kroner, 2011). They express low levels of membrane ligands and receptors that are important for mediating or inducing typical macrophage functions including major histocompatibility complex (MHC) class II molecules typical of professional antigen-presenting cells (Aloisi, 2001).

Furthermore, resting microglia may secrete low levels of growth factors to support the viability of the surrounding neurons and other glia. Kim and Joh (2006) have claimed that the neurons play a role in maintaining resting microglia phenotype through CD200 and

glycoprotein expressed on the surface of neurons linked with the microglia and involved in the regulation of phagocytic activity (Wright *et al.*, 2000). In transgenic mice in which CD200 has been deleted, microglia are spontaneously stimulated and express high levels of CD45 and CD11b (Hoek *et al.*, 2000).

Under normal conditions during adult life, resting microglia numbers remain relatively constant with a slow turnover (Chew *et al.*, 2006). Responding to chemical signals and directing the responses for tissue repair and induction of protective immune responses is one of the most important characteristics of microglia. To carry out these different functions, microglia need to be activated (Aloisi, 2001; Hanisch, 2002). There are two different types of activated microglia according to their phagocytic activity; one sort is hypertrophic with increased expression of the surface marker molecules but these are not phagocytic. They are found mainly in areas of secondary reaction, for example, as a result of nerve transection. The other type is fully phagocytic microglia, found in areas of primary trauma, infection or neural necrosis but also in the developing brain (Gehrmann *et al.*, 1995).

Microglia appear to have a spectrum of activation states; minor changes in morphology and functional state can even be observed in the process of preparing cultured microglia cells which have been found to express CD14, a marker not present in ramified microglia (Wright *et al.*, 1990). At the extreme end of the activity spectrum, stimulation with lipopolysaccharide (LPS) to simulate infection, leads to marked alterations in function (Hayakawa *et al.*, 1997). Fully activated microglia are present in the foetal brain where they act as

scavengers of pruned cell materials during the remodeling stages of development (Voyvodic, 1996; Watnab *et al.*, 1997).

Microglial activation is characterized by proliferation and migration to the site of injury which requires a change in morphology to one different from resting cells; their processes retract into the soma giving an amoeboid shape and they develop a generally more rounded appearance (Vilhardt, 2005) as shown in Figure 1.1. In addition to morphological modifications during this multi-step activation process, microglia also undergo differential gene expression of a host of surface receptors including Fc receptors (Fcγ-RI, RII and RIII); CD14 receptors; Toll-like receptors (TLR); chemokine receptors (CCR2, CCR3, CCR5, CXCR4, CX3CR1), interferon-gamma receptors (IFN-α, β, γ), tumor necrosis factor-alpha (TNF-α) receptors (TNFRI, TNFRII) and transforming growth factor-beta (TGF-β) receptors (TGFβ-RI, RII and RIII) (Qin *et al.*, 2005; Rock *et al.*, 2004) in addition to other antigens including, MHC class II, CD45, CD11b (Kim and Joh, 2006).

Microglia detect pathogens by means of pattern recognition receptors (PRRs) on the cell surface which recognize pathogen-associated molecular patterns (PAMPs), molecular structures associated with host cells (Medzhitov and Janeway, 2000). Most PRRs are expressed only at low levels on ramified microglia, if at all, and are upregulated upon microglial activation (Aloisi, 2001). Previous studies have postulated that microglia have the dual, contrasting functions of mediating both neurotoxicity and neuroprotection, because they stimulate neuronal cell death, by releasing neurotoxic factors such as nitric oxide, glutamate, or unknown neurotoxins, as well as

supporting the survival of neurones, by releasing neurotrophic factors (Streit, 2005; Takahashi 2005; Chao *et al.*, 1992).

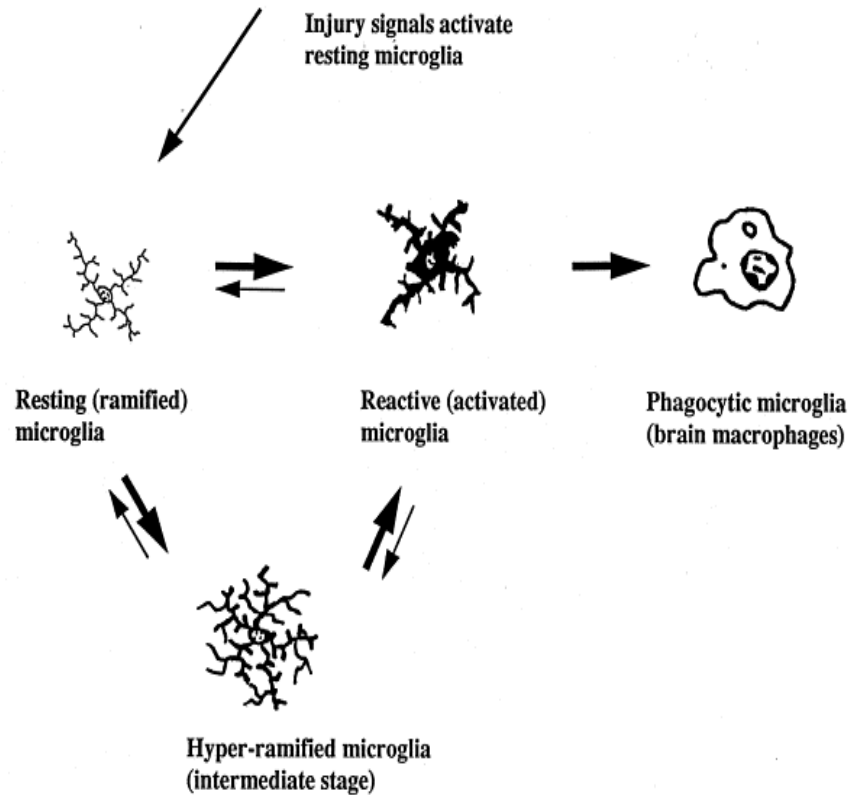


**Figure 1.1** Diagrammatic representations of the stages of microglia cell during activation, adapted from Streit, (1999).

Microglia polarization is routinely classified into classical (M1) and alternative (M2) activation. Although this classification might be an over simplification, microglia can be polarized into an activation state that is intermediate between a neuro-harmful and a protective state. Lipopolysaccharide (LPS) is known as a representative M1 polarization inducer, and these are highly aggressive against bacteria and produce large amounts of lymphokines (Murray and Wynn, 2011). M1 microglia express proinflammatory molecules that include tumor necrosis factor- $\alpha$  (TNF- $\alpha$ ), interleukin-1 $\beta$  (IL-1 $\beta$ ), interferon- $\gamma$  (IFN- $\gamma$ ), and nitric oxide (NO) as well as cell surface markers, CD86 and

CD68. On the other hand, IL-4 induces M2 polarization (Liao *et al.*, 2012; Kigerl *et al.*, 2009; Meissner *et al.*, 2012). M2 microglia express different molecules, such as IL-4, arignase1, Ym1, CD206, and IL-10, and show neuroprotective effects (Liao *et al.*, 2012; Kigerl *et al.*, 2009; David and Kroner, 2011; Ponomarev *et al.*, 2007).

Microglial activation has protective functions in the destruction of pathogens, such as microorganisms, neoplastic cells, removal of debris and enhancement of tissue repair and release of neurotrophic factors. However, excessive activation can be damaging and can exacerbate the effects of inflammation leading to neurodegenerative disease (Banati *et al.*, 1993). Microglial activation has been implicated in Alzheimer's disease, multiple sclerosis, chronic pain, Parkinson's disease, and in the animal model experimental allergic encephalomyelitis (EAE), and numerous other disorders, including Pick's and Huntington's diseases, amyotrophic lateral sclerosis, Shy-Drager syndrome (Banati *et al.*, 2004; McGeer *et al.*, 1988); post-traumatic injury and aging also involve activated microglia (Figure 1.1). In fact, activation of microglia may be a common feature of all neurological damage. This activation could contribute further insult through immune-mediated cellular damage (Fontana *et al.*, 1987) and this will be discussed in more detail later in a separate section.

### **1.2.1 Microglia migration**

Movement of microglia can be the result of a random, non-vectorial motility (chemokinesis), or a directed migration that depends from a chemical gradient to organize the movement (chemotaxis), or both (Devreotes and Janetopoulos, 2003; Miller and Stella, 2009). Cell migration can be triggered by a diverse array of chemoattractants.

Consistent with their role in the immune response in the CNS, microglia express an array of receptors for chemokines which are involved in the intercellular communication in brain and contribute to intracerebral recruitment of immune cells (Aloisi, 2001; Hanisch, 2002; Kim and de Vellis, 2005). Fractalkine, as mentioned in the previous section, is a chemokine that can exist in two different forms, membrane-anchored or as a soluble glycoprotein (Harrison *et al.*, 1998). Under normal conditions, CX3CL1 is constitutively associated to the neuronal membrane, stimulating higher intracellular calcium mobilization in responding cells. This process is apparently needed for adhesion properties. However, after an excitotoxic stimulus, the chemokine undergoes a cleavage by matrix metalloproteinases (MMPs) triggered by the NMDA (N-methyl-D-aspartate) receptor pathway (Chapman *et al.*, 2000).

The soluble glycoprotein can then interact with its receptor expressed on microglia inducing their chemotaxis (Harrison *et al.*, 1998). Thus, the release of this molecule is an early event in the inflammatory response leading to neuronal death after an excitotoxic injury (Chapman *et al.*, 2000). Moreover, microglial migration is also induced, among others, by the lymphoid chemokine CCL21, which involves chloride channels (Rappert *et al.*, 2002), and by secondary lymphoid-tissue (Biber *et al.*, 2001), both expressed by damaged neurons and acting on CXCR3 receptor expressed by microglia.

Microglial cells also migrate towards neurotrophic factors such as the epidermal growth factor (Nolte *et al.*, 1997) and nerve growth factor (De Simone *et al.*, 2007), corroborating the role of microglia in brain development. Pathological protein aggregates, such as amyloid- $\beta$ , have been shown to induce microglial migration (Gyoneva *et al.*, 2009).

Purines that are released from injured tissue in higher levels into the extracellular space by neurotransmission, lead to microglia chemotaxis (Parkhurst and Gan, 2010). Indeed, the baseline motility of microglial processes in the intact brain is modulated by some of the ATP signaling mechanisms mediating injury-induced microglial responses (Davalos *et al.*, 2005).

ATP G protein-coupled purine receptors (P2YR) (Honda *et al.*, 2001; Haynes *et al.*, 2006), In fact, microglial cells from mice lacking P2Y12R receptor are unable to polarize, migrate or extend processes towards nucleotides, either *in vitro* or *in vivo* (Haynes *et al.*, 2006). Besides P2YR, ATP acts on ionotropic P2X receptors (P2XR) and P2X4R which are also involved in microglial chemotaxis as demonstrated by Ohsawa and his colleagues (2007). Furthermore, microglial cells themselves can release ATP so that a positive feedback mechanism may exist to perpetuate migration.

Intriguingly, Duan *et al.*, (2009), and more recently Samuels and his colleagues (2010), claim that nitric oxide (NO) is the true responsible for directing the movement of microglia after nerve injury in leech. According to these studies, ATP released by damaged cells activates microglia and induces their initial movement, whereas NO directs migration of the cells to CNS lesions. In fact, NO mediates microglial response to acute spinal cord injury *in vivo*, but this process is under the control of ATP (Dibaj *et al.*, 2010). Nucleotide uridine diphosphate (UDP) is released by dying neurons and recognized by P2Y6 receptor (P2Y6R), specifically expressed on microglia.

### **1.3 Mechanisms of microglial activation**

Many molecules and conditions can trigger a transformation of resting to activate microglia. Activation can result from damage to brain parenchyma or imbalances in ion homeostasis. Microglia do respond to neuronal depolarization and associated increased potassium fluxes across membranes in the absence of neuronal damage (Gehrmann *et al.*, 1993). Furthermore, ATP and other P<sub>2</sub> receptor agonists change the electrophysiological properties of microglia, by facilitating depolarization, and ATP can be released as a co-transmitter by several cell types during injury.

Several molecules stimulate microglial cells such as the gram-negative bacterial endotoxin lipopolysaccharide (LPS), interferon- $\gamma$  (IFN- $\gamma$ ), amyloid- $\beta$  peptide (A $\beta$ ), CD40 ligand (CD40L), chemokines, neurotransmitters and gangliosides, thrombin, tissue plasminogen activator (tPA) and matrix metalloproteinase-3 (MMP-3). Some activators can be derived from pathogens, or from neurons, for instance ATP, and also from the microglia themselves, such as TNF- $\alpha$ , plasminogen and NO (Abd-el-Basset and Fedoroff, 1995; Vogel and Noelle, 1998).

The most commonly used compound to stimulate microglial activation experimentally *in vitro* and *in vivo* is the bacterial endotoxin lipopolysaccharide (LPS), the major mediator of shock induced by gram-negative bacteria (Rietsehel *et al.*, 1994). This, therefore, mimics gram-negative bacterial infection of the brain, which is prevented under normal circumstances by the BBB. The pattern recognition receptor (PRR) Toll-like receptor 4 (TLR4) (Kalis *et al.*, 2003) and cluster of differentiation (CD 14) are expressed by

microglia and other cells of the monocyte/macrophages lineage; this is a GPI-anchored glycoprotein which reacts with LPS to form LPS-binding protein in serum (Wright *et al.*, 1990). LPS also activates microglia through CD4, CD11c, CD18.

Myeloid differentiation primary response gene 88 (MyD88) is the primary TLR4 signalling mechanism (Figure 1.2); the interaction of MyD88 with TLR recruits IL-1 receptor (IL-1R) -associated kinase 4 (IRAK4) to death domains of both MyD88 and TLR (O'Neill *et al.*, 2003; Hacker *et al.*, 2006). The interaction of IRAK4 with the death domains acts to facilitate the phosphorylation of IRAK1, the activated IRAK1 then binds to the tumour necrosis factor receptor associated factor 6 (TRAF6) (Kobayashi *et al.*, 2002). Two distinct pathways are activated by TRAF6. The first pathway activated is transforming growth factor  $\beta$ -activated kinase (TAK1) pathway. The other pathway activated by TRAF6 is the Nuclear Factor KappaB (NF- $\kappa$ B) and activator protein-1 (AP-1) system (Kobayashi *et al.*, 2002).

Both of these pathways lead to transcription factors like NF- $\kappa$ B being up-regulated and an increase in the activation of mitogen-activated protein (MAP) kinases (Akira and Takeda, 2004). Protein tyrosine kinases, MAP kinases, protein kinase C, small G proteins and ceramide-activated protein kinase are all intracellular signalling molecules for LPS-mediated monocyte, macrophage and also microglial activation. LPS activates transcription factors, including NF-IL6, C/EBP and activated PKCs may facilitate Fos/ Jun families and cytokine genes (Sweet and Hume, 1996; Koistinaho and Koistinaho, 2000; Fiebich *et al.*, 1998). As a consequence of pro-inflammatory activation, ramified microglia morphologically transform into an amoeboid shape and migrate towards the lesion spot.

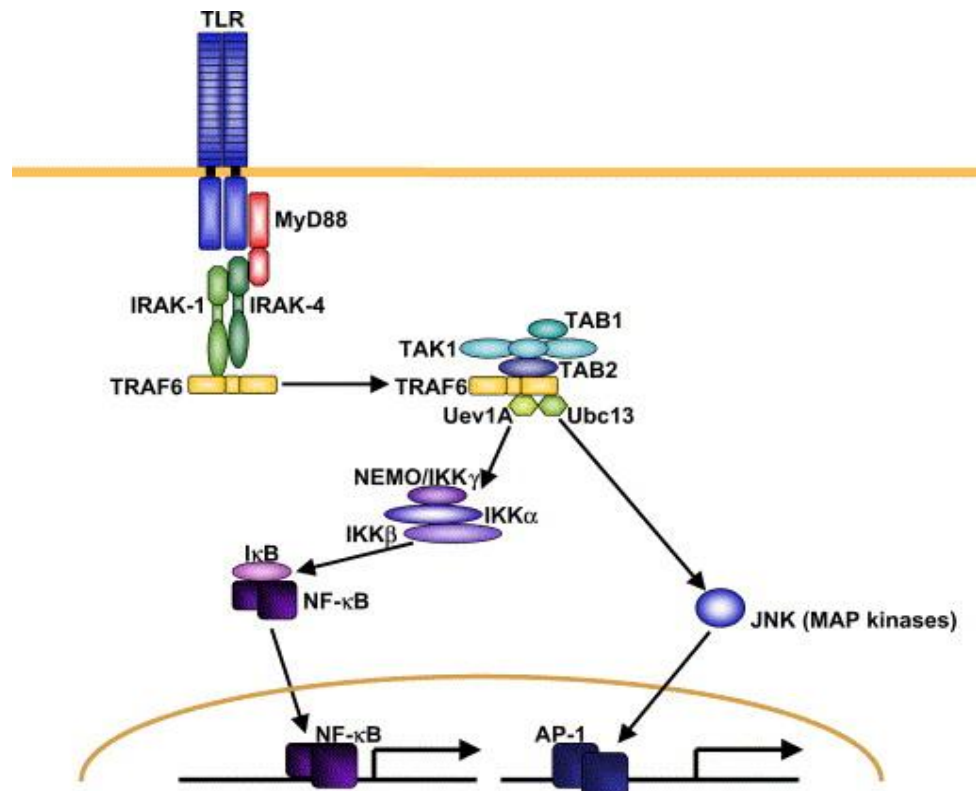


**Figure 1.2:** Diagrammatic representation of the LPS/TLR4 signalling. LPS recognition is assisted by LBP and CD14, and is mediated by TLR4/MyD88 receptor. TRAF6, which mediates the activation of pro-inflammatory cytokine (Adapted from Takeda and Akira, 2004).

Activated microglia express increased levels of chemokine (C-C) motif ligand 2 (CCL2), a modulator of microglial migration and proliferation (Hinojosa *et al.* 2011), building a chemoattractant gradient at the lesion spot to attract further cells and shield the adjacent tissue environment from neurotoxic substances (Ambrosini and Aloisi 2004). Activated microglia sequester effector cytokines like interleukin-6 (IL-6) and interleukin-1 $\beta$  (IL-1 $\beta$ ) leading to paracrine activation of migrating microglia (Ferreira *et al.* 2010).

Other PRRs expressed by microglia include TLR2, TLR9 and other mannose receptors. In addition, microglial receptors exist allowing detection and phagocytosis of other pathogens which have been opsonised (coated) by soluble components of the immune system

(Aloisi, 2001). The receptors expressed by microglia which allow detection of pathogens are discussed in detail in Chapter three.

### **1.3.1 Microglial effector molecules**

Different receptors and signaling pathways are involved in the detection of and response to different molecules which activate microglia (Pocock and Liddle, 2001). It is, therefore, likely that different microglial activators cause the up-regulation of specific genes and lead to slightly different activated phenotypes. Microglial activation may lead to the release of reactive oxygen and nitrogen species (ROS and RNS), proteolytic enzymes, prostanoids and glutamate. Microglia can also release glutamate through increased expression or activity of the cystine/glutamate antiporter Xc or the reversal of excitatory amino acid transporters.

The release of ROS and RNS by activated microglia represents a cytotoxic attack mechanism against invading pathogen. Microglial activation may induce the rapid generation of superoxide by reduced nicotinamide adenine dinucleotide phosphate (NADPH) oxidase known as the respiratory burst (Sankarapandi *et al.*, 1998). Either superoxide may be cytotoxic alone; alternatively they may combine together to form the highly reactive species peroxynitrite (Noack *et al.*, 1999). ROS and RNS have the potential to cause cell damage and death by reacting with proteins, nucleic acid and lipids of neighboring cells (Volko *et al.*, 2007). Peroxynitrite causes the dysregulation of mitochondrial respiration (Bolaños *et al.*, 1997). However, in some cells peroxynitrite may be protective through the up-regulation of the pentose phosphate pathway, leading to stimulation of NADPH levels

to regenerate the reduced form of the antioxidant glutathione (Almeida *et al.*, 2005).

Activated microglia may also express inducible nitric oxide synthase (iNOS) allowing the production of the inflammatory mediators, nitric oxide (NO) (Brown and Bal-Price 2003; Michelucci *et al.* 2009), tumour necrosis factor (TNF)- $\alpha$ , interleukins (IL) IL-1 $\beta$ , IL-6, transforming growth factor- $\beta$ 1 (TGF- $\beta$ 1), macrophage-colony stimulating factors (M-CSF) (Sgeng *et al.*, 2005), brain-derived neurotrophic factor (BDNF), neurotrophin-3 (NT-3) and neural growth factor (NGF). Moreover, activated microglia secrete proteinases, for instance, cathepsin B/L and plasminogen activator, which could be involved in neuronal remodeling during repair (Gehrmann *et al.*, 1995; Merrill, 1992).

Activated brain microglial cells release NO which has protective activity in the central nervous system by keeping iNOS expression suppressed via preventing NF- $\kappa$ B activation or alternatively NO may cause up-regulation of glycolysis leading to compensatory ATP production and maintenance of the mitochondrial membrane potential (Almeida *et al.*, 2005). Moreover, NO may act as an antimicrobial defense (Chao *et al.*, 1992). By contrast, excessive release of NO has been found to cause brain injury and to mediate neurodegenerative inflammatory processes (Cabral, 2001; Colasanti *et al.*, 1995).

There are three isoforms of nitric oxide synthase (NOS) that have been cloned, two of them are constitutively active; endothelial NOS (eNOS) and neuronal NOS (nNOS), which are responsible for the production of transient, low level bursts of NO and both are calcium/calmodulin-dependent. The third type is inducible by

inflammation, endotoxin, cytokines and oxidative stress, but not by calcium, and its expression is induced in many cell types including macrophages (Brown, 1997). Under normal conditions, the release of NO from microglial cells is insignificant, but when it is released, it can pass from the cell of origin into surrounding tissue to act on other cells because it is small and without charge (Brown, 1997). However, upon stimulation with LPS or cytokines such as TNF- $\alpha$  and (IFN- $\gamma$ ), inhibition of NO release has been found to increase microglial cell survival in several models (Gibbons and Dragunow, 2006). The modulation of NO release from microglia by cannabinoids will be addressed in Chapter Two.

#### **1.4 Microglial receptors**

Microglial cells express a variety of cytokine and chemokine receptors, as discussed previously. They also contain receptors for the major excitatory neurotransmitter glutamate including metabotropic glutamate receptors, which can be neuroprotective through group III mGluR (mGlu4, mGlu6 and mGlu8 receptors) or neurotoxic via group II mGluR (mGlu2 and mGlu3) (Taylor *et al.*, 2002; Taylor *et al.*, 2003; Taylor *et al.*, 2005). Receptors for the main inhibitory transmitter, gamma-amino butyric acid (GABA), GABA<sub>A</sub> and GABA<sub>B</sub> receptors, are also expressed in microglia. Activation of GABA<sub>B</sub> receptors inhibits the LPS-induced release of IL-6, IL-12 and p40 (Kuhn *et al.*, 2004; Lee *et al.*, 2011).

Dopamine receptors have been found in rat and mouse microglia in culture and in brain slices (Farber *et al.*, 2005). D1 and D2 receptors generate the inhibition of the constitutive potassium inward rectifier currents and stimulated potassium outward currents in a

subpopulation of microglia. Chronic dopamine receptor stimulation increases migratory activity and attenuates the LPS-induced NO release (Farber *et al.*, 2005).

Microglia express  $\beta_1$  and  $\beta_2$ -adrenoceptors which, upon activation with noradrenaline or adrenaline, both increase the level of cAMP production and IL-1 $\beta$  mRNA. Selective  $\beta_2$ -adrenoceptor agonists inhibit LPS-induced release of IL-12, p40 and cAMP (Prinz *et al.*, 2001). Moreover, microglia contain endothelin (ET $_B$ ) receptors which, when stimulated, lead to increased intracellular Ca $^{2+}$  release from cytoplasmic stores (Moller *et al.*, 1997). Cultured rat microglia also express mRNA for Ca $^{2+}$ -mobilizing bradykinin type 2 (B $_2$ ) receptors (Noda *et al.*, 2003); bradykinin increases microglial motility and induces the release of NO and PGE $_2$  (Noda *et al.*, 2006).

A $_{2A}$  adenosine receptor-mediated neuroprotective effects might be a result of the release of neurotrophic factors including nerve growth factor (NGF). Activation of A $_{2A}$  receptors also induces cyclooxygenase-2 (COX-2 mRNA) expression (Fiebich *et al.*, 1996). Moreover, activation of microglial adenosine A $_3$  receptors inhibits LPS-induced TNF- $\alpha$  formation (Lee *et al.*, 2006).

Microglia express the P2 receptors P2X and P2Y in both resting and activated states, leading to increases in cytosolic calcium upon stimulation. Activation of P2X7 receptors by high concentrations of ATP induces the release of IL-1 $\beta$  and plasminogen as well as reducing the LPS-mediated production of IL-6, IL-12, TNF- $\alpha$  and macrophage inflammatory protein 1-alpha (MIP1- $\alpha$ ). P2Y receptors can be stimulated by ATP or ADP leading to alterations in microglial chemotaxis (Honda and Kohsaka, 2001).

Microglia also expresses glucocorticoid (GR) and mineralocorticoid (MR) receptors in primary cultures from the forebrain of newborn rats. Stimulation of GR inhibited proliferation of cultured microglia and enhanced lysosomal formation (Tanaka *et al.*, 1997). Furthermore, the vasoactive intestinal polypeptide (VIP) acts via the VPAC (VIP/pituitary adenylyl cyclase activating peptide) G protein-coupled receptors. VPAC1 receptors are found in rat microglia, and stimulation of these receptors with VIP (0.1  $\mu$ M) or with its functional/structural analogue pituitary adenylyl cyclase-activating polypeptide leads to inhibition of TNF- $\alpha$  production in LPS-activated cultured rat microglia (Kim *et al.*, 2000).

### **1.5 Cannabinoid signalling system.**

Microglia are reported to express cannabinoid CB<sub>1</sub> and CB<sub>2</sub> receptors which play an important role in microglial activation states and have been linked to cannabinoid modulation of chemokine and cytokine action.

#### **1.5.1 CB<sub>1</sub>/CB<sub>2</sub> receptors**

The CB<sub>1</sub> receptor was identified in 1988 by Devane *et al.*, 1992 and cloned in 1990; since then it has been cloned from mouse and human tissues and there is 97-99% sequence identity between them. In humans, the CB<sub>1</sub> receptor is expressed extensively throughout the central nervous system (CNS) particularly in the hippocampus, basal ganglia, hypothalamus and amygdala (Herkenham *et al.*, 1990; Mechoulam *et al.*, 2012). CB<sub>1</sub> receptors have also been recognized peripherally in tonsils, spleen, sympathetic nerve terminals, and in preparations such as the guinea-pig small intestine (Pertwee *et al.*,

1996), the mouse urinary bladder, the mouse vas deferens, hamster smooth muscle cells (Filipeanu *et al.*, 1997) and cat vascular smooth muscle cells (Gebremedhin *et al.*, 1999).

The CB<sub>1</sub> receptor is considered to be the most highly expressed GPCR in the brain (Maccarrone *et al.*, 2011). Regional expression density correlates well with the observed acute central effects of cannabinoids, such as impairment in cognition, memory, learning and motor coordination (Huffman *et al.*, 2005; Patel and Hillard, 2006). In rodents, cannabinoid drugs produce a “cannabinoid tetrad” of characteristic pharmacological effects: antinociception, hypothermia, a decrease in general mobility (sedation), and catalepsy, the combination of which has achieved acceptability as a screening procedure (Martin *et al.*, 1991). In addition, CB<sub>1</sub> receptor activation for minutes to hours changes gene expression inducing neuroprotective proteins, for example BDNF, to reduce cell damage (Stella, 2004).

CB<sub>2</sub> receptors were cloned from human promyelocytic leukaemia (HL-60) cells (Munro *et al.*, 1993). This receptor shares with the CB<sub>1</sub> receptor the structural features typified by seven transmembrane-spanning domains and coupling to G proteins. The human CB<sub>2</sub> receptor has 68% amino acid sequence homology to the CB<sub>1</sub> receptor within the transmembrane domains, but only 44% homology throughout the total protein (Begg *et al.*, 2005; Fernandez-Ruiz *et al.*, 2007). Both CB<sub>1</sub> and CB<sub>2</sub> receptors belong to the group of rhodopsin-like G protein-coupled receptors (GPCRs) which comprise one subdivision of the GPCR superfamily (Pertwee *et al.*, 2010). CB<sub>1</sub> and CB<sub>2</sub> receptors both signal through the G<sub>i/o</sub> class of heterotrimeric G proteins (Bosier *et al.*, 2010; Pertwee *et al.*, 2010).

Activation of CB<sub>1</sub> or CB<sub>2</sub> receptors via binding of endogenous or synthetic agonists causes dissociation of the G<sub>α</sub> subunit from the Gβγ subunits and the consequent initiation of a number of intracellular signaling cascades. Both CB<sub>1</sub> and CB<sub>2</sub> activation result in inhibition of adenylyl cyclase and the associated inactivation of protein kinase A through the G<sub>α</sub> subunit, and activation of elements of the mitogen-activated protein kinase (MAPK) signaling mediated by Gβγ (Bosier *et al.*, 2010; Pertwee *et al.*, 2010).

Furthermore, in addition to the G<sub>i/o</sub> subtype of G alpha, the CB<sub>1</sub> receptor is also reported to signal through G<sub>s</sub> and G<sub>α</sub> subunits to stimulate a rise in intracellular Ca<sup>2+</sup> (Bosier *et al.*, 2010). CB<sub>1</sub> receptor activation is linked to the modulation of ion channel signaling pathways including activation of inwardly rectifying K<sup>+</sup> channels (Demuth and Molleman, 2006).

CB<sub>2</sub> receptor expression has traditionally only been associated with cells of the immune system, although in recent years, evidence has emerged for its presence on neurons (Mechoulam *et al.*, 2012; den Boon *et al.*, 2012; Viscomi *et al.*, 2009). Munro *et al.* (1993) suggested that CB<sub>2</sub> receptors are absent in healthy brain. They are also present on glial cells where their roles include modulation of cytokine release and immune cell migration, especially activated microglial cells (Waksman *et al.*, 1999; Walter *et al.*, 2003).

Little is known about CB<sub>2</sub> homomers or heteromers although a recent study demonstrated the formation of functional CB<sub>1</sub>/CB<sub>2</sub> heteromers in transfected neuronal cells and in brain tissue (Callen *et al.* 2012). Of particular interest was their observation of bidirectional cross-antagonism in the heteromers with CB<sub>1</sub> antagonists able to block the

effects of CB2 agonists and vice versa. CB1 receptors are located both pre- and post-synaptically, whereas CB2 receptors are thought to display a preferentially post-synaptic distribution (Callen *et al.* 2012; Brusco *et al.* 2008). CB1 but not CB2 receptor distribution is also affected by membrane cholesterol content, with lower cholesterol levels resulting in increased CB1 signalling (Maccarone *et al.* 2011; Bari *et al.* 2005).

The CB<sub>2</sub> receptor is implicated in the neuroprotective activity of cannabinoids, mainly through a series of glia-dependent anti-inflammatory actions (Pertwee, 2006; Fernandez-Ruiz *et al.*, 2007). Activation of CB<sub>2</sub> receptors contributes to an inhibition of pro-inflammatory responses *in vitro* and the most relevant pro-inflammatory agents that seem to be under control of CB<sub>2</sub> receptors are TNF- $\alpha$ , IL-1 and IL-6 (Ashton *et al.*, 2006; Fernandez-Ruiz *et al.*, 2007).

### **1.5.2 Non-CB<sub>1</sub>/CB<sub>2</sub> receptors**

Reports of the existence of additional cannabinoid receptors continue to accumulate, and these are based on investigations using CB<sub>1</sub> knockout or CB<sub>1</sub>/CB<sub>2</sub> double-knockout mice which demonstrate that some pharmacological responses to endogenous, exogenous and synthetic cannabinoids are exerted through mechanisms independent of CB<sub>1</sub> and CB<sub>2</sub> (Breivogel *et al.*, 2001; Alexander, 2012).

Previous reports have proposed that the orphan GPR55 receptor and the transient receptor potential vanilloid 1 (TRPV1) may potentially be novel cannabinoid receptors. In addition, McHugh *et al.*, (2012) found that two cannabinoid receptor agonists, anandamide (AEA) and

tetrahydrocannabinol (THC), are full agonists and the non-psychoactive phytocannabinoid cannabidiol (CBD) is a weak partial agonist at the GPR18 receptor.

N-arachidonoylglycine (NAGLY; an endogenous fatty acid) is a full agonist at GPR18 (McHugh *et al.*, 2012). GPR18 expression is reported in human lymphoid cells (Kohno *et al.*, 2006), BV-2 microglial cells, HEC-IB human endometrial cells (McHugh *et al.*, 2012) and metastatic melanoma (Qin *et al.*, 2011). Several reports have suggested that there is sufficient evidence for GPR18 to be considered as a third cannabinoid receptor (Pertwee *et al.*, 2010).

#### **1.5.2.1 GPR55 receptor**

Some recent studies indicate that GPR55, an orphan G protein-coupled receptor, could also be considered as a novel cannabinoid receptor. GPR55 pharmacology is a controversial issue and the inconsistencies in the literature are likely attributed to the differences in assay protocols and /or cellular backgrounds employed by different workers (Henstridge *et al.*, 2010).

GPR55 belongs to the class A family of GPCRs and has been found to be activated by endogenous, synthetic and phytocannabinoids (Sawzdargo *et al.*, 1999). However, a clear classification of GPR55 as a cannabinoid receptor is not well supported. Some cannabinoid receptor agonists such as CP-55,940, as well as endocannabinoids and endocannabinoid-like molecules including anandamide, virodhamine and palmitoylethanolamine activate [<sup>35</sup>S]-GTP-γ-S binding via this receptor with nanomolar potency. On the other hand, Kapur and colleagues (2009) have reported that CP-55,940 is an

antagonist of the GPR55 receptor in common with abnormal cannabidiol, O-1602, HU 210, JWH 015 and AM 251 (Baker, 2006; Johns *et al.*, 2007). GPR55 is also reported to be antagonized by cannabidiol (CBD), independent of CB<sub>1</sub> or CB<sub>2</sub> activity (Ryberg *et al.*, 2007). Kapur and colleagues (2009) have found that the CB<sub>1</sub> antagonist rimonabant (SR141716A) activated GPR55 at a concentration of 10 µM (Johns *et al.*, 2007; Ryberg *et al.*, 2007).

Several reports concerning the pharmacology of GPR55 are controversial and divergent and some groups have also reported that cannabinoids that have been previously described as ligands for GPR55 may not actually have affinity for the receptor (Ross, 2009; Oka *et al.*, 2009; Henstridge *et al.*, 2009). Lauckner and his colleagues (2008) observed a significant intracellular calcium rise in human GPR55-expressing HEK293 cells and in large dorsal root ganglion (DRG) cells when GPR55 was stimulated by the classical cannabinoid THC, JWH015, AEA, myristoylethanolamine (MEA) and lysophosphatidylinositol (LPI) requiring G<sub>αq</sub>, PLC, G<sub>α13</sub> and RhoA, whereas, there was less calcium release in non-transfected HEK cells (Edeeb *et al.*, 2009). GPR55 pharmacology will be discussed in greater detail in Chapter Two.

The latter agents described appear to have more potency at GPR55 than CB<sub>1</sub> and CB<sub>2</sub> cannabinoid receptors (Pertwee, 2007). Ryberg and colleagues (2007) have claimed that GPR55 is activated by endocannabinoid-related ligands, especially PEA and OEA. However, other studies have reported that GPR55 is not activated by endocannabinoid-like ligands (Yin *et al.*, 2009). GPR55 is thus unlikely to be reclassified as a cannabinoid receptor in the near future and more recent evidence has suggested that it may be a receptor for

endogenous phospholipids with the arachidonic acid containing species 2-arachidonoyl-*sn*-glycero-3-phosphoinositol (LPI), having the highest affinity (Oka *et al.*, 2010).

#### **1.5.2.2 PPARs**

The peroxisome proliferator-activated receptors (PPARs) belong to a family of nuclear receptors. Three PPAR isoforms are known to date:  $\alpha$ ,  $\beta/\delta$  and  $\gamma$  which have different expression patterns (Wahli *et al.*, 2012). PPAR  $\alpha$  is predominantly expressed in tissues catabolising a high volume of fatty acids, such as liver, heart and kidney (Wahli *et al.*, 2012; O'Sullivan *et al.*, 2010). PPAR  $\beta/\delta$  displays the broadest expression pattern with levels in certain tissues determined by cell proliferation and differentiation (Michalik *et al.*, 2006). PPAR  $\beta/\delta$  is found in the skin, gut, adipose tissue, brain, skeletal and heart muscle amongst others (Wahli *et al.*, 2012). PPAR $\gamma$  has two splice variants;  $\gamma 1$  is found in the brain, vascular, immune and inflammatory cells.  $\gamma 2$  is expressed predominantly in adipose tissue (Berger and Moller, 2002; Michalik *et al.*, 2006). PPARs mediate a wide variety of biological processes such as regulation of lipid metabolism, inflammation, energy homeostasis and cell differentiation (O'Sullivan, 2009).

There are several studies reporting that PPARs can be activated by cannabinoids; Kozak and his colleagues (2002) found the first evidence of interaction between PPAR  $\alpha$  and cannabinoids by demonstrating increasing transcriptional activity of PPARs from stimulation by the endogenous cannabinoids 2-AG and OEA in concentrations of 0.1-10 $\mu$ M. Furthermore, Rockwell and Kaminski, (2004) found that AEA inhibited pro-inflammatory cytokines and this

was reversed by PPAR $\gamma$  antagonists. Other cannabinoids which activate the transcriptional activity of PPAR $\gamma$  include WIN55212-2, CP-55,940, cannabidiol (1–20  $\mu$ M) and HU-210 (100 nM) (O’Sullivan *et al.*, 2006). Studies focused on the cannabinoid mechanism of stimulation of PPARs, Yano *et al.* (2007) reported that cannabinoids activate the receptors at the cell surface, initiating intracellular signaling that may lead to PPAR activation, whereas another possibility demonstrated by Rockwell and Kaminski, (2004) might be that metabolites of cannabinoids are the active ligands of PPARs. O’Sullivan *et al.* (2005) identified that THC caused slowly developing vasorelaxation through activation of PPAR $\gamma$  dependent on the generation of hydrogen peroxide (H<sub>2</sub>O<sub>2</sub>), NO production and superoxide dismutase (SOD) activity (Kozak *et al.*, 2002; O’Sullivan *et al.*, 2005).

### **1.5.2.3 Transient receptor potential channels**

Transient receptor potential channels type V1 (TRPV1 or vanilloid receptors) are ligand-gated ion channels that have a role in cannabinoid functions. TRPV1 are non-selective cation channels activated by both chemical (e.g. capsaicin, the active component of chili peppers) and physical (noxious heat and low pH) stimuli (Battista *et al.* 2012; De Petrocellis *et al.* 2010). They are not only found on sensory neurons, partly co-expressed with CB<sub>1</sub> receptors (Ahluwalia *et al.*, 2000), but are also found in several central nuclei including those in the hypothalamus and basal ganglia, hippocampus, cerebellum and striatum (Cristino *et al.*, 2006).

Di Marzo (1998) found that anandamide, which has some chemical similarities to capsaicin, activates the channel resulting in vasodilator

effects, production of pro-apoptotic kinases in neuronal and immune cells, increased mitochondrial uncoupling, release of cytochrome c and increased intracellular  $\text{Ca}^{2+}$ ,  $[\text{Ca}^{2+}]_i$ . The sensitivity to anandamide led to the proposal that TRPV1 may be considered to be a cannabinoid receptor (Ross, 2003; Battista *et al.*, 2012).

The transient receptor potential channel type V2 (TRPV2) protein, also known as vanilloid receptor-like 1 (VRL-1), is distributed in medium- to large-diameter  $\text{A}\beta$  mechanosensitive and thermosensitive sensory neurons in the rat dorsal root ganglion (DRG) (Caterina *et al.*, 1999), the trigeminal ganglion (Ichikawa and Sugimoto, 2000), and the spinal cord (Lewinter *et al.*, 2004). Moreover, TRPV2 is upregulated in rat DRG after nerve injury (Frederick *et al.*, 2007) and inflammation (Shimosato *et al.*, 2005). TRPV2 receptors can be activated by noxious heat, (with an activation threshold  $>52^\circ\text{C}$ ), swelling, and 2-aminoethoxydiphenylborate (Caterina *et al.*, 1999; Muraki *et al.*, 2003). The activation of this receptor leads to translocation of the protein from an intracellular compartment to the plasma membrane as result of stimulation by insulin-like growth factor-1, PDGF, or the neuropeptide (Boels *et al.*, 2001) and PI3-kinase signalling pathways (Penna *et al.*, 2006).

## **1.6 Cannabinoid receptor ligands**

### **1.6.1 General information**

For thousands of years, preparations of the marijuana plant *Cannabis sativa* (e.g. hashish) have been known to interact with the human body on many levels. In 1964, identification of the chemical structure of the principal psychoactive compound of marijuana,  $\Delta^9$  –

tetrahydrocannabinol ( $\Delta^9$ -THC), by Gaoni and Mechoulam was made. It was previously thought that the effects of this and other highly lipophilic cannabinoid compounds were due to non-specific membrane perturbation but the radioligand binding studies of Devane *et al.*, (1988) clearly indicated the presence of a receptor protein in the plasma membrane that recognized cannabinoid ligands.

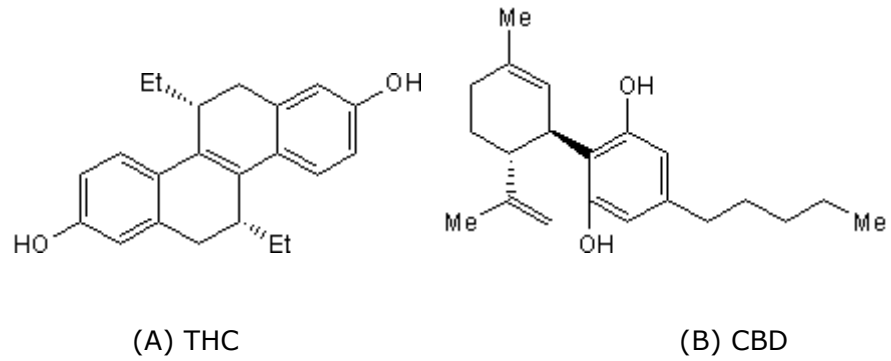
Since the discovery and elucidation of the chemical structure of  $\Delta^9$ -THC, many highly affinity, selective and non-selective cannabinoid receptor ligands have been synthesised and evaluated in animal models and in cell lines. This classification of cannabinoid receptor ligands is done according to their chemical classes and pharmacological activity. This has encouraged the classification of cannabinoids into five chemical groups; classical, non-classical, aminoalkylindol, eicosanoid and diarylpyrazole (Pertwee, 1997; Huffman, 2005; Pertwee, 2006).

### **1.6.2 Classical cannabinoids**

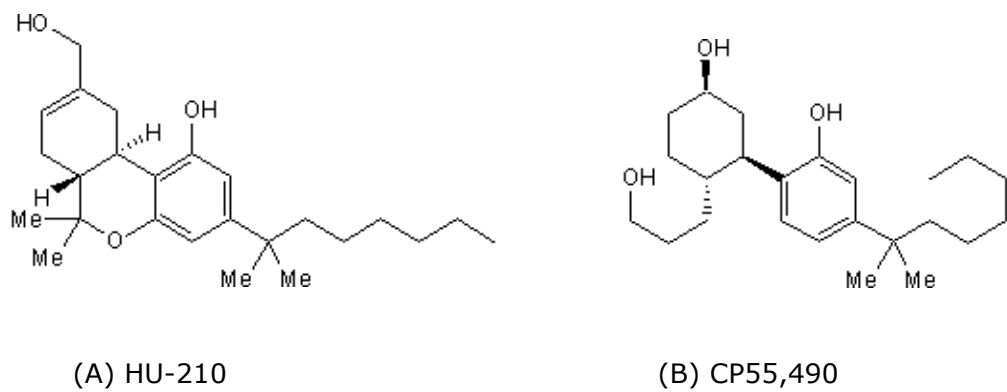
This group is represented by plant-derived cannabinoids (e.g.  $\Delta^9$ -THC, ( $\Delta^8$ -THC) Figure 1.3 A), cannabinol (CBN), cannabidiol (CBD) Figure 1.3 B], (low affinity for CB<sub>1</sub> as well as for CB<sub>2</sub>) (Sharir and Abood, 2010). In recent years, other phytocannabinoids have been isolated and characterized (see below).

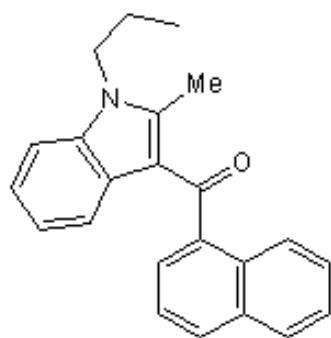
Phytocannabinoids are synthesised in the cannabis plant by glandular trichomes as carboxylic acids from geranyl pyrophosphate and olivetolic acid to yield the parent phytocannabinoid compound, cannabigerolic acid (CBGA). Subsequent reactions involving different enzymes catalyze the transformation of CBGA into other

phytocannabinoids. The presence of these enzymes differs between various strains and species of cannabis, resulting in a different content of phytocannabinoids (Russo, 2007).

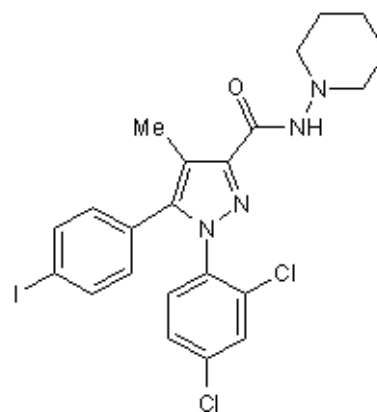


**Figure 1. 3:** structures of phytocannabinoids THC and CBD.





(D) JWH 015



(E) AM 251

**Figure 1.4:** Structures of synthetic cannabinoids HU210, CP55,940, JWH015 and AM251.

Further phytocannabinoids include CBDV (cannabidivarin), CBDVA (cannabidivarinic acid), CBC (cannabichromene), CBG (cannabigerol), CBGV (cannabigerovarin), CBN (cannabinol), CBNV (cannabinovarin), THCA (tetrahydrocannabinolic acid) THCV (tetrahydrocannabivarin), and CBDA (cannabidiolic acid) (Gaoni and Mechoulam, 1966; Vollner *et al.*, 1969; Gill *et al.*, 1970).

Synthetic analogs such as HU-210 and CP-55940 (Figure 1.4 A) have high affinity for CB<sub>1</sub> and CB<sub>2</sub> receptors and JWH-133, L-759633 and L-759656 are CB<sub>2</sub> selective agonists, the main part of their structure contains a dibenzopyran ring (Kapur *et al.*, 2009; Felder *et al.*, 1995; Pertwee, 1997).

### 1.6.2.1 Cannabidiol (CBD)

The phytocannabinoid cannabidiol (CBD) is a non-psychoactive substance (Ross *et al.*, 2008) and is one of the major constituents, forming up to 40% of *Cannabis sativa* (marijuana) extract (Mechoulam *et al.*, 2002). The action of CBD could involve other

cannabinoid receptors including an abnormal cannabidiol receptor, a non-CB<sub>1</sub> and non-CB<sub>2</sub> receptor (Franklin *et al.*, 2003) and it was proposed to be a GPR55 receptor ligand; either an antagonist or agonist depending on the authors reporting the data (Oka *et al.*, 2007; Ryberg *et al.*, 2007). Recent reports showed that CBD exerted analgesic effects and it is suggested that the analgesic effect of CBD is mediated, at least in part, by TRPV1 (McHugh *et al.*, 2008). CBD has also been found to activate TRPV2 ion channels and to produce TRPV2-mediated elevation of [Ca<sup>2+</sup>]<sub>i</sub> and to cause the release of CGRP from sensory neurons (Bisogno *et al.*, 2001; Qin *et al.*, 2008).

Furthermore, CBD inhibits serotonin reuptake and increases catecholamine activity in rat brain synaptosomes. It has been reported to activate serotonin (5-HT<sub>1A</sub>) receptors which might be involved in its proposed antidepressant, anxiolytic, and neuroprotective properties (Russo *et al.*, 2005; Zanelati *et al.* 2009; Resstel *et al.*, 2009; Mishima *et al.* 2005). It also inhibits adenosine uptake (Russo *et al.*, 2005; Carrier *et al.*, 2006) and can antagonise the psychotropic effects of Δ<sup>9</sup>-THC. However, CBD displays all of these effects only at micromolar concentrations (Russo *et al.* 2005) and the molecular mechanisms underlying the effects are still unclear (Petit *et al.*, 1998).

CBD is suggested to produce different pharmacological effects including anti-inflammatory, anticonvulsant, hypnotic, anxiolytic, and antipsychotic effects via GPR55, whereas it has no activity at CB<sub>1</sub> and CB<sub>2</sub> receptors. Furthermore, CBD inhibits anandamide degradation and transport and was suggested to possess antioxidant capacities and neuroprotective actions (Mechoulam *et al.*, 2002; Malfait *et al.*, 2000; Carlini *et al.*, 1981) and CBD was reported to protect from

brain damage in gerbils caused by cerebral ischaemia (Braidia *et al.*, 2003).

Cannabidiol has also been shown to inhibit cancer cell growth, albeit with low potency. Although the inhibitory mechanism is not yet fully understood, Ligresti *et al.* (2006) suggested that CBD exerts its effects on these cells through multiple mechanisms that include either direct or indirect activation of CB<sub>2</sub> and TRPV1 receptors, and induction of oxidative stress, all contributing to induce apoptosis. CBD has the ability to induce apoptosis in cultures of human HL-60 myeloblastic leukaemia cells and human U87 and U373 glioma cells (Gallily *et al.*, 2003) and recent reports have shown promise for controlling the spread of metastatic breast cancer by down-regulating the activity of the gene ID1 which is responsible for tumor metastasis (McAllister *et al.*, 2007).

Ryan *et al.*, (2009) have found that CBD protect human neuroblastoma cell lines (SH-SY5Y) against mitochondrial toxins (FCCP, a mitochondria uncoupler), oligomycin and hydrogen peroxide, moreover CBD may prove beneficial in preventing apoptotic signalling via a restoration of Ca<sup>2+</sup> homeostasis.

### **1.6.3 Non classical cannabinoids**

The group of bicyclic and tricyclic analogs of Δ<sup>9</sup>-THC lacking a pyran ring was developed by Pfizer (Groton, CT, USA). It includes CP-55,940 (Figure 1.4 B), a high affinity cannabinoid receptor agonist with a similar affinity for CB<sub>1</sub> and CB<sub>2</sub> receptors. When radiolabelled, it is an important tool in determining the activity of compounds at the cannabinoid receptors and was used by Devane *et al.* (1988) to

characterize the CB<sub>1</sub> receptor. More recently synthesized compounds in this class are CP47497, CP55244 and HU-308 which have a higher affinity for CB<sub>2</sub> than CB<sub>1</sub> receptors (Felder *et al.*, 1995).

#### **1.6.4 Aminoalkylindoles (hybrid cannabinoids)**

These compounds differ structurally from the members of the first two groups and were developed by Sterling Winthrop (Collegeville, PA, USA). WIN55212-2 is the most widely investigated aminoalkylindole and it is high affinity agonist for CB<sub>1</sub> and CB<sub>2</sub> with a slight selectivity towards CB<sub>2</sub> receptors (Felder *et al.*, 1995). Since the synthesis of these aminoalkylindoles, several others have been developed, such as the CB<sub>2</sub>-selective ligands L768242 (GW405833) and JWH015 (Gallant *et al.*, 1996; Howlett *et al.*, 2002).

#### **1.6.5 Eicosanoids**

The arachidonate-containing compounds in this class are the endocannabinoids, (discussed in section 1.8) but it also includes noladin ether, oleamide, virodhamine (VIR) and synthetic analogues of AEA, such as methanandamide, arachidonyl-2'-chloroethylamide (ACEA), arachidonylcyclo-propylamide (ACPA), 2-methylarachidonoyl-(2-fluoroethyl)-amide (O-689) (potent CB<sub>1</sub> agonists) and O-1812. Methanandamide (more potent at CB<sub>2</sub> receptors) and O-1812 are more resistant to enzymatic hydrolysis than AEA, ACEA and ACPA (Hillard *et al.*, 1999).

#### **1.6.6 Diarylpyrazoles**

The best characterized CB receptor antagonist is SR141716 (rimonabant) discovered by Sanofi (Paris, France) which has high

selectivity for the CB<sub>1</sub> receptor. It is an antagonist with nanomolar affinity for the CB<sub>1</sub> and micromolar affinity for CB<sub>2</sub> receptor, but it has been widely reported to have inverse agonist properties at CB<sub>1</sub> (Huestis *et al.*, 2001). Other CB<sub>1</sub> selective antagonists include LY 320135, AM 251 (Figure 1.4 D) and AM 281; the latter two are synthetic analogues of SR141716. AM 251 also acts as a GPR55 agonist. Selective CB<sub>2</sub> antagonists/inverse agonists include SR144528 and AM 630 (both having much higher affinity towards CB<sub>2</sub> than to CB<sub>1</sub> receptors) (Pertwee, 2005; Rinaldi-Carmona *et al.*, 1994; Kapur *et al.*, 2009; Barth and Rinaldi-Carmona, 1999).

### **1.7 Allosteric modulators**

In addition to the presence of the orthosteric (primary) binding site on the cannabinoid receptors with which agonists, antagonists and inverse agonists interact, studies have recently found evidence for an allosteric binding site on the CB<sub>1</sub> receptor through which certain drugs interact and cause a conformational change in the receptor structure, modifying the affinity and/or intrinsic effectiveness of cannabinoids acting at the orthosteric binding site (Price *et al.*, 2005; Ross, 2007). Recent reports suggest that CBD is a positive allosteric modulator at low micromolar concentrations for both strychnine-sensitive  $\alpha_1$  and  $\alpha_1\beta$  glycine receptors (Ahrens *et al.*, 2009). 2AG is reported to be an allosteric modulator at other receptors such as the hA3 adenosine receptor (Lane *et al.*, 2009).

### **1.8 Endogenous cannabinoids**

The cloning of the cannabinoid receptors led to a search for endogenous cannabinoid receptor agonists (Pertwee, 2008). Several

fatty acid ligands of cannabinoid receptors (known as endocannabinoids) have been identified, of which *N*-arachidonoyl ethanolamine (anandamide) and 2-arachidonoylglycerol (2-AG) are the best characterized (Pertwee *et al.*, 2010). Endocannabinoids synthesis and release are thought to be in response to elevation of intracellular calcium concentrations and, in contrast to many other neurotransmitters, AEA and 2-AG are not stored in vesicles but they are widely believed to be released on "demand" when and where they are needed (Piomelli *et al.*, 2000) in response to cellular depolarization and influx of  $\text{Ca}^{2+}$  to act on cannabinoid receptors present in the cells surrounding the region of production to operate as neuromodulators and immunomodulators (Stella *et al.*, 1997; Giuffrida *et al.*, 2000). However, Sarmad *et al.*, (2011) produced data which suggest that the dogma of calcium-driven endocannabinoid synthesis, at least in complex tissues, might not be universally true.

One of the most well known functions of endocannabinoids is their role as retrograde messengers (Kano *et al.*, 2009). Endocannabinoids released from the post-synaptic neurons traverse the synaptic cleft and bind to pre-synaptic  $\text{CB}_1$  receptors reducing  $\text{Ca}^{2+}$  and potassium ( $\text{K}^+$ ) conductance ultimately decreasing release of neurotransmitter (Ohno-Shosaku *et al.*, 2001). The membrane phospholipid *N*-arachidonoyl phosphatidyl ethanolamine (NAPE) is the precursor for anandamide, whose formation is catalysed by *N*-arachidonoyl phosphatidyl ethanolamine-selective phospholipase D (NAPE-PLD) whereas; 2-AG synthesis is derived from diacylglycerols catalysed by diacylglycerol lipase (DGL) (Stella and Piomelli, 2001). The levels of 2-AG in the brain are 170 times more than anandamide

and both are similar in their binding affinity for cannabinoid receptors (Mechoulam *et al.*, 1995; Stella *et al.*, 1997; Sugiura *et al.*, 1996).

Anandamide expresses typical pharmacological and biochemical effects of cannabinoid agonists at CB<sub>1</sub> and CB<sub>2</sub> receptors (Stella, 2009) and inhibits adenylyl cyclase by binding to both receptors. The main mechanisms involved in termination of endocannabinoid signalling are transport across membranes into cells, intracellular hydrolysis and oxygenation (Mackie and Stella, 2006).

Following cellular uptake, endocannabinoids are degraded by intracellular enzymes. Anandamide is predominately metabolised by fatty acid amide hydrolase (FAAH) (Cravatt *et al.*, 2001; Kaczocha, 2009) and also by N-Acylethanolamine-hydrolyzing Acid Amidase (NAAA), cyclooxygenase-2, lipoxygenase and some cytochromes P450. Whereas 2-AG is degraded by Monoacylglycerol Lipase (MGL) and also by FAAH (Cravatt *et al.*, 2001). Furthermore, palmitoylethanolamide (PEA) and other fatty acid amides are also metabolized by fatty acid amide hydrolase (FAAH) and N-acylethanolamine-hydrolyzing acid amidase (NAAA), the latter has more specificity toward PEA than other fatty acid amides (Tsuboi *et al.*, 2007) as shown in Figure 1.5. Whilst PEA interacts with PPAR- $\alpha$  receptors and/or an unknown G<sub>i/o</sub> protein-coupled receptor (Muccioli and Stella, 2008), it also appears to enhance the activation by AEA of cannabinoid receptors and TRPV1 channels (Petrosino *et al.*, 2009).

There are also other endocannabinoid-like agents including *N*-dihomo- $\alpha$ -linolenylethanolamine, *N*-docosatetraenylethanolamine, oleamide, *N*-arachidonoyl dopamine, *N*-oleoyl dopamine, oleylethanolamide (OEA) and virodhamine which

have little or no affinity for CB receptors but can modify cannabinoid function possibly via entourage effects (Pertwee, 2009).

Microglia, which play an important role in modulating nociceptive responses, are capable of synthesising and catabolising endocannabinoids (Franklin *et al.*, 2003, Guasti *et al.*, 2009). Microglia, which play an important role in modulating nociceptive responses, are capable of synthesising and catabolising endocannabinoids (Franklin *et al.*, 2003, Guasti *et al.*, 2009). Recently, it has been demonstrated that mouse microglia produce a number of putative endocannabinoids (Walter *et al.*, 2003). Carrier *et al.*, 2004 have found that cultured microglial cells produce the endocannabinoid 2-arachidonoylglycerol (2-AG) as well as anandamide in smaller quantities.

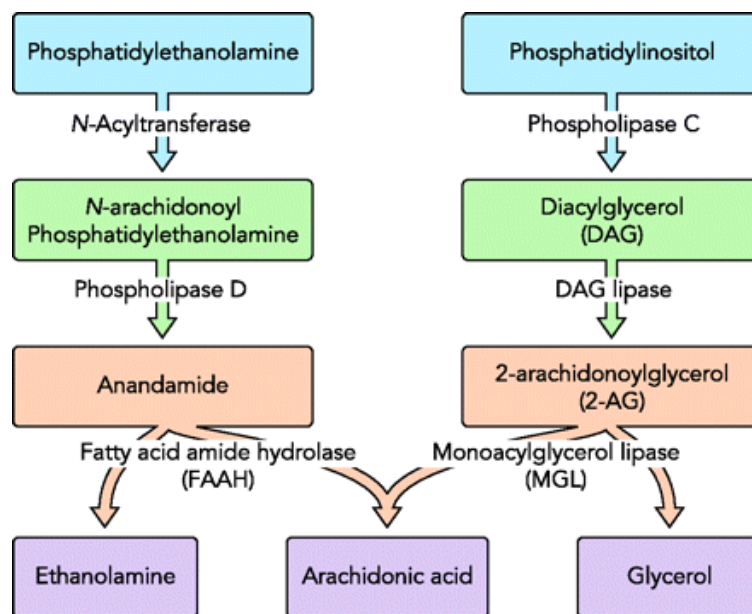


**Figure 1.5:** Diagrammatic representation of the Main pathways of synthesis and degradation of the endocannabinoids anandamide and 2-arachidonoylglycerol (2-AG) adapted from El Manira and Kyriakatos (2010).

## 1.9 Cannabinoids and Neuroinflammation

Since the 1970s, a few studies have suggested that marijuana use was associated with an increased incidence of viral infection and found that cannabinoids suppressed immune resistance to such microbes as Friend leukemia virus, herpes simplex viruses (HSV), *Acanthamoeba*, *Listeria monocytogenes*, *Staphylococcus albus*, *Treponema pallidum* and *Legionella pneumophila* (Cabral and Staab, 2005; Morahan *et al.*, 1979; Juel-Jensen, 1972; Cabral and Dove-Pettit, 1998; Marciano-Cabral *et al.*, 2001, Newton *et al.*, 1994; Klein *et al.*, 1998).

Proteins which are up-regulated in neurological diseases characterized by an inflammatory component have been found to activate microglia *in vitro*. These include components of the blood such as albumin (Hooper *et al.*, 2009) and thrombin (Choi *et al.*, 2003) which may be encountered at elevated concentrations by microglia following BBB damage. In addition, proteins present in the lesions characteristic of particular neurodegenerative diseases such as amyloid beta plaques, intracellular neurofibrillary tangles (NFTs) and prion proteins in spongiform encephalopathies (Fabriz *et al.*, 2001) are associated with activated microglial and astrocytes (Campbell and Gowran., 2007; Meda *et al.*, 1995; Ramírez *et al.*, 2005).

However, activated microglia have been cited as a direct cause of, or a contributor to, the progress of chronic neurodegenerative diseases that are characterized pathologically by an atypical production of pro-inflammatory factors. Microglia *in vivo* tend to become progressively more activated with age (Streit *et al.*, 1999); indeed an age-related microglia dystrophy have been reported in human brain (Streit *et al.*,

2004) and microglia are activated after traumatic brain injury (d'Avila *et al.*, 2012).

Release of pro-inflammatory and other neurotoxic factors from other cells in the CNS, such as astrocytes and perivascular macrophages, and from peripheral immune cells that have penetrated the BBB, contribute towards the pathology of neurodegenerative and neuroinflammatory diseases (Perry, 2004).

Exogenous cannabinoids have been shown to suppress both cell-mediated and humoral immune responses in a variety of immune cells.  $\Delta^9$ -THC suppressed the antibody response of B-cells (Carayon *et al.*, 1998; Kaminski *et al.*, 1994), and diminished B and T cell proliferation in response to cell-specific mitogens (Carayon *et al.*, 1998; Derocq *et al.*, 1995). Both  $\Delta^9$ -THC and CP-55,940 prevented macrophage cell contact-dependent cytolysis of tumor cells by macrophages and macrophage-like cells, to inhibit the processing of antigens by macrophages and to suppress proliferation of B lymphocytes (Wang *et al.*, 1991; McCoy *et al.*, 1999), while  $\Delta^9$ -THC suppresses the cell-killing activity of natural killer cells (Wang *et al.*, 1991). Moreover,  $\Delta^9$ -THC and CP-55,940 have been found to affect chemotaxis of immune cells to sites of infection and/or injury (Sacerdote *et al.*, 2000). This modulatory effect was investigated in a mouse model of granulomatous amoebic encephalitis (GAE), where migration to the site of infection was decreased in  $\Delta^9$ -THC-exposed macrophages and macrophage-like cells (Marciano-Cabral *et al.*, 2001; Cabral and Marciano-Cabral, 2005).

There is a suggestion that, via their interactions with cannabinoid receptors, the immune modulatory effects of cannabinoids are down-

stream consequences of the inhibition of adenylyl cyclase activity by a pertussis toxin-sensitive G protein-coupled mechanism (Kaminski *et al.*, 1992; Kaminski., 1996). A significant downstream effect of cannabinoid signaling is the modulation of gene expression of pro-inflammatory mediators.  $\Delta^9$ -THC has been shown to inhibit pro-inflammatory cytokine (IL-1 $\alpha$ , IL-1 $\beta$ , IL-6 and TNF- $\alpha$ ) mRNA expression, as well as to ablate TNF- $\alpha$  release (Fernandez-Ruiz *et al.*, 2007; Facchinetti *et al.*, 2003).

There is growing evidence that cannabinoids could be developed as therapeutic agents in neurological diseases, by attenuation of pro-inflammatory factors from infiltrated peripheral immunocytes. Cannabinoids easily penetrate the blood brain barrier (BBB) and are not toxic to the brain (Cabral and Griffin-Thomas., 2008). Because cannabinoids can inhibit expression of pro-inflammatory mediators, and improve blood supply to injured brain, as a result of inhibiting endothelium-derived mediators, they have therapeutic potential for neuropathies characterized by chronic formation of pro-inflammatory factors (Chen *et al.*, 2000).

The therapeutic benefits of cannabinoids have been investigated both *in vitro* and *in vivo* models of multiple sclerosis (MS), Alzheimer's disease (AD), HIV encephalitis (HIVE), amyotrophic lateral sclerosis (ALS), closed head injury (CHI) and granulomatous amoebic encephalitis (GAE) (Cabral and Griffin-Thomas., 2008; Ramírez *et al.*, 2005). Benefit has also been shown in Parkinson's disease and Huntington's disease (Tanveer *et al.*, 2012). This potential is largely based on the antioxidant, anti-inflammatory and anti-excitotoxic properties exhibited by these compounds that allow them to afford

neuroprotection in different neurodegenerative disorders (de Lago and Fernández-Ruiz, 2007).

AD is a very common neurodegenerative disorder that leads to senile dementia as result of deposit beta-amyloid protein ( $\beta$ -A) (Mattiace et al., 1990). MS is a chronic inflammatory disease that is characterized by T-cell mediated demyelination of axonal myelin sheaths that protect axons. MS patients suffer from cognitive impairment, muscle weakness, and impaired coordination, balance, speech and sight (Mitrovic et al., 1994). HIVE, also known as Acquired Immune Deficiency Syndrome (AIDS)-dementia complex, is a neuroinflammatory disorder caused by the production of pro-inflammatory cytokines and neurotoxins, including glutamate and reaction oxygen species (ROS), produced by HIV-infected monocytes and microglia (Soontornniyomkij et al., 1998).

PD is a neurodegenerative disease characterized by the selective loss of dopaminergic neurons in the substantia nigra pars compacta and deposition of  $\alpha$ -synuclein aggregates in nigral neurons (Hirsch et al., 2012; Nakajima and Kohsaka, 2004). In the neuroinflammatory diseases described above, there is a failure to maintain the immunological and overall homeostatic balance within the brain, and activated microglia and astrocytes play a vital role in this imbalance (Nakajima and Kohsaka, 2004).

Recent reports have found that CB<sub>1</sub> receptor activation by HU-210 and WIN55212-2 protects against mutant Huntingtin-induced cell death (Scotter et al., 2010) and Sagredo et al., (2012) suggested that the ability of cannabinoids to improve the symptoms of Huntington's disease is due to their anti-inflammatory,

neuroprotective and neuroregenerative properties. Treatment with the synthetic cannabinoid agonists WIN55,212-2 and HU-210 improved motor function in Theiler's murine encephalomyelitis virus (TMEV)-infected mice (Croxford and Miller, 2003; Arevalo-Martin *et al.*, 2003), a model of chronic demyelinating disease that resembles MS. These same cannabinoid agonists were shown to prevent microglial activation and cognitive impairment in AD based on examination of brain samples and primary microglial function (Ramirez *et al.*, 2005). Thus, by using cannabinoid receptors as molecular targets, it might be possible to improve the various neuropathological processes associated with chronic brain inflammation (Croxford and Yamamura, 2005).

## **1.10 Models used in microglial function**

### **1.10.1 Primary microglial cells**

Perhaps the most appropriate *in vitro* model used for gaining insight into the biology of microglia is that of brain microglia in primary cell culture. However, it is time-consuming and technically difficult to prepare almost pure primary microglial cultures in sufficient quantities for study and the cells cannot be kept in culture for prolonged periods of time (Tamashiro *et al.*, 2012). Immortalized microglial cell lines have been generated and characterized to avoid some of these challenges (Cheepsunthorn *et al.*, 2001).

### **1.10.2 BV-2 cells**

BV-2 cells (a murine microglial cell) were generated by immortalizing primary mouse microglia. These cells possess functional and phenotypic properties common to primary microglial, including

phagocytic ability, secretion of pro-inflammatory cytokines and expression of surface receptors and antigens. These cells have been used extensively as *in vitro* models to study microglial function, immune responses and the role of microglia in neurodegenerative diseases. BV-2 cells have been shown to become activated upon exposure to IFN- $\gamma$  (Han *et al.*, 2002; Han *et al.*, 2002; Hwang *et al.*, 2004) and LPS (Blasi *et al.*, 1990; Kim *et al.*, 2004) and they have been employed to study the effects of anti-inflammatory agents on pro-inflammatory cytokine and iNOS gene expression (Kim *et al.*, 2004; Han *et al.*, 2002), and to study the expression profiles of chemokines and chemokine receptors upon microglial activation (Kremlev *et al.*, 2004).

### **1.10.3 HAPI cells**

Highly aggressive proliferating cell type [HAPI] cells were derived from primary microglia-enriched cultures. This rat cell line retains phenotypic and morphological characteristic of activated microglia. Thus, HAPI cells offer a model of activated primary microglial cells and are the only available model of rat-derived microglial cells (Cheepsunthorn *et al.*, 2001).

## **1.2 Aim and Objectives**

The main aim of this project is to determine the role of cannabinoids in modulation of microglial cell function using *in vitro* approaches, and to investigate the molecular mechanisms underlying such modulation.

First, the aim of this study was to examine the potential effects and mechanisms of action of cannabidiol and related phytocannabinoids

on the function of microglial cells (nitric oxide formation as indicator for microglia activation) *in vitro*.

Second, to evaluate the effects of phytocannabinoids on microglial migration and phagocytosis and to gain insight into the mechanisms of drug action.

It is hoped that the findings will address the potential of cannabinoids to be therapeutic agents for neuroinflammatory diseases that are pathologically hallmarked by a chronic elevation of pro-inflammatory mediators and microglial activation.

## 2. 1 Introduction

Microglia are considered to be the resident macrophages of the central nervous system (CNS). Chronic activation of microglia is characterized by proliferation, migration to the site of injury, altered morphology and cell surface marker changes (Kim and Joh, 2006). Microglial activation has protective functions in the destruction of pathogens, neoplastic cells, removal of debris and accelerated tissue repair, and release of neurotrophic factors (Hanisch and Kettenmann, 2007).

However, excessive activation can be damaging and can exacerbate the effects of inflammation leading to neurodegenerative disease e.g. as seen in AIDs dementia and Alzheimer's disease (Banati *et al.*, 1993). Activated microglia may act as intrinsic brain phagocytes or by secretion of neurotoxins such as TNF- $\alpha$  (Banati *et al.*, 1998), nitric oxide (NO), proteinases, reactive nitrogen species, plasminogen activator and cytokines, for instance IL-1, and other factors which could cause neuronal injury (Gehrmann *et al.*, 1995; Waksman *et al.*, 1999; Izzo *et al.*, 2009). Activated microglia and astrocytes are thought to be the main sources for reactive oxygen and nitrogen species within the CNS (Hanisch and Kettenmann, 2007).

Activated microglia synthesize, release and/or up-regulate a plethora of mediators including cytokines, chemokines and prostaglandin E<sub>2</sub> (PGE<sub>2</sub>) (Ryu *et al.*, 2000; Barger *et al.*, 2007; Wang *et al.*, 2008; Rock *et al.* 2004) while both iNOS (Ryu *et al.*, 2000, Barger *et al.*, 2007, Wang *et al.*, 2008), and COX-2 (Akundi *et al.*, 2005) are enzymes up-regulated by inflammatory stimuli.

Brain microglial cells release substantial amounts of the radical nitric oxide (NO) (Weinstein *et al.*, 2008, Kawahara *et al.*, 2009). Although NO has protective activity in the central nervous system, excessive release has been found to cause brain injury and to mediate neurodegenerative inflammatory processes (Boje *et al.*, 1992; Martinez-Orgado *et al.*, 2012). Under normal conditions, the release of NO from microglial cells is insignificant, but when it is released in abundance, it can pass from the cell of origin into surrounding tissue to act on other cells because it is small and without charge (Brown, 1997).

There are three isoforms of nitric oxide synthase (NOS) that have been cloned, two of which are constitutively active; endothelial NOS (eNOS) and neuronal NOS (nNOS). These are responsible for the production of transient low level bursts of NO and both are calcium/calmodulin-dependent (Kone *et al.*, 2003). The third type is inducible by inflammatory stimuli, such as endotoxin, cytokines and oxidative stress, but not calcium; its expression is induced in many cell types including macrophages (Brown, 1997). An accumulation of reports have indicated that cannabinoids may modulate formation of inflammatory factors, such as NO, released by activated brain microglial cells. One of the earliest links between cannabinoids and NO (Stefano *et al.*, 1996, Stefano *et al.*, 1997) showed that anandamide (AEA) and the CB<sub>1</sub>/CB<sub>2</sub> receptor agonist CP55940 initiated the release of NO in a concentration-dependent manner from invertebrate microglia.

Cannabinoids have been found to alter the functional activity of macrophages and macrophage-like cells (Makriyannis *et al.*, 1990; Friedman *et al.*, 1986) and have been suggested as potential future treatments for different types of neurodegenerative disease (Klein and Newton, 2007), especially those compounds that lack psychoactive effects,

such as cannabidiol (CBD). The anti-inflammatory and immunosuppressive properties of cannabinoids have been reported to modulate the host immunity response against infections (Klein *et al.*, 1998). However, the mechanisms underlying these actions are not fully understood.

CBD exerts a wide variety of anti-inflammatory properties and regulates cell cycle and function of various immune cells. These effects include inhibition of humoral responses such as release of cytokines, chemokines and growth factors. For example, CBD decreases the activity of the NF- $\kappa$ B pathway, up-regulates the activation of STAT3 and reduces the activation of LPS-induced STAT1 transcription factors to interfere with inflammatory pathways in LPS-treated BV-2 microglial cells (Kozela *et al.*, 2010). CBD is reported to up-regulate the transcription of nuclear factor-erythroid 2 (Nrf2), which is responsible for regulation of protective antioxidant and detoxification activities (Juknat *et al.*, 2012).

Cannabinoid compounds produce their biological effects by acting through at least three G protein-coupled cannabinoid receptors. These include CB<sub>1</sub> and CB<sub>2</sub> receptors that are reported to be expressed in activated microglial cells (Walter *et al.*, 2003) and the abnormal-cannabidiol-sensitive receptors (abn-CBD receptors) (Ja'rai *et al.*, 1999). Alternatively, cannabinoids including CBD could act through the orphan GPCR GPR55 (Staton, *et al.*, 2008). Pietr *et al.*, (2009) have reported the expression of GPR55 mRNA in mouse primary microglial cultures and the BV-2 cell line. Following its identification in 1998, two patents from GlaxoSmithKline, in 2001, and AstraZeneca, in 2004, suggested that GPR55 represents a novel cannabinoid receptor in spite of having only 13.5% and 14.5% sequence homology to CB<sub>1</sub> and CB<sub>2</sub> receptors, respectively (Kreitzer and Stella, 2009).

The orphan receptor GPR55 has been suggested to be an additional member (non-CB<sub>1</sub>/CB<sub>2</sub> receptor) of the cannabinoid receptor family based largely on reports indicating that a variety of different cannabinoid ligands interact with it, including antagonism by CBD (Ryberg *et al.*, 2007; Sharir and Abood, 2010). There are, however, significant doubts about its classification as a CB receptor with a lack of agreement between different authors concerning its pharmacological profile (Baker *et al.*, 2006; Pertwee, 2007; Ryberg *et al.*, 2007; Ross, 2009). Putative endocannabinoids such as anandamide and virodhamine are reported to activate GTP-γ-S binding via the GPR55 receptor (Baker *et al.*, 2006).

The suggested physiological roles of GPR55 include pain signalling, and control of vascular tone. Moreover, GPR55 might play a role in lipolysis and immune cell migration (Pertwee, 2007). Recent studies have now implicated GPR55 receptors in the neuroprotective activity of cannabinoids through an anti-inflammatory action (Pietr *et al.*, 2009; Staton *et al.*, 2008).

Studies of mitogen-activated protein kinase (MAPK) phosphorylation in GPR55-expressing cells lead to it being classified as a lysophosphatidylinositol (LPI) receptor (Oka *et al.*, 2007). More recently, LPI acting on GPR55 has been reported to couple to increasing intracellular calcium inducing phosphorylation of P38 MAPK and activating transcription factor 2 (Oka *et al.*, 2009; Oka *et al.*, 2010). On the other hand, various types of lysolipids as well as a number of cannabinoid receptor ligands did not induce phosphorylation of the extracellular signal-regulated kinase in GPR55 receptor-expressing cells (Oka *et al.*, 2007).

Human brain GPR55 mRNA is more predominantly expressed in the caudate nucleus and putamen than the hippocampus, thalamus, pons,

cerebellum and frontal cortex (Sawzdargo *et al.*, 1999), whereas, in rat brain, GPR55 mRNA is highly expressed in hippocampus, thalamic nuclei and regions of the midbrain (Brown, 2007). In mice, the highest levels of GPR55 mRNA were found in adrenal tissue, ileum, frontal cortex and striatum. GPR55 mRNA is also found in spleen and gut in both humans and rodents (Sawzdargo *et al.*, 1999). Furthermore, GPR55 mRNA is found in omental adipose tissue, testis and breast but, it was not detected in subcutaneous fat tissue (Brown, 2007; Sawzdargo *et al.*, 1999).

The GPR55 receptor is implicated in modulation of inflammation via alterations in microglial activity, and their pharmacological treatment might be worthy for delaying the development of neurodegenerative diseases and inflammatory pain. Furthermore, GPR18 is involved in modulation of microglial, endothelial and glioma cell migration (McHugh *et al.*, 2010).

**2.2 The aim** of this study was to examine the potential effects and mechanisms of action of cannabidiol and related phytocannabinoids on the function of microglial cells (nitric oxide formation) *in vitro*.

## **2.3 Material and Methods**

### **2.3.1 Reagents**

The studies performed for this project included the use of phytocannabinoids and synthetic exogenous cannabinoid agonists and antagonists. All cannabinoids were purchased from Tocris Cookson (Bristol, UK) unless otherwise stated. Phytocannabinoids were a gift from GW Pharmaceuticals, (Salisbury, UK), GSK agonist and antagonist provided by Andrew Brown (Investigator in GlaxoSmithKline) and VSN16R (This compound tested by Prof David Baker (Barts and the London School of Medicine and Dentistry)).

All other chemicals used in this work were purchased from Sigma-Aldrich Chemical Company (Poole, UK) or Tocris Bioscience (Bristol, UK). Plant-derived and synthetic cannabinoid ligands were dissolved in ethanol to 10 mM stock solutions except for the GSK agonist/antagonist. Ionomycin was dissolved in 50% DMSO and VSN16R and SNP, in media. All drugs were stored in stock solutions at 10 mM from which serial dilutions were made. Fluo-4-AM and pluronic acid were from Invitrogen (Carlsbad, CA), XAC (Tocris Bioscience, Bristol, UK), 1400W (Ascent Scientific). The maximum ethanol concentration used in this study was 0.01%.

For cell activation, bacterial lipopolysaccharide (LPS) from *Escherichia coli* strain 0127: B8, was purchased from Sigma Aldrich (Poole, Dorset, UK). A stock solution of 1mg/ml was made in complete growth medium and stored at -20°C. Working solutions of 100ng/ml were made from dilution of the stock solution for all experiments.

### **2.3.2 Cell culture conditions**

The effects of cannabinoid drugs on LPS-induced NO generation were determined in BV2 mouse microglial cells (which have been extensively used for the study of microglial activity), in HAPI cells (an aggressively proliferating rat microglial cell line) and primary mouse microglia.

All cell culture was performed under sterile conditions in class II, laminar air flow hoods; cells were generally passaged twice a week at a split ratio of 1:5. Almost confluent (BV-2 75-90%, HAPI cells, 70-80%; with passages number 10-25) cells were seeded into a new 75 mm culture flask. First the medium was removed and cells were washed with 10 ml phosphate-buffered saline (PBS). Approximately 10 ml of a trypsin/EDTA solution 1x (Invitrogen) was added and the flasks was incubated at 37°C

for 3-5 minutes to displace the cells. Trypsinization was inhibited by the addition of 10 ml growth medium. Cells were mixed well by pipetting up and down, and then pelleted by centrifugation (1300 x g, 5 minutes), re-suspended in growth medium and seeded at the appropriate density.

#### **2.3.2.1 Cell counts**

The cell number was determined using a cell chamber haemocytometer.

#### **2.3.2.2 BV-2 cell line**

BV-2 cells, a mouse microglial cell line, (a gift from Prof. Nephi Stella, Washington University, USA) were grown in Dulbecco's Modified Eagle Medium (DMEM) with Ham-F12 obtained sterile from Sigma, supplemented with penicillin (100 U/ml) / streptomycin (100 µg/ml) solution, HEPES (15 mM), NaHCO<sub>3</sub> (5mM), L-glutamine (2 mM) and 10% fetal bovine serum (FBS) which was heat inactivated. All cell culture solutions were stored at 4°C and pre-warmed to 37°C in a water bath prior to use. The cells were grown to 95% confluence in 75cm<sup>2</sup> flasks at 37°C with 5% CO<sub>2</sub> and 95% atmosphere.

#### **2.3.2.3 HAPI cell line**

HAPI cells, an aggressively proliferating rat microglial cell line employed as a model of activated microglia, were a gift from Dr J.R. Connor, (Pennsylvania State University, USA.). Cells were expanded in Dulbecco's Modified Eagle Medium (DMEM) with 5% heat inactivated FBS, L-glutamine (2 mM), penicillin (100 U/ml) / streptomycin (100 µg/ml) solution and maintained in a humidified incubator with 5% CO<sub>2</sub> at 37°C.

#### **2.3.2.4 Primary mouse microglial cultures**

Two male adult 8-10 week old C57bl6 mice were deeply anesthetized with sodium pentobarbital, transcardially perfused with heparinised 1U/ml 0.9% saline and decapitated according to UK Home Office guidelines and the whole spinal cord (C1-S1) was dissected. The brain and spinal cord were put in ice cold Modified Hibernate A media (MHibA) ( trademark of Life Technologies) [20 ml Hibernate A, 0.4 ml B27 supplement, 50 µl 200 mM glutamine and 174 µl 454 mM EGTA].

Meninges were removed and the brain and spinal cord cut into 0.5 mm slices using a McIlwain tissue chopper. The tissue was incubated in MHibA containing (20 ml Hibernate A, 0.4 ml B27 supplement, 50 µl 200 mM glutamine and 174 µl, 454 mM EGTA plus papain 12 mg, Worthington) at 30°C for 30 minutes on shaker. The tissue is allowed to settle for 5 minutes, the media is removed and replaced by 2mls of DFP media (DMEM, glutamax-1, 15% heat inactivated fetal bovine serum and 1% penicillin, streptomycin). The tissue is quickly triturated 3 times using a 1ml pipette, the tissue is allowed to settle for 2 minutes, and the supernatant layer is removed and kept. The trituration process is repeated twice more; this results a total of 6mls of supernatant containing suspended cells. The cell suspension was centrifuged, and the pellet re-suspended in 1 ml of 15% FBS of DMEM (see above for details).

Cell density is adjusted to 80,000 cells/ml. 500µl of the cell suspension is added to the wells, then the cells are incubated at 37°C with 5% CO<sub>2</sub> for between 2 and 24 hours media from the wells was aspirated to remove additional debris and non-adherent cells, and then rinsed once with 500µl warm 15% FBS of DMEM media before finally replaced with another 500µl fresh warm 15% FBS of DMEM. The cells are incubated for a further 4

days. A purity of 99% microglia cells with little or no neuronal or astrocytic contamination can be achieved by this protocol.

Our protocol contains several steps to prevent cellular contamination, which is important when there is a need to study pure microglia alone. Other monocytic lineage cells such as circulating macrophages may be one potential contaminant of microglia cultures (Chan *et al.*, 2007). This contaminant is removed by transcardial perfusion with heparinised saline. Other contaminants include neurones and astrocytes present in the spinal cord. However, under the conditions described in this study, no neurones, and very few astrocytes were observed. One possibility for the high purity obtained may be due to the absence of any substrata, such as poly-L-lysine or laminin which is often used to culture neurones and astrocytes due to their adhesive properties (Wong *et al.*, 2006; Imura *et al.*, 2006). We also suggest the limited astrocytic presence under our conditions may be due, at least in part, to the short time in culture, which reduces the possibility for these cells to proliferate.

### **2.3.3 Nitric oxide (NO) assay**

In the Griess NO assay, BV-2, HAPI and primary mouse microglia cells were used. BV-2 or HAPI cells were plated onto 24 well plates (Costar, UK) at ( $5 \times 10^5$  cells/well) overnight. All cell culture was performed under sterile conditions in a laminar airflow hood. The cells were activated by incubation with bacterial LPS (1 – 4000ng) for 24 hours to choose an appropriate concentration. 100ng LPS was used in most experiments because this concentration did not adversely affect the viability of the cells. Cells were co-incubated with LPS and cannabinoids (over the concentration range 10nM-10 $\mu$ M). For experiments with the intracellular Ca<sup>2+</sup> chelator

BAPTA-AM (10-50 $\mu$ M) and the microglial inhibitor minocycline (1-20 $\mu$ M), cells were exposed to the drug for 1 hour prior to LPS and/or cannabinoids.

NO formation was monitored by measuring nitrite accumulation following the method of Griess (Green *et al.*, 1982). After 24 hours of incubation, 100 $\mu$ l of the cell culture supernatant from each well was collected and an equal volume of Griess reagent (2% sulfanilamide and 0.1% N-naphthylethylenediamine dihydrochloride in 1mM HCL) was added after 10 minutes and the reaction mixture incubated at room temperature. The standard curve for NO formation using a serial dilution of sodium nitrite standard ranging from 6.25  $\mu$ M to 100 $\mu$ M is shown in (Figure 2.1).

The optical density of the samples was determined spectrophotometrically at 540 nm. Results are expressed as the means of 3 separate experiments, each performed in duplicate.

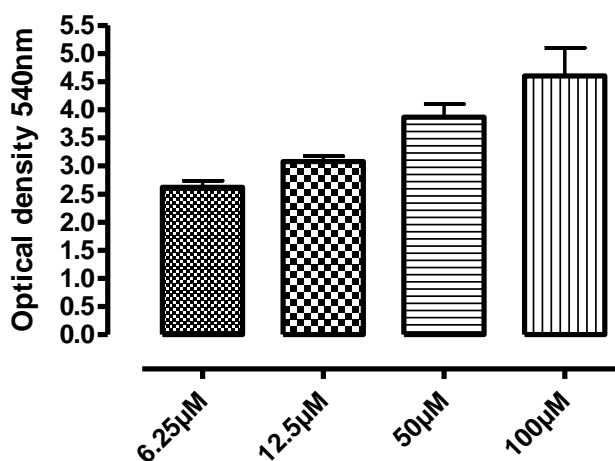


**Figure 2.1:** Sodium nitrite standard curve in BV-2 cell media. Standards were measured using the Griess reaction as described in Methods. The figure represents means of three determinations.

### **2.3.4 Cell viability**

The Neutral Red (NR) cytotoxicity assay procedure is a measure of the ability of viable cells to incorporate and bind to the supravital dye NR in lysosomes. The cells were grown and treated using the same protocols to those used for measuring LPS-induced NO release or the effects of cannabinoids or other drugs. The 24 well plates were incubated for 1 hour with serum-free medium containing NR; the cells were subsequently washed twice with phosphate-buffered saline (PBS), the NR dye was extracted into fixative solution (50% ethanol, 45% water and 5% glacial acetic acid) and incubated for 1 hour. 200µl aliquots of desorbed NR were transferred to a 96 well plate and absorption was read spectrophotometrically at a wavelength of 540 nm.

### **2.3.5 Intracellular $\text{Ca}^{2+}$ ( $[\text{Ca}^{2+}]_i$ ) measurement using the Flexstation**

BV-2 cells were seeded onto black-walled, clear-bottomed, 96-well microtitre plates poly-L-lysine coated at 40,000 cells per well and allowed to proliferate overnight at 37 °C in 5% CO<sub>2</sub> to achieve 95% confluence.

The cells were loaded with 100µl/well of media containing Fluo4-AM (1µM), 10% FCS, 2.5 mM probenecid and incubated in the dark at 37°C for 45mins. Then the cells were washed twice with HEPES buffer saline (HBSS; 25 mM HEPES, 10 mM glucose, 146 mM NaCl, 5 mM KCl, 1 mM MgSO<sub>4</sub>, 2 mM sodium pyruvate, and 1.3mM CaCl<sub>2</sub>) containing 2.5 mM probenecid and incubated for 30 minutes at 37°C in the absence and presence of antagonists prior to monitoring intracellular calcium responses using a FlexStation II plate-reader (Molecular Devices, Sunnyvale, CA). Fluorescence was measured (excitation, 485 nm, and emission detected at

525 nm with a 515 nm cut off filter) every 1.52 second intervals for up to 200 seconds. Analysis of the data was conducted using SOFTmax PRO<sup>®</sup> Software. Responses to a positive control stimulant (100  $\mu$ M ATP) were used to normalize responses across the plates.

A subset of experiments involved exposure of cells to 100  $\mu$ M ATP; in these experiments, cells were incubated either with LPS (1  $\mu$ g or 100 ng) in the absence and presence of 10 $\mu$ M BAPTA-AM. Ionomycin was used as a positive control.

### **2.3.6 Immunoblotting**

#### **2.3.6.1 Whole Cell Protein Extraction and protein determination**

Whole cell protein lysates of BV-2 cells were used in immunoblotting assays. BV-2 cells ( $5 \times 10^5$  cells/well) were plated onto 24-well tissue culture plates and allowed to attach overnight. Triplicate wells of cells were treated with fresh media or treatments for the times indicated; BV-2 cells were then washed twice in cold PBS. The cells were suspended in cold lysis buffer (50 mM Tris-HCl, pH 8.0; 150 mM NaCl and 1% NP-40) containing 1 tablet of protease inhibitor cocktail (4-(2-Aminoethyl) benzenesulfonyl fluoride hydrochloride (AEBSF), Bestatin hydrochloride, Leupeptin, E-64, Aprotinin, Pepstatin A, and Phosphoramidon disodium salt; Sigma) for 15 minutes on ice. The lysed cells were centrifuged at 13,000g for 1 minute at 4°C, and the supernatant (protein lysate) was collected and assayed for total protein.

Lysed cell pellets were assayed for total protein content using the Lowry method (Lowry et al., 1951). Serial dilutions of standards were prepared by using 1 mg/ml BSA as a stock solution. 200 $\mu$ l of each standard concentration and 200 $\mu$ l of diluted samples were transferred into a new

microfuge tube. 1 ml of Lowry reagent was added into the samples and the standards. After 10 minutes 100 µl of Folin phenol reagent were added into the samples and standards left for 45 minutes. Then 200µl of samples, blank and standards were loaded in 96-well plate in triplicate. The absorbance was measured at 750 nm using a spectrophotometric plate reader (Dynatech Laboratories, MRX) with Dynex Revelation software. The protein concentrations were expressed in mg/ml.

The supernatant fractions were kept in solubilisation buffer (2.5 ml Tris buffer, 2.0 ml glycerol, 2.0 ml 10% SDS, 2.5 ml DH<sub>2</sub>O, 1.0 ml 2-mercaptoethanol and 40 µl 2.5% Bromophenol Blue). The samples were used immediately or stored at -20 C until needed.

#### **2.3.6.2 Cytoplasmic and Nuclear Protein Extraction**

Cytoplasmic and nuclear protein fractions were prepared from BV-2 cells (approximately 500,000). Cell pellets were re-suspended in 150 µl of hypotonic lysis buffer [10 mM HEPES (pH 7.9), 10 mM KCl, 1.5 mM MgCl<sub>2</sub>, 0.1% NP40, and 5% protease inhibitor (0.2 mM DTT, 10 mM benzamidine, 7 µg/ml leupeptin, 50 µg/ml soybean trypsin inhibitor, 2 µg/ml aprotinin, 2 µg/ml antipain, 0.7 µg/ml pepstatin, 0.5 mM phenylmethylsulfonyl fluoride, and 0.5 mM 4-(2-aminoethyl) benzenesulfonyl fluoride)] and incubated on ice for 15 minutes, then briefly vortexed and centrifuged (16,000g) for 5 min at 4°C. The supernatant containing the cytoplasmic protein fraction was collected and stored at -80°C until used in experiments.

The pellet containing nuclei was washed with hypotonic buffer and centrifuged (16,000g) for 5 minutes at 4°C (3 times) and was re-suspended in complete lysis buffered (1 mM DTT, lysis buffer AM1, protease inhibitor cocktail) and incubated on ice for 30 minutes. Re-

suspended nuclei were vortexed briefly and centrifuged (16,000g) for 5 minutes, and these nuclear extracts were stored at -80°C until use.

### **2.3.6.3 Gel electrophoresis**

The 10% sodium dodecyl sulphate (SDS) polyacrylamide gels were transferred into an electrophoresis tank (Bio-Rad, USA). The combs were removed from the gels and 500 ml electrophoresis buffer 1x (30.3g Tris, 144g glycine and 10 g SDS in 1L distilled water) was added into the tank. 20 µg of denatured protein samples were loaded into the wells with 2 µl of the All Blue standard molecular weight markers (Bio-Rad laboratories Ltd, UK); electrophoresis was conducted at 200 V for 45 minutes.

1 membrane and 2 filter papers were placed in sequence in transfer buffer (30.3g Tris, 144g glycine dissolved in 8 litres distilled water, to which another 2 litres of methanol was added) and then the proteins were transferred at 100V for 60 minutes at 4°C using Bio-Rad kit. The protein transfer was checked by using a few drops of Ponceau S solution. The membranes were incubated with 5% fat-free dried milk powder in TBST (30.3g Tris, 73.12g NaCl, in 1L distilled water adjusted to pH 7.6 and then diluted to 10 litres with water and the addition of Tween 20 to a final concentration of 0.1%) on a shaker at room temperature for 60 minutes and then washed with 0.1% TBS-Tween twice.

The indicated primary antibodies were diluted in 5% milk powder in TBST then the membranes with diluted primary antibodies and GAPDH were incubated in small plastic bags on a shaker at 4°C overnight. The membranes were washed with TBS-Tween on a shaker at room temperature for 3 times of 10 minutes each and then incubated with 5% milk in TBST diluted [IRDye infrared LI-COR, USA] -secondary antibodies

(1:2000, dilution) goat anti-Rabbit IgG or goat- anti-mouse IgG with shaking for 1 hour at 37°C.

The membranes were washed with TBS-Tween on a shaker at room temperature for 3 times of 10 minutes each. Then washed once with Milli-Q-water and the blots were scanned using the Li-COR Odyssey Infrared Imaging system (Li-Cor Bioscience), in the 700 and 800 nm channels, with a resolution of 42  $\mu\text{m}$ , quality, an intensity of 5, and focal offset of 2mm. The data were analyzed by Odyssey application software. The membranes were kept at 4°C for future reference.

#### **2.3.6.3.1 Antibodies Used**

Anti-ERK1/2 (1:1000), NF-KB, pNF-KB (1:1000, Signaling Technology, # 3034, 3036), IKB  $\alpha$ , P-IKB  $\alpha$  (1:1000, Cell Signaling Technology, # 4812, 9246), JNK, P-JNK (1: 1000, , P-JNK (1: 1000, Life Technologies, # 44-682G), iNOS (1: 1000; Cell Signaling Technology, #2977), COX 2 (1: 1000, Cell Signaling Technology, #4812) and anti-GAPDH (1:2000, Sigma).

#### **2.3.7 Immunocytochemistry**

BV-2 cells ( $5 \times 10^5$ ) were seeded on poly-L-lysine-coated 13 mm glass coverslips and allowed to attach overnight in the conditioned medium. The following day, cells were serum-starved for 24 hours in a medium containing no fetal bovine serum (FBS), when indicated 10% FBS was added to other cells. The cells were incubated with medium alone or with LPS with or without drug for indicated times. Cells were fixed with 4% paraformaldehyde in phosphate buffered saline (PBS) for 30 minutes at room temperature, washed with PBS and then permeabilized using 0.1% Triton-X100 for 30 minutes.

Blocking of non-specific binding sites was performed by incubating cells with PBS containing 1% bovine serum albumin (BSA) for 1 hour at room temperature. Cells were incubated with the indicated primary antibody overnight at 4 °C.

After 3 times washes with PBS, FIT-C-conjugated goat anti-rabbit IgG (1:800) or FIT-C-conjugated goat anti-mouse IgG (1:500, both IgG from Jackson Immuno Research) was incubated for 1 hour at 37 °C. To visualize all the cells present on coverslips, the cell nuclei were stained with 4, 6-diamidino-2-phenylindole (DAPI, Molecular Probes) dye (1:1000) for 5 minutes at room temperature. After extensive washing, coverslips were mounted with mounting medium without DAPI (Vectashield) and viewed through a 63 x glycerine immersion lens objective or 40 magnifications oil immersion with a Leica DMRA2 fluorescent microscope.

Images were cropped and brightness and contrast were adjusted equally using Image J Software. The intensity of immunoreactivity was defined as the product of relative optical density (ROD) and area of immunoreactivity was measured using Image J Software and velocity Demo 6 software was used for confirmation. Negative controls without primary antibody were included to identify non-specific staining.

#### **2.3.7.1 Antibodies used**

GPR55; 1:250, Cayman Chemical, USA # 10225, iNOS 1:250, Cell Signaling Technology, NF-KB; 1:500, Cell Signaling Technology and LB $\alpha$ -1; 1:100, alpha laboratories; # 019-19741, Hampshire, UK.

### **2.3.8 Dichlorofluorescein (DCF) assay**

To measure ROS released into the medium by the cells, a DCF (2',7'-dichlorodihydro-fluorescein diacetate) assay was employed. BV-2 cells were seeded in 24 well plates then loaded with 10 $\mu$ M of DCF in PBS for 30 minutes in the dark at 37°C. Cells were washed twice with PBS then stimulated with LPS with or without CBD at different times and concentrations. At the end of the time course, cells were washed with PBS. The fluorescence of the supernatant was determined using a spectrofluorometer (Synergy-2 plate reader; BioTek Instruments Inc, Winooski, VT) with 485 nm excitation and 520 nm emission.

### **2.3.10 Antioxidant effect of CBD**

BV-2 cells were cultured in 24 well plates then treated with 10 $\mu$ M CBD for 24 hours before exposure to hydrogen peroxide for 2 hours in the presence and absence of CBD. Cell viability was measured using the Neutral Red (NR) assay. Fluorescence was measured at 540 nm in a microplate reader and normalized to the negative control.

### **2.3.11 Reverse transcription polymerase chain reaction (RT-PCR)**

#### **2.3.11.1 RNA extraction**

Cultured BV-2 cells (5 x 10<sup>5</sup> cells/ well) were plated onto 6-well tissue culture plates and incubated overnight until attached. Triplicate wells were treated with vehicle and CBD for 24 hours, cell cultures were washed twice with PBS.

The BV-2 cell pellets were homogenized in lysis reagent (Tri-reagent<sup>®</sup>, Ambion, UK). The homogenate was incubated for 5 minutes on ice to promote a complete dissociation of nucleoprotein complexes before

addition of 1-bromo-3-chloro-propane (BCP) and centrifugation (10,000g for 15 minutes at 4 °C) to separate the mixture into an aqueous, RNA phase and an organic, protein phase separated by thin layer of DNA. The upper aqueous phase was used for RNA precipitation at 20 °C for 30 minutes with 2 M sodium acetate and isopropanol at pH 4.

The organic phase was kept at -80°C for further protein extraction. RNA was collected by centrifugation (10000 g for 15 min at 4 °C) and washed twice with 70% ethanol. 50 µl of DEPC-treated water was added to dissolve pellets; the concentration of total RNA and purity were assessed using a NanoDrop (ND-1000 Spectrophotometer, NanoDrop Technologies, USA) at 260 nm.

#### **2.3.11.2 Complementary DNA (cDNA) synthesis**

5 µl (1 µg/µl) purified RNA was used to synthesis cDNA with superscript III reverse transcriptase (Invitrogen, UK) and another 5 µl underwent the same reaction but with superscript III reverse transcriptase replaced by HPLC water to generate a non-reverse transcriptase control (NRTs). To each 5 µl of RNA, 1 µl of random primer and 1 µl of dNTP were added, made up to a volume of 13 µl with 6 µl of HPLC grade water; the mixture was incubated at 65 °C for 5 minutes and quickly chilled on ice followed by addition of the following to make up the final reaction volume of 20µl (4 µl first strand buffer X5; 1 µl 0.1 M DDT; 1 µl RNase inhibitor and 1 µl superscript III for cDNA sample or 1 µl NRTs sample). Finally, the mixture underwent an incubation period of 20 minutes at 37 °C then 60 minutes at 50 °C and at 70 °C for 15 minutes. cDNA and NRTs synthesized were stored at -20 °C for future use.

### 2.3.11.3 Designing the Primers and Probe

Primers for the target gene were designed using Primer Express 2 (Applied Biosystems, UK) following the manufacturer's instructions and purchased through Eurofins MGW Operon. Primer and probe were "blasted" using the National Center for Biotechnology Information (NCBI) BLAST to ensure that the chosen sequence was specific for the gene of interest. Primer and probes were constituted and diluted to 10 $\mu$ M prior to use. Mouse actin, beta (ACTB) endogenous control (FAMTM Dye/MGB probe, Non-Primer limited) Part Number 4352933E from Applied Biosystems (UK) was used as control.

Gene	Primers	sequence
<b>Mouse</b>	Forward Primer	GAGCAGATATGGACTGCAGCTGCAA
	Reverse Primer	GAGGCACGAACATGA
<b>GPR55</b>	Probe	CCAGAGCGTGACAACACTGCTCATTCGA

### 2.3.11.4 Taqman Real-Time PCR

A mix of cDNA from different samples of positive control was used to form the standard curve and 2 fold dilutions (1:2, 1:4, 1:8, etc) of each cDNA and non-template control to quantify relative concentrations of the target and reference genes in the samples, cDNA samples were diluted.

A master mix prepared for the reference and target gene were calculated according to desired number of wells each containing a mix of Taqman master mix, forward primer, and reverse primer, probe and HPLC water. 10  $\mu$ l from this mix was added to each well of a 96 well reaction plate (Applied Bioscience, USA) then 3  $\mu$ l from each cDNA sample or standard was added

in triplicate. The StepOne plus real time PCR system (Applied Biosystem, UK) was setup.

### **2.3.12 [<sup>35</sup>S]-GTPγS binding assay**

Cannabinoid receptor-effector coupling efficiency was determined using the [<sup>35</sup>S] GTPγS binding assay following optimisation (Happe et al., 2001).

#### **2.3.12.1 Reagents**

Tris, hydrated magnesium chloride (MgCl<sub>2</sub>.6H<sub>2</sub>O), bovine serum albumin (BSA), guanosine diphosphate (GDP), theophylline and guanosine 5'-[γ-thio]triphosphate tetralithium (GTPγ) salt were purchased from Sigma Aldrich (UK), sodium chloride (NaCl) from Fisher Scientific, [<sup>35</sup>S]guanosine 5'-[γ-thio]triphosphate was purchased from Perkin Elmer (MA, USA) and all cannabinoids used in this section were purchased from Tocris Bioscience (Bristol, UK).

#### **2.3.12.2 Brain membranes**

Membrane fractions were prepared using tissue from the whole rat brain. Rats were sacrificed by decapitation and brain was weighed and excess fluid was removed and homogenised in 10 ml of ice-cold Tris-Mg<sup>2+</sup> buffer (50 mM Tris-HCl/3 mM MgCl<sub>2</sub>/1 mM EGTA, pH 7.4) using 10 strokes of a motor-driven ground glass pestle and homogenate was diluted to 10 volumes of brain tissue with cold Tris buffer. The homogenate was centrifuged at 20,000g at 4 °C for 10 minutes, and the supernatant was removed. Samples were re-suspended in a further 20 x volume of 50mM Tris and the process repeated 4 times in total. Following the final centrifugation step, samples were re-suspended to final concentration of 2mg/ml and divided into 1 ml aliquots then stored at -80 °C until needed.

Protein levels were determined using the Lowry method (Lowry *et al.*, 1951).

### **2.3.12.3 [<sup>35</sup>S]-GTPγS assay**

Using whole rat brain, homogenates were re-suspended in binding buffer (50 mM Tris, 100 mM NaCl, 10 mM MgCl<sub>2</sub>.6H<sub>2</sub>O, 0.2 mg/ml BSA in distilled water). 10 μg of brain membrane was added to each tube, 2 mM theophylline. [<sup>35</sup>S]-GTPγS binding along with 40 μM GDP (optimized value, Figure 2.56). GDP was included in the assay to promote G protein inactivation. Increasing GDP decreased basal binding of [<sup>35</sup>S] GTPγS and allowed a higher percent stimulation of binding by agonist (Breivgel *et al.*, 1998).

Samples were vortexed and incubated at 30°C for 30 minutes. Following incubation, samples were separated into one of three conditions: basal, non-specific binding and drug-stimulated. Each assay was conducted in triplicate for each drug concentration. Drug buffer was added to basal samples, 1μM unlabelled GTPγS to non-specific binding samples and different concentration range samples. All samples were subsequently incubated with 0.02 nM [<sup>35</sup>S]-GTPγS for 90 minutes in a shaking water bath at 30°C to attain steady state. Following incubation, the reaction was terminated by rapid filtration of membrane samples through a Brandel Tissue Harvester (Gaithersburg, MD, USA) onto Whatman GF/B glass-fibre filters (Clifton, NJ) for 4 times washing by cold distilled water. Filter discs were subsequently transferred to scintillation vials and covered with Ultima Gold XR scintillant (Perkin Elmer, MA, USA) and the radioactivity measured using a Packard Tri-Carb 2100 TR scintillation counter (Isotech, Chesterfield, UK) with a count time of 3 minutes.

### 2.3.13 Statistical analysis

Data were collected from three or more independent experiments (using different passages of cells) and are expressed as mean  $\pm$  S.E.M. Statistical analysis was performed, where indicated, using repeated measures one way ANOVA, with post-hoc Bonferonni's multiple comparison test or a Dunnett's *post hoc* analysis assessed using *GraphPad Prism*<sup>®</sup> version 5 software (GraphPad Software, La Jolla, CA). Differences were considered statistically significant at  $p < 0.05$ . Prism was also used to fit sigmoidal curves to concentration-response data.

[<sup>35</sup>S]-GTP $\gamma$ S data analysis; the mean was calculated for triplicates. The non-specific binding was measured which was subtracted from the total binding without drugs then calculated as dpm (every concentration) – dpm (basal)/ dpm (total) %. The data are the mean of three independent assessments each performed in triplicate. Radioligand binding data were analysed by non-linear regression analyses, agonist concentration–effect curves using the software *GraphPad Prism*<sup>®</sup> version 5. The agonists increase nucleotide binding above basal levels, and therefore display percentage activation above 100%. Inverse agonists decrease nucleotide binding below basal levels and therefore give a percentage below 100%. Finally, neutral antagonists, that do not affect nucleotide binding, display a percentage activation of 100%. EC<sub>50</sub> values were calculated for compounds which displayed a half affinity.

## **2.4 Results**

### **2.4.1 Characterization of LPS-evoked nitric oxide production in BV2 cells**

#### **2.4.1.1 The influence of LPS concentration, time, serum and minocycline**

The BV-2 mouse microglial cell line, which has been reported to express cannabinoid receptors (Walter, Franklin et al. 2003), was employed to investigate the effects of cannabinoids on NO formation. BV-2 cells showed a concentration-dependent increase in NO formation in response to bacterial lipopolysaccharide (LPS) application (1ng-4µg/ml), measured by nitrite accumulation, in a concentration-dependent manner as shown in Figure 2.2; A. Maximum NO formation occurred between 24 and 30 hours of LPS exposure (Figure 2.2; B).

The LPS-stimulated enhancement of nitrite accumulation was abolished in the presence of minocycline, a microglial inhibitor, in a concentration-dependant manner (5-20 µM) (Figure 2.3; A). LPS-stimulated NO formation was inhibited by approximately 50% when incubated in 5% serum-containing media and was completely blocked in serum-free media (Figure 2.3; B). Ethanol (0.01%) vehicle had no effect on basal or LPS-stimulated NO formation.

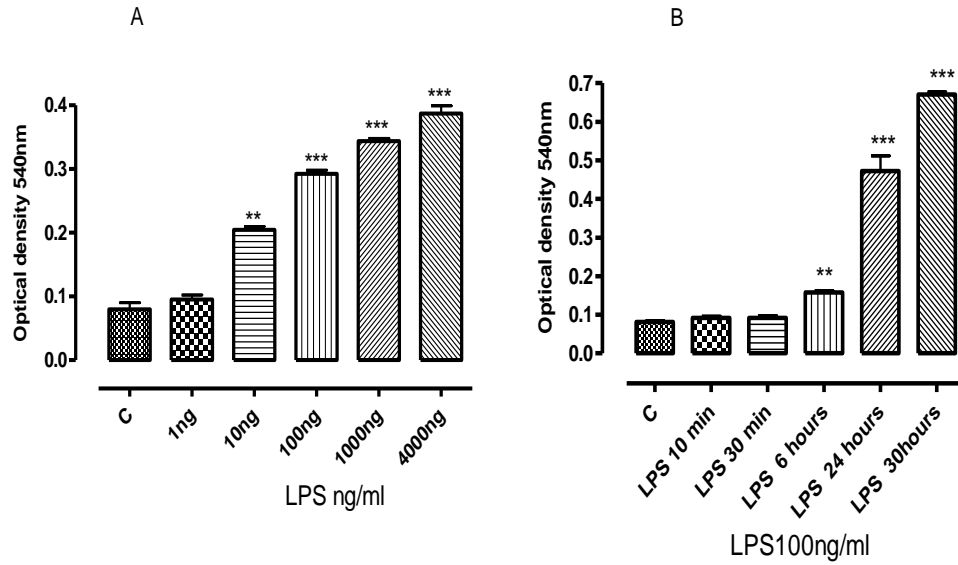


**Figure 2.2: (A)** Histogram represent the concentration-dependence of LPS effects on NO production in BV-2 cells. **(B)** Time-dependence of LPS effects on NO formation in BV-2 cells (by time). BV-2 cells ( $5 \times 10^5$  cells/well) were pre-treated with LPS at the indicated concentrations for the indicated time. Control wells were incubated in culture medium alone. Culture supernatant was assayed for nitrite levels using the Griess reagent. Data are mean  $\pm$  SEM of triplicates from three separate experiments. Data were analysed using one-way ANOVA followed by Dunnett's test Panel A and B; \*\* $p < 0.01$  compared with (C) control, \*\*\* $p < 0.001$  compared with (C) control.

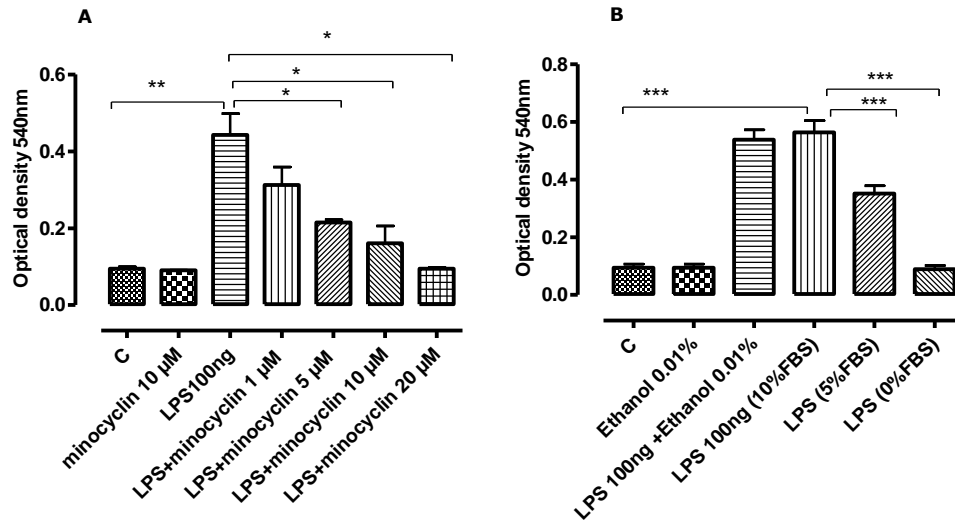


**Figure 2.3: (A)** Histogram represent the effects of a selective microglial inhibitor, minocycline, on LPS-mediated NO release in the BV-2 cell line. **(B)** Effect of fetal bovine serum (FBS) and ethanol (01%) on LPS-induced NO production in BV-2 cells. BV-2 cells ( $5 \times 10^5$  cells/well) were pre-treated with minocycline at the indicated concentrations for 1 hour then incubated with LPS (100ng) for 24 hours. Control wells in culture medium 10% FBS (C) or at the indicated concentrations of FBS for 24 h. Culture supernatant was assayed for nitrite levels using the Griess reaction as described in Methods. The figure represents means  $\pm$  SEM of triplicates of three independent experiments. Data were analysed using one-way ANOVA followed by Dunnett's test compared with LPS alone.

#### 2.4.1.2 The influence of calcium ions

BV-2 cells were incubated with BAPTA-AM (a cell-permeant calcium chelator)  $40 \mu$ M for 1 hour, then in the absence or presence of LPS (100ng/ml) for 24 hours and NO was measured by the Griess assay. BAPTA-AM alone had no effect but significantly reduced LPS-stimulated NO in a concentration-dependent fashion (Figure 2.4). To exclude any toxic effect of BAPTA-AM, cell viability was assessed using the Neutral Red assay. Cells were 98-100% viable under all conditions (data not shown). BV-2 cells were treated with different concentrations of the calcium ionophore ionomycin in the absence of LPS (24 hours) and release of NO was measured by the Griess assay. Ionomycin had no effect on microglial

NO formation (Figure 2.5), despite its ability to increase intracellular calcium concentration (Figure 2.6).

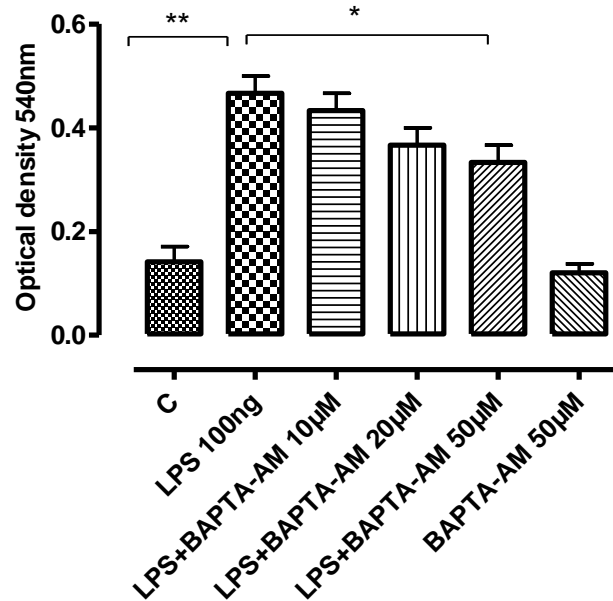


**Figure 2.4:** Histogram represents the effect of BAPTA-AM on LPS-induced NO formation. BV-2 cells ( $5 \times 10^5$  cells/well) were pre-treated with BAPTA-AM (at indicated concentrations) 1 hour prior to LPS (100ng) or LPS alone, and then incubated for 24 hours. Culture supernatant was assayed for nitrite levels using the Griess reaction as described in Methods. The figure represents means  $\pm$  SEM of triplicates of three independent experiments. Data were analysed using one-way ANOVA followed by Dunnett's test  $*P < 0.01$ , LPS+BAPTA-AM compared with LPS alone.

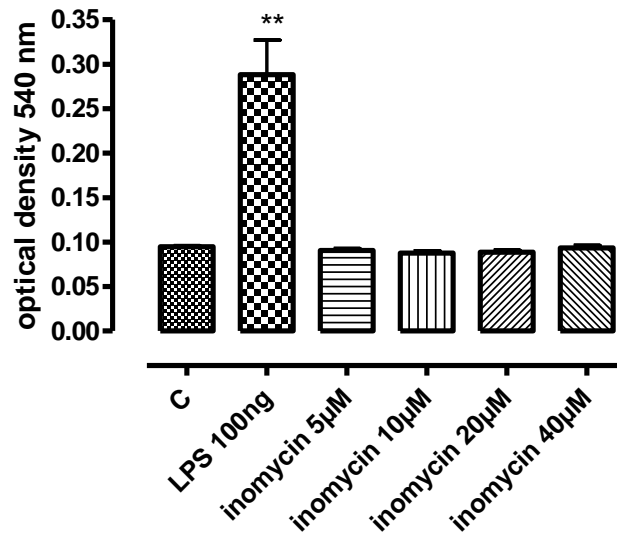


**Figure 2.5:** Histogram represents the effect of ionomycin-induced elevation of the basal  $\text{Ca}^{2+}$  on NO formation. BV-2 ( $5 \times 10^5$  cells/well) treated with different concentrations of ionomycin or LPS 100ng/ml 24 hours. Culture supernatant was assayed for nitrite levels using the Griess reaction as described in methods. The figure represents means  $\pm$ SEM of triplicates of three independent experiments. Data were analysed using one-way ANOVA followed by Dunnett's test  $**P < 0.01$ , compared with control.

#### 2.4.1.2.1 The role of intracellular $\text{Ca}^{2+}$ [ $\text{Ca}^{2+}$ ]<sub>i</sub> in microglial activation

Intracellular  $\text{Ca}^{2+}$  concentrations [ $\text{Ca}^{2+}$ ]<sub>i</sub> in BV2 cells were assessed in the presence of LPS and ionomycin and in the presence of the calcium chelator BAPTA-AM. There was a marked concentration-dependant increase in the levels of [ $\text{Ca}^{2+}$ ]<sub>i</sub> in the LPS-activated cells (Figure 2.6; A). Ionomycin (40  $\mu\text{M}$ ) also increased [ $\text{Ca}^{2+}$ ]<sub>i</sub> and this was partially inhibited by BAPTA-AM (50  $\mu\text{M}$ ). In addition, ATP (100  $\mu\text{M}$ ), another widely employed microglial activator, significantly increased [ $\text{Ca}^{2+}$ ]<sub>i</sub> and this was, again, partially reduced by BAPTA-AM (10  $\mu\text{M}$ ) (Figure 2.6; B).

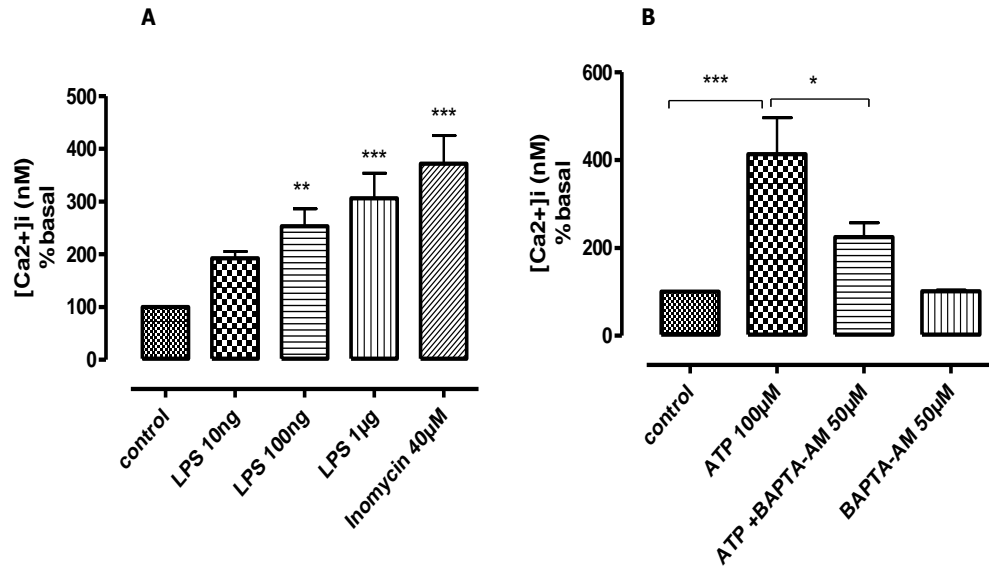


**Figure 2.6: (A)** Histogram shows the effect of LPS on  $[Ca^{2+}]_i$  in BV-2 ( $1 \times 10^6$  cells/well). Cells were treated with LPS at indicated concentrations (10ng, 100ng and  $1 \mu\text{g} / \text{ml}$ ). **(B)** Effect of ATP ( $100 \mu\text{M}$ ) on  $[Ca^{2+}]_i$  in the presence or absence of BAPTA-AM ( $50 \mu\text{M}$ ) on  $[Ca^{2+}]_i$  in BV-2 cells and control cells (basal). Using fura-4-based imaging,  $[Ca^{2+}]$  was measured at baseline ( $1'' - 14''$ ), peak ( $15'' - 60''$ ). The data represent means  $\pm$  SEM of three independent experiments. Data present as % basal values. Data were analysed using one-way ANOVA followed by Dunnett's test Panel A; \*\* $P < 0.01$  and \*\*\* $P < 0.001$  compared with the control. Panel B; test \*\*\* $P < 0.001$  compared with control and \* $P < 0.05$  (ATP+BAPT-AM) compared with ATP alone.

#### 2.4.1.2 The involvement of inducible NOS

1400W (a selective iNOS inhibitor (Jarvinen et al., 2008);  $10 \mu\text{M}$ ) significantly attenuated NO formation in BV-2 cells (Figure 2.7; A). In order to characterize our model further, we tested dexamethasone, a synthetic glucocorticoid receptor agonist, reported to inhibit iNOS and NO production at  $1 \mu\text{M}$  (Hamalainen et al., 2008). Dexamethasone at  $1 \mu\text{M}$  reversed significantly LPS-induced NO release (Figure 2.7; B).

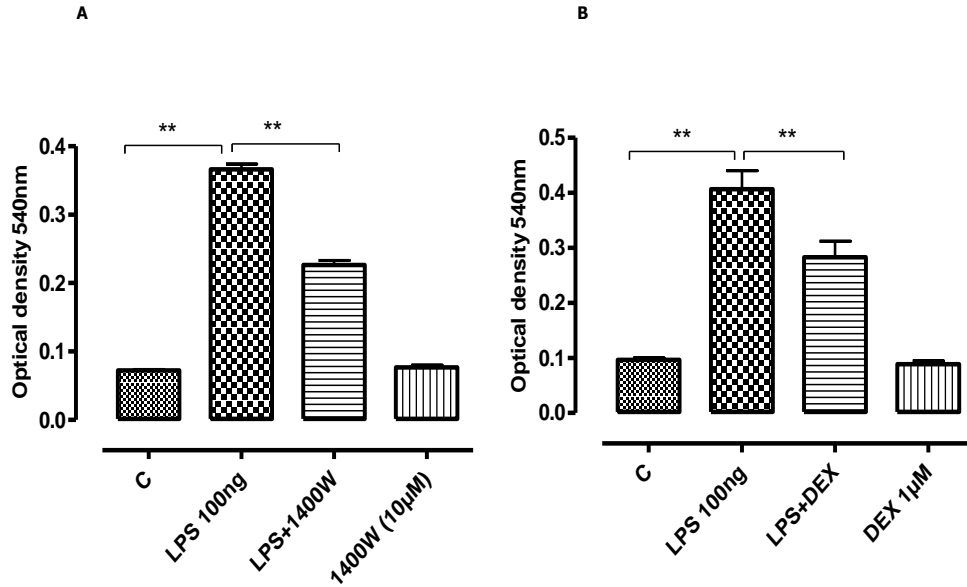


**Figure 2.7: (A)** Histogram shows the effect of 1400W, an iNOS inhibitor, on LPS-induced NO production in BV-2 cells. **(B)** Effect of dexamethasone (DEX) on LPS-induced NO production in BV-2 cells. BV-2 cells ( $5 \times 10^5$  cells/well) were pre-treated with 1400W (10µM) for 1 hour with and without LPS (100 ng/ml) for 24 hour or DEX. Control wells were incubated in culture medium alone. Culture supernatant was assayed for nitrite levels using the Griess reagent. Figure represents mean  $\pm$  SEM of triplicates from three separate experiments. Data were analysed using one-way ANOVA followed by Dunnett's test Panel A  $**p < 0.01$  compared with LPS alone.

## 2.4.2 The effect of cannabinoid ligands on LPS-evoked nitric oxide production in BV2 cells

### 2.4.2.1 Endocannabinoids and related compounds

A number of endocannabinoids and endocannabinoid-like compounds, N-oleoyl- (OEA), N-palmitoyl- (PEA), N-arachidonylethanolamine (AEA), 2-arachidonoyl-glycerol (2-AG) and N-stearoyl-ethanolamine (SEA), all at 10 µM concentrations failed to alter significantly basal NO or LPS (100ng)-evoked increases in NO formation (Figure 2.8).

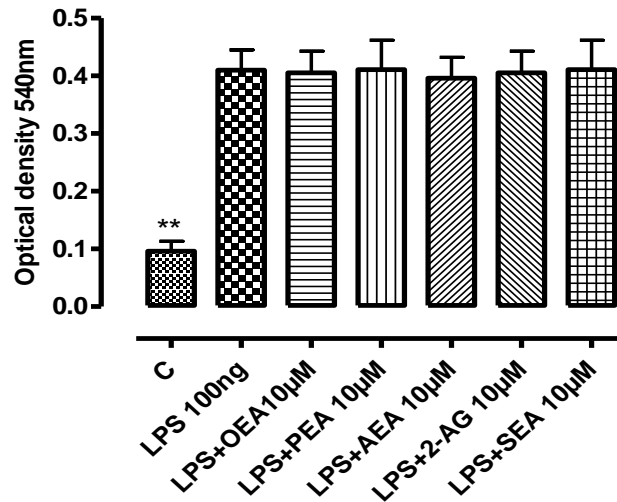


**Figure 2.8:** Histogram shows the effect of endocannabinoids on LPS-induced NO in BV-2 cells. BV-2 cells ( $5 \times 10^5$  cells/well) were pre-treated with endocannabinoid-like molecules N-oleoyl- (OEA), N-palmitoyl- (PEA), N-arachidonylethanolamine (AEA), 2-arachidonoyl-glycerol (2-AG) and N-stearoyl-ethanolamine (SEA), (all at  $10\mu\text{M}$ ) for 1 hour before LPS (100 ng/ml) for 24 hour. Control wells were incubated in culture medium alone. Culture supernatant was assayed for nitrite levels using the Griess reagent. Figure represents means  $\pm$  SEM of triplicates from three separate experiments. Data were analysed using one-way ANOVA followed by Dunnett's test  $**p < 0.01$  compared with LPS alone.

#### 2.4.2.2 Cannabinoid receptor ligands

On the other hand, the synthetic cannabinoid ligand, CP-55,940, and AM251 ( $\text{CB}_1$  antagonist and putative GPR55 antagonist) significantly attenuated LPS-induced NO release only at the highest concentration ( $10\mu\text{M}$ ), when LPS (100 ng/ml) was applied to the BV-2 cells for 24 hours. At the same concentration ( $10\mu\text{M}$ ), the phytocannabinoid-related ligand, HU-210 and the  $\text{CB}_2$  receptor-selective agonist, JWH015, all failed to alter significantly LPS-evoked increases in NO formation. The  $\text{CB}_1$  and  $\text{CB}_2$  receptor-agonist, WIN55212-2 and AM251 inhibited LPS-induced NO formation at  $10\mu\text{M}$  (Figure 2.9 - 2.13).

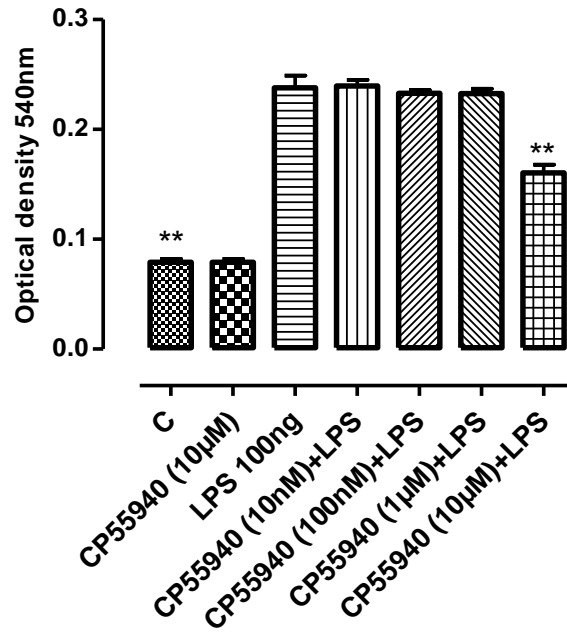


**Figure 2.9:** Histogram shows the effect of CP-55,940 on LPS-induced NO in BV-2 cells. BV-2 cells ( $5 \times 10^5$  cells/well) were pre-treated with CP55940 at the indicated concentrations for 1 hour prior to LPS (100ng/ml). Control wells were incubated in culture medium alone. Culture supernatant was assayed for nitrite levels using the Griess reagent. Figure represents mean  $\pm$  SEM of triplicates from three separate experiments. Data were analysed using one-way ANOVA followed by Dunnett's test  $**p < 0.01$  compared with LPS alone.

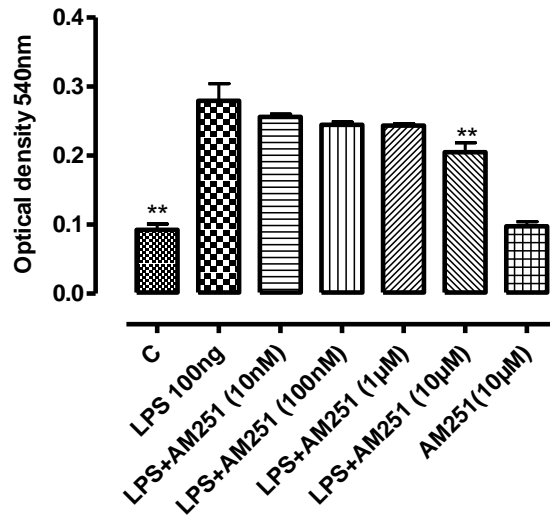


**Figure 2.10:** Effect of AM251 on LPS-induced NO in BV-2 cells. BV-2 cells ( $5 \times 10^5$  cells/well) were pre-treated with AM251 at the indicated concentrations for 1 hour prior to LPS (100 ng/ml). Control wells were incubated in culture medium alone. Culture supernatant was assayed for nitrite levels using the Griess reagent. Figure represents mean  $\pm$  SEM of triplicates from three separate experiments. Data were analysed using one-way ANOVA followed by Dunnett's test  $**p < 0.01$  compared with LPS alone.

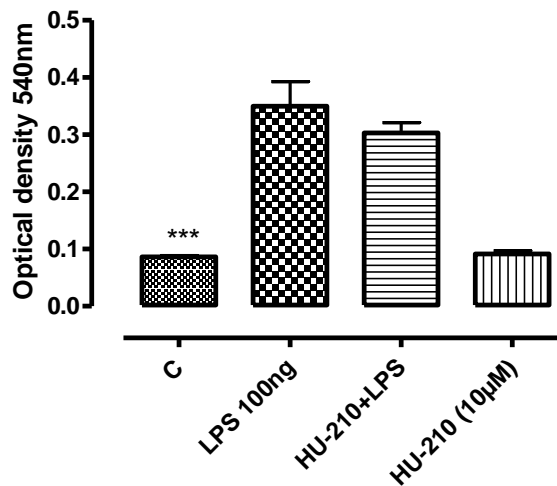


**Figure 2.11:** Effect of HU-210 on LPS-induced NO in BV-2 cells. BV-2 cells ( $5 \times 10^5$  cells/well) were pre-treated with HU-210 (10  $\mu$ M) for 1 hour prior to LPS (100 ng/ml). Control wells were incubated in culture medium alone. Culture supernatant was assayed for nitrite levels using the Griess reagent. Figure represents mean  $\pm$  SEM of triplicates from three separate experiments. Data were analysed using one-way ANOVA followed by Dunnett's test  $***p < 0.001$  compared with LPS alone.

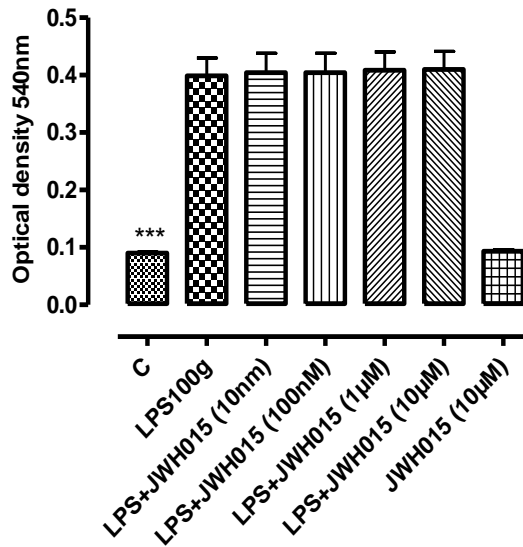


**Figure 2.12:** Histogram shows the effect of JWH015 on LPS-induced NO in BV-2 cells. BV-2 cells ( $5 \times 10^5$  cells/well) were pre-treated with JWH015 at the indicated concentrations for 1 hour prior to LPS (100ng/ml). Control wells were incubated in culture medium alone. Culture supernatant was assayed for nitrite levels using the Griess reagent. Figure represents mean  $\pm$  SEM of triplicates from three separate experiments. Data were analysed using one-way ANOVA followed by Dunnett's test  $**p < 0.01$  compared with LPS alone.

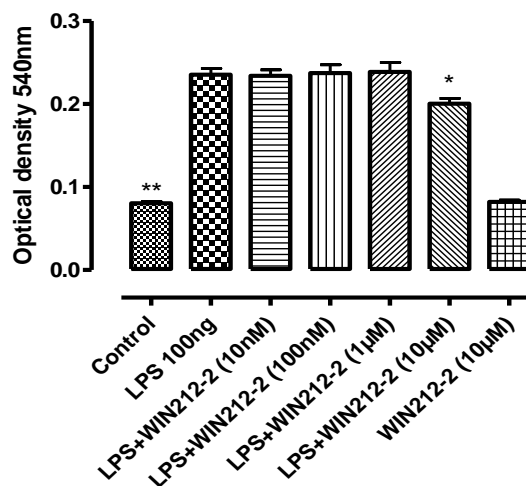


**Figure 2.13:** Histogram shows the effect of WIN55212-2 on LPS-induced NO in BV-2 cells. BV-2 cells ( $5 \times 10^5$  cells/well) were pre-treated with WIN55212-2 at the indicated concentrations for 1 hour prior to LPS (100 ng/ml). Control wells were incubated in culture medium alone. Culture supernatant was assayed for nitrite levels using the Griess reagent. Figure represents mean  $\pm$  SEM of triplicates from three separate experiments. Data were analysed using one-way ANOVA followed by Dunnett's test  $**p < 0.01$  compared with LPS alone.

### 2.4.2.3 Phytocannabinoids

A number of phytocannabinoids and their acids including cannabigerol (CBG), cannabidivarin (CBDV), tetrahydrocannabivarin (THCV), cannabidiolic-acid (CBDA) and cannabigerol acid (CBGA)] and THC, all failed to alter significantly LPS-stimulated NO formation in BV-2 cells at concentrations of 10  $\mu$ M (Figure 2.14 and 2.15). However, cannabidiol (CBD) also a putative GPR55 antagonist (10  $\mu$ M) significantly inhibited LPS-stimulated NO formation (Figure 2.16). HAPI cells (highly aggressive proliferating rat microglia) and primary mouse microglial cells were employed to confirm that the effects of CBD on NO release were not cell line-specific. HAPI cells and primary mouse microglial cells showed a significant increase in LPS-stimulated NO formation and this was inhibited by CBD (10 $\mu$ M) as shown in Figure 2.17.

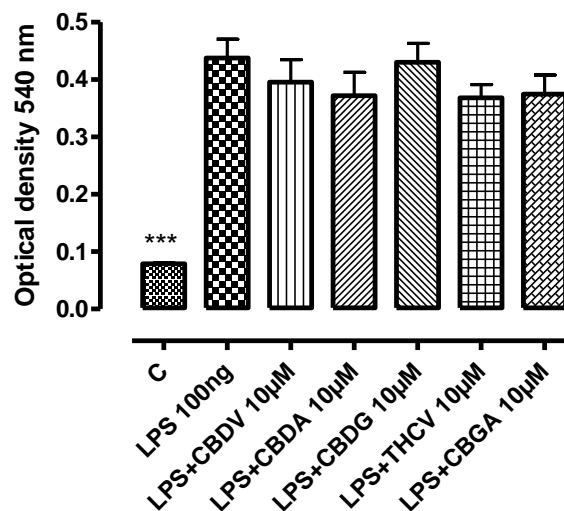


**Figure 2.14:** Histogram shows the effect of phytocannabinoids on LPS-induced NO in BV-2 cells. BV-2 cells ( $5 \times 10^5$  cells/well) were pre-treated with phytocannabinoids; CBDV, CBDA, CBDG, THCV and CBGA all at 10  $\mu$ M) for 1 hour before LPS (100ng/ml) for 24 hours. Control wells were incubated in culture medium alone. Culture supernatant was assayed for nitrite levels using the Griess reagent. Figure represents mean  $\pm$  SEM of triplicates from three separate experiments. Data were analysed using one-way ANOVA followed by Dunnett's test \*\*\* $p < 0.001$  compared with LPS alone.

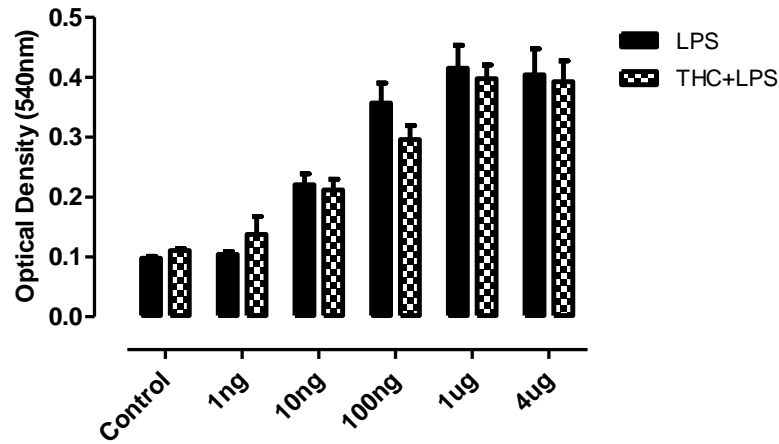


**Figure 2.15:** Histogram shows the effect of THC on LPS-induced NO in BV-2 cells. BV-2 cells ( $5 \times 10^5$  cells/well) were pre-treated with THC  $10\mu\text{M}$  for 1 hour prior to LPS (10-4000 ng/ml). Control wells were incubated in culture medium alone. Culture supernatant was assayed for nitrite levels using the Griess reagent. Figure represents mean  $\pm$  SEM of triplicates from three separate experiments. Data were analysed using Two-way ANOVA followed by Dunnett's test  $**p < 0.01$  compared with LPS alone.

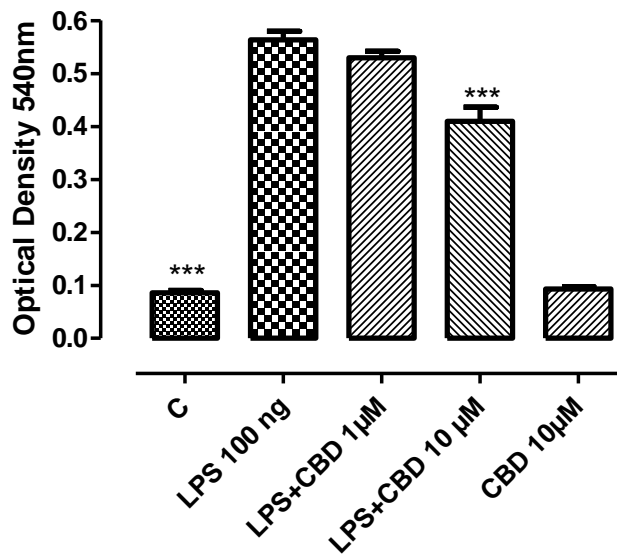


**Figure 2.16:** Histogram shows the effect of CBD on LPS-induced NO in BV-2 cells. BV-2 cells ( $5 \times 10^5$  cells/well) were pre-treated with CBD  $10\mu\text{M}$  for 1 hour with or without LPS (100 ng/ml) for 24 h. Control wells were incubated in culture medium alone. Culture supernatant was assayed for nitrite levels using the Griess reagent. Figure represents mean  $\pm$  SEM of triplicates from three separate experiments. Data were analysed using one-way ANOVA followed by Dunnett's test  $***p < 0.001$  compared with LPS alone.

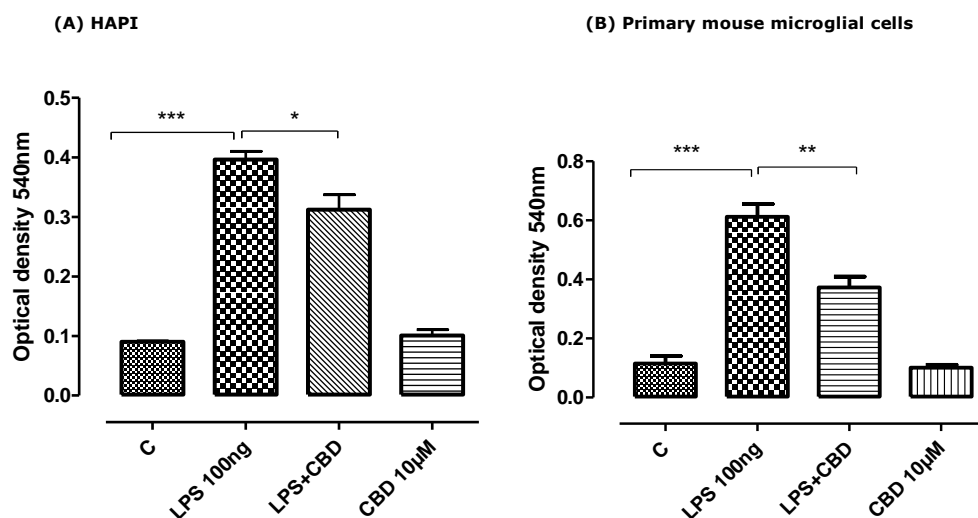


**Figure 2.17:** Histogram shows the effect of CBD on LPS-induced NO in (A) HAPI cells ( $5 \times 10^5$  cells/well) (B) primary microglial mouse cells were pre-treated with CBD at  $10\mu\text{M}$  concentrations for 1 hour prior to LPS 100 ng/ml. Control wells were incubated in culture medium alone. Culture supernatant was assayed for nitrite levels using the Griess reagent. Figure represents mean  $\pm$  SEM of triplicates from three separate experiments. Data were analysed using one-way ANOVA followed by Dunnett's test (A)  $*p < 0.05$  LPS+CBD compared with LPS alone;  $***P < 0.001$  C (control). (B)  $**p < 0.01$  LPS+CBD compared with LPS alone;  $***P < 0.001$  C (control).

#### 2.4.2.4 GPR55

The actions of different putative GPR55 receptor ligands on LPS (100ng/ml)-stimulated NO formation were investigated. The putative GPR55 ligand VSN16R and O-1602 (both  $10\mu\text{M}$ ) were without effect (Figure 2.18 and 2.19) as was the endogenous GPR55 activator lysophosphatidylinositol (LPI) and a novel GPR55 receptor agonist from GSK Pharmaceuticals also failed to significantly affect NO formation (Figure 2.20 and 2.21), whereas a GSK-supplied selective GPR55 receptor *antagonist*, produced significant inhibitions of LPS-stimulated NO formation (Figure 2.22).

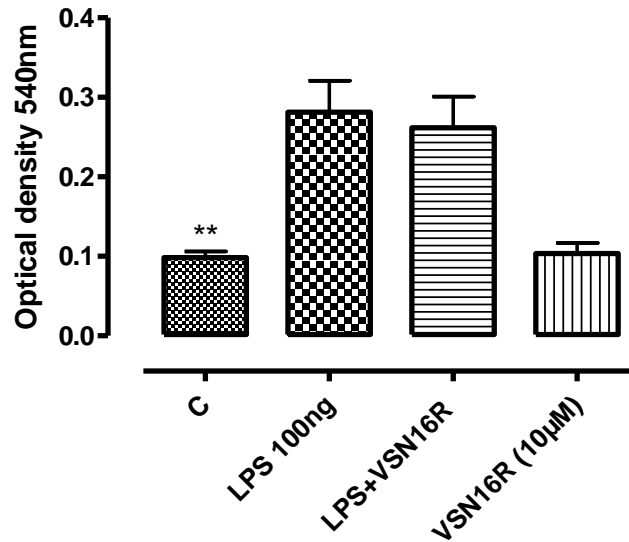


**Figure 2.18:** Effect of VSN16R on LPS-induced NO production in BV-2 cells. BV-2 cells ( $5 \times 10^5$  cells/well) were pre-treated with VSN16R at  $10\mu\text{M}$  for 1 hour prior to LPS (100 ng/ml) for 24 hours. Control wells were incubated in culture medium alone. Culture supernatant was assayed for nitrite levels using the Griess reagent. Figure represents mean  $\pm$  SEM of triplicates from three separate experiments. Data were analysed using one-way ANOVA followed by Dunnett's test  $**p < 0.01$  compared with LPS alone.

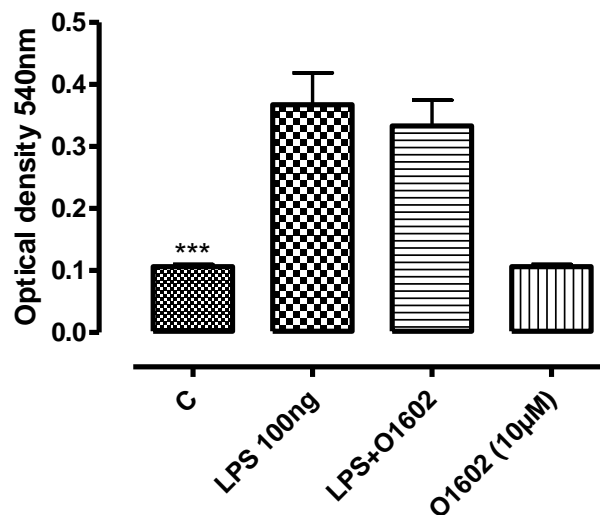


**Figure 2.19:** Histogram shows the effect of O1602 on LPS-induced NO release. BV-2 cells ( $5 \times 10^5$  cells/well) were pre-treated with O1602 ( $10\mu\text{M}$ ) for 1 hour with or without LPS (100 ng/ml) for 24 hours. Control wells were incubated in culture medium alone. Culture supernatant was assayed for nitrite levels using the Griess reaction as described in Methods. The figure represents means  $\pm$  SEM of triplicates of three independent experiments. Data were analysed using one-way ANOVA followed by Dunnett's test  $***P < 0.001$  compared with LPS alone.

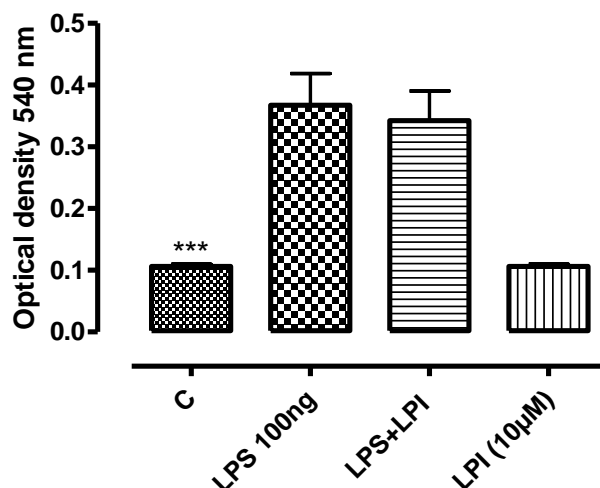


**Figure 2.20:** Histogram shows the effect of LPI on LPS-induced NO release. BV-2 cells ( $5 \times 10^5$  cells/well) were pre-treated with LPI ( $10 \mu\text{M}$ ) for 1 hour with or without LPS (100 ng/ml) for 24 hours. Control wells were incubated in culture medium alone. Culture supernatant was assayed for nitrite levels using the Griess reaction as described in Methods. The figure represents means  $\pm$  SEM of triplicates of three independent experiments. Data were analysed using one-way ANOVA followed by Dunnett's test  $***P < 0.001$  compared with LPS alone.

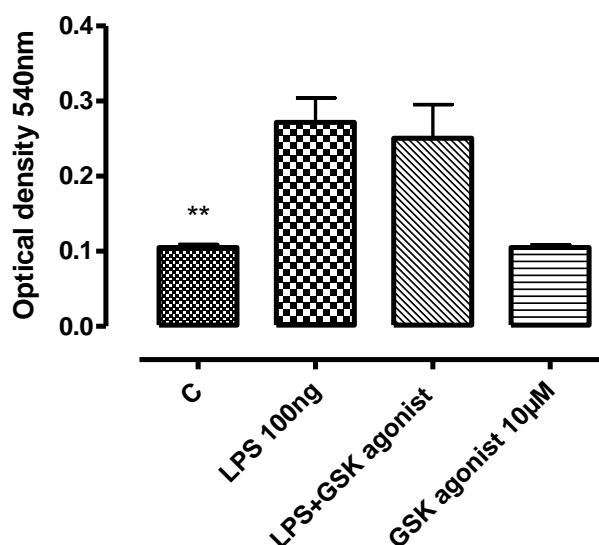


**Figure 2.21:** Histogram shows the effect of GSK agonist on LPS-induced NO production in BV-2 cells. BV-2 cells ( $5 \times 10^5$  cells/well) were pre-treated with GSK agonist at the  $10 \mu\text{M}$  concentrations for 1 hour with or without LPS (100 ng/ml). Control wells were incubated in culture medium alone. Culture supernatant was assayed for nitrite levels using the Griess reagent. Data are mean  $\pm$  SEM of triplicates from three separate experiments. Data were analysed using one-way ANOVA followed by Dunnett's test  $**p < 0.01$  compared with LPS alone.

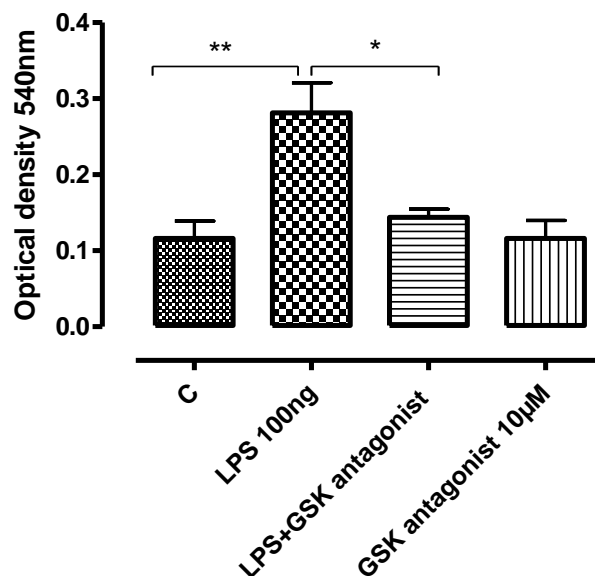


**Figure 2.22:** Histogram shows the effect of GSK antagonist on LPS-induced NO production in BV-2 cells. BV-2 cells ( $5 \times 10^5$  cells/well) were pre-treated with GSK antagonist  $10\mu\text{M}$  for 1 hour with or without LPS (100 ng/ml). Control wells were incubated in culture medium alone. Culture supernatant was assayed for nitrite levels using the Griess reagent. Data are mean  $\pm$  SEM of triplicates from three separate experiments. Data were analysed using one-way ANOVA followed by Dunnett's test  $**p < 0.01$  compared with LPS alone;  $*p < 0.05$  LPS+GSK antagonist compared with LPS alone.

#### 2.4.2.5 GPR18 /abn-CBD

The role of the GPR18 receptor on NO formation was examined using N-arachidonoyl glycine (NAGLY), an endogenous metabolite of the endocannabinoid anandamide which acts as an agonist at GPR18 (McHugh et al, 2010), and O-1918 which is an abn-CBD antagonist. NAGLY had no effect on LPS-stimulated NO release and O-1918 did not reverse the inhibition due to CBD (Figure 2.23; 2.24) suggesting that GPR18 and abn-CBD have no role to play in the effects of the phytocannabinoid.

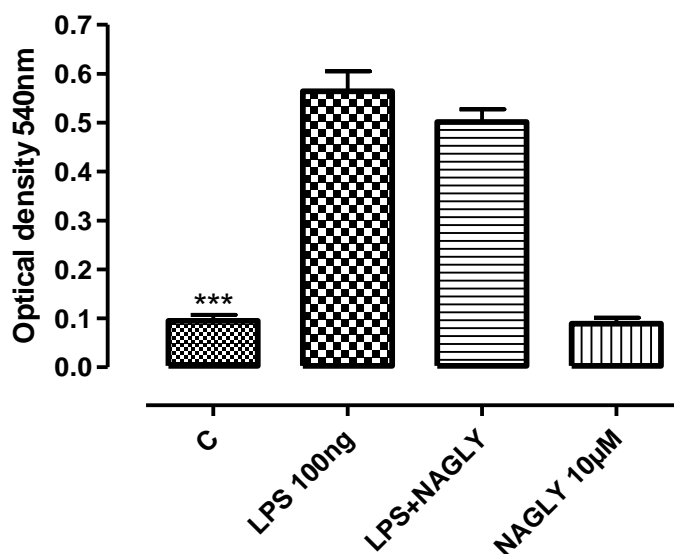


**Figure 2.23:** Histogram shows the effect of NAGLY, a GPR18 agonist. BV-2 cells ( $5 \times 10^5$  cells/well) were treated with NAGLY ( $10 \mu\text{M}$ ) 1 hour prior to LPS  $100 \text{ ng/ml}$  for 24 hours. NO levels in supernatant were measured using the Griess reaction as described in Methods. The figure represents means  $\pm$ SEM of triplicates of three independent experiments. Data were analysed using ANOVA followed by Dunnett's test. \*\*\*  $P < 0.001$  compared with LPS alone.

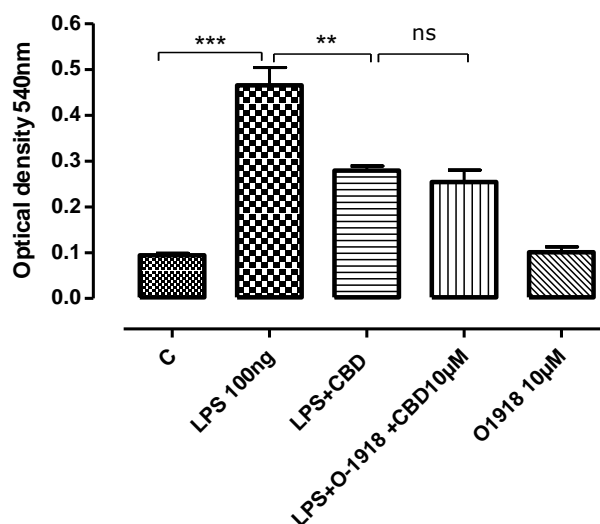


**Figure 2.24:** Histogram shows the effect of O-1918, a GPR18 antagonist, on CBD inhibition of NO induced by LPS. BV-2 cells ( $5 \times 10^5$  cells/well) were treated with O1918 1hour ( $10 \mu\text{M}$ ) then with CBD prior to LPS ( $100 \text{ ng/ml}$ ) for 24 hours. NO levels in supernatant were measured using the Griess reaction as described in Methods. The figure represents means  $\pm$ SEM of triplicates of three independent experiments. Data were analysed using one-way ANOVA followed by post-hoc Bonferonni's multiple comparison test \*\* $P < 0.01$  LPS+CBD vs. LPS; not significant LPS+O-1918+CBD vs. LPS+CBD; \*\*\* $p < 0.001$  compared with LPS alone.

#### 2.4.2.6 TRPV channels

In order to test the possibility that CBD might exert its effect via TRP channels, the TRPV1 antagonist capsazepine (CPZ) and the non-selective TRP channel blocker ruthenium red (RR) were administered, at the indicated concentrations, prior to CBD and LPS. Neither antagonist reversed the CBD inhibition of LPS-stimulated NO release (Figure 2.25).

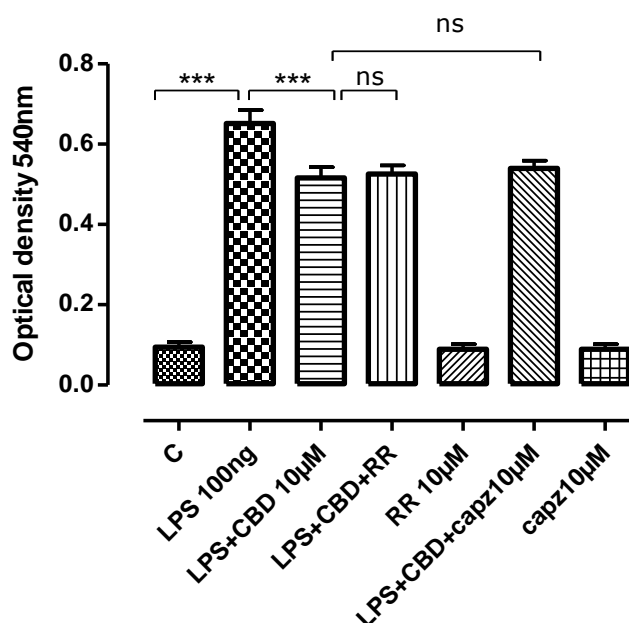


**Figure 2.25:** Histogram shows the effect of TRPV channel blockade on CBD inhibition of NO in BV-2 cells. BV-2 ( $5 \times 10^5$  cells/well) were treated with RR a non-selective TRP inhibitor ( $10 \mu\text{M}$ ) or with capsazepine ( $10 \mu\text{M}$ ) (TRPV1 antagonist) for 1 hour then with CBD prior to LPS ( $100 \text{ ng/ml}$ ) for 24 hours. NO levels in supernatant were measured using the Griess reaction as described in Methods. The figure represents means  $\pm$ SEM of triplicates of three independent experiments. Data were analysed using ANOVA followed by post-hoc Bonferonni's multiple comparison test \*\*\* $P < 0.001$  LPS+CBD vs. LPS alone; not significant LPS+CBD+RR vs. LPS+CBD; not significant LPS+CBD+Capz. vs. LPS+CBD.

#### 2.4.2.7 PPARs receptors

The peroxisome proliferator-activated receptors (PPAR  $\alpha$  and  $\gamma$ ) play an important role in lipid metabolism and inflammation (Storer et al, 2005). Potential PPAR involvement in the effects of CBD was tested using

GW6471, a PPAR  $\alpha$  antagonist, and GW9662, an antagonist of PPAR- $\gamma$ . Neither antagonist reversed CBD-induced inhibition of LPS-stimulated NO release or altered basal NO levels in cells (Figure 2.26; A-B).

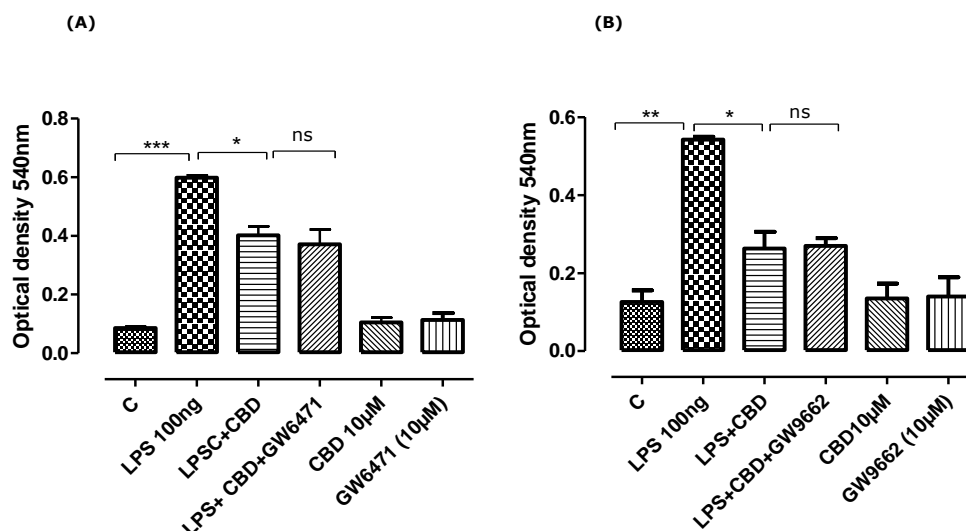


**Figure 2.26:** Histogram shows the effect of PPAR antagonists on NO release in BV-2 cells. BV-2 cells ( $5 \times 10^5$  cells/well) were treated with GW6471, a PPAR $\alpha$  antagonist, or with GW6471, a PPAR $\gamma$  antagonist ( $10 \mu\text{M}$ ), for 1 hour then treated with CBD prior to LPS ( $100 \text{ ng/ml}$ ) for 24 hours. NO levels in supernatant were measured using the Griess reaction as described in Methods. The figure represents means  $\pm$  SEM of triplicates of three independent experiments. Data were analysed using one-way ANOVA followed by post-hoc Bonferonni's multiple comparison test (A) \* $P < 0.05$  LPS+CBD vs. LPS; \*\*\* $P < 0.001$  compared with LPS alone; (B) \*\* $p < 0.01$  compared with LPS alone; not significant compared with LPS+CBD.

### 2.4.3 Characterization of CBD effects on LPS-evoked nitric oxide production in BV2 cells

#### 2.4.3.1 Effect on Cell viability

To investigate the potential non-specific toxicity of CBD on the viability of BV-2 microglial cells,  $5 \times 10^5$  cells/well were incubated with LPS alone or with CBD in combination in the Neutral Red (NR) cell viability assay. LPS slightly reduced viability of BV-2 cells in a concentration-dependent manner and this was totally reversed by  $10 \mu\text{M}$  CBD (Figure 2.27). To confirm this CBD-mediated protection against cell toxicity, we used  $\text{H}_2\text{O}_2$  as a well-

known cellular toxin. Remarkably, CBD again completely reversed the reduced cell viability due to H<sub>2</sub>O<sub>2</sub> (Figure 2.28).

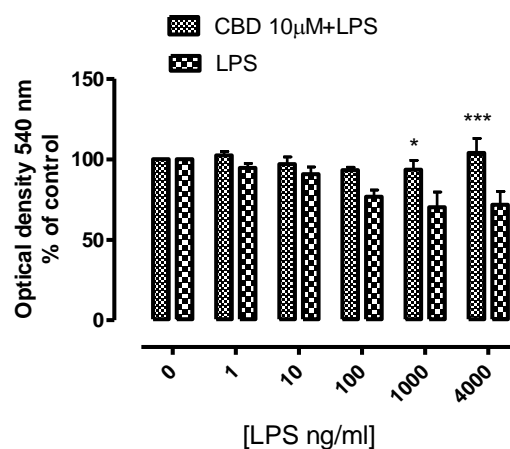


**Figure 2.27:** Histogram shows the effect of LPS on BV-2 cell viability by NR assay. Cells were treated with LPS (100 ng) prior to CBD (10µM) for 1 hour. Control wells were incubated in culture medium alone after that media was removed and fresh media with NR was added for 1 hour then optical density at 540 nm. The figure represents means ±SEM of triplicates of three independent experiments. Data were analysed using two-way ANOVA post-hoc test \*\*\*P<0.001 CBD+LPS compared with LPS (4000ng/ml); \*P< 0.05 CBD+LPS compared with LPS 1000 ng/ml.

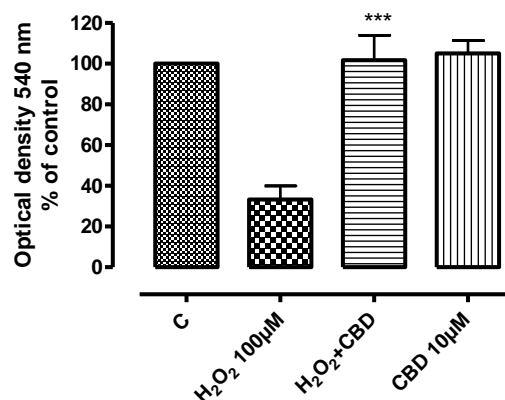


**Figure 2.28:** Histogram shows the effect of CBD on H<sub>2</sub>O<sub>2</sub> toxicity in BV-2 cell viability by NR assay. Cells were pre-treated with CBD for 1 hour prior to H<sub>2</sub>O<sub>2</sub> (100 µM). Control wells were incubated in culture medium alone after that media was removed and fresh media with NR was added for 1 hour then optical density at 540 nm. The figure represents means ±SEM of triplicates of three independent experiments. Data were analysed using one-way ANOVA post hoc Bonferonni's multiple comparison test. \*\*\* P<0.01 compared with H<sub>2</sub>O<sub>2</sub> alone.

### 2.4.3.2 Reactive oxygen species

ROS generated from nicotinamide adenine dinucleotide phosphate (NADPH) oxidase (an enzyme that reduces  $O_2$  to superoxide ( $O_2^{\cdot-}$ )). Activation of microglia leads to produce ROS (Mao et al, 2007). LPS-induced neurotoxicity was shown to be mediated through ROS-mediated microglial activation, the generation of microglial-derived extracellular neurotoxic ROS, and the amplification of microglial proinflammatory gene expression. Therefore, we investigated whether apocynin, a NADPH oxidase inhibitor, was able to reduce LPS-induced NO release in microglia. BV-2 cells were treated with apocynin in different concentrations 1 hour prior to LPS alone or together with CBD for 24 hours. Although apocynin did not alter the basal level of NO, it was able significantly to reduce the LPS response in a concentration-dependant manner (Figure 2.29).

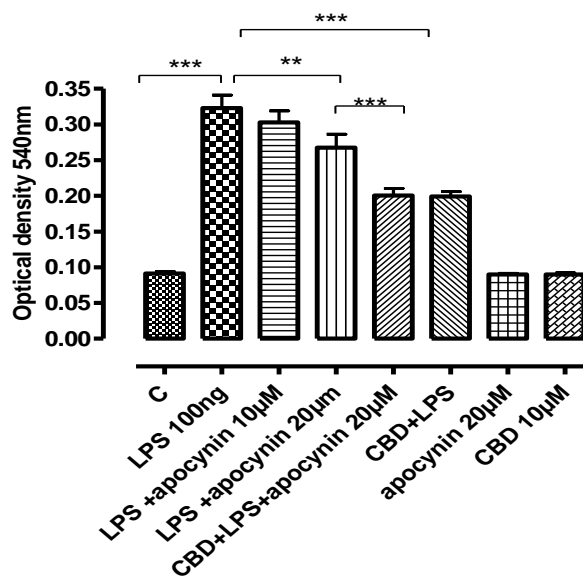


**Figure 2.29:** Histogram shows the effect of apocynin, a NADPH oxidase inhibitor (10-20µM) treatment on CBD-mediated NO inhibition LPS-induced in BV-2. BV-2 cells ( $5 \times 10^5$  cells/well) were pre-treated with apocynin (10-20µM) for 1 hour in presence or absent of LPS (100 ng/ml) and CBD (10 µM) for 24 hours. Control wells were incubated in culture medium alone. Culture supernatant was assayed for nitrite levels using the Griess reagent. Data were analysed using one-way ANOVA followed by post-hoc Bonferonni's multiple comparison test \*\*P<0.01 compared with LPS alone; \*\*\*P<CBD+LPS+ apocynin compared with LPS+CBD.

### 2.4.3.3 cannabinoid receptor antagonists

In this series of experiments, the cells were pre-incubated with either cannabinoid receptor antagonist or vehicle for 60 minutes followed by CBD for 30 minutes before exposure to 100 ng/ml LPS for 24 hours. Under these conditions, inhibition of nitric oxide release by LPS was not significantly attenuated by pre-incubation with 1  $\mu$ M of the CB<sub>1</sub>-selective receptor antagonist, SR141716A. The same concentration of the CB<sub>2</sub>-selective receptor antagonist, SR144528, had no significant effect on the inhibition of nitric oxide release by LPS (data not shown). Neither antagonist had a significant effect on the inhibition of nitric oxide release by LPS (100ng/ml), when administered alone; neither did 1  $\mu$ M SR141716A (SR1) or SR144528 (SR2) have any significant effect on LPS-induced nitric oxide production (Figure 2.30).

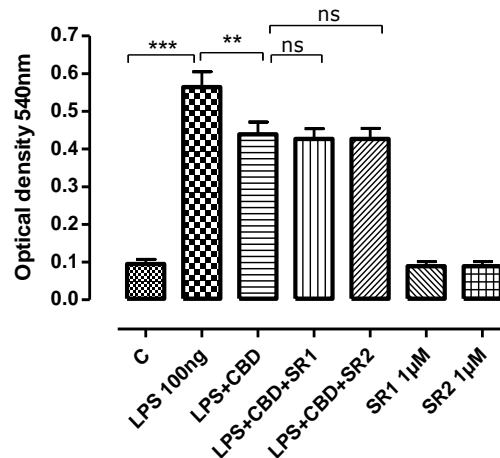


**Figure 2.30:** Histogram shows the effect of CB<sub>1</sub>/CB<sub>2</sub> antagonist treatment on CBD-mediated NO inhibition LPS-induced in BV-2. BV-2 cells ( $5 \times 10^5$  cells/well) were treated with LPS (100 ng/ml) in presence or absence of CBD (A) CB<sub>1</sub>-selective receptor antagonist, SR141716A (SR1) (B) CB<sub>2</sub>-selective receptor antagonist, SR144528 (SR2) at 1  $\mu$ M concentrations for 24 hours. Control wells were incubated in culture medium alone. Culture supernatant was assayed for nitrite levels using the Griess reagent. Data were analysed using one-way ANOVA followed by post-hoc Bonferonni's multiple comparison test P\*\*\*<0.001, \*\*P<0.01compared with LPS alone; not significant compared with LPS+CBD.

#### 2.4.3.4 Other receptors

##### 2.4.3.4.1 (5-HT) receptors

CBD acts as an agonist at the human 5-HT<sub>1A</sub> receptor and this action could possibly be involved in the protective effect of CBD in ischemia (Russo et al., 2005; Mishima et al., 2005). We, therefore, tested the effects of the 5-HT<sub>1A</sub> receptor antagonist (WAY 100635) on the CBD inhibition of LPS-mediated nitric oxide release from BV-2 cells (Figure 2.31). The cells were incubated at 37°C for 1 hour with 10 μM WAY 100635, then for 30 minutes with 10 μM CBD prior to the addition of 100 ng/ml LPS for 24 hours. WAY 100635 had no effect on basal levels, neither did it affect the inhibition of LPS-mediated NO formation by CBD.

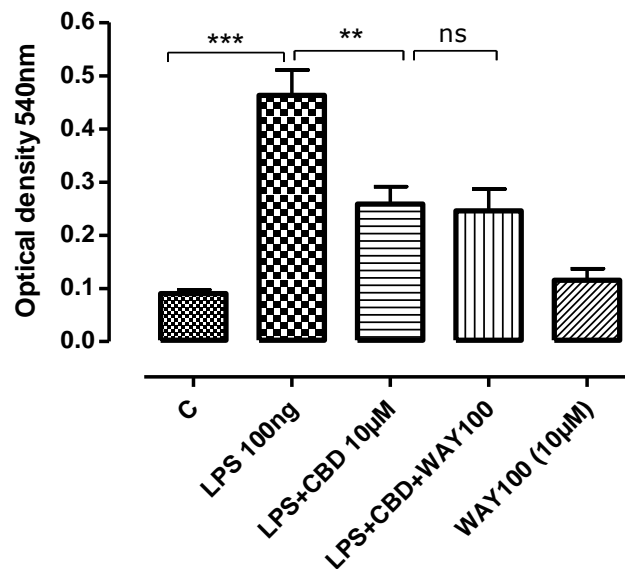


**Figure 2.31:** Histogram shows the effect of WAY100635 (a 5-HT antagonist) on CBD-inhibited NO formation induced by LPS. BV-2 cells ( $5 \times 10^5$  cells/well) were pre-treated WAY100635 (10 μM) for 1 hour with CBD (10 μM) and with LPS (100 ng) for 24 hours. Control wells were incubated in culture medium alone. Culture supernatant was assayed for nitrite levels using the Griess reaction as described in Methods. The figure represents means  $\pm$  SEM of triplicates of three independent experiments. Data were analysed using one-way ANOVA followed by post-hoc Bonferonni's multiple comparison test.  $P^{***} < 0.001$  and  $P^{**} < 0.01$  compared with LPS alone; not significant compared with LPS+CBD.

#### 2.4.3.4.2 Adenosine receptors

We investigated the role of adenosine receptors on CBD inhibition of NO induced by LPS. Adenosine receptors have been shown to have both pro-inflammatory and anti-inflammatory effects and to regulate the inflammatory process in the brain; moreover, CBD exerts anti-inflammatory effects via blockade of adenosine uptake (Liou *et al.*, 2008). We used the non-selective adenosine receptor antagonist xanthine amine congener (XAC) at 10  $\mu$ M for 1 hour before CBD, followed by LPS (100ng/ml) for 24 hours. XAC failed to reverse the CBD inhibition of NO induced by LPS and did not affect the basal NO release (Figure 2.32).

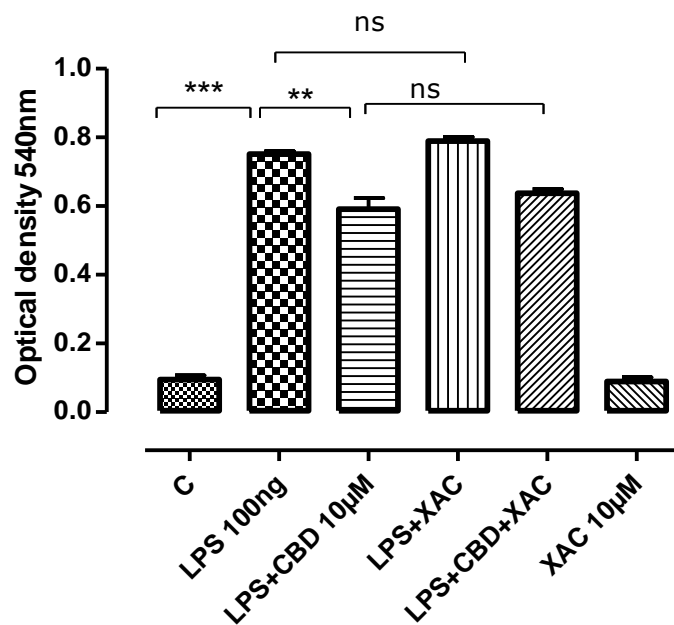


**Figure 2.32:** Histogram shows the effect of xanthine amine congener (XAC), an adenosine receptor antagonist, on CBD-inhibited NO formation induced by LPS. BV-2 cells ( $5 \times 10^5$  cells/well) were pre-treated XAC (10  $\mu$ M) for 1 hour with CBD (10  $\mu$ M) and with LPS (100ng) for 24 hours. Control wells were incubated in culture medium alone. Culture supernatant was assayed for nitrite levels using the Griess reaction as described in Methods. The figure represents means  $\pm$ SEM of triplicates of three independent experiments. Data were analysed using one-way ANOVA followed by post-hoc Bonferonni's multiple comparison test.  $P^{**} < 0.01$  compared with LPS; not significant compared with LPS+CBD.

### 2.4.3.4.3 Purinergic receptors

We tested the potential involvement of P2X and P2Y receptors on microglial activation (NO formation) using ATP and UDP-glucose as stimuli. ATP (100 nM to 400  $\mu$ M) failed to induce nitric oxide release from BV-2 cells in comparison to LPS (100 ng/ml). It also failed to alter LPS-induced NO release Figures (2.33-A and B). Moreover, UDP-glucose did not attenuate the NO release from BV-2 cells (Figure 2.34).

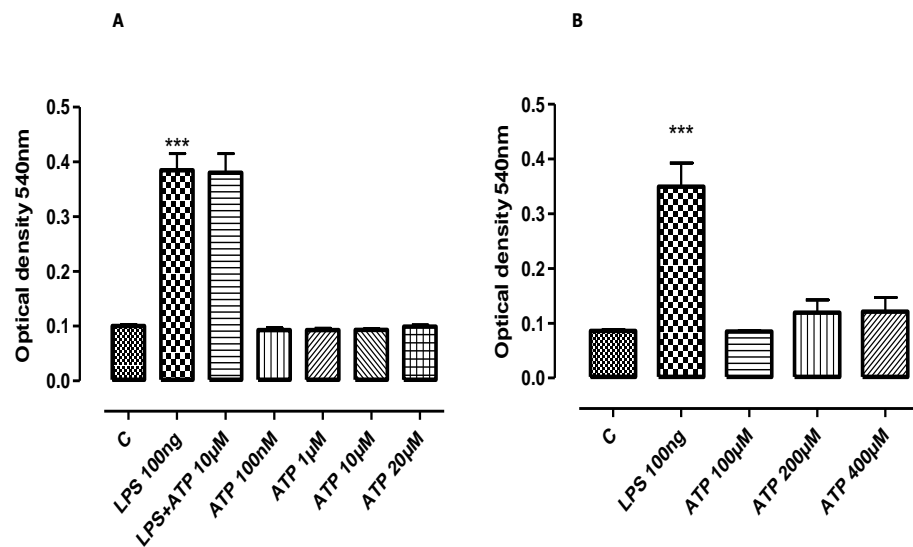


**Figure 2.33:** Histogram shows the effect of different concentrations of ATP on NO production in BV-2 cells. BV-2 cells ( $5 \times 10^5$  cells/well) were pre-treated with LPS (100 ng/ml) and ATP at the indicated concentrations for 24 hours. Control wells were incubated in culture medium alone. Culture supernatant was assayed for nitrite levels using the Griess reagent. Figure represents mean  $\pm$  SEM of triplicates from three separate experiments. Data were analysed using one-way ANOVA followed by Dunnett's test \*\*\* $p < 0.001$  compared with (C) control.

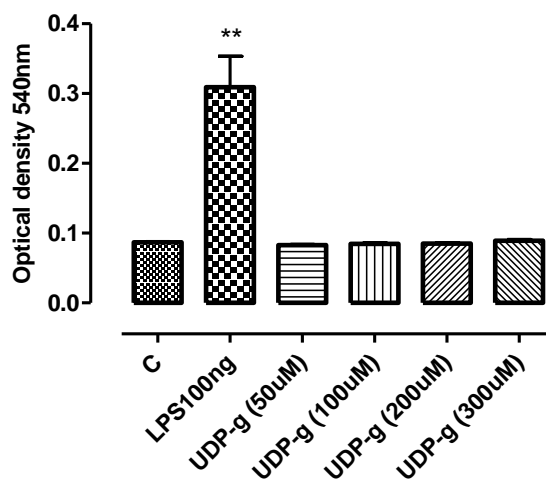


**Figure 2.34:** Histogram shows the effect of UDP-glucose on NO production in BV-2 cells. BV-2 cells ( $5 \times 10^5$  cells/well) were pre-treated with LPS (100ng/ml) and UDP-glucose at the indicated concentrations for 24 hour. Control wells were incubated in culture medium alone. Culture supernatant was assayed for nitrite levels using the Griess reagent. Figure represents mean  $\pm$  SEM of triplicates from three separate experiments. Data were analysed using one-way ANOVA followed by Dunnett's test \*\*p < 0.01 compared with (C) control.

#### 2.4.3.5 The effect of pertussis toxin on CBD mechanism of action

To further exclude any interaction with classical cannabinoid receptors and /or Gi/o protein-coupled receptors, in subsequent experiments, we pre-treated cells with 50 ng/ml of PTX for 18 hours to inactivate susceptible G proteins. This did not impair CBD inhibition of NO formation induced by LPS (Figure 2.35).

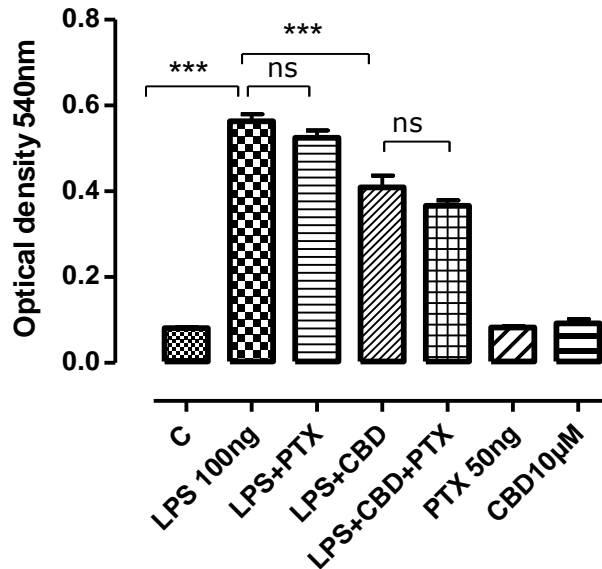


**Figure 2.35:** Histogram shows the effect of PTX treatment on CBD-mediated NO inhibition LPS-induced NO in BV-2. BV-2 cells ( $5 \times 10^5$  cells/well) were pre-treated with 50 ng/ml PTX for 18 hours at 37°C then followed with LPS (100 ng/ml) in presence or absence of CBD 10  $\mu$ M for 24 hours. Control wells were incubated in culture medium alone. Culture supernatant was assayed for nitrite levels using the Griess reagent. Figure represents means  $\pm$  SEM of triplicates from three separate experiments. Data were analysed using one way ANOVA followed by post-hoc Bonferonni's multiple comparison test.  $P^{***}<0.001$  compared with LPS alone; not significant compared with LPS+CBD.

#### 2.4.3.6 Kinases

Previous evidence has shown that inhibition of different MAPK pathways is associated with decreases in LPS-induced NO production (Kaminska et al., 2009). To further clarify which pro-inflammatory pathways might be involved in mediating the inhibition of LPS-induced NO by CBD, selective inhibitors for p38 MAPK (SB203580 10 $\mu$ M), a selective inhibitor of MEK-1/2 (U0126 10  $\mu$ M), PI3K inhibitor (wortmannin 10 $\mu$ M) and the Rho/Rock inhibitor (Y27632 10 $\mu$ M) were administered 1 hour before CBD with or without LPS stimulation for 24 hours (Figures 2.36 A- B -2.38). The results show that although SB203580 inhibited LPS-induced NO production, the p38 inhibitor was unable to block the inhibitory effects of CBD. These results suggest that p38 MAPK is associated with LPS-mediated NO

regulation. However, wortmannin, Y27632 and U0126 did not affect NO formation.

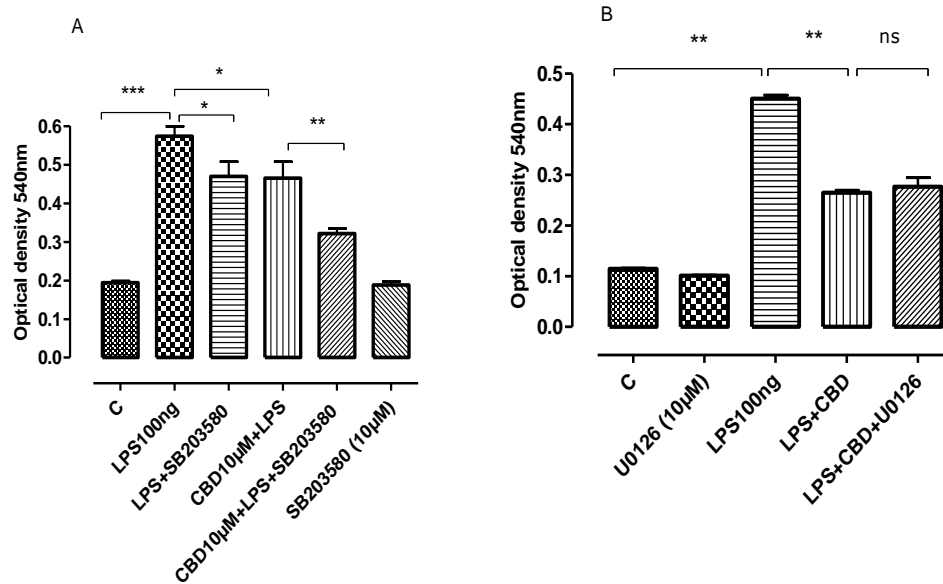


**Figure 2.36:** (A) Histogram shows the effect of P38 inhibitor (SB203580) treatment and (B) MEK1 (ERK 1/2) inhibitor (U0126) on CBD-mediated NO inhibition LPS-induced in BV-2. BV-2 cells ( $5 \times 10^5$  cells/well) were pre-treated with SB203580 or U0126 ( $10 \mu\text{M}$ ) for 1 hour in presence or absence of LPS ( $100 \text{ ng/ml}$ ) and CBD ( $10 \mu\text{M}$ ) for 24 hours. Control wells were incubated in culture medium alone. Culture supernatant was assayed for nitrite levels using the Griess reagent. Figure represents means  $\pm$  SEM of triplicates from three separate experiments. Data were analysed using ANOVA followed by post-hoc Bonferonni's multiple comparison test (A)  $*P < 0.05$  compared with LPS alone  $***P < 0.001$  (C) control vs. LPS alone and  $**P < 0.01$  vs. LPS+ CBD. (B)  $**p < 0.01$  LPS alone vs. (C) control, LPS+ CBD.

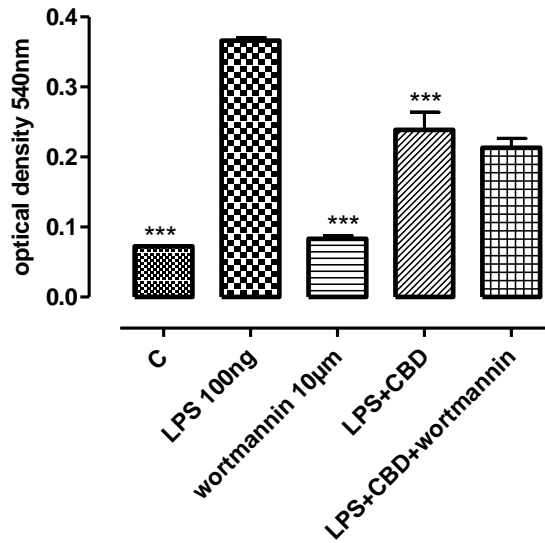


**Figure 2.37:** Histogram shows the effect of PI3K inhibitor (wortmannin) treatment on CBD-mediated NO inhibition LPS-induced in BV-2. BV-2 cells ( $5 \times 10^5$  cells/well) were pre-treated with wortmannin ( $10 \mu\text{M}$ ) for 1 hour in presence or absence of LPS ( $100 \text{ ng/ml}$ ) and CBD ( $10 \mu\text{M}$ ) for 24 h. Control wells were incubated in culture medium alone. Culture supernatant was assayed for nitrite levels using the Griess reagent. Figure represents means  $\pm$  SEM of triplicates from three separate experiments. Data were analysed using one-way ANOVA followed by post-hoc Bonferonni's multiple comparison test \*\*\* $P < 0.001$  compared with LPS alone; not significant compared with LPS+CBD.

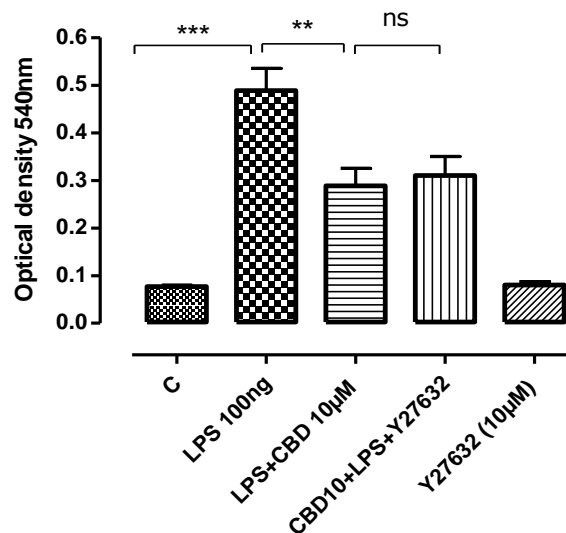


**Figure 2.38:** Histogram shows the effect of Rho/ROCK inhibitor (Y27632,  $10 \mu\text{M}$ ) treatment on CBD-mediated NO inhibition LPS-induced in BV-2. BV-2 cells ( $5 \times 10^5$  cells/well) were pre-treated with Y27632 ( $10 \mu\text{M}$ ) for 1 hour in presence or absent of LPS ( $100 \text{ ng/ml}$ ) and CBD ( $10 \mu\text{M}$ ) for 24 hours. Control wells were incubated in culture medium alone. Culture supernatant was assayed for nitrite levels using the Griess reagent. Data were analysed using ANOVA followed by post-hoc Bonferonni's multiple comparison test \*\* $P < 0.01$  and \*\*\* $P < 0.001$  compared with LPS alone.

## **2.4.4 Characterization of CBD effects on LPS-evoked changes in inflammatory markers**

### **2.4.4.1 iNOS expression**

Cannabidiol (CBD) at 10  $\mu\text{M}$  significantly inhibited LPS-stimulated NO formation (see Figure 2.16). Using Western blotting, we found that LPS application (100ng/ml for 24h) significantly stimulated iNOS protein expression in BV-2 cells. CBD was able to significantly inhibit LPS-induced increases in expression at 1 $\mu\text{M}$  and completely blocked it at 10 $\mu\text{M}$ . In the presence of 1400W, a selective inhibitor of iNOS activity, (Saura, 2007) CBD significantly affected LPS-induced iNOS stimulation only at 10 $\mu\text{M}$ . there was a strong trend towards a reduction in the presence of 1  $\mu\text{M}$  CBD. This was not apparently secondary to a reduction in iNOS activity since the iNOS inhibitor 1400W was without effect (Figure 2.39 A-B).

In order to determine whether the increase in NO by LPS was due to enhanced iNOS expression; we tested the effect of various MAPK and NADPH oxidase inhibitors on BV2 iNOS expression. We examined the effect of the NADPH oxidase inhibitor (apocynin 15 $\mu\text{M}$ ) on LPS-induced iNOS expression in BV-2 cells. LPS significantly stimulated iNOS protein expression at 5, 24 and 30 hours (Figure 2.40 A-B) and this was completely blocked by apocynin at 24 hours. Also, to examine the role of MAPKs in LPS's enhancement of iNOS expression, a variety of inhibitors (used in NO release experiments described earlier in this chapter) were employed. We found that SB203580, a P38 inhibitor, and wortmannin, a PI3K inhibitor, significantly reduced iNOS induced by LPS, whereas Y27632, a ROCK inhibitor, and U0126, a MEK 1/2 inhibitor, were not able to attenuate the LPS-mediated induction of iNOS protein (Figure 2.41 A-B). To confirm that the microglial cells had actually been activated to increase expression of iNOS, we used an immunohistochemical approach to visualize

iNOS expression in primary microglial and BV-2 cells. LPS enhanced iNOS expression in both cell types and this was completely reversed by CBD (Figure 2.42; A-C). To distinguish between microglia and other glial cells, LB $\alpha$ -1 a microglia marker was employed (Figure 2.42; D-F).

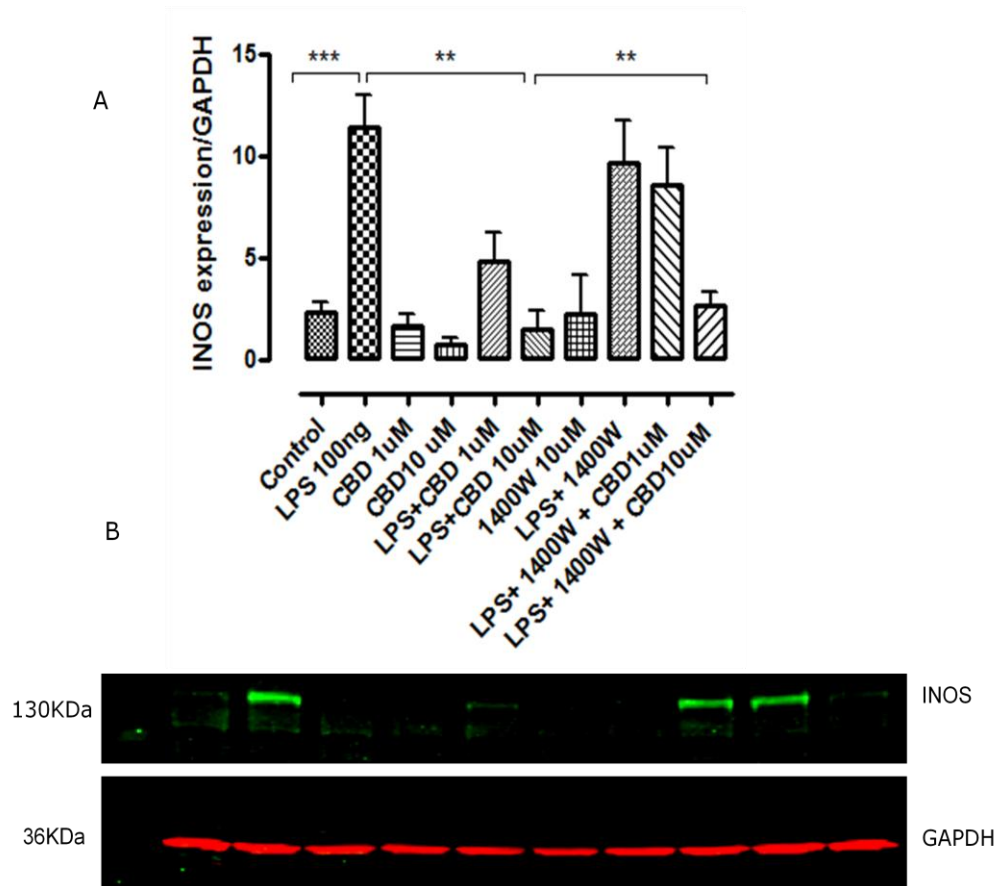


**Figure 2.39:** Western blot and histogram show increase in the expression of the ratio of iNOS expression and GAPDH in whole cell lysates of BV-2 (20 $\mu$ g protein) at 24 hours. BV-2 cells ( $5 \times 10^5$ ) treated with 1400W (10  $\mu$ M) for 1 hour prior to CBD then stimulated LPS 100 ng/ml and control cell (basal) blots were incubated with Rabbit antibody to iNOS followed by IRDY<sup>®</sup> conjugatesgoat anti-Rabbit IgG. **(A)** Histogram; Data shown are the mean of 3 experiments $\pm$  SEM. **(B)** green presented of the iNOS at 130KDa, red is GAPDH. Data were analysed using one-way ANOVA followed by post-hoc Bonferonni's multiple comparison test  $**P < 0.01$ .

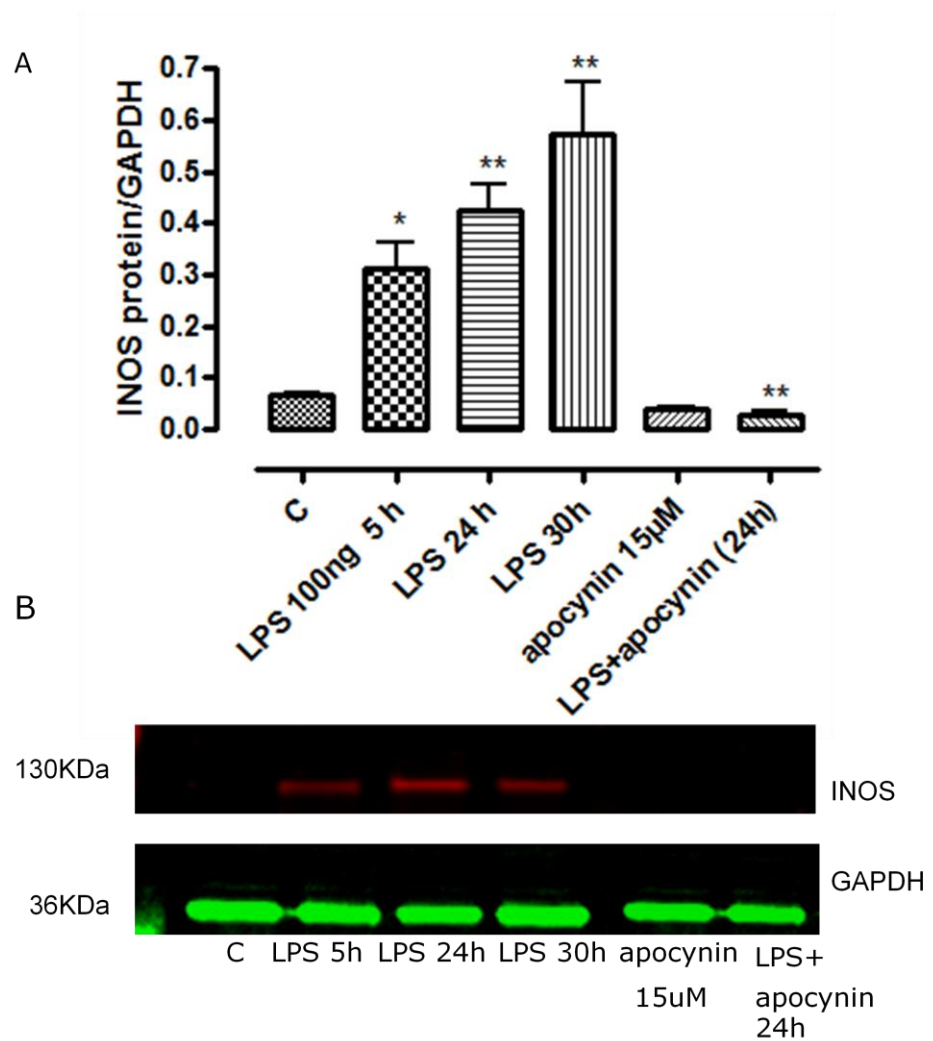


**Figure 2.40:** Western and histogram show the effect of apocynin on the ratio of iNOS expression and GAPDH levels in whole cell lysates of BV-2 cells (20µg protein). BV-2 cells ( $5 \times 10^5$ ) were treated with LPS 100 ng/ml at indicated times alone or with apocynin 15µM and control cell (C) blots were incubated with a rabbit antibody to iNOS followed by IRDY<sup>®</sup> conjugatesgoat goat anti-Rabbit IgG. **(A)** Histogram; Data shown are the mean of 3 experiments  $\pm$  SEM. **(B)** Red bands represents iNOS 130 KDa, green is GAPDH. Data were analysed using one-way ANOVA followed by Dunnett's test. \*  $P < 0.05$ , \*\* $P <$  compared with control; \*\* $P <$  LPA+apocynin compared with LPS alone.

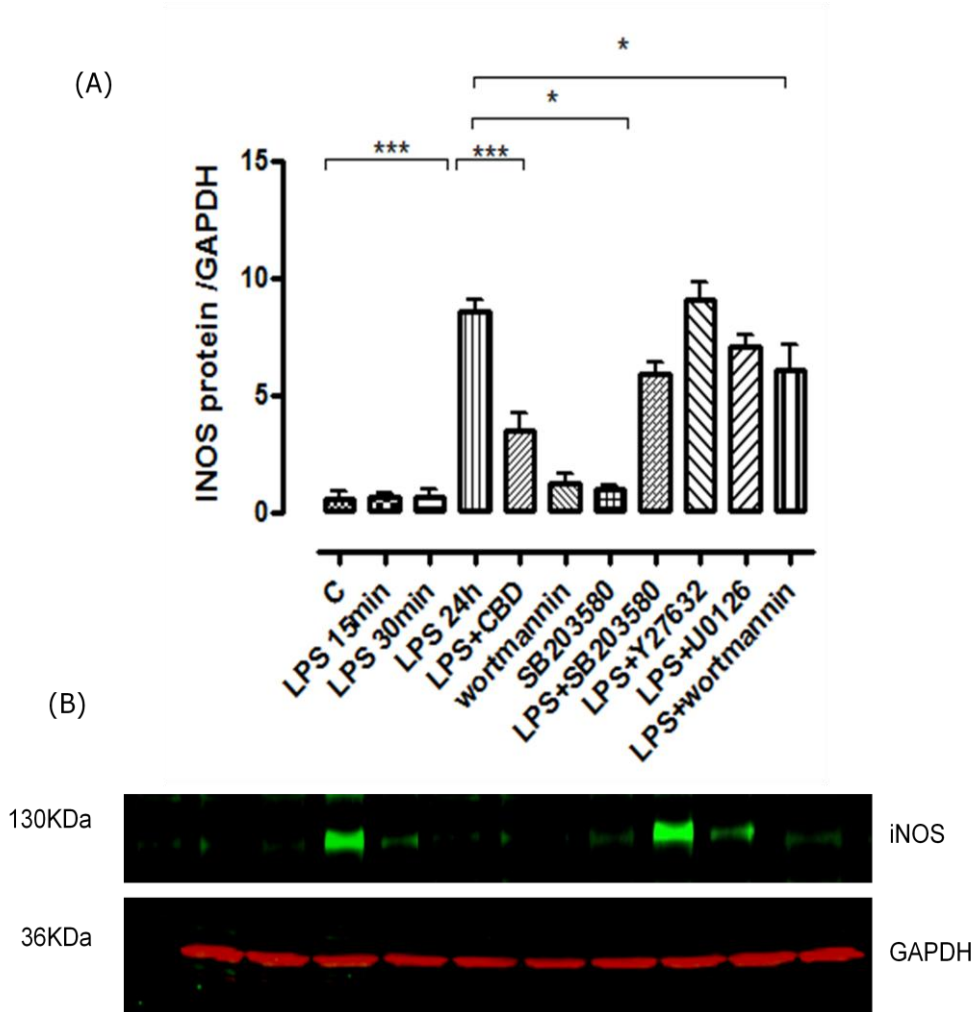
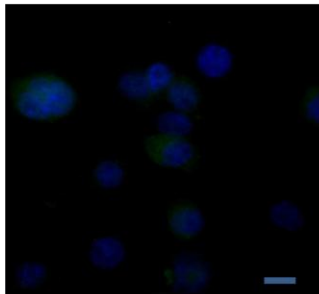


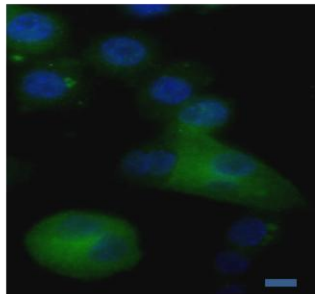
**Figure 2.41:** Western and histogram show the effect of MAPKs on the ratio of iNOS expression and GAPDH levels in whole cell lysates of BV-2 cells (20µg protein). BV-2 cells ( $5 \times 10^5$ ) were treated with LPS 100 ng/ml or 10 ng/ml incubated at indicated times alone or with CBD (10 µM), p38 inhibitor SB203580 (10 µM), PI3K inhibitor wortmannin, Y27632 and U0126 (all 10 µM) for 24 hours and basal (vehicle) blots were incubated with rabbit antibody to iNOS followed by IRDY<sup>®</sup> conjugatesgoat anti-Rabbit IgG anti-rabbit IgG. **(A)** Histogram; Data shown are the mean of 3 experiments± SEM. **(B)** Red represents GAPDH, green is iNOS. Data were analysed using one-way ANOVA followed by Dunnett’s test. \*\*\* P<0.001and \*P<0.05 compared with control (C) or with LPS alone.

## 1. BV- 2

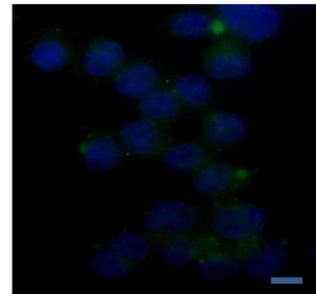
**A. Control**



**B. LPS 100ng**

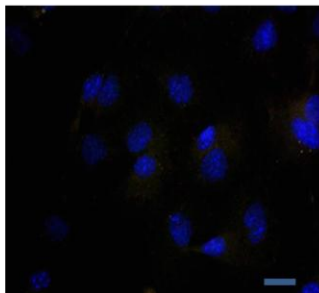


**C. LPS+CBD**

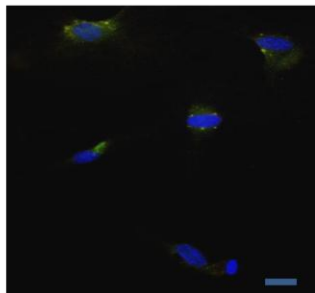


## 2. Primary microglia

**D. Control**



**E. LPS 100ng**



**F. LPS+CBD**

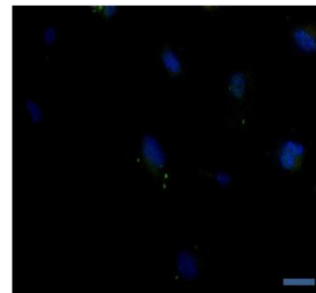


**Figure 2.42:** Immunocytochemistry shows the effect of CBD on iNOS expression induced by LPS in BV-2 and mouse primary microglial cells. **(A)** control **(B)** LPS stimulated cells for 24 hours **(C)** Cells were pretreated with CBD for 1 hour before stimulation by LPS (100 ng/ml) for 24 hours **(D)** primary microglia control **(E)** LPS stimulated cells for 24 hours **(F)** Cells were pretreated with CBD for 1 hr before stimulation by LPS (100 ng/ml) for 24 hrs. (A-B) Green; iNOS and Blue; DAPI (40 x), (D-F) Green; iNOS, Red; LBa-1 microglia marker and Blue DAPI nucleus (40 X magafication).

### 2.4.4.2 Reactive Oxygen Species (ROS)

It is reported that many stress factors, including oxidative stress, lead to inflammation. Therefore, to test whether both apocynin and CBD were capable of reducing ROS production in BV-2 after stimulation with LPS, we determined ROS formation after 100 ng/ml LPS treatment in the presence and absence of CBD. The DCF assay (Keston and Brandt, 1965) showed that stimulation of the cells with LPS resulted in time- and concentration-dependent increases in ROS (30 minutes); gradually increasing at 60 minutes (Figure 2.43; A-B). Pretreatment of BV-2 cells with either 10  $\mu$ M

CBD or apocynin (15  $\mu$ M; a selective NADPH oxidase assembly inhibitor) for 1 hour prior to LPS (100 ng/ml) for 24 hours, significantly reduced ROS formation (Figure 2.44; A). To investigate the effect of CBD on ROS formation at different times, we also treated BV2 cells with CBD for 1 hour prior to LPS and LPS alone (Figure 2.44; B). DCF assay showed that stimulation of the cells with LPS caused increases in ROS formation whereas CBD (10  $\mu$ M) significantly reduced LPS-induced superoxide formation at 30 minutes. In contrast, CBD alone stimulated basal ROS formation, (Figure 2.44; B)

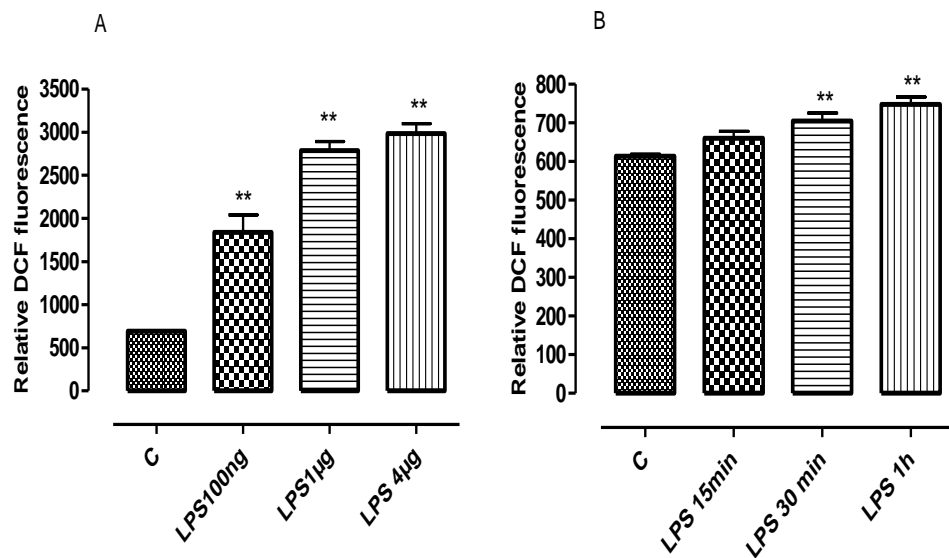


**Figure 2.43:** Histograms show the effect of LPS on ROS formation in BV-2 by DCF assay. BV-2 ( $5 \times 10^5$  cells/well) treated with LPS 100ng/ml or vehicle for indicated time. Maximal ROS formation and then intracellular ROS level was quantified using DCF assay (A): LPS concentration response data. (B) LPS time dependence. Data shown are the mean  $\pm$ SEM of 3 samples. Data were analysed using ANOVA followed by post-hoc Bonferonni's multiple comparison test \*\* $P < 0.01$  compared with control (A and B).

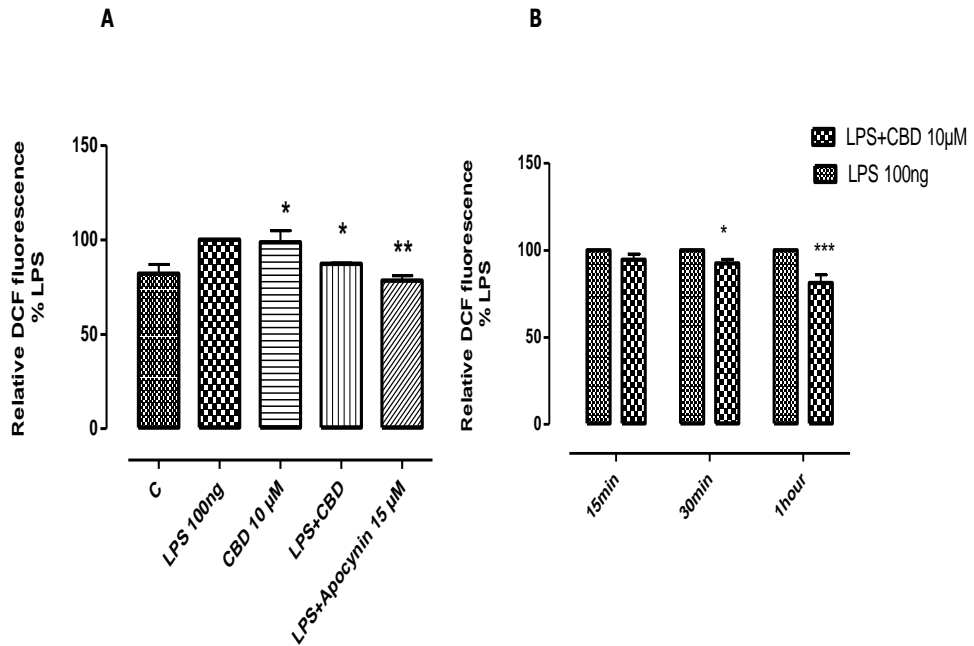


**Figure 2.44:** Histograms show the effect of CBD on LPS-induced ROS in BV-2 by DCF assay. BV-2 ( $5 \times 10^5$  cells/well) treated with CBD (10  $\mu$ M) for 1 hour, followed by vehicle or LPS 100ng/ml for indicated time. Maximal ROS formation and then intracellular ROS level was quantified using DCF assay (A) Comparison of ROS formation measured by DCF assay on BV-2 cells pretreated with CBD at 1 hour, apocynin, and treated with vehicle (control) or LPS 100ng/ml. (B) Effect of CBD on LPS-induced ROS at indicated time. Data shown are the mean  $\pm$ SEM of 3 samples. Data were analysed using one-way ANOVA or Two-way ANOVA followed by post-hoc Bonferonni's multiple comparison test. (A) \* $P < 0.05$  LPS+CBD compared with LPS alone; \*\* $P < 0.01$  LPS+Apocynin vs. LPS alone; \* $P < 0.05$  CBD vs. control. (B) \*\*\* $P < 0.001$  CBD+LPS compared with LPS alone; \* $p < 0.05$  LPS+CBD vs. LPS alone.

#### 2.4.4.3 COX-2 expression

The effects of LPS on cyclooxygenase 2 (COX-2) activity were investigated by Western blot analysis. Under basal conditions, microglial cells did not appear to express COX-2, but protein levels were significantly increased by 24 hours stimulation in the presence of LPS. CBD completely reversed the LPS-mediated COX-2 induction (Figure 2.45; A, B).

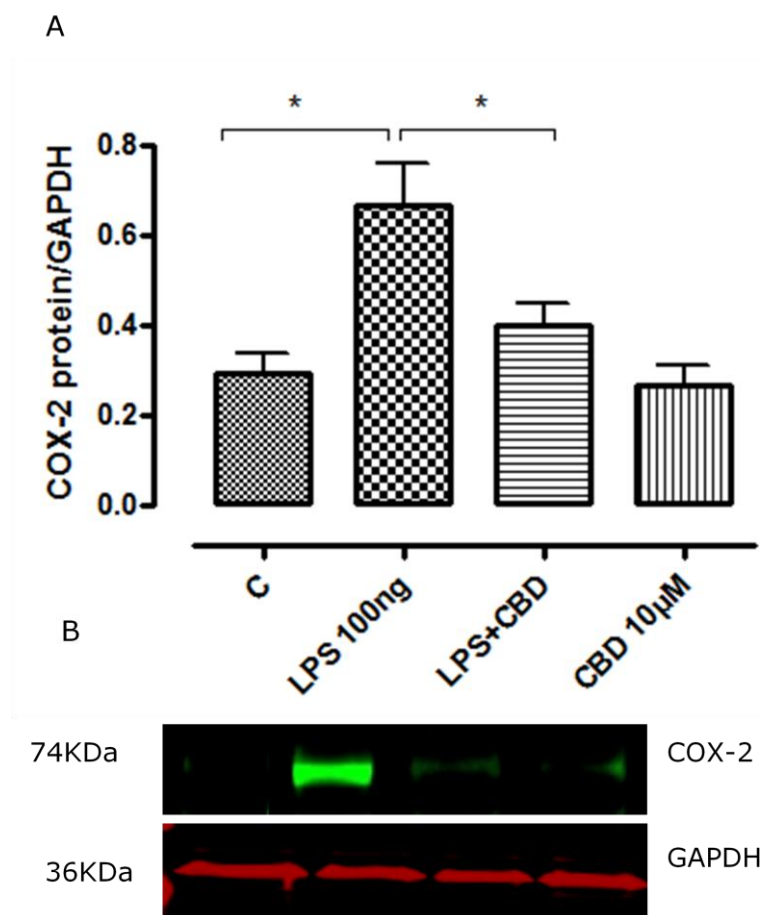


**Figure 2.45:** Western blot and histogram show increase the expression of ratio of COX-2 expression to GAPDH levels in whole cell lysates of BV-2 (20µg protein) at 24 hours. BV-2 cells ( $5 \times 10^5$  cells/ell) treated with LPS 100 ng/ml incubated at times alone or with CBD 10 µM or vehicle. Blots were incubated with rabbit antibody to COX-2 followed by IRDY<sup>®</sup> conjugates goat anti-Rabbit IgG. (A) Histogram; Data shown are the mean of 3 experiments  $\pm$  SEM. (B) Red represents GAPDH; green is COX-2 at 74KDa. Data were analysed using one-way ANOVA followed by Bonferonni's multiple comparison test \*  $P < 0.05$  LPS alone compared with control (C); \* $P < 0.05$  LPS+CBD compared with LPS alone.

#### 2.4.4.4 MAPK activation

MAPKs are thought to be important in the signaling pathways that control the production of pro-inflammatory mediators by activated microglia and LPS activates MAPK signal-transduction pathways (Hill and Treisman, 1995). Therefore, we investigated the potential effects of CBD on phosphorylation/activation of the MAP kinases P38, JNK, and ERK in response to LPS in BV-2 cells by Western blot analysis.

Stimulation of cells with LPS resulted in increased phosphorylation of all three MAPKs, and this peaked at 30-60 minutes. We investigated also the effect of LPS on P38 activation (phosphorylation) at early times (15, 30 and 1 hour and at 24 hours. LPS stimulated P38 activation at 30 minutes until 24 hours and, CBD 10  $\mu$ M significantly inhibited P38 activation induced by LPS at 30 minutes and at 24 hours (Figure 2.46-2.47; A-B).

Moreover, we investigated if reactive oxygen species (ROS) and SB203580 had any effect on activation of the P38 MAPK pathway induced by LPS in BV-2 cells. The NADPH oxidase inhibitor (15  $\mu$ M), added 60 minutes before stimulation with LPS for 24 hours, significantly inhibited LPS-induced P38 activation (Figure 2.47; A-B).

Using Western blotting, protein bands representing ERK1/2 and phosphorylated ERK were detected at 44/42 KDa, Figure 2.48 showed that LPS activated ERK1/2 significantly at 15 and 30 minutes. But CBD failed to activate phospho-ERK or total ERK and the phospho-ERK/ERK ratio (Figure 2.49). To verify the role of the endogenous GPR55 ligand LPI on ERK phosphorylation as positive control for ERK 1/2 activation in BV-2, Figure 2.49 shows that p-ERK/ERK ratio following treatment with LPI was activated. We examine the role of CBD and LPS on c-Jun N-terminal kinases (JNKs/SAPKs). We collected samples at different time points ranging from 15 minutes-24 hours. Western blot analysis showed that LPS triggered an early (30 minutes) increase in the activation of stress-activated JNKs/SAPKs. CBD (10 $\mu$ M) inhibited LPS-induced JNK 1/2 phosphorylation in BV-2 cells (Figure 2.50).

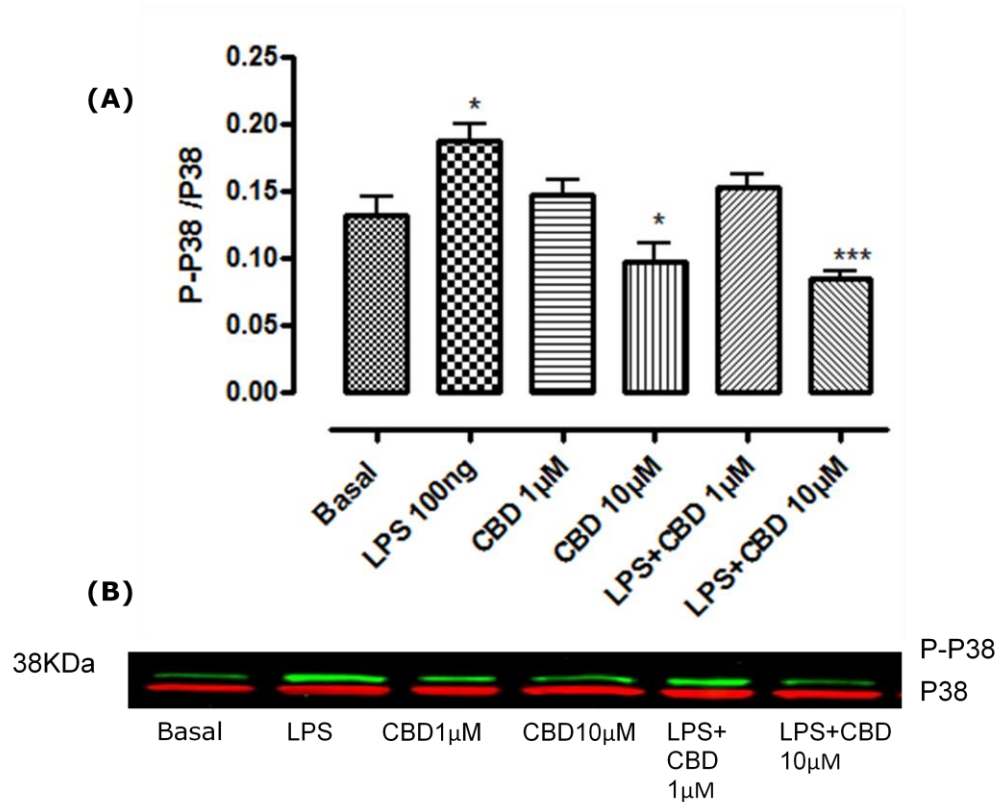


**Figure 2.46:** Western blot and histogram show increase the ratio of phospho-P38 to total P38 expression in whole cells lysates (20μg protein) of BV-2 cells by LPS and inhibited by CBD. BV-2 cells ( $5 \times 10^5$ ) were treated with LPS 100 ng/ml alone and CBD at indicated concentrations alone or with LPS or basal (control) for 24 hours. Blots were incubated with P38 antibody followed by IRDY<sup>®</sup> conjugates goat anti-mouse and anti-rabbit IgG. (A) Histogram; Data shown are the mean of 3 experiments  $\pm$  SEM (B) Red represents total P38, green is phospho-P38. Data were analysed using ANOVA followed by Dunnett's test. \*  $P < 0.05$  and \* $P < 0.05$  compared with basal; \*\*\* $p < 0.001$  LPS+CBD compared with LPS alone.

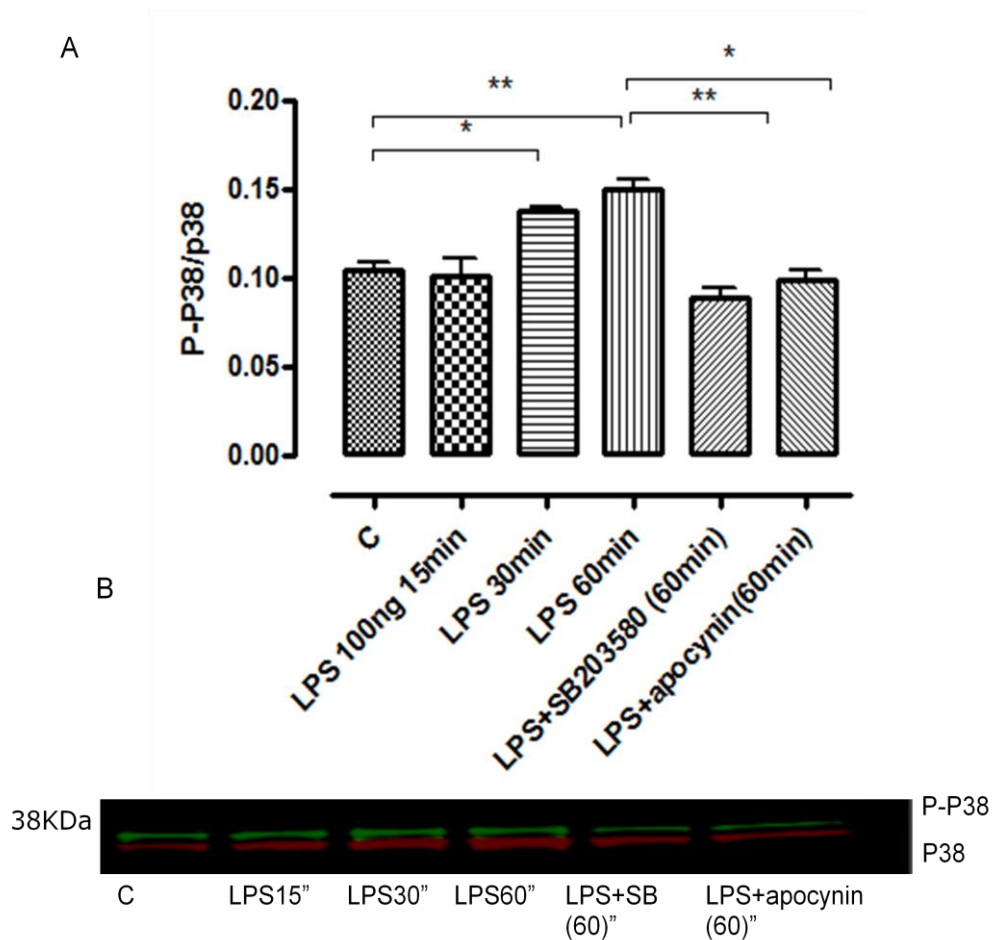


**Figure 2.47:** Western blot and histogram show increase the ratio of phospho-P38 to total P38 expression in whole cells lysates at 30 and 60 minutes (20 $\mu$ g protein) by LPS at 30" and 60" and inhibited by SB203580 and apocyanin. BV-2 cells ( $5 \times 10^5$ ) treated with LPS 100 ng/ml incubated at indicated times alone or with P38 inhibitor SB203580 10 $\mu$ M or with apocyanin 10 $\mu$ M or control (C) and blots were incubated with P38 antibody followed by IRDY<sup>®</sup> conjugates goat anti-mouse and anti-rabbit IgG. (A) Histogram; Data shown are the means of 3 experiments $\pm$  SEM. (B) Red represents total P38, green is phospho-P38 at 38KDa. Data were analysed using ANOVA followed by Dunnett's test. \*  $P < 0.05$  and \*\* $P < 0.01$  compared with (C) control or \*\* $p < 0.01$  with LPS alone.

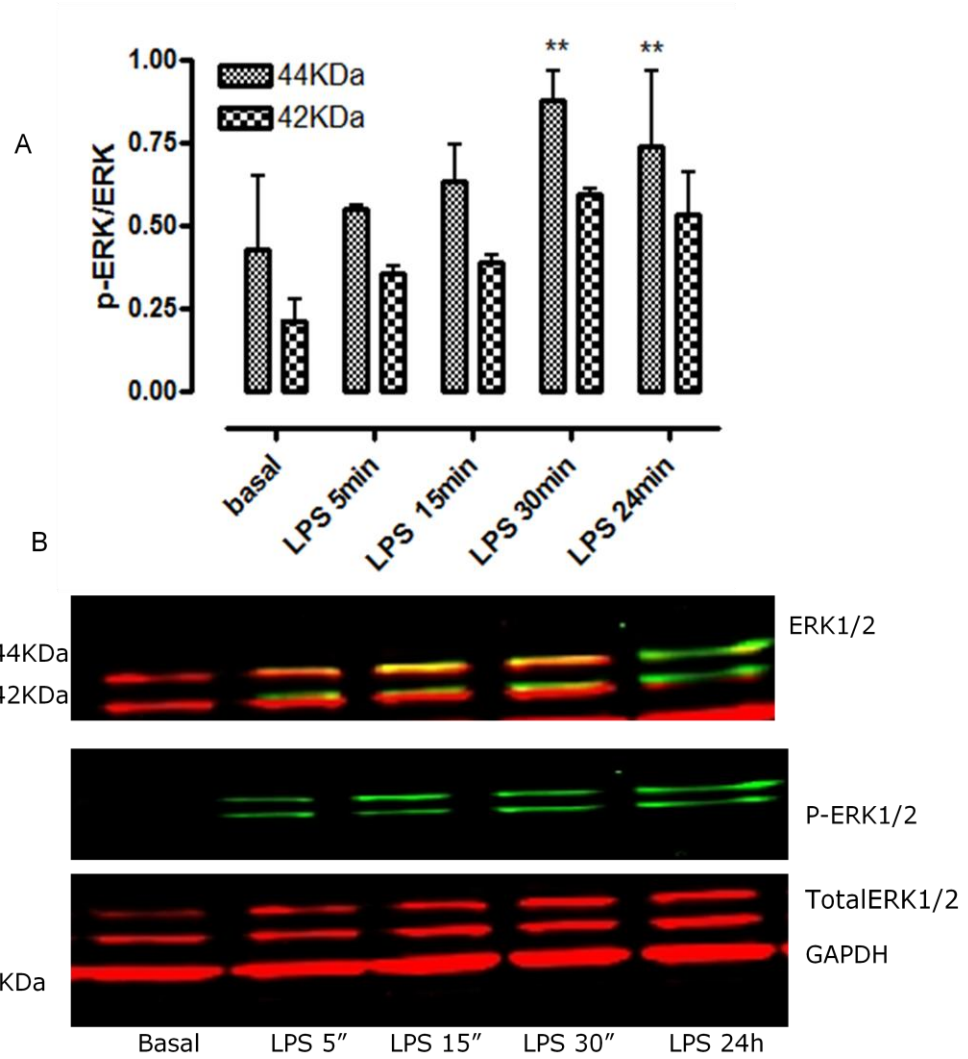


**Figure 2.48:** Western blot and histogram show the increase the ratio of phospho ERK 1/2 to total ERK 1/2 expression in whole cell lysates by LPS (20 μg protein) of BV-2 by LPS at 30" and 24 hrs. BV-2 cells (5x10<sup>5</sup>) were treated with LPS (100ng/ml) or basal for indicated times. Blots were incubated with mouse antibody to ERK 1/2 followed by IRDY<sup>®</sup> conjugates goat anti-mouse and anti-rabbit IgG. (A) Histogram Data shown are the mean of 3 experiments ± SEM. Two way ANOVA post-hoc Test; \*\*p < 0.01 LPS vs. basal (control) ; (B) ERK1/2, at 44 KDa and 42KDa.

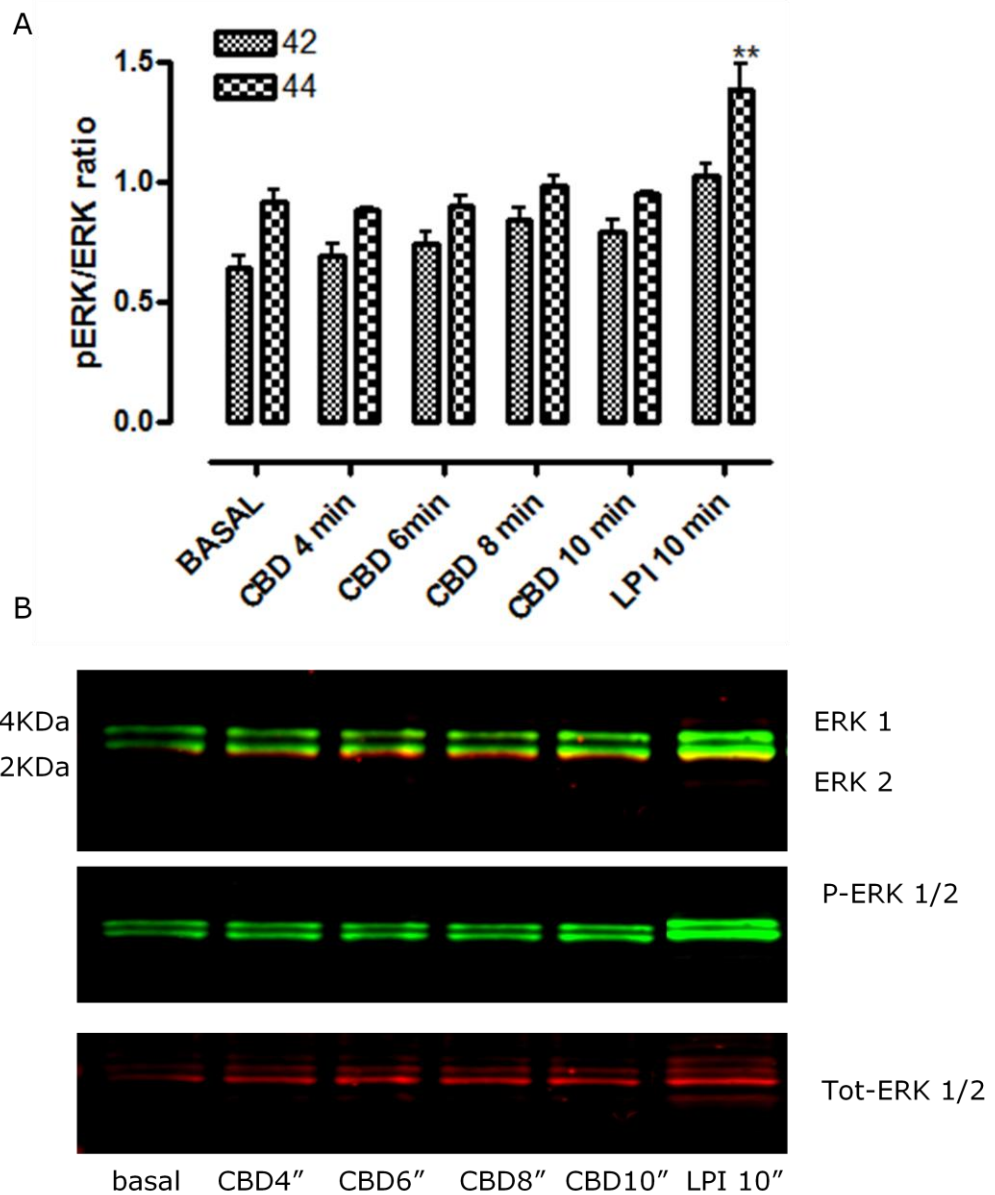


**Figure 2.49** Western blot and histogram show the increase of phospho-ERK 1/2 and the ratio phospho ERK 1/2 to total ERK 1/2 expression in whole cell lysates BV-2 by LPI at 10". BV-2 cells ( $5 \times 10^5$ ) were treated with CBD ( $10 \mu\text{M}$ ) for indicated times and LPI ( $10 \mu\text{M}$ ). Blots were incubated with mouse antibody to ERK1/2 followed by IRDY<sup>®</sup> conjugates goat anti-mouse and anti-rabbit IgG. (A) Histogram data shown are the mean of 3 experiments  $\pm$  SEM. Two way ANOVA post-hoc Test\*\* $p < 0.01$  LPI vs. Basal (B) ERK 1/2 at 44 KDa and 42K Da.

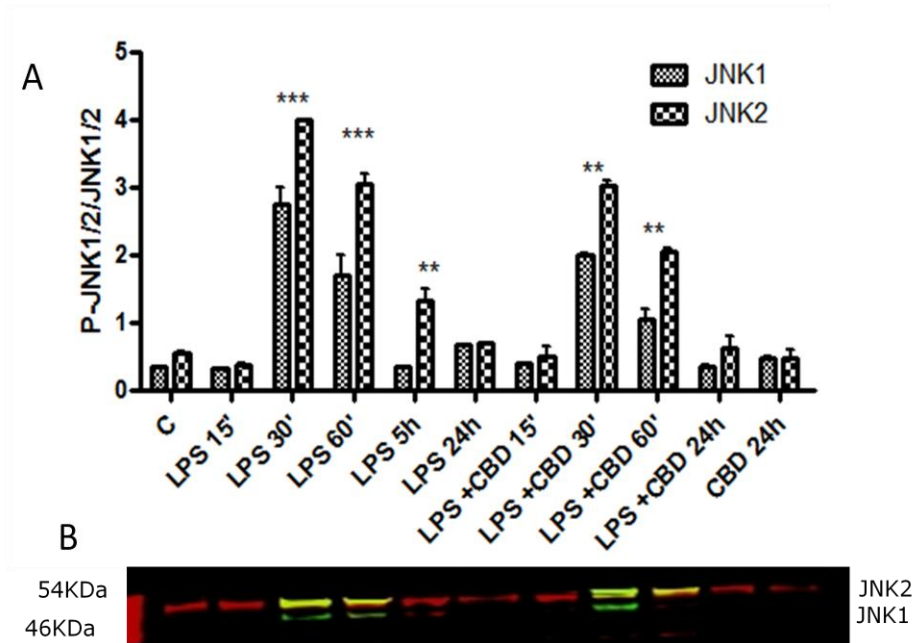


**Figure 2.50:** Westren blot and histogram show increase of the ratio of phaspho JNK 1/2 to total JNK 1/2 expression in whole cell extracts of BV-2 cells by LPS at 30" and 60" and inhibited by CBD at the same times. ( $5 \times 10^5$ ) treated with LPS (100 ng/ml) alone or with CBD 10  $\mu$ M for indicated times or control (C). Blots were incubated with mouse antibody to JNK1/2 followed by IRDY<sup>®</sup> conjugates goat anti-mouse and anti-rabbit IgG. (A) Data is the mean of 3 experiments  $\pm$  SEM, Two way ANOVA post-hoc Test\*\*\* $p < 0.001$  LPS alone vs. control; \*\* $p < 0.01$  LPS+CBD at (30 and 60 mins) vs. LPS alone. (B) Red presented of the total JNK1/2, green is phosho JNK1/2.

#### 2.4.4.5 NF $\kappa$ B/I $\kappa$ B alpha expression

NF- $\kappa$ B is an important transcription factor in the regulation of pro-inflammatory mediators and enzymes; including iNOS (Xie *et al.*, 1994). It can be activated by LPS or inflammatory cytokines. We analyzed NF- $\kappa$ B activation by measuring (using immunocytochemistry) the levels of the p65 subunit upon cell stimulation by LPS. Induction of the p65 subunit was investigated because p65 plays a major role in NF- $\kappa$ B activation and function, and it contains the transactivation domain responsible for the transcriptional activity of NF- $\kappa$ B. LPS treatment induced the nuclear translocation of p65 NF- $\kappa$ B within 1 hour of incubation.

Exposure of BV2 cells to LPS resulted in intensified nuclear staining, compared with the diffuse cytosolic staining in untreated cells. In the unstimulated condition, NF- $\kappa$ B p65 protein was mainly located in the cytoplasm and there was little staining for p65 in the nuclei (Figure 2.51; A). In microglial cells that were activated by LPS increased NF- $\kappa$ B nuclear translocation was observed (there are more yellowish areas visible in the nucleus than in the cytoplasm (Figure 2.51; B). Pretreatment with CBD inhibited this LPS-induced nuclear translocation of p65 NF- $\kappa$ B (Figure 2.51; C).

To confirm the inhibitory effect of CBD on the LPS-induced nuclear translocation of NF- $\kappa$ B, immunoblotting was conducted with whole cell lysates and nuclear fractions (Figure 2.52-2.53). NF- $\kappa$ B is a heterodimeric cytosolic protein which, in resting cells, is kept inactive by binding with a member of the I $\kappa$ B $\alpha$  inhibitor protein family (O'Neill and Kaltschmidt., 1997). After phosphorylation, I $\kappa$ B $\alpha$  is ubiquitinated and degraded by the proteasome system and NF- $\kappa$ B can translocate to the nucleus promoting transcription of a number of pro-inflammatory proteins including iNOS. We first determined the time course of I $\kappa$ B $\alpha$  phosphorylation in whole cell lysates. For these experiments BV-2 cells were treated with LPS 100 ng/ml for 5, 15, 30 and 60 minutes. We found that LPS significantly activated I $\kappa$ B $\alpha$  within 30 minutes (Figure 2.54).

Results from these cytosolic analyses demonstrated that phosphorylation of I $\kappa$ B $\alpha$  at 24 hours was not detectable in unstimulated cells or after exposure to CBD alone (Figure 2.55). Phosphorylation of I $\kappa$ B $\alpha$  occurred upon LPS stimulation and the level of phosphorylation was inhibited in cells pretreated with CBD. These results suggest that the inhibitory effects of CBD on NF- $\kappa$ B function are dependent on I $\kappa$ B $\alpha$ .

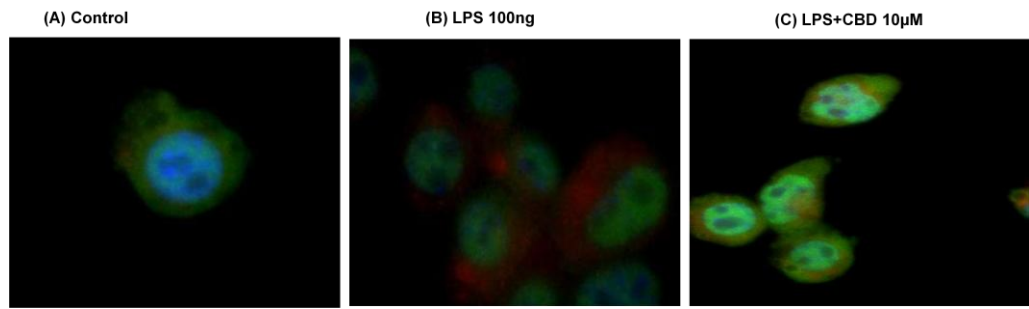


**Figure 2.51:** Immunocytochemistry; Inhibition of LPS-induced NF-κB by CBD in BV-2 cells **(A)** control **(B)** LPS 100ng/ml stimulated cells for 1 hour **(C)** Cells were pretreated with CBD for 1 hour before stimulation by LPS (100 ng/ml) for 1 hr. Untreated cells displayed diffuse cytoplasmic staining, whereas intensified staining in the nucleus was observed in LPS-treated cells is indicative of NF-κB nuclear translocation. Pretreatment of cells with CBD (10 μM) attenuated the LPS-induced translocation of NF-κB. Three independent experiments were analysed by Velocity Demo 6 software. Green p-NF-κB, Red total NF-κB and blue DAPI.

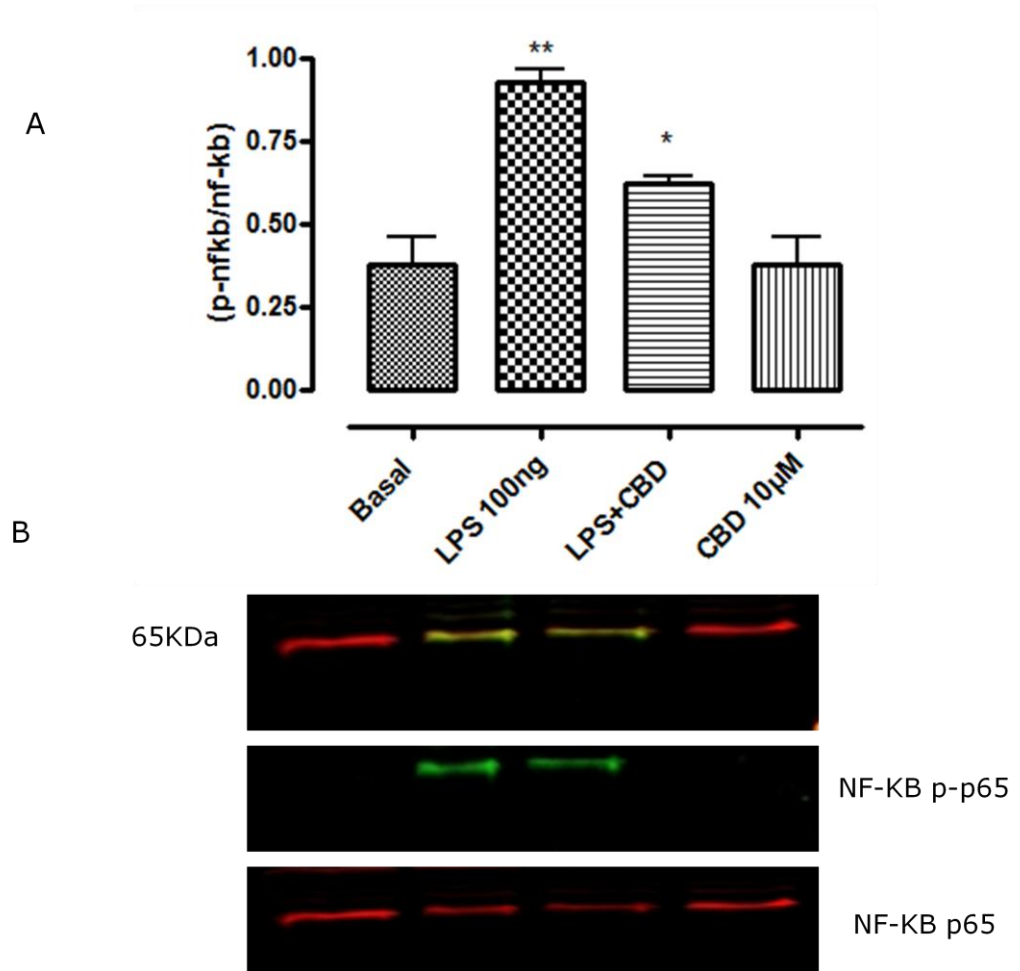


**Figure 2.52:** Western blot and histogram show increase of phaspho-NF-KB and the ratio of phosphor-NF-KB to total NF-KB expression of nuclear lysates of BV-2 cells (protein 5µg) at 1hour by LPS and inhabited by CBD. BV-2 cells ( $5 \times 10^5$  cells/well) were treated with LPS 100 ng/ml alone or with CBD (10 µM) or basal (control) for 1 hour prior stimulated with LPS) for 1 hour. Blots were incubated with mouse antibody to NF-KB followed by IRDY<sup>®</sup> conjugates goat anti-rabbit and anti-mouse IgG. Red represents the total NF-KB, green is phospho-NF-KB. Data shown are the mean of 3 experiments  $\pm$ SEM, Data were analysed using one-way ANOVA followed by Dunnett's test \* \*P<0.01 compared with basal and \*P<0.05 with LPS alone.

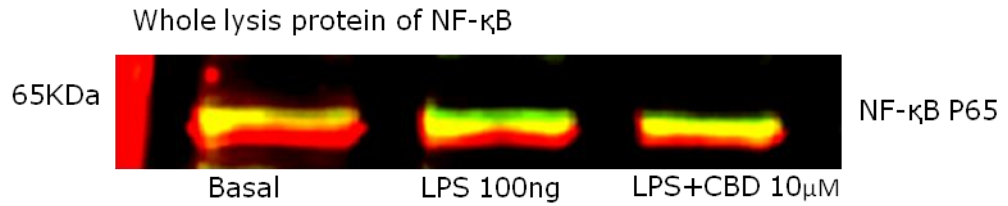


**Figure 2.53:** Western blot shows both total NF-KB and phospho-NF-KB expression in whole lysis of BV-2 (protein 20 $\mu$ g) at 24 hours. BV-2 cells ( $5 \times 10^5$ ) treated with LPS 100 ng/ml alone or with CBD (10  $\mu$ M for 1 hour prior stimulated with LPS (100ng/ml) for 24 hours or basal cell blots were incubated with mouse antibody to NF-KB followed by IRDY<sup>®</sup> conjugates goat anti-rabbit and anti-mouse IgG. LPS activated NF-KB, CBD treatment prior to LPS inhibits NF-KB. Red represents the total NF-KB, green is phospho NF-KB.

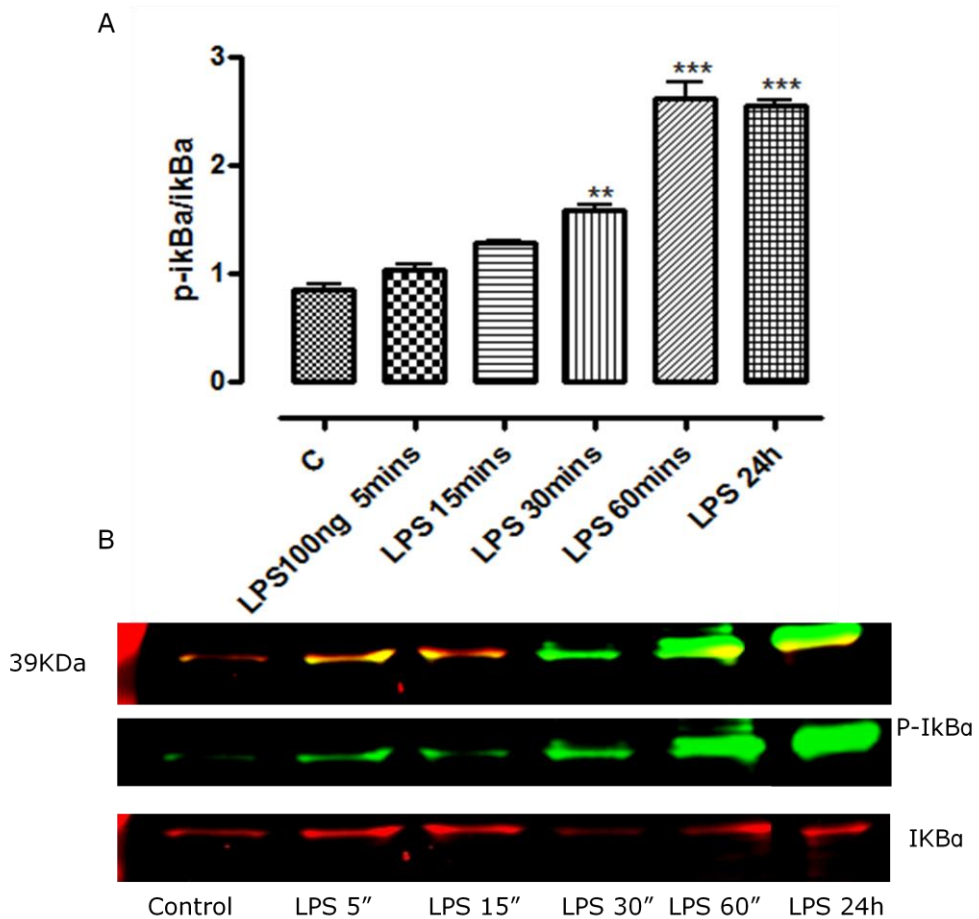


**Figure 2.54:** Western blot and histogram show the increase the phospho-IκBa and the ratio of phospho-IκBa to total IκBa expression in cytoplasmic lysates of BV-2 (protein 20 $\mu$ g) by LPS. BV-2 cells ( $5 \times 10^5$  cells/well) treated with LPS (100 ng/ml) or vehicle at indicated times. Blots were incubated with mouse antibody to IκBa followed by IRDY<sup>®</sup> conjugates goat anti-rabbit and anti-mouse IgG. Red represents the total IκBa, green is phospho IκBa and yellow both. Data shown are the mean of 3 experiments  $\pm$  SEM. Data were analysed using one-way ANOVA followed by Dunnett's test \*\* $P < 0.01$ ; \*\*\* $P < 0.001$  LPS compared with (C) control.

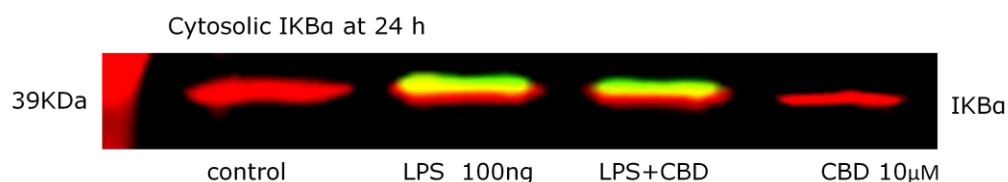


**Figure 2.55:** Western blot shows the total of IKBa and phospho-IKBa expression of cytoplasmic lysates (protein 20 $\mu$ g) of BV-2 at 24 hours. BV-2 cells ( $5 \times 10^5$  cells/well) treated with LPS 100 ng/ml alone or with CBD (10  $\mu$ M) or control for 1 hour prior stimulated with LPS (100ng/ml) for 24 hours. Blots were incubated with mouse antibody to IKBa followed by IRDY<sup>®</sup> conjugates goat anti-rabbit and anti-mouse IgG. LPS activated IKBa, CBD treatment prior to LPS inhibits IKBa. Red presented of the total IKBa, green is phospho IKBa and yellow both.

## 2.4.5 Molecular investigation of BV2 cells

### 2.4.5.1 GTP gamma S binding

In order to further confirm the activity of cannabinoids in rat whole brain membranes, experiments of [<sup>35</sup>S]GTP $\gamma$ S binding assay in this tissue were carried out.

#### 2.4.5.1.1 Optimization of assay method

First, we tested the requirement of GDP to find the proper amount required for activation of [<sup>35</sup>S]-GTP $\gamma$ S binding assay in the whole rat brain membrane using different concentrations of GDP (0-40 $\mu$ M) in the presence and absence of an effective concentration of the cannabinoid receptor agonist HU-210 (Figure 2.56). The percentage stimulation of [<sup>35</sup>S]-GTP $\gamma$ S binding by HU-210 was increased by increasing concentration of GDP, up to a maximum of 215% at 46  $\mu$ M GDP.

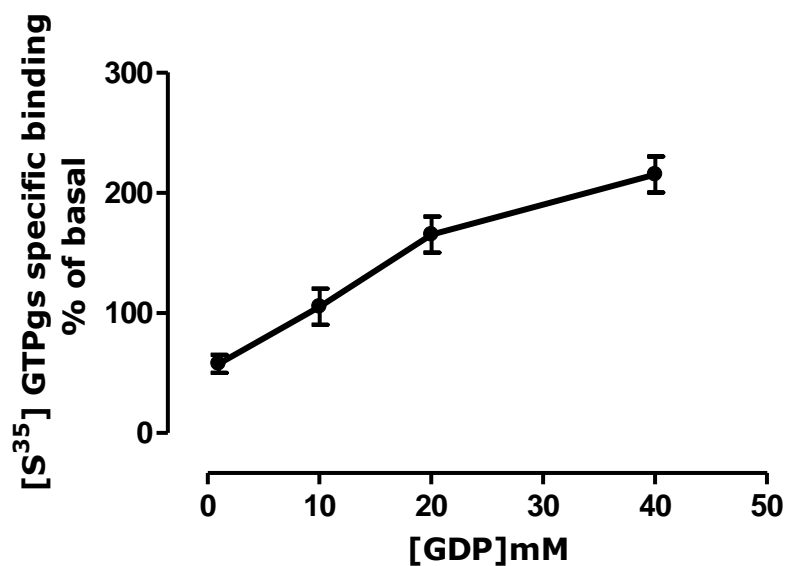


**Figure 2.56:** Histogram shows HU210 (10  $\mu$ M)-induced [<sup>35</sup>S] GTP $\gamma$ S binding with increasing GDP concentration (mean  $\pm$  SEM). Percentage binding above basal elicited by the cannabinoid receptor agonist HU210 to cannabinoid receptors in the brain membrane higher concentrations of GDP produce greater binding.

#### 2.4.5.1.2 The effect of saponin in GTP $\gamma$ S binding assays

We investigated the role of saponin in the activation of the [<sup>35</sup>S]-GTP $\gamma$ S binding assay in whole rat brain membranes using different concentrations of saponin (3-1000nM) in the presence and absence of an effective concentration of HU210 (10 $\mu$ M) (Figure 2.57) the stimulation of [<sup>35</sup>S]-GTP $\gamma$ S binding was increased after treatment with saponin.

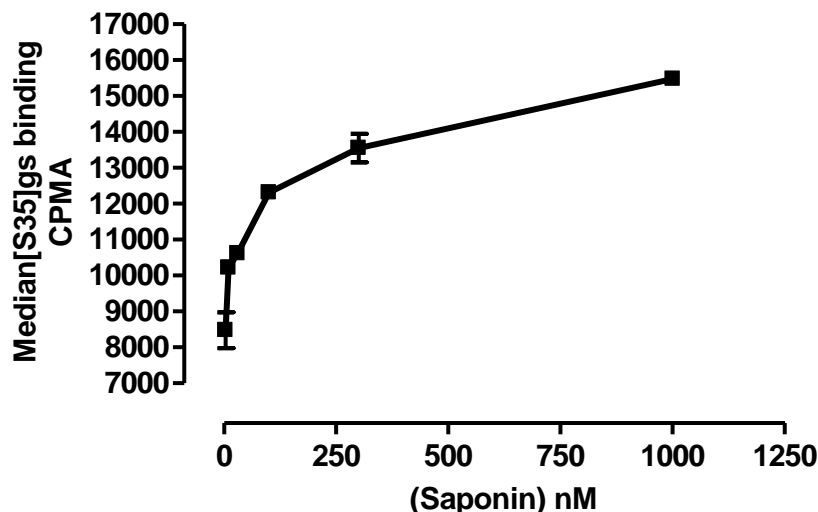


**Figure 2.57;** HU-210 (10  $\mu$ M)-induced [ $^{35}$ S]-GTP $\gamma$ S binding to rat brain membranes with increasing saponin concentrations (mean  $\pm$  SEM 3 independent experiments). Percentage binding above basal elicited by the cannabinoid receptor agonist HU-210 was enhanced with higher concentrations of saponin.

#### 2.4.5.1.3 Effects of cannabinoids ligands on [ $^{35}$ S] GTP $\gamma$ S

The actions of different putative GPR55 receptor ligands on [ $^{35}$ S]-GTP $\gamma$ S binding were investigated), As shown in Figure (2.58; A), CP-55,940 (cannabinoid CB $_1$ /CB $_2$  receptor agonist and putative GPR55 antagonist), as expected, was able to stimulate [ $^{35}$ S] GTP $\gamma$ S binding to the whole rat brain membranes, with an EC $_{50}$  value of -8; %127.7, which was not different to the previous reported in [ $^{35}$ S]-GTP $\gamma$ S binding.

HU-210 increased the binding of [ $^{35}$ S]-GTP $\gamma$ S in the rat whole brain membrane the percentage of basal binding the agonists (CB $_1$ /CB $_2$ ) HU-210 (EC $_{50}$ ; -8.6; %133.5) (Figure 2.58; B). Conversely, cannabidiol (CBD) (EC $_{50}$  -7.6; % 89.55), in the same experimental conditions, was unable to stimulate or inhibit [ $^{35}$ S] GTP $\gamma$ S binding at any of the concentrations tested (Figure 2.58; C). These results rule out the ability of CBD, in this range of concentrations, to directly bind to and activate CB $_1$  or CB $_2$  receptors.

The activation of cannabinoid receptors with Win55-212, a CB<sub>1</sub>/CB<sub>2</sub> agonist with uncertain GPR55 activity also stimulated [<sup>35</sup>S] GTPγS binding in rat brain membranes (EC<sub>50</sub>; -8; %151.9) (Figure 2.58; D).

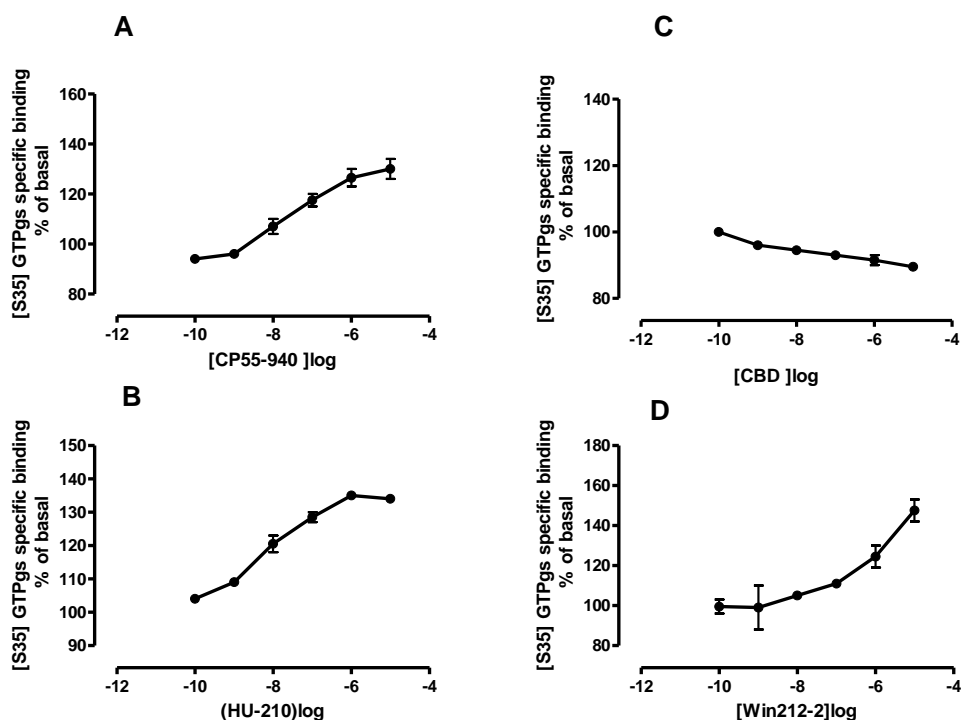


**Figure 2.58;** Histograms show the effects of cannabinoids on [<sup>35</sup>S]-GTPγS binding in rat brain membranes. Membranes were incubated with 0.05nM [<sup>35</sup>S]-GTPγS and 20 μM GDP as described in Methods, with various concentration of (A) CP-55,940, (B) HU210, (C) CBD, (D) WIN55212-2. Data are expressed as percentage basal [<sup>35</sup>S]-GTPγS binding and represent mean values ± SEM from three separate experiments.

## 2.4.5.2 GPR55 and cannabinoids receptors expression

### 2.4.5.2.1 Cannabinoid receptors expression in BV-2 cells

The expression of CB<sub>1</sub> and CB<sub>2</sub> receptor mRNA in BV-2 cells was measured by RT-PCR. Mouse brain and CHO cells transfected with CB<sub>2</sub> receptors were employed as positive controls for CB<sub>1</sub> and CB<sub>2</sub> in BV-2 cells. The RT-PCR results showed no measurable expression of CB<sub>1</sub> or CB<sub>2</sub> mRNA in BV-2 cells (Edeeb, 2009).

#### 2.4.5.2.2 Expression of GPR55 receptors in BV-2

Using RT-PCR, we found that GPR55 mRNA was present in BV-2. Interestingly, CBD inhibited GPR55 mRNA expression after 24 hours exposure; mouse brain was used as a positive control in this experiment (Figure 2.59).

In order to validate this finding, BV-2 cells were stained with a GPR55 antibody using an immunocytochemistry approach. GPR55 receptor-like immunoreactivity was observed in unstimulated BV2 cells (Figure 2.60; A); furthermore, immunoreactivity was increased in cells stimulated with 100ng LPS for 24 hours (Figure 2.60; B) and this was partially reversed by pre-treatment with CBD (Figure 2.60; C).

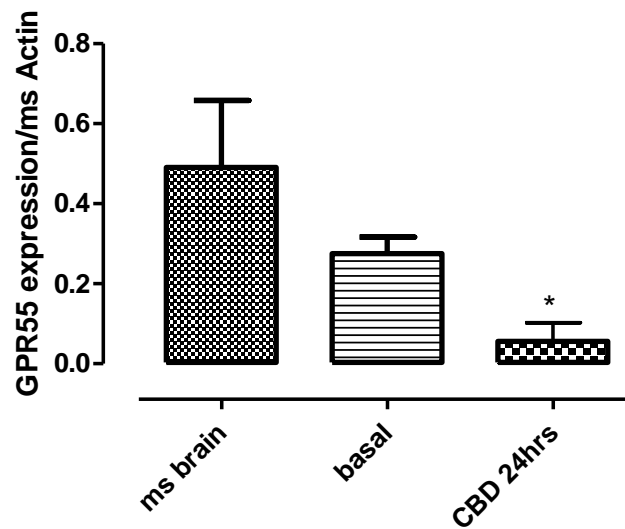


**Figure 2.59:** mRNA expression levels of GPR55 receptor by RT-PCR in mouse and BV-2 cells. RNA was extracted using Trizole reagent and RNA samples were reverse transcribed using the superscript reverse transcription. Data are mean  $\pm$ SEM of triplicate determinations of GPR55/mouse actin ratio. Data were analysed using 2-tailed t -test \* $P < 0.05$  compared with the basal.

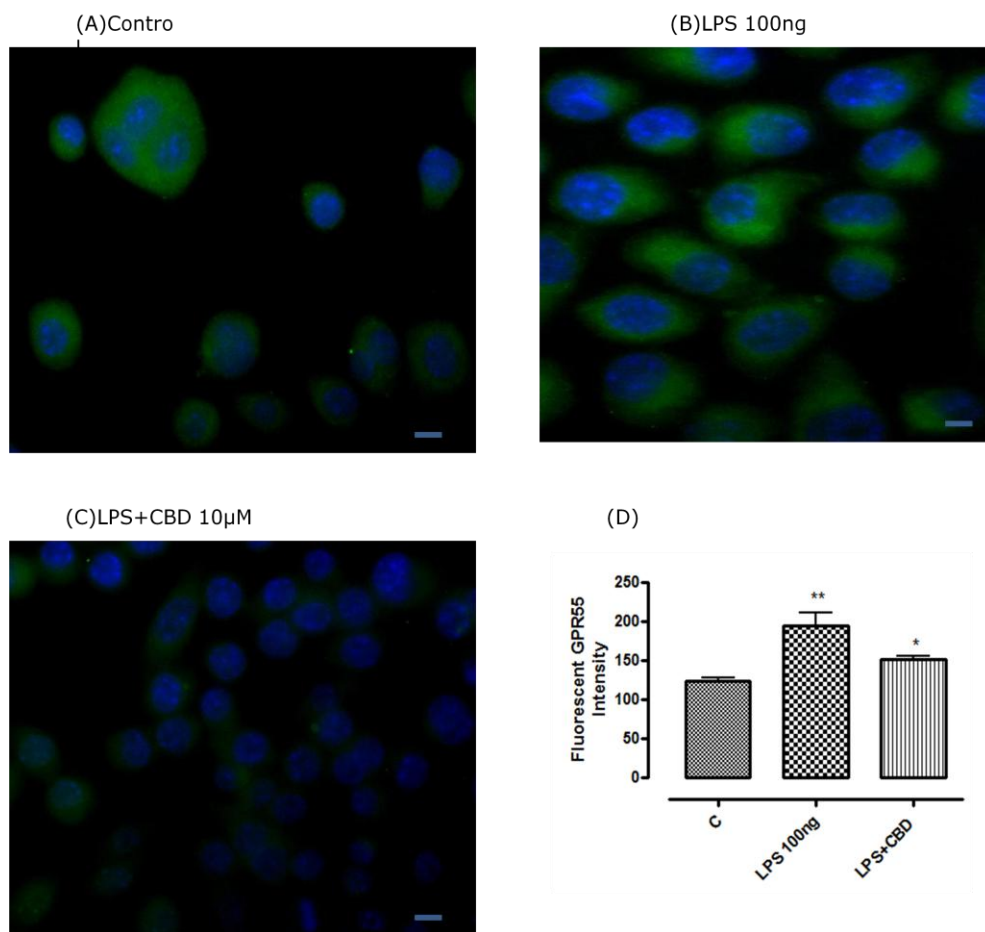


**Figure 2.60:** Images show the effect of CBD on GPR55 expression in BV2 cells shown by immunofluorescent staining **(A)** control **(B)** LPS stimulated cells for 24 hours **(C)** Cells were pretreated with CBD for 1 hr before stimulation by LPS (100 ng/ml) for 24 hrs **(D)** mean of fluorescent GPR55 intensity of three independent experiments were analysed by Volocity Demo 6 software. Untreated cells showed small amounts of cytoplasmic staining, whereas intensified staining in the cytoplasm was observed in LPS-treated cells indicative of GPR55 receptor activation. Pretreatment of cells with CBD (10 µM) attenuated the LPS-induced activation of GPR55 (40 X).

## 2.5. Discussion

The anti-inflammatory and immunosuppressive properties of cannabinoids have been reported to modulate the immune function of macrophages and macrophage-like cells such as microglia (Cabral and Griffin-Thomas, 2008). However, the mechanisms of these actions are not fully known. Microglia become fully activated upon infection or injury and are able to elicit a

whole host of immune responses, including releasing pro-and anti-inflammatory chemokines, cytokines, reactive nitrogen species and other factors may be beneficial or damaging (Waksman et al., 1999). Microglia are also activated after exposure to LPS, interferon or  $\beta$ -amyloid protein (Zielasek and Hartung, 1996).

Nitric oxide (NO) plays a role in host defense against intracellular pathogens but, at the same time, may also contribute to neurodegeneration and neuronal damage (Molina-Holgado *et al.*, 2002). We used lipopolysaccharide (LPS) as a microglial activator and release of pro-inflammatory NO as an end-point of activation.

The BV-2 cell line used in the study possesses functional and phenotypic properties common to primary microglia including phagocytic ability, secretion of pro-inflammatory cytokines and expression of surface receptors and antigens (Blasi *et al.*, 1990) and, as such, is a suitable *in vitro* model for investigation of microglial function. Upon LPS stimulation, NO release from BV-2 cells was observed at 6 hours post-stimulation and more robustly at 24 and 30 hours, after which, 24 hours was the time point used in all subsequent LPS-stimulation studies. The results of the NO assay showed that basal NO formation was more pronounced with adult mouse microglial cells when compared with BV-2 cells and HAPI cells.

In order to validate our BV-2 model, the effects of ethanol and serum-free medium were examined; ethanol failed to significantly affect LPS-induced NO in BV-2. When BV-2 cells were cultured in serum free medium, they showed retracted processes and nitric oxide release by LPS was not apparent in contrast to cells cultured in 5-10% serum-containing medium. It, therefore, appears that the LPS-induced NO release requires a serum protein in the medium. LPS binds to the serum protein LPS-binding protein

(LBP), which facilitates binding to CD14; LPS/LBP complexes bind to CD14, which interacts with Toll-like receptor 4 (TLR4) to activate the cells and stimulate NF-KB (Haziot et al., 1996; Wright *et al.*, 1990; Schumann et al., 1990).

As a control we investigated the effect of minocycline on microglial activation; minocycline is a second generation tetracycline which inhibits NO formation by blocking iNOS or P38 and it has been reported as an anti-inflammatory agent (Tikka and Koistinaho, 2001). Minocycline reversed the NO release in LPS-stimulated BV-2 in a concentration-dependent manner. The effects of minocycline as a microglial inhibitor have been documented previously (Wu *et al.*, 2002).

In this work, we have focused on the effects of LPS as a representative inflammatory stimuli. Treatment of microglial cells with LPS alone induced NO production. Sodium nitroprusside, (SNP) a NO donor was used to investigate the effects of NO on activation of microglia. Our data indicate that exogenous NO did not modulate the microglia, at least in the BV-2 cell line. Therefore, this is not likely to be the main mechanism to activate microglia in NO production. Since, in several cell types, iNOS is responsible for the high-output production of NO after exposure to LPS (Bogdan, 2001).

In order to confirm our model, dexamethasone (DEX) and 1400W were also examined. Dexamethasone is able to prevent LPS-induced NO formation in microglial BV-2 cells (Hinkerohe *et al.*, 2010). DEX may decrease iNOS mRNA/protein expression by inhibition of NF-KB (Golde et al., 2003; Bauer et al., 1997). Moreover, 1400W attenuated NO formation in BV-2 cells. These results indicate that iNOS was the likely enzyme responsible for LPS-induced NO production.

To test the mechanism of LPS-activated NO release; the role of calcium was examined. Using BAPTA-AM (a cell-permeable  $\text{Ca}^{2+}$  chelator) a concentration-dependent attenuation in NO production was seen consistent with previously reported calcium-dependency (Hoffmann et al., 2003; Toescu *et al*, 1998). However, despite this apparent calcium dependency of the LPS activation of NO release, direct elevation of intracellular  $\text{Ca}^{2+}$  using ionomycin failed to increase NO release from BV-2 cells, indicating that LPS signaling requires other elements in addition to elevation of intracellular  $\text{Ca}^{2+}$  as suggested previously (Hoffmann et al., 2003).

The aim of this chapter was to investigate the effects of cannabinoids on NO release (as a measure of microglial activation). In order to examine the role of cannabinoid ( $\text{CB}_1$ ,  $\text{CB}_2$ ) receptors in inhibition of lipopolysaccharide stimulated nitric oxide release in BV-2 microglia. Various cannabinoid receptor ligands were examined. Waksman et al (1999) reported an inhibitory effect of the  $\text{CB}_{1/2}$  agonist CP55,940 on endotoxin/cytokine-activated NO formation in rat cortical microglial cells mediated by  $\text{CB}_1$  receptors, but in the present study, CP55,940 was only effective at  $10\mu\text{M}$ , well above the concentration range selective for  $\text{CB}_1$  activation (Ross *et al.*, 2000; Pertwee, 1997) and its effect was not inhibited by a  $\text{CB}_1$  antagonist. However, CP55,940 is also reported to be an agonist of the GPR55 receptor (Ryberg *et al.*, 2007).

Also AM251 ( $\text{CB}_1$  antagonist and putative GPR55 agonist) inhibited NO induced by LPS in BV-2 at micromolar concentrations, which indicated that it acts via GPR55 (Kapur *et al.*, 2009; Pertwee, 2007). It was somewhat unexpected that none of the cannabinoid receptor agonists in concentrations expected to activate CB receptors affected LPS-stimulated NO formation, but it is clear that, under the culture conditions employed, the BV-2 cells failed to express either  $\text{CB}_1$  or  $\text{CB}_2$  receptors significantly. It

does seem that BV-2 cell expression of CB receptors is not well maintained with increasing passage number (Stella, personal communication) which might explain this deficit. Facchinetti *et al.*, (2003) have reported that only micromolar concentrations of CP55, 940, WIN55, 212-1 regulate cytokine release from cultured microglia which is consistent with our data.

In the present study, the phytocannabinoids CBG, CBDV, THCV, CBDA, CBGA and THC (is the main psychoactive component of marijuana) were all without effect. However, CBD attenuated LPS-induced NO formation. The phytocannabinoid cannabidiol (CBD) is widely reported to have anti-inflammatory properties (Tubaro *et al.*, 2010) although its mechanism of action is unclear; it has also been reported to be a GPR55 antagonist (Ryberg *et al.*, 2007).

The pharmacology of the GPR55 receptor is controversial with no well characterized selective ligands; nevertheless, we sought to investigate the role of GPR55 receptors in inhibition of LPS-stimulated nitric oxide formation in BV-2 microglia using various cannabinoids and other putative GPR55 receptor ligands. A novel selective GPR55 agonist (a gift from GSK) failed to produce significant inhibition consistent with the similar lack of effect of the synthetic agonists VSN16R and putative GPR55 agonist O-1602 and the endogenous GPR55 activator lysophosphatidylinositol (LPI). Interestingly, given that CBD is reported to be an antagonist of GPR55 (Ryberg *et al.*, 2007), a novel GPR55 antagonist (also from GSK) also inhibited LPS-induced NO release. Whether this indicates that LPS releases an endogenous GPR55 agonist that mediates its effects seems unlikely since other agonists did not increase NO formation and an off-target effect of the GSK antagonist is possible.

Neither LPI nor O1602, another GPR55 agonist (Johns *et al.*, 2007), affected LPS-stimulated NO formation lending little support to the possibility that the effect of CBD is GPR55-mediated. Nevertheless, it is conceivable that the GPR55 receptors in the BV-2 are constitutively activated and that CBD acts as a GPR55 antagonist/inverse agonist under the prevailing culture conditions. In support of this model, Oka *et al.*, (2010) reported that LPI enhances activity of P38 MAP kinase (Obata *et al.*, 2000). We found by immunoblotting, that LPI activated ERK 1/2 in BV-2 cell line this finding to support that GPR55 is target receptor (Kapur *et al.*, 2009).

To evaluate the effects of cannabinoids on NO production and hence microglial activation, a number of endocannabinoids, arachidonylethanolamide (AEA), and endocannabinoid-like compounds (palmitoylethanolamide (PEA), oleoylethanolamide (OEA) were studied. All failed, however, to inhibit LPS-induced NO formation. PEA is a potent anti-inflammatory and GPR55 ligand (Mackie and Stella, 2006). This result argues the involvement of GPR55 receptor.

CB receptor agonists did nothing and antagonists did not reverse CBD's effects and crucially, despite previous reports of CB receptors in BV 2 cells, there was no CBR expression by RT-PCR. Furthermore, CBD in the present study was found not to be a CB<sub>1</sub> agonist because it failed to enhance brain GTPγS binding although other CB agonists did.

When CBD was given alone without LPS it did not alter the basal level of NO formation. The GPR55 receptors in the BV-2 cells appeared to be functional since the putative endogenous agonist LPI (Oka *et al.*, 2007) produced a concentration-dependent elevation of intracellular Ca<sup>2+</sup> which

was attenuated by CBD (Eldeeb *et al.*, 2009), in agreement with its designation as a GPR55 antagonist.

It is possible that the inhibition of NO production in LPS stimulated cells could be ascribed to cytotoxic effects of CBD; however, there were only very minor reductions in cell viability at high CBD concentration and in fact, CBD provided remarkable protection against toxic challenge by hydrogen peroxide.

CBD has been frequently described as a potent neuroprotective and anti-oxidant agent, which reduces glutamate excitotoxicity and peroxide-induced oxidative neuronal damage (Hampson *et al.*, 1998). Lastres-Becker *et al.*, (2005) have reported that, in animal models of Parkinson's disease, there is an improvement of toxic effects of 6-hydroxydopamine by administration of CBD as a result of anti-oxidative effects.

The neuroprotective effects of a non-psychoactive cannabinoid, cannabidiol (CBD), are reported to be largely mediated by its ability to scavenge reactive oxygen species (ROS) (Mechoulam *et al.*, 2007). ROS can also function as second messengers to regulate several downstream signaling molecules, including mitogen-activated protein kinase, and PI3K/Akt pathways (Kwon *et al.*, 2004).

We examined the effect of NADPH oxidase enzyme activity of LPS-treated microglial cells. LPS appears to stimulate NO formation via ROS as its effects are blocked by apocynin. Previous studies have reported that microglial NADPH oxidase can regulate the bioavailability of NO and the production of peroxynitrite (Bal-Price *et al.*, 2001).

CBD also blocked LPS stimulated ROS formation despite having a positive effect alone (the mechanism is unclear but it is partially consistent with an

anti-oxidant effect of CBD). CBD has been shown to be effective in attenuating oxidative and nitrosative stress in a number of disease models (Booz, 2011). Both apocynin and CBD blocked LPS-mediated enhancement of iNOS expression showing that the effects of CBD appear to be at the level of iNOS expression and not via regulation of NO availability. Although its mechanism of action is uncertain, it is possible that CBD may act directly at the level of the mitochondrion or nucleus to oppose or promote oxidative/nitrosative stress in a cell type-selective manner. There is evidence that, in some systems, ROS at lower, non-toxic levels can actually enhance cell proliferation and survival (Blanchetot and Boonstra, 2008).

Therefore, the inhibitory effect CBD on LPS stimulated NO was not due to any cytotoxic action on BV-2 microglia. Although neither cannabinoids nor cannabinoids-related receptors were implicated in the effect. In this study, neither CB<sub>1</sub> nor CB<sub>2</sub> receptors were seen to be expressed in the BV-2 cells. Furthermore, there was no evidence for the involvement of 5-HT, adenosine, PPARs and TRPVs receptors. Furthermore, the PTX data argue against the involvement of any G<sub>i/o</sub> linked GPCR.

There is evidence to show the involvement in microglia activation of purine receptors such as P2X7 receptors, whose activation is considered a strong inflammatory stimulus (Skaper *et al.*, 2006; Inoue, 2008). Our data show that ATP failed to induce nitric oxide release in BV-2 cells, consistent with previous studies showing that ATP alone did not alter iNOS activation, but enhanced IFN- $\gamma$  induced iNOS in BV-2 cells (Ohtani *et al.*, 2000). It is likely that ATP itself does not have a direct effect on microglial processes, and that other signaling is required (Inoue *et al.*, 1998). However, high concentrations of ATP have been shown to stimulate inducible nitric synthase mRNA leading to NO release from rat microglia through P2X7 receptors (Ohtani *et al.*, 2000; Honda and Kohsaka, 2001).

Another purine receptor P2Y<sub>14</sub> has recently been found to be expressed by BV-2 cells (unpublished data, Eldeeb and Hassan) so its potential role in activation of microglia and LPS-induced release of NO was examined. UDP glucose, a selective agonist for P2Y<sub>14</sub> (Malin and Molliver, 2010) failed, however, to alter NO production.

Cannabidiol is remarkable in the diversity of its actions on receptor and non-receptor targets when employed in the micromolar concentration range (Pertwee, 2004; 2008). Whilst BV-2 cells are widely used as a surrogate model for studying microglial function it is worth remembering that the microglial phenotype is very plastic and that differences do exist compared with microglia in primary culture and adult brain. Thus, it could be argued that the effects of CBD described here are relevant only to BV-2 cells and not to microglia in general. However, it is notable that in a very different cell line, HAPI (highly aggressively proliferating immortalized rat brain microglia) (Cheepsunthorn *et al.*, 2001), CBD also inhibited LPS-activated NO formation and, indeed its potency, seemed to be somewhat greater in the primary microglial cells.

Consistent with the report from Pietr *et al.*, (2009) describing GPR55 expression in both primary microglial and BV-2 cells we were also able, using RT-PCR to show that GPR55 mRNA was expressed with reasonable quantity in BV-2 when compared with rat brain . Although no evidence was found implicating GPR55 in the effect of CBD on NO formation, it is interesting that LPS increased GPR55 expression in BV-2 cells and CBD was able to reduce it. What the functional significance of this might be requires further investigation.

The radiobinding assay demonstrate a wide range of activities, ranged from the highly potent and efficacious through to compounds displaying little or

weak- dependent stimulation of [<sup>35</sup>S]GTPγS binding. Of the range of compounds tested; WIN 55212-2, CP55, 940, HU210, and CBD. WIN 55212-2 was selected as a standard cannabinoid receptor agonist, acting as a potent full agonist, in many different assays (Howlett, 1995; Martin et al., 1995). It also displays a high affinity for both subtypes of cannabinoid receptor CB1/CB2 (Pertwee, 2006). The results obtained confirmed previous finding that WIN55212-2 stimulated [<sup>35</sup>S] GTPγS binding (Burkey et al., 1997).

Similar experiments were performed using CP55,940, an identical result was observed a full agonist at potency lower than previous reports at CB1/CB2. It has not been shown to have any significant effect on CB<sub>1</sub> and CB<sub>2</sub> receptor signaling (Ryberg et al., 2007).

Evidence has shown that inhibition of different MAPK pathways is associated with decreases in LPS-induced NO production (Kaminska et al., 2009). Therefore, we investigated MAPKs involvement in NO formation in BV-2 cells. In the present study, the effect of CBD was independent of particular kinase signaling pathways including MEK 1/2, PI3K, Rho/ROCK pathways suggesting that these may not be important downstream TLR4 targets in NO release by LPS. These results are supported by recent studies using Rho/ROCK pathway inhibitors showing that the Rho-dependent activation of ROCK kinase has structural effects but is not involved in functional signaling including attenuation of NO or cytokine release (Hoffman et al., 2008). However, some evidence was gathered showing involvement of p38 MAPK (which can be activated by microenvironmental stress and regulates inflammatory cytokines release (Rajesh et al., 2008)) in the LPS-dependent release of NO. LPS enhanced p38 activation and this was reduced by CBD. However with regard to NO formation both CBD and

the p38 inhibitor SB203580 reduced the effects of LPS and their effects were additive, possibly suggesting independent actions.

We evaluated the effect of LPS and CBD on ERK1/2 and JNK/SAPK signaling, in this study, LPS activated ERK1/2, JNK/SAPK and p38 MAPK in a time dependent manner. CBD failed to inhibit ERK1/2, whereas it did inhibit JNK/SAPK and p38 MAPK. It has been documented that JNK is an essential mediator of relevant pro-inflammatory function in microglia (Waetzig *et al.*, 2005) and inhibition of this pathway may be a therapeutic approach for treating inflammatory neurological disease (Borsello and Forloni, 2007). Immunoblotting analysis showed that LPS treatment induced a time-dependent enhancement of P38 protein phosphorylation at 30 minutes with a further increase at 60 minutes and this was attenuated by 10  $\mu$ M SB03580 and 15  $\mu$ M apocynin, a NADPH oxidase inhibitor. Oxidative stress and pro-inflammatory cytokines have been previously reported to activate the MAP kinases including P38 (Obata *et al.*, 2000). Indeed, in this study, 10 $\mu$ M CBD inhibited LPS-induced P38 phosphorylation as suggested by Esposito *et al.*, (2006). P38 MAPK has been implicated in the regulation of pro-inflammatory cytokines and apoptosis *in vitro* (Walton *et al.*, 1998).

The NF- $\kappa$ B pathway is a primary intracellular pathway controlling the transcription of many inflammatory genes (Rothwarf and Karin, 1999). The NF- $\kappa$ B p65-p50 protein complex is present in the cytoplasm through association with the inhibitor protein, I $\kappa$ B, which masks the nuclear localization signal present within the NF- $\kappa$ B p65 subunit. The activation of NF- $\kappa$ B by extracellular stimulation depends on the rapid phosphorylation of I $\kappa$ B by upstream IRAK-1 followed by ubiquitination and targeting for proteasome degradation of both proteins. The NF- $\kappa$ B p65 subunit then undergoes phosphorylation, followed by translocation to the nucleus where

it regulates the expression of various inflammatory genes, including IL-1 $\beta$  and IL-6 (Covert *et al.*, 2005).

Our results showed that CBD reduced the activation of NF- $\kappa$ B which could result in the attenuation of downstream cytokine production (Wang *et al.*, 2002). The inhibition of NF- $\kappa$ B transcriptional activity exerted by CBD appears to be a consequence of inhibiting I $\kappa$ B $\alpha$  which would result in the retention of the I $\kappa$ B $\alpha$ /NF- $\kappa$ B complex in the cytoplasm, and reduced NF- $\kappa$ B translocation to the nucleus. Several previous reports have suggested the involvement of the NF- $\kappa$ B pathway in cannabinoid-induced immunosuppression in macrophages (Jeon *et al.*, 1996) including inhibition of iNOS gene expression (Burstein and Zurier, 2008).

Microglial cells in the healthy brain do not express iNOS, but they become activated to produce iNOS and to release a large amount of NO following ischemic, traumatic, neurotoxic or inflammatory damage (Hanisch, 2002). In order to investigate whether the inhibition of CBD on NO and PGE<sub>2</sub> production was related to a modulation of iNOS and COX-2 induction, we evaluated iNOS and cyclooxygenase-2 (COX-2) expression in BV-2 cells. COX-2 expression has been associated with inflammatory and neurodegenerative processes of several human neurological diseases (Minghetti and Pocchiari, 2007). In this study, we found that LPS activated expression of both iNOS and COX-2 in BV-2 cells. On the other hand, the effects of LPS were completely blocked by CBD (10  $\mu$ M) but not by 1400W, an iNOS inhibitor, indicating that the effects of CBD are not secondary to inhibition of iNOS activity.

MAPKs have been shown to play important roles in LPS-induced iNOS, COX-2, and proinflammatory cytokine expression in many types of cells (Gorina *et al.*, 2011). It also has been reported that LPS-induced pro-

inflammatory cytokines expression is mediated by MAPKs signalling in BV-2 cells (Kim *et al.*, 2004). We found that iNOS protein expression was blocked by selective inhibitors of p38 MAPK and PI3K but not by U0126, a MEK 1/2 inhibitor. or by Y27632, a ROCK inhibitor. These data suggest that MAPK signaling regulates iNOS expression at the transcriptional level in BV2 cells mediated via both p38 MAPK and PI3K signaling pathways, but not via ERK MAPK and ROCK pathways.

This is consistent with previous reports that P38 phosphorylation can increase the activity of the transcription factor NF- $\kappa$ B (Wilms *et al.*, 2003) which enhances the transcription of a wide range of pro-inflammatory genes including inducible nitric oxide synthase (iNOS) and COX-2 (Bauer *et al.*, 1997; Iuvone *et al.*, 2004). Moreover, the involvement of PI3K in the regulation of iNOS expression was previous reported (Jang *et al.*, 2004).

The major source of ROS during inflammation is NADPH oxidase (Qin *et al.*, 2004), although other sources may also contribute (Sastre *et al.*, 2003). NADPH oxidase is expressed mainly by microglia in the brain and its activity is increased by LPS (Green *et al.*, 2001; Mayer *et al.*, 2011). In this study, we tested the hypothesis that iNOS induction by LPS is conditional upon microglial NADPH oxidase activation. The NADPH oxidase inhibitor apocynin significantly inhibited iNOS protein expression in BV-2 cells. Therefore, it is possible that CBD could reduce iNOS expression by interacting with ROS generation. CBD has been shown to be effective in attenuating oxidative and nitrosative stress in a number of disease models (Booz, 2011).

It was previously demonstrated that application of LPS to cultured spinal microglia produced a profound increase in the activated form of p38 MAPK, phospho-p38 (Hua *et al.*, 2005) suggesting that production of nitric oxide is

dependent on p38 activation. p38 may affect the activity of iNOS, or by acting on transcription factors such as nuclear factor- $\kappa$ B (NF- $\kappa$ B) (Wilms *et al.*, 2003) and, recently, CBD was shown to inhibit LPS-stimulated, NF- $\kappa$ B-dependent pro-inflammatory cytokine release in BV-2 cells (Kozela *et al.*, 2010).

Whilst these sequences of events could explain the consequent inhibitory effects of CBD on NO formation, the involvement of the GPR55 receptor, fully activated by a component of the cell culture system, is tenuous. Whether CBD is initially recognized by a cell surface receptor or has its effects on a downstream component of the signaling cascade is uncertain. Although its recognition site in relation to microglial modulation is unclear, CBD might have potential for delaying the development of neurodegenerative diseases and inflammatory pain.

## **2.6. Conclusion**

The data presented demonstrate that CBD inhibits microglial cells activity, as judged by NO formation, and this appears to be mediated by reduction of NF- $\kappa$ B P38 MAPK, JNK and ROS activity.

### 2.6.1 Summary of chapter 2

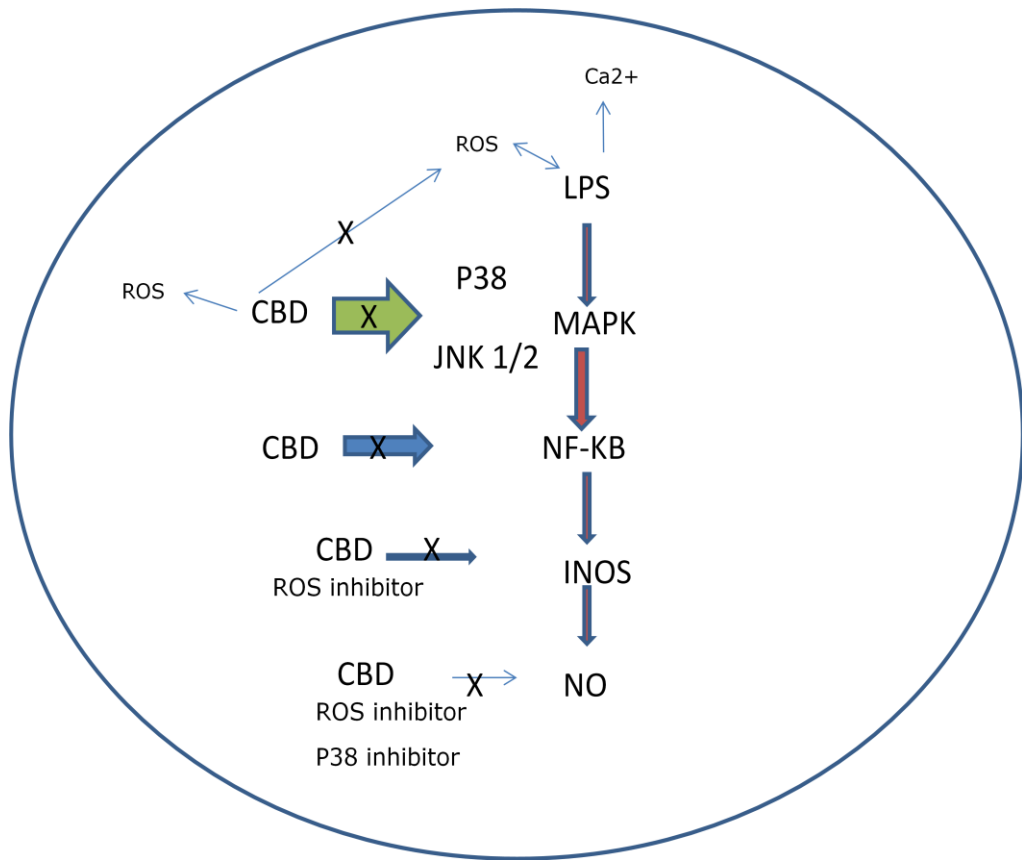


**Figure 2.61:** The summary graph shows the mechanism of inhibition of LPS induced NO. Inhibition of p38, NF-κB and iNOS. Moreover, CBD attenuate ROS induced by LPS.

### 3.1 Introduction

The immune system, in which microglia play a crucial central role, exists to detect and eliminate invading pathogens and to clear debris associated with damage (Janeway, 1992; Aderm and Underil, 1999). Several different functions have been identified for microglia, including migration into the site of infection or damage and phagocytosis. The stimuli for these functions are still to be fully characterized (Frank-Cannon *et al.*, 2009).

Phagocytosis can be defined as a mechanism for internalizing and destroying particles that are more than 0.5  $\mu\text{m}$  in diameter ( Botelho and Grinstein, 2011). Microglia function as the primary phagocytotic cells in the brain, acting to engulf invading microbes and pathological proteins. For example, it has been shown that the Alzheimer's disease associated accumulation of amyloid  $\beta$  can be engulfed by microglia (Bard *et al.*, 2000). Microglia migrate to the site of injury in other pathological conditions including stroke, neurodegenerative disease and tumor invasion (Kettenmann *et al.*, 2011). Phagocytosis has been reported in microglia studied in tissue culture where they have been shown to ingest foreign objects (latex beads), immunoglobulin-coated erythrocytes, dead cells and infectious agents such as bacteria and fungi (Giulian and Baker, 1986; Hassan *et al.*, 1991; Rieske *et al.*, 1989; Williams *et al.*, 1992; Lee *et al.*, 1992).

Phagocytosis is initiated by activation of receptors on the cell surface including Fc gamma receptors (Fc $\gamma$ R) which interact with antibody-opsonised (coated) pathogens and facilitate phagocytosis through pathways affecting reorganization of the actin cytoskeleton and activation of NADPH oxidase resulting in ROS formation. The complement system facilitates phagocytosis by opsonising pathogens, and operates through

signaling pathways which are different from those of Fc receptor-mediated phagocytosis (Zhou and Brown, 1994; Caron and Hall, 1998; Pollard and Borisy, 2003).

Ligated FcRs on macrophage plasma membranes induce phosphorylation of tyrosines within the immunoreceptor tyrosines-based activation motif (ITAM) of FcR, leading to intracellular signals required for phagocytosis such as Syk, phosphatidylinositol 3-kinase (PI3K) and protein kinase C $\epsilon$  (PKC $\epsilon$ ) (Cox and Greenberg, 2001; Srinivasan *et al.*, 2003). The reorganization of the actin cytoskeleton and increased synthesis of PIP<sub>3</sub>, PI-(4,5)-P<sub>2</sub> and diacylglycerol also stimulate the tyrosine kinase receptor-associated phospholipase C $\gamma$ , leading to increased intracellular calcium and Rho GTPase protein (Garcia-Garcia and Rosales, 2002; Srinivasan *et al.*, 2003). However, morphological and signalling characteristics of phagocytosis may differ depending on the local environment, substrate, etc (Aderem and Underhill, 1999).

In order to phagocytose target material, microglia must respond to appropriate physiological stimuli and migrate to the areas of brain injury or inflammation (Noda and Suzumura, 2012). It has been recognized that injury to central nervous system (CNS) tissue results in the release of chemotactic factors that initiate microglial migration to the site of insult. These include the chemokines monocyte chemoattractant protein 1 (MCP-1), macrophage inflammatory protein 1 $\alpha$ , macrophage inflammatory protein 1 $\beta$ , regulated upon activation normal T cell expressed and secreted (RANTES), interleukin 8 and interferon gamma inducible protein-10 (IP-10) (Cross and Woodroffe, 1999). Transforming growth factor  $\beta$  and brain-derived chemotactic factor are also chemoattractants. Gradients of these chemokines have been found to be responsible for migration *in vitro* and in

injury models of the developing CNS (Cartier *et al.*, 2005; Cross and Woodroffe, 1999).

ATP and ADP are released upon acute injury to the CNS and have been found to be chemoattractant for microglial cells (Honda *et al.*, 2001; Davalos *et al.*, 2005). Purine receptors responsible for recognition of these chemoattractants and migration of microglial cells include P2Y<sub>12</sub> (which controls chemotaxis of amoeboid microglia and motility of ramified microglia), and P2X<sub>4</sub> and P2Y<sub>13</sub> (Ohsawa *et al.*, 2010; Ohsawa *et al.*, 2007; Parkhurst *et al.*, 2010; Farber *et al.*, 2005). Some matrix proteins, including the  $\beta$ 2-integrin CD11b, have been shown to be necessary to allow normal migration in response to injury (Isaksson *et al.*, 2009).

Cannabinoids have been shown to engage neuroprotective mechanisms against acute brain damage and toxicity both *in vivo* and *in vitro*. These include decreases in pro-inflammatory cytokines, nitric oxide, antioxidant activity and reductions in calcium influx (Mechoulam *et al.*, 2002).

Cannabidiol (CBD) comprises up to 40% of *Cannabis sativa* extracts and represents one of the most promising cannabinoid drugs in clinical development due to its lack of psychoactive effects and its high level of tolerability in humans (Mechoulam *et al.*, 2002; Mechoulam *et al.*, 2007). Recently, CBD has attracted much interest due to pharmacological effects such as anticonvulsant, hypnotic, anti-inflammatory, anxiolytic, antipsychotic and neuroprotective actions (Barichello *et al.*, 2012). Furthermore, in preclinical research, administration of CBD has been shown to reduce neuroinflammation in mice injected with intracerebral amyloid  $\beta$  (Martin-Moreno *et al.*, 2001). Low doses of CBD protect oligodendrocyte progenitor cells during immune system insult (Mecha *et al.*, 2012) and it has been found that CBD has anti-inflammatory effects by inhibiting iNOS

expression, COX-2, nitric oxide generation and by reducing pro-inflammatory cytokine production induced by LPS (Kozela *et al.*, 2010).

CBD has very low affinity for either CB<sub>1</sub> or CB<sub>2</sub> receptors (Showalter *et al.*, 1996); however, the action of CBD could involve other non-CB<sub>1</sub>/CB<sub>2</sub> receptors including abnormal cannabidiol receptors, (GPR18) (McHugh *et al.*, 2010) and CBD can activate vanilloid (TRPV1) as well as TRPV2 receptors (Oka *et al.*, 2007; Ryberg *et al.*, 2007). Agonist and antagonist actions of CBD at GPR55, an orphan protein coupled-receptor (see Chapter 2), have been described (Oka *et al.*, 2007; Ryberg *et al.*, 2007). In addition, it activates 5-HT<sub>1A</sub> receptors (Russo *et al.*, 2005) and it also blocks the reuptake of anandamide (Bisogno *et al.*, 2001) and adenosine (Carrier *et al.*, 2006).

An accumulation of studies has indicated that cannabinoids may modulate inflammation, by enhancing microglial phagocytosis and migration to the sites of inflammation (Martín-Moreno *et al.*, 2011). However, previous studies have provided no insights into the mechanisms of action of CBD on phagocytosis.

### **3.2 The aim of this study**

To evaluate the effects of phytocannabinoids on microglial migration and phagocytosis and to gain insight into the mechanisms of drug action.

### **3.3 Methods**

#### **3.3.1 Materials**

All cell reagents were obtained from Sigma-Aldrich Co (UK). All cannabinoids were from Tocris Cookson (Bristol, UK); unless otherwise

stated. Mounting medium (VECTASHIELD) was purchased from Vector laboratories, Rhodamine phalloidin from (Cytoskeleton, Molecular Probes, Eugene, USA) and DAPI from (Vector Laboratories, Petersborough, U.K.).

Ruthenium red and N-arachidonylglycine were from Tocris Cookson (Bristol, UK). 1400W (an iNOS inhibitor) was from Abcam Biochemicals® (Bristol, UK) oligomycin was from Acros Organics (Leicestershire, UK ) and dexamethasone was purchased from Organon (Cambridge, UK). All cannabinoid drugs were diluted in 100% ethanol to  $10^{-2}$ M stocks, then in assay buffer to give final ethanol concentrations less than 0.1%. PEA, OEA, AEA and SEA were synthesized in the School of Chemistry, University of Nottingham, by Dr S.P.H. Alexander.

### **3.3.2 Cell culture conditions**

Please see Chapter 2 for details.

#### **3.3.2.1 Murine microglial (BV-2) cell line**

BV-2 cells, a mouse microglial cell line, (a gift from Prof. Nephi Stella, Washington University, USA) were grown in Dulbecco's Modified Eagle Medium (DMEM) with Ham-F12 obtained sterile from Sigma, supplemented with penicillin (100 U/ml) / streptomycin (100 µg/ml) solution, HEPES (15 mM), NaHCO<sub>3</sub> (5 mM), L-glutamine (2 mM) and 10% fetal bovine serum (FBS) which was heat inactivated. All cell culture solutions were stored at 4 °C and pre-warmed to 37 °C in a water bath prior to use. The cells were grown to 95% confluence in 75cm<sup>2</sup> flasks at 37°C with 5% CO<sub>2</sub> and 95% atmosphere.

### **3.3.2.2 HAPI cell line**

HAPI cells, an aggressively proliferating rat microglial cell line employed as a model of activated microglia, were a gift from Dr J.R. Connor, (Pennsylvania State University, USA). Cells were expanded in Dulbecco's Modified Eagle Medium (DMEM) with 5% heat inactivated FBS, L-glutamine (2 mM), penicillin (100 U/ml) / streptomycin (100 µg/ml) solution and maintained in a humidified incubator with 5% CO<sub>2</sub> at 37 °C.

### **3.3.2.3 Macrophage like cells (RAW-264.7)**

RAW-264.7 cells, a monocyte/macrophage-like line were expanded in Dulbecco's Modified Eagle Medium (DMEM) with 10% heat inactivated FBS, L-glutamine (2 mM), penicillin (100 U/ml) / streptomycin (100 µg/ml) solutions. The cells were maintained in a humidified incubator with 5% CO<sub>2</sub> at 37 °C.

### **3.3.2.4 Primary mouse microglial cultures,**

Please see Chapter 2 for details.

### **3.3.3 Cell counts**

Please see Chapter 2 for details.

### **3.3.4 Assessment of cell membrane integrity**

Staining of cells with Trypan blue, a derivative of toluidine, allows distinction between live/ necrotic cells. Live cells maintain membrane integrity and exclude compounds that can enter the intracellular compartments. In contrast, necrotic cells have disrupted membranes and the above-mentioned selectivity is lost.

Thus, upon staining, Trypan blue can freely traverse the membrane and stain necrotic cells. Cells are then examined under the light microscope, counted and the percentage of necrotic cells can be evaluated. In all experiments, where the viability of microglia in phagocytosis was assessed by this method, cells were first trypsinised and harvested to 1.5 ml Eppendorf™ tubes. Subsequently, an equal volume of 0.4% Trypan blue was added to 150 µl of cell suspension and incubated in room temperature for 5–15 minutes. Following incubation, 10 µl of cell suspension was placed on the haemocytometer and the number of both stained and unstained cells was assessed.

### **3.3.5 Assessment of phagocytosis**

In this study, phagocytosis was assessed in BV-2, HAPI, and RAW 264.7 cell lines and in primary microglial cells and two methods used for assessment of phagocytosis.

#### **3.3.5.1 Phagocytosis assay**

Latex (amino-modified polystyrene) beads with or without fluorescent tagging (1-0.8 µm diameter respectively; Sigma; excitation/emission 470/540) were used as phagocytosis targets.

##### **3.3.5.1.1 Fluorescent BSA latex beads**

To observe the phagocytic activity of microglia, BV-2 ( $5 \times 10^5$  cells) were cultured on glass coverslips (19 mm) in 12 well plates, and treated with cannabinoids (as indicated in individual experiment descriptions) for 24 hours after which the medium was removed and different volumes of fluorescent latex beads from original stocks were re-suspended in 0.1% bovine serum albumin with PBS without  $\text{Ca}^{2+}$  and  $\text{Mg}^{2+}$  for 2 hours at 37°C.

Each volume (addition of 0.25  $\mu$ l, 0.5  $\mu$ l and 1  $\mu$ l) of beads was tested to determine the optimum bead concentration that the cells would phagocytose. Following the 2-hours incubation, the assay was stopped and non-phagocytosed beads removed by applying several rinses of 1ml cold PBS to each well. The cells were then fixed onto coverslips with 500  $\mu$ l of warm paraformaldehyde (4% paraformaldehyde/400 mM sucrose in PBS) at room temperature for 30 minutes.

The cells were then washed several times with warm PBS and permeabilized with 500  $\mu$ l of 0.1% Triton X-100 in 1% bovine serum albumin-containing PBS for 15 min at room temperature. To visualize the phagocytosed beads, F-actin was detected by staining with rhodamine phalloidin (a high-affinity F-actin probe conjugated red fluorescent dye) was purchased from Molecular Probes® Life technology which binds to the polymerised form of actin (F-actin) diluted in PBS for 15 min at room temperature. Coverslips were then incubated with DAPI (1:1000) for staining of cell nuclei. The coverslips were mounted on glass slides by one drop of warm mounting medium without DAPI. The cells were viewed by confocal microscopy under 20X magnification using an oil immersion lens.

All images of the cells were recorded using the same microscope, objective lens, and exposure time to allow comparison of measurements. Fluorescence intensity in each channel was corrected for background noise and quantified using Velocity 6 Demo image analysis software. Fluorescent beads were quantified on consecutive images using Velocity 6 Demo software to measure pixel intensity along the line scans at the bead site. The number of ingested beads per cell and total cells was counted to determine the rate of phagocytic cells and the mean number of ingested beads per cell.

#### **3.3.5.1.2 Non-fluorescent latex beads**

Phagocytosis was assessed in BV-2 and HAPI cells. Cells were cultured at  $5 \times 10^5$  cells per well in 12 well-plates for 24 hours until cells were approximately 70% confluent. Cells were stimulated with LPS alone or with CBD for 24 hours then incubated with latex beads (0.8 $\mu$ m) for 2 hours. The cells were washed with cold PBS 3 times then fixed with paraformaldehyde (4%) for 30 minutes at room temperature. Images were taken using inverted microscope. To analyse the amount of phagocytosis that occurred in this culture. 3 images per conditions were randomly captured and then analysed by manually counting the number of beads engulfing and number of total cells per field.

#### **3.3.6 Migration**

We designed a cell migration assay using an in-house designed and built "Compass" device (University of Nottingham Medical Engineering Unit). This system (details withheld subject to patent application) allows migration to be measured in a 96-well plate, where cell migration into a vacant space can be recorded by image capture at regular intervals over a 48 hour period using an inverted microscope with an attached camera. Images were analyzed using PowerPoint to measure the degree of cellular incursion into the vacant space.



**Figure 3.1;** “Compass” cell migration assay device

### **3.3.7 Western blotting**

#### **3.3.7.1 Whole Cell Protein Extraction**

Whole cell protein lysates of BV-2 cells were used in immunoblotting assays (see chapter 2).

#### **3.3.7.2 Membrane fractionation**

Procedures for fractionation were adapted from the method of Rockstroh et al., (2011). Cells were plated 24 hours before the experiment. On the day of the experiment, BV-2 cells ( $5 \times 10^4$ ) were centrifuged for 5 min at  $250 \times g$  and washed twice with 3 ml with 1.5 ml buffer A (250 mM sucrose, 50 mM Tris-HCl, 5 mM  $MgCl_2$  and protease inhibitor).

The cell pellet was re-suspended in 1.5 ml buffer B (1 M sucrose, 50 mM Tris-HCl, 5 mM  $MgCl_2$  and [protease inhibitor tablet; containing 1 tablet of protease inhibitor cocktail (4-(2-Aminoethyl) benzenesulfonyl fluoride hydrochloride (AEBSF), Bestatin hydrochloride, Leupeptin, E-64, Aprotinin, Pepstatin A, and Phosphoramidon disodium salt; Sigma)]) by vortexing. The

suspension was incubated for 10 minutes while continuously rocking. After 15 minutes centrifugation at 16,000 x g and 4 °C, the supernatant (S1) contained the cytosolic proteins. The pellet (P1) was dissolved in 1 ml buffer C (20 mM Tris-HCl, 0.4 M NaCl, 15% glycerol, 1.5% Triton X-100 and protease inhibitor) and the mixture was incubated for 30 minutes shaking. The suspension was centrifuged for 15 minutes at 16,000 x g and 4 °C. The supernatant (S2) contained the solubilised membrane proteins, the cell debris containing pellet (P2) was discarded. The protein determination for both fractions was carried out using the Lowry method.

### **3.3.7.3 Gel electrophoresis**

The 10% sodium dodecyl sulphate (SDS) polyacrylamide gels were transferred into an electrophoresis tank (Bio-Rad, USA). The combs were removed from the gels and 500 ml electrophoresis buffer 1x (30.3g Tris, 144g glycine and the 10 g SDS in 1L distilled water) was added into the tank. 20 µg of denatured protein samples were loaded into the wells with 2 µl of the All Blue standard molecular weight markers (Bio-Rad laboratories Ltd, UK); electrophoresis was run at 200 V for 45 minutes.

1 membrane and 2 filter papers were placed in sequence in transfer buffer (30.3g Tris, 144g glycine dissolved in 8 litres distilled water, to which a another 2 litres of methanol was added) and then the proteins were transferred at 100V for 60 minutes at 4 °C using Bio-Rad apparatus. The protein transfer was checked by using a few drops of Ponceau's solution.

The membranes were incubated with 5% fat-free dried milk powder in TBST (30.3g Tris, 73.12g NaCl, in 1L distilled water adjusted to pH 7.6 and then diluted to 10 litres with the addition of Tween 20 to a final concentration of 0.1%) on a shaker at room temperature for 60 minutes

and then washed with 0.1% TBS-Tween twice. The indicated primary antibodies were diluted in 5% milk in TBST. The membranes with diluted primary antibodies were incubated in small plastic bags on a shaker at 4°C overnight.

The membranes were washed with TBS-Tween on a shaker at room temperature for 3 times of 10 minutes each and then incubated with 5% milk in TBST diluted secondary antibodies ([IRDye infrared LI-COR, USA] - 1:2000, dilution) goat anti-rabbit IgG or goat anti-mouse IgG with shaking for 1 hour at 37 °C. The membranes were washed with TBS-Tween on a shaker at room temperature for 3 times of 10 minutes each. Then washed one time with Milli-Q-water and the blots were scanned using the Li-COR Odyssey Infrared Imaging system (Li-Cor Bioscience), in 700 and 800 nm channels, with a resolution of 42 µm, quality, an intensity of 5, and focal offset of 2mm. The data were analyzed by Odyssey application software. The membranes were kept at 4°C for future reference.

#### **3.3.7.3.1 The primary antibodies used**

Anti-TRPV2 (1:1000, Calbiochem; PC421), anti-TRPV1 (1:1000, Santa Cruz Biotechnology; sc-28759), Phospho-Akt (Thr308) (244F9) Rabbit mAb, (1:1000, Cell Signaling Technology; 4056), Akt (40D4) Mouse mAb (1:1000, Cell Signaling Technology; 2920) and anti-GAPDH (1:2000; Sigma).

#### **3.3.8 Immunocytochemistry**

BV-2 cells ( $5 \times 10^5$ ) were seeded on poly-L-lysine-coated 13 mm glass coverslips and allowed to attach overnight in the conditioned medium. The following day, cells were serum-starved for 24 hours in a medium containing no fetal bovine serum (FBS); when indicated, 10% FBS was

added to some cells. The cells were incubated with medium alone, with LPS, or with drug for indicated times.

Cells were fixed with 4% paraformaldehyde in phosphate-buffered saline (PBS) for 30 minutes at room temperature, washed with PBS and then permeabilized using 0.1% Triton X-100 for 30 minutes. Blocking of non-specific binding sites was performed by incubating cells with PBS containing 1% bovine serum albumin (BSA) for 1 hour at room temperature. Cells were incubated with indicated primary antibody overnight at 4 °C.

After 3 washes with PBS, FIT-C-conjugated goat anti-rabbit IgG (1:800) or FIT-C-conjugated goat anti-mouse IgG (1:500, both IgG from Jackson Immuno Research) was added and incubation proceeded for 1 hour at 37 °C. To visualize the cells present on coverslips, the cell nuclei were stained with 4, 6-diamidino-2-phenylindole (DAPI, Molecular Probes) dye (1:1000) for 5 minutes at room temperature. After extensive washing, coverslips were mounted with mounting medium without DAPI (Vectashield) was from (Vector Laboratories, inc Burlingame) and viewed through a 63x glycerin immersion objective lens or 40x oil immersion lens with a Leica DMRA2 fluorescent microscope. Images were cropped and brightness and contrast were adjusted equally using the ImageJ Software. The intensity of immunoreactivity was defined as the product of relative optical density (ROD) and area of immunoreactivity was measured using the ImageJ Software and velocity Demo 6 software was used for confirmation. Negative controls without primary antibody were included to identify non-specific staining.

### **3.3.8.1 The primary antibodies used**

TRPV2; 1:500, CalBiochem, TRPV1; 1:100, Santa Cruz Biotechnology, PKC alpha (H-7) AC, Monoclonal Antibody; 1:250, Santa Cruz Biotechnology; sc-8393-AC), PKC $\epsilon$ , Polyclonal Antibody; 1:250, Santa Cruz Biotechnology; sc-638, PLC Gamma2 (Q-20), Polyclonal Antibody (1:250; Santa Cruz Biotechnology; sc-407) or (IB $\alpha$ -1; 1:100, alpha laboratories; 019-19741, Hampshire, UK)

### **3.3.9 Reverse transcription polymerase chain reaction (RT-PCR)**

#### **3.3.9.1 RNA extraction**

The cell pellets from confluent 24 well plates of BV-2 cells or mouse whole brain tissue were homogenized in 1 ml lysis reagent (Tri-reagent®, Ambion, UK). The homogenate was incubated for 5 minutes on ice to promote a complete dissociation of nucleoprotein complexes before addition of BCP (1-bromo-3-chloro-propane) and centrifugation (10 864 g for 15 minutes at 4°C) to separate the mixture into an aqueous RNA phase and an organic protein phase. The upper aqueous phase was used for RNA precipitation at 20°C for 30 minutes with sodium acetate (2 M pH 4) and isopropanol (500  $\mu$ l, 700  $\mu$ l/1 ml of aqueous phase respectively). The organic phase was kept at -80°C for further protein extraction. RNA was collected by centrifugation (10 864 g for 10 minutes at 4°C) and washed twice with 70 % ethanol. 50  $\mu$ l of DEPC-treated water was added to dissolve pellets before measuring the concentration of total RNA obtained using a NanoDrop device (ND-1000 Spectrophotometer, NanoDrop Technologies, USA).

### **3.3.9.2 mRNA Preparation**

As the target gene is a single exon gene, Dynabeads® mRNA purification kit (Invitrogen, UK) was used to extract mRNA from total RNA to overcome the problem of genomic DNA contamination. The manufacturer's instructions were followed using a magnet (Magna-Sep™, Invitrogen, UK) to remove the suspending, binding and washing buffer from oligo (dT) coated Dynabeads. mRNA was eluted from Dynabeads using 20 µl of 10 mM Tris-HCl and heating for 2 min in 65-80°C.

### **3.3.9.3 Complementary DNA (cDNA) synthesis**

5 µl (1 µg/µl) purified RNA was used to synthesis cDNA with superscript III reverse transcriptase (Invitrogen, UK) and another 5 µl underwent the same reaction but with superscript III reverse transcriptase replaced by HPLC water to generate a non-reverse transcriptase control (NRTs). To each 5 µl of RNA, 1 µl of random primer and 1 µl of dNTP were added, made up to a volume of 13 µl with 6 µl of HPLC grade water; the mixture was incubated at 65 °C for 5 minutes and quickly chilled on ice followed by addition of the following to make up the final reaction volume of 20µl (4 µl first strand buffer X5; 1 µl 0.1 M DDT; 1 µl RNase inhibitor and 1 µl superscript III for cDNA sample or 1 µl NRTs sample). Finally, the mixture underwent an incubation period of 20 minutes at 37°C, then 60 minutes at 50 °C and at 70 °C for 15 minutes. cDNA and NRTs synthesized were stored at -20°C for future use.

### **3.3.9.4 Designing the Primers and Probes**

Primers for the target gene were designed using Primer Express 2 (Applied Biosystems, UK) following manufacturer's instructions and purchased through Eurofins MGW Operon. Primers and probes were assessed using

the National Center for Biotechnology Information Basic Local Alignment Search Tool (NCBI BLAST) to ensure that the chosen sequence was specific for the gene of interest. Primer and probes were re-constituted and diluted to 10 $\mu$ M prior to use.

Mouse beta actin (ACTB) endogenous control (FAMTM Dye/MGB probe, non-Primer limited) Part Number 4352933E from (Applied Biosystems, UK) was used as control.

<b>Gene</b>	<b>Primers</b>	<b>sequence</b>
<b>Mouse Trpv2</b>	Forward Primer	ACTAAGGTGGAGGGTGGACGAT-3'
	Reverse Primer	CCAAGCCTAGCGGGACTCT-3'
	Probe	CCAGCTACGGAGGCTCCGCG-3'

### **3.3.9.5 Taqman Real-Time PCR**

A mixture of cDNA from different samples of positive control was used to form the standard curve and 2 fold dilutions (1:2, 1:4, 1:8 etc) of each cDNA and non-template control to quantify relative concentrations of the target and reference genes in the samples, cDNA samples were diluted. A master mix prepared for the reference and target gene was calculated according to the desired number of wells each containing a mix of Taqman master mix, forward primer, and reverse primer, probe and HPLC water. 10  $\mu$ l from this mix was added to each well of a 96 well reaction plate (Applied Bioscience, USA) then 3  $\mu$ l from each cDNA sample or standard was added in triplicate. The StepOne plus real time PCR system (Applied Biosystem, UK) was used for assay.

### **3.3.10 Fura-2 AM Ca<sup>2+</sup> imaging**

Experiments were typically conducted using BV-2 cultures at  $5 \times 10^5$  cells seeded onto 19 mm glass coverslips coated with poly-L-lysine. Cultures were washed 3 times in buffer (NaCl 145mM, KCl 5mM, CaCl<sub>2</sub> 2mM, MgSO<sub>4</sub> 7H<sub>2</sub>O 1mM, HEPES 10mM, glucose 10mM and 2g BSA) and loaded for 30 minutes in the dark at 37°C, with 10 μM cell-permeable fluorescent Ca<sup>2+</sup> indicator, Fura-2-AM (Cambridge Bioscience, Cambridge, UK). Cells were then washed again with buffer and all experiments performed at room temperature in the dark. Cultures were superfused at a rate of 2 ml/min. Using the laser scanning microscope, emission intensity was measured up to 20 min, every 200 - 400 ms using excitation at 430 nm and emission detection range from 480 to 536 nm. Stimulating drugs were added after 10 to 30 seconds.

### **3.3.11 Statistical analysis**

Data were collected from three or more independent experiments (using different passages of cells) and are expressed as mean ± S.E.M. Statistical analysis was performed, where indicated, using repeated measures one-way and two-way ANOVA, with post-hoc. Comparison of more than two groups was done by ANOVA followed by Dunnett's multiple comparison tests or Bonferonni's multiple comparison test as appropriate. Statistical analysis was performed using *GraphPad Prism*® version 5 software (GraphPad Software, La Jolla, CA). Statistical significance was considered for a p value less than 0.05.

### 3.4 Results

#### 3.4.1 Phagocytic response after non- fluorescent latex beads exposure

The phagocytic response of BV-2 to 0.8  $\mu\text{m}$  latex beads after 2 hours exposure was assessed. The total proportion of cells that could phagocyte latex beads and the total beads were recorded. A significant stimulation of phagocytosis after incubation with either 10  $\mu\text{M}$  CBD or 100 ng/ml LPS in the BV-2 cells is shown in Figure 3.2.

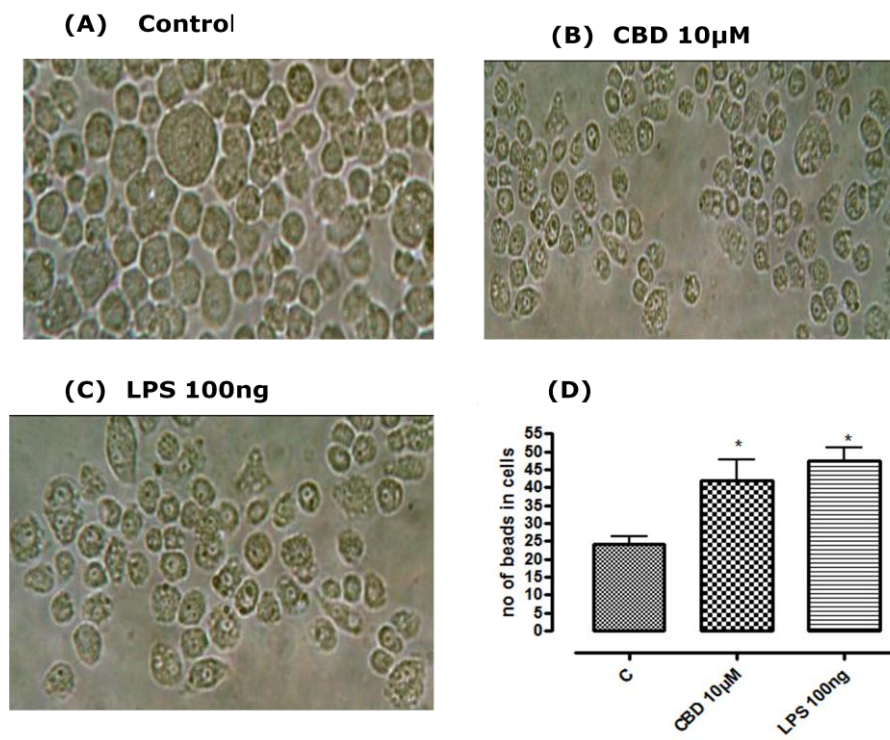


**Figure 3.2:** Phagocytosis of non-fluorescent latex beads assessed using an inverted microscope. BV2 cells were treated with (A) C; control (B) CBD 10 $\mu\text{M}$  (C) LPS 100ng/ml for 24 hours and incubated with latex beads (0.8  $\mu\text{m}$  in size; 0.5u/ml) for 2 hours then washed with PBS, fixed with PFD (4%) and visualized with an inverted microscope. manually counting the number of beads engulfing and number of total cells per field (D) Histogram of number of beads /number of total cells. Data were analysed using one-way ANOVA followed by post-hoc Dunnett's test; \*P<0.05 CBD compare with (C) control; \*P<0.05 LPS compare with (C) control.

### 3.4.2 Fluorescent BSA latex beads

#### 3.4.2.1 Optimization of protocol

Microglial phagocytosis was monitored by assessing the ingestion of latex beads (Figure 3.3). The influence of bead concentration and time-course on phagocytosis was investigated (Figure 3.4). The number of fluorescent beads accumulated by BV-2 cells tended to increase with increasing bead-load ( $0.25 \mu\text{l/ml} < 0.5 \mu\text{l/ml} < 1 \mu\text{l/ml}$ ). At a bead concentration of  $0.5 \mu\text{l/ml}$ , phagocytosis of beads increased over the period 0.5 to 2 hours (Figure 3.5). We further tested the effects of temperature and ethanol (as drug vehicle) on microglial phagocytic activity. BV-2 cells were incubated with  $0.5 \mu\text{l/ml}$  fluorescent latex beads for 2 hours in the presence of (1%) bovine serum albumin at  $37^\circ\text{C}$  (control) or  $4^\circ\text{C}$  and in the presence of 0.1% ethanol. We found that low temperature inhibited phagocytosis but phagocytic activity was not significantly affected by 0.1% ethanol (the maximum amount used as vehicle in any experiment) (Figure 3.6).

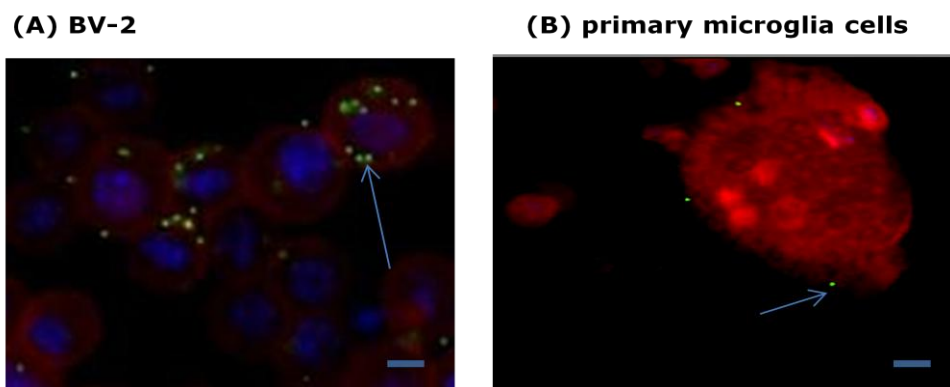


**Figure 3.3:** Images show the phagocytic cells in BV-2 cells and primary mouse primary microglia. BV-2 cells ( $5 \times 10^5$  cells/well) or primary cells were loaded with BSA fluorescent beads for 2 hours then incubated at  $37^\circ\text{C}$  with medium then stained with rhodamine phalloidin (a high-affinity F-actin probe conjugated red fluorescent dye) (red) and DAPI (blue). (A) BV-2 phagocytic cells (40X) (B) in primary mouse phagocytic microglia (red IBa-1 microglial marker), arrow indicates yellow fluorescent beads (40X).

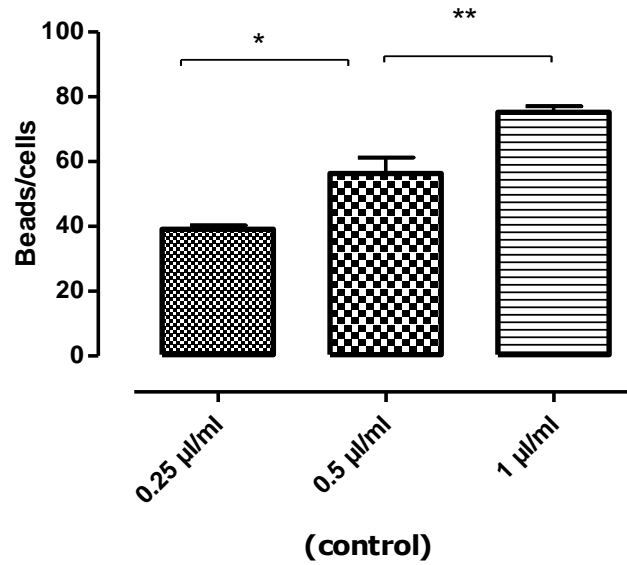


**Figure 3.4:** Histogram shows the effect of BSA latex bead concentration on phagocytic activity in BV-2 cells. BV-2 cells ( $5 \times 10^5$  cells/well) were incubated with medium for 24 hours. Fluorescent BSA beads ( $1 \mu\text{m}$  size) were then added at the concentrations indicated for 2 hrs. Data were analysed using one-way ANOVA followed by post-hoc Bonferroni;  $**P < 0.01$ ,  $1 \mu\text{l/ml}$  concentration compare with  $0.5 \mu\text{l/ml}$  concentration;  $*P < 0.25 \mu\text{l/ml}$  concentration compared with  $0.5 \mu\text{l/ml}$  concentration.

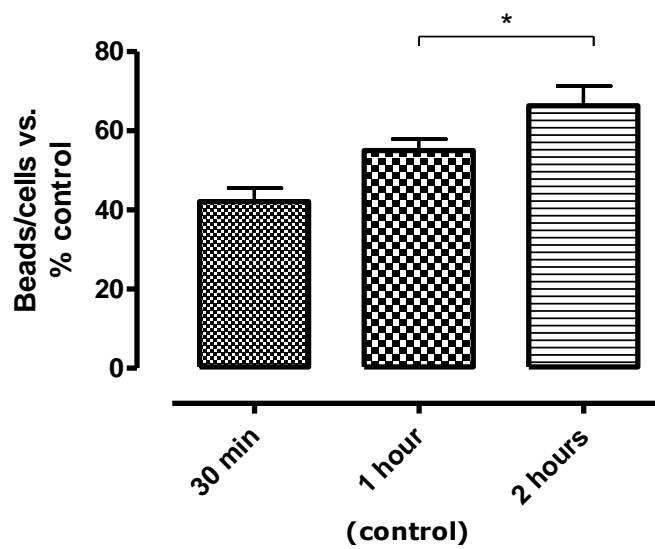


**Figure 3.5:** Histogram shows the effect of incubation time on phagocytosis in BV2 cells. BV-2 cells ( $5 \times 10^5$  cells/well); Cells were incubated with the fluorescent beads ( $1 \mu\text{m}$ -size,  $0.5 \mu\text{l/ml}$  concentrations) for the times indicated. Data were analysed using one-way ANOVA followed by post-hoc Bonferroni;  $*P < 0.05$ , 2h compare with 1 h.

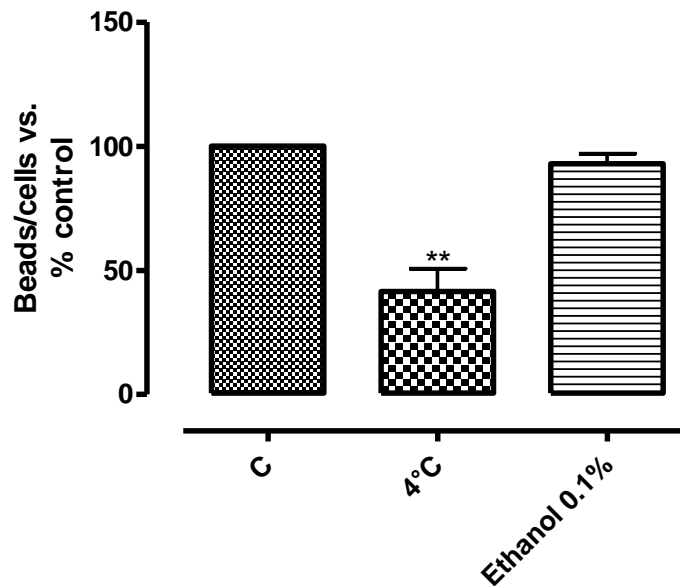


**Figure 3.6:** Histogram shows the effect of temperature and ethanol on phagocytosis in BV-2 cells. BV-2 cells ( $5 \times 10^5$  cells/well); were loaded with fluorescent BSA latex beads ( $1 \mu\text{m}$ ,  $0.5 \mu\text{l/ml}$ ) for 2 hours then incubated at  $4^\circ\text{C}$  or  $37^\circ\text{C}$  with or without ethanol. The figure represents means  $\pm$  SEM of triplicate determinations in three independent experiments. The data are presented as a percentage of control. Data were analysed using one-way ANOVA followed by post-hoc Dunnett's test;  $**P < 0.01$  C  $4^\circ\text{C}$  compare with C.

#### 3.4.2.2 The role of the cytoskeleton in phagocytosis

To assess cytoskeletal involvement in phagocytic BV-2 phagocytosis, the effect of cytochalasin D, an inhibitor of actin polymerization, was assessed. This drug disrupts actin microfilaments and activates p53-dependent signaling pathways causing arrest of the cell cycle at the G1-S transition. Bead phagocytosis is expected to require pseudopod extension which is an actin-based movement of the microglial cells. Cytochalasin D ( $1 \mu\text{M}$ ) was added to BV-2 cells for 1 hour before incubation with fluorescent BSA beads at  $37^\circ\text{C}$  for 2 hours, and the cultures were gently washed in PBS to eliminate uningested beads, fixed using 4% formaldehyde for 20 min and washed with PBS. Samples were analyzed by fluorescence microscopy.

Cytochalasin D completely inhibited phagocytosis, indicating the dependence of phagocytosis on actin polymerization (Figure 3.7).

### 3.4.2.3 The role of mitochondria in phagocytosis

In order to assess the requirement for mitochondrial activity, the effects of oligomycin (a mitochondrial ATPase inhibitor) and FCCP (a mitochondrial uncoupler that blocks oxidative phosphorylation) on BV-2 phagocytosis were monitored. BV-2 cells were incubated with oligomycin (1 $\mu$ M) or with FCCP (1 $\mu$ M) for 1 hour then 0.5 $\mu$ l/ml fluorescent BSA latex beads were added for 2 hours. 1 hour treatments with oligomycin or FCCP failed to affect the ability of BV-2 to phagocytose latex beads (Figure 3.7).

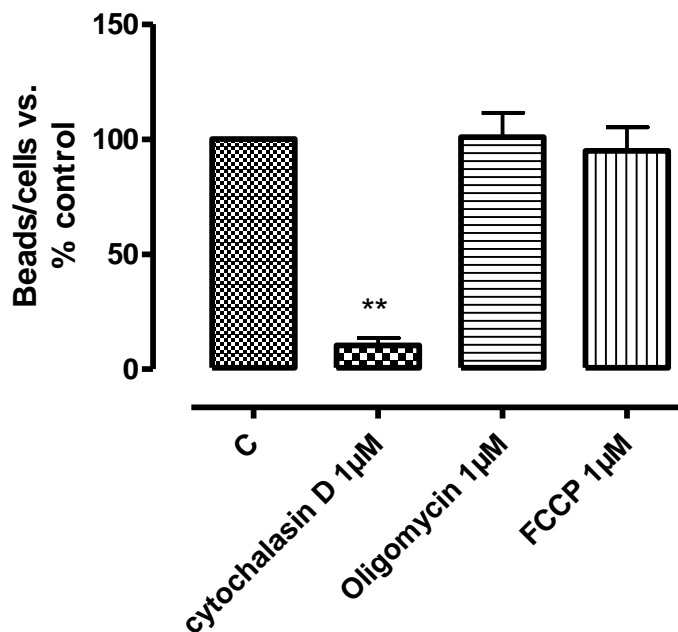


**Figure 3.7:** Histogram shows the effect of the cytochalasin D (a cytoskeleton inhibitor), oligomycin (a mitochondrial ATPase inhibitor) and FCCP (a mitochondrial uncoupler) on phagocytosis in BV-2 cells. ( $5 \times 10^5$  cells/well); BV-2 were pre-incubated with indicated drugs at (1 $\mu$ M) for 1 hour. Control wells (C) were incubated with culture medium alone. BV-2 cells were loaded with 0.5  $\mu$ l/ml fluorescent beads (0.5  $\mu$ l/ml) for 2 hours. The figure represents means  $\pm$ SEM of triplicates of three independent experiments. The data are presented as a percentage of control. Data were analysed using one-way ANOVA followed by post-hoc Dunnett's test; \*\* $P < 0.01$  cytochalasin compare with control.

#### 3.4.2.4 The role of myosin II in BV-2 phagocytosis

Non-muscle myosin II, an actin-based motor protein, plays an important role in actin cytoskeleton organization and cellular motility. We examined the localization of myosin II and whether myosin light chain II (MLCII) is involved in the BSA latex bead phagocytosis using antibodies against MLCII, incubated with BSA latex beads ( $1\mu\text{m}$ - $0.5\ \mu\text{L}/\text{ml}$  for 2 hours at  $37\ ^\circ\text{C}$ ). MLCII antibody was added overnight. Myosin II accumulates at the edges of BV-2 cells to form tight filaments through the edge of the cells during phagocytosis (figure 3.8; B). It seems likely that myosin II contributes to some aspect of phagocytosis localized around the BSA latex beads.

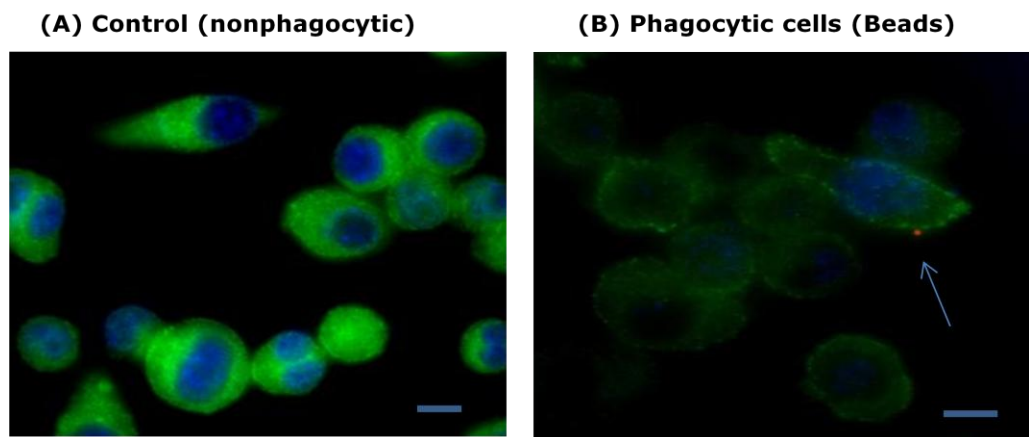


**Figure 3.8:** Images show The role of myosin light chain II protein on phagocytosis by immunocytochemistry **(A)** non-stimulated staining with MLCII antibody (green) and DAPI (blue) **(B)** BV-2 cells stimulated with fluorescent BSA latex beads ( $1\ \mu\text{m}$  –  $0.5\ \mu\text{l}/\text{ml}$  for 2 hours (arrow beads). The cells were visualized by confocal microscopy under 63X magnification glycerin immersion.

#### 3.4.2.5 Expression of CD11b in microglial cells

Microglia were assessed for changes in the extent and intensity of CD11b expression during phagocytosis of latex beads as this protein is used as an indicator of microglial activation. The expression in phagocytic microglia (i.e. exposed to beads) was compared to that in non-phagocytic microglia.

As a positive control, BV-2 microglia were treated with bacterial lipopolysaccharide (LPS), which induces an inflammatory response and activates microglia. The expression of CD11b in BV-2 phagocytic microglia was similar to that of BV-2 (control) non-phagocytic cells (Figure 3.9; A, B) while a significant increase in average intensity of CD11b expression in LPS-treated cells was observed (Figure 3.9; C).

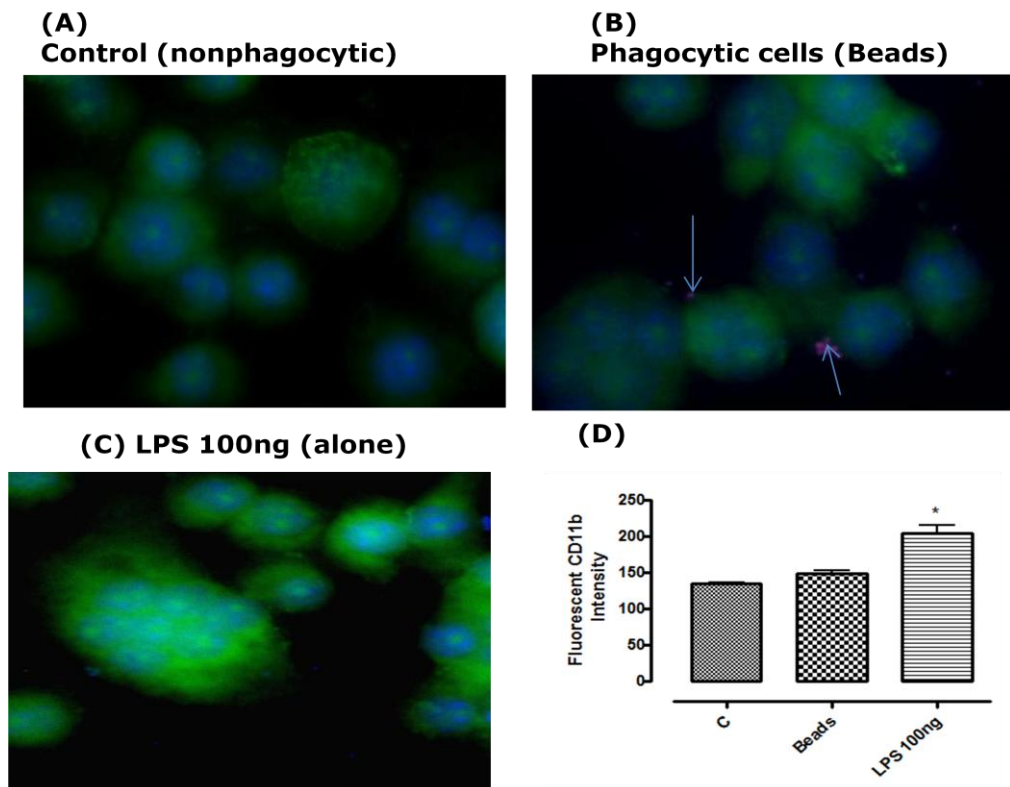


**Figure 3.9:** Confocal images showing expression of CD11b receptor immunocytochemical analysis of BV-2 cells stained with CD11b antibody (green) and blue DAPI. (A) Control non-phagocyte cells (B) phagocytes, BV-2 incubated with fluorescent BSA latex beads (0.5  $\mu$ l/ml; 1  $\mu$ m) for 2 hours (C) BV-2 incubated with LPS for 1hour (D) Fluorescent CD11b RFU The cells were visualized by confocal microscopy under 63X magnification using a glycerin immersion objective lens. The figure represents means  $\pm$ SEM of triplicate determinations in three independent experiments. Data were analysed using one-way ANOVA followed by post-hoc Dunnett's test; \*P<0.05 LPS compare with (C) Control.

#### **3.4.2.6 The role of phospholipase C $\gamma$ 2 (PLC $\gamma$ 2) in BV-2 phagocytosis**

PLC $\gamma$  is activated during phagocytosis in phagocytic cells, where it is essential for particle ingestion and bactericidal response (Scott *et al.*, 2005). We first examined the expression pattern of PLC $\gamma$ <sub>2</sub> in BV-2 cells. Next, we examined whether PLC $\gamma$ 2 could be activated by phagocytosis of latex beads. The images confirm that PLC $\gamma$ 2 is strongly expressed in BV-2 cells (Figure 3.10; A) and appeared to be translocated to areas around the beads during phagocytosis (Figure 3.10; B) and (C) cells in the presence of latex beads plus CBD with PLC $\gamma$ 2 translocated around the beads inside vesicles.

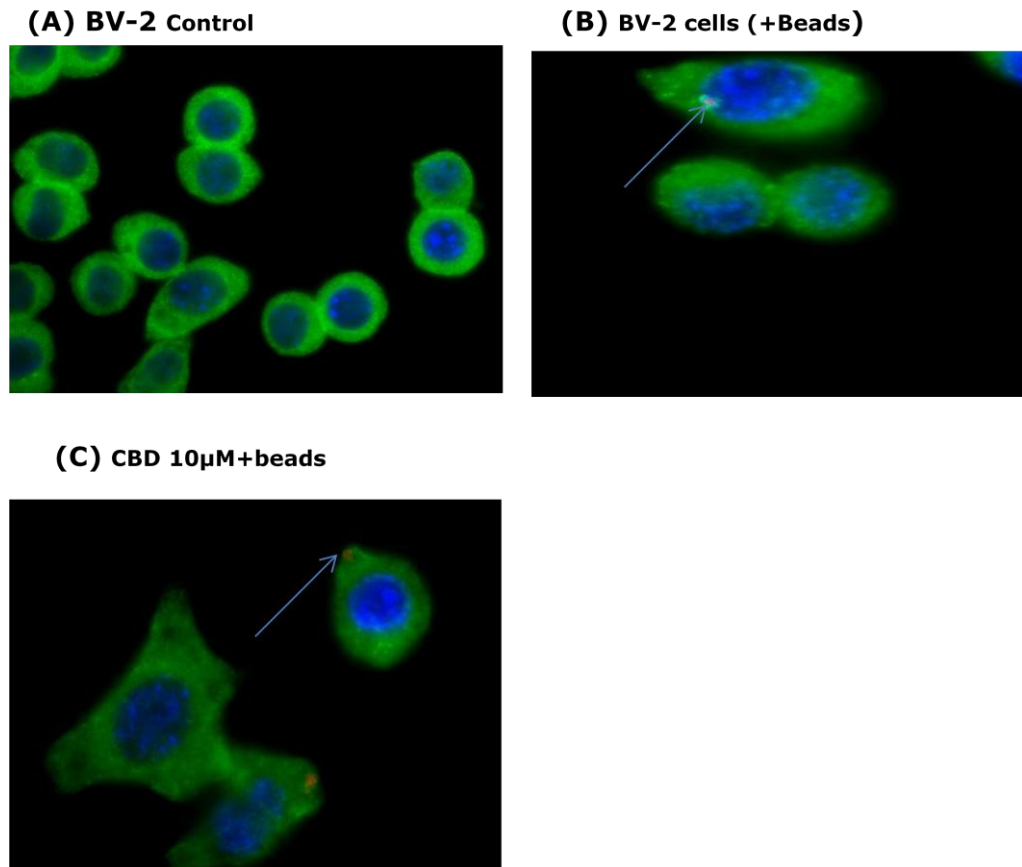


**Figure 3.10:** Confocal images showing expression of PLC $\gamma_2$  protein immunocytochemical analysis of BV-2 cells stained with PLC  $\gamma$  2 antibody (green) and blue DAPI. (A) Control BV-2 cells (40X) (B) Phagocytosing BV-2 cells incubated with fluorescent BSA latex beads 0.5 $\mu$ l/ml; 1  $\mu$ m for 2 hours, arrows indicate expression of PLC  $\gamma$ 2 around the beads (63X). (C) BV-2 cells pre-incubated with CBD 10 $\mu$ M for 24 hrs, then incubated with BSA latex beads 0.5 $\mu$ l/ml for 2hrs, arrows indicate beads with translocation of PLC $\gamma$ 2 inside the vesicles (63X).

### 3.4.2.7 The role of protein kinase C (PKC) in BV-2 phagocytosis

#### 3.4.2.7.1 PKC $\alpha$

Protein kinase C  $\alpha$  (PKC $\alpha$ ) contributes to F-actin remodeling during phagocytosis and phagosomal maturation in phagocytic cells. A previous report indicates a role for PKC $\alpha$  in signaling CR3/MAC-1-mediated phagocytosis of iC3b opsonized particles (Fallman et al., 1992; Makranz et al., 2003). To examine the role and expression of in phagocytosis of latex beads in microglial cells, BV-2 cells were incubated with or without latex

beads overnight with PKC $\alpha$  antibody. The results indicate apparent translocation of PKC $\alpha$  to the cell membrane and suggest that PKC $\alpha$  might play a role in latex bead phagocytosis in these cells (Figure 3.11; A-B).

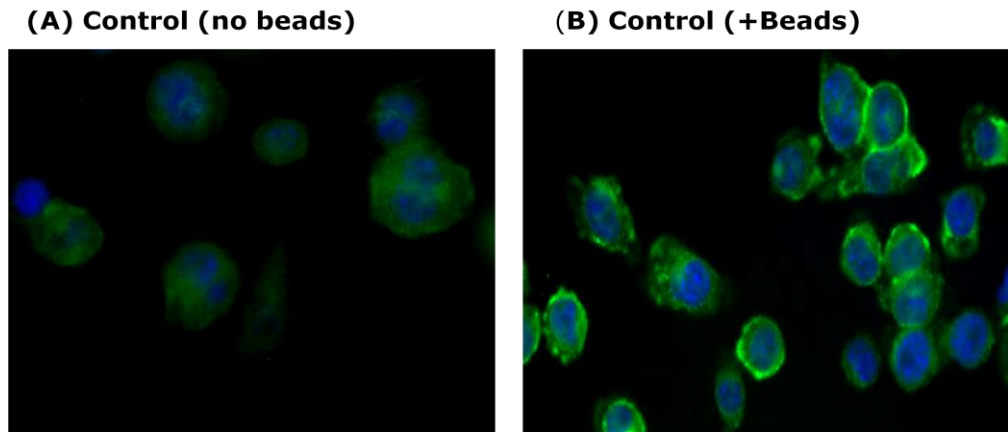


**Figure 3.11:** Images show the expression of PKC $\alpha$  protein by immunocytochemical analysis. BV-2 cells stained with PKC $\alpha$  antibody (green) and blue DAPI. (A) Control non-phagocytosing cells (B) BV-2 cells incubated with non-fluorescent latex beads (0.5 $\mu$ l/ml) for 2 hours. The cells were visualized by confocal microscopy under 63X magnification using a glycerin immersion objective lens.

#### 3.4.2.7.2 PKC $\epsilon$

PKC ( $\epsilon$ ) have been reported to translocate to membranes during Fc $\gamma$ R cross-linking or phagocytosis (Zheng *et al.*, 1995). To investigate the role and expression of PKC $\epsilon$  in microglial cells during phagocytosis, BV-2 cells were incubated with or without latex beads overnight with PKC- $\epsilon$  antibody. The results show apparent up-regulation of PKC $\epsilon$  to the cell membrane and suggest that PKC $\epsilon$  might play a role in BSA latex bead phagocytosis according to immunocytochemistry (Figure 3.12; A-B).

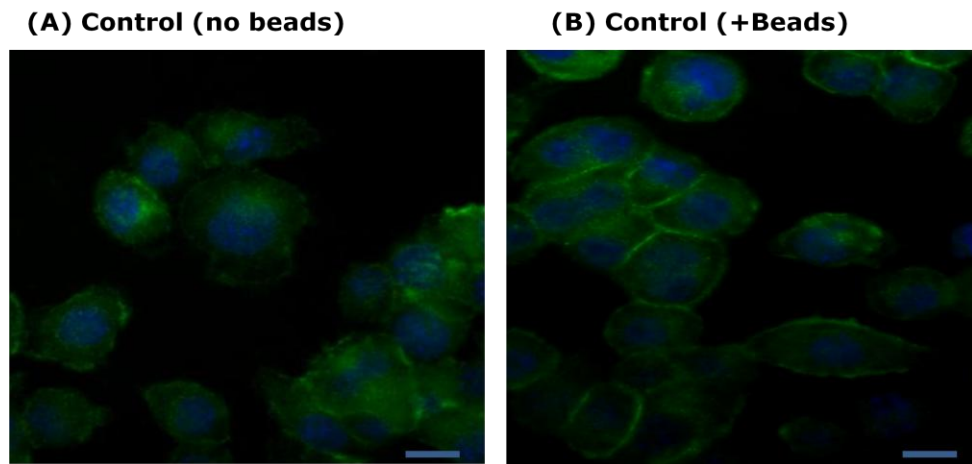


**Figure 3.12:** Images show the expression of PKC $\epsilon$  protein in BV-2 by immunocytochemical analysis. BV-2 cells stained with PKC- $\epsilon$  antibody (green) and blue DAPI. (A) Control cells without beads (B) BV-2 cells incubated with non-fluorescent BSA latex beads (0.5 $\mu$ l/ml) for 2 hours. The cells were visualized by confocal microscopy under 63X magnification using a glycerin immersion objective lens.

#### 3.4.2.8 The role of P2Y or P2X receptors in phagocytosis

ATP and UDP trigger a dynamic change in the motility of microglia *in vitro* and *in vivo* (Koizumi et al., 2007). To evaluate whether P2Y or P2X receptors are involved in microglial phagocytic activity the role of these purinoceptors in BV2 phagocytosis was investigated. BV-2 cells were incubated with UDP or ATP for 24 hours then loaded with 0.5  $\mu$ l/ml BSA latex beads for 2 hours. UDP (10  $\mu$ M) a P2Y<sub>6</sub> receptor agonist, but not ATP, produced a significant increase in phagocytosis (Figure 3.13).

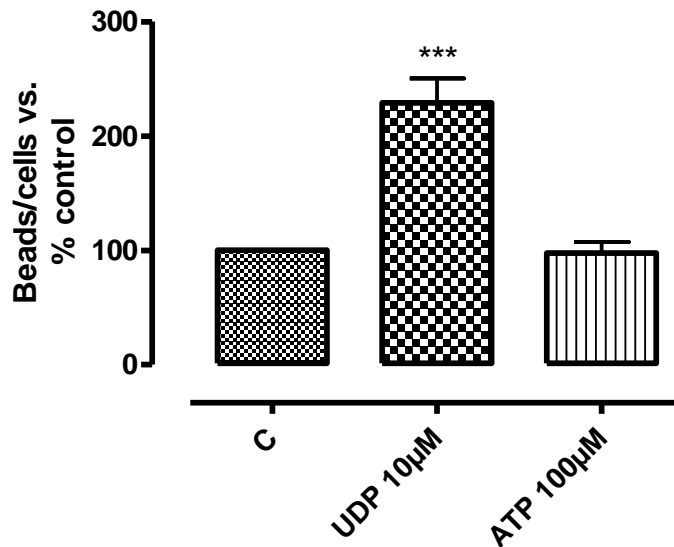


**Figure 3.13:** Histogram shows the effect of UDP and ATP (10 µM) on phagocytosis in BV-2 cells. ( $5 \times 10^5$  cells/well); BV-2 cells were incubated with indicated drugs for 24 hours and control wells (C, control) were incubated with culture medium alone. The cells were loaded with 0.5 µl/ml fluorescent BSA beads for 2 hours. The figure represents means  $\pm$  SEM of triplicate determinations from three independent experiments. The data are presented as a percentage of control. Data were analysed using one-way ANOVA followed by post-hoc Dunnett's test; \*\*\* $P < 0.001$  UDP compare with (C) Control.

### 3.4.2.9 The role of pro-inflammatory mediators in BV-phagocytosis

In order to determine whether nitric oxide has a direct effect on phagocytosis in BV2 cells, the selective iNOS inhibitor 1400W (N-[3-(aminomethyl) benzyl] acetamide) was incubated with BV-2 cells 1 hour prior to CBD (10 µM) for 24 hours then with added latex beads. 1400W failed to affect phagocytosis in the basal BV-2 cells (Figure 3.14), providing no evidence of a controlling influence of NO in BV2 phagocytosis.

We also investigated the effect on phagocytic activity in BV-2 cells activated with bacterial lipopolysaccharide (LPS, 100ng/ml) and interferon (50 U/ml). Figure 3.14; shows that, in the presence of BSA latex beads, LPS and interferon respectively led to an increase in phagocytosis after 24 hours incubation.

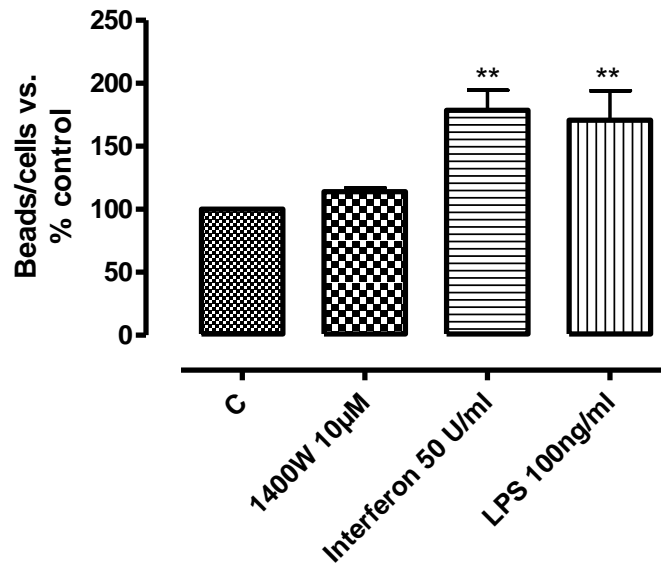


**Figure 3.14:** Histogram shows the effect of 1400W (selective iNOS inhibitor 1400W), interferon and LPS on phagocytosis in BV-2 cells ( $5 \times 10^5$  cells/well); cells were pre-treated with 1400W ( $10 \mu\text{M}$ ), SNP ( $10 \mu\text{M}$ ), interferon- $\gamma$  ( $50 \text{ U/ml}$ ) and LPS ( $100 \text{ ng/ml}$ ). Control wells (C) were incubated with culture medium alone. The cells were loaded with fluorescent BSA beads ( $0.5 \mu\text{l/ml}$ ) for 2 hours. The figure represents means  $\pm$ SEM of triplicates of three independent experiments. Data presented as a percentage of control. Data were analysed using one-way ANOVA followed by post-hoc Dunnett's test; \*\* $P < 0.01$ , INF- $\gamma$  compare with (C) control; \*\* $P < 0.01$ , LPS compare with (C) control.

#### 3.4.2.10 The role of anti-inflammatory drugs on BV-2 phagocytosis

To test the effects of anti-inflammatory agents on microglial phagocytosis, BV-2 cells were incubated with minocycline which has been shown to have anti-inflammatory and neuroprotective effects and to prevent microglial activation (Familian et al., 2007). Cells were incubated with minocycline ( $10 \mu\text{M}$ ) 1 hour prior to CBD ( $10 \mu\text{M}$ ) for 24 hours then incubated for 2 hours with latex beads ( $0.5 \mu\text{l/ml}$ ). The results show that minocycline failed to affect phagocytosis in BV-2 cells (Figure 3.15).

Glucocorticoids, including the synthetic glucocorticoid, dexamethasone, are recognised for their anti-inflammatory properties and ability to inhibit production of pro-inflammatory mediators such as nitric oxide synthase

(iNOS) (Lieb et al., 2003; Golde et al., 2003). Furthermore, they are reported to increase phagocytosis of apoptotic cells (Hodrea et al., 2012; Giles et al., 2001). The phagocytosis of BSA latex beads was investigated after exposure of BV-2 cells to different concentrations of dexamethasone (DEX) for 24 hours. Dexamethasone, as expected, augmented phagocytosis in a concentration-dependent manner as indicated in Figure 3.15.

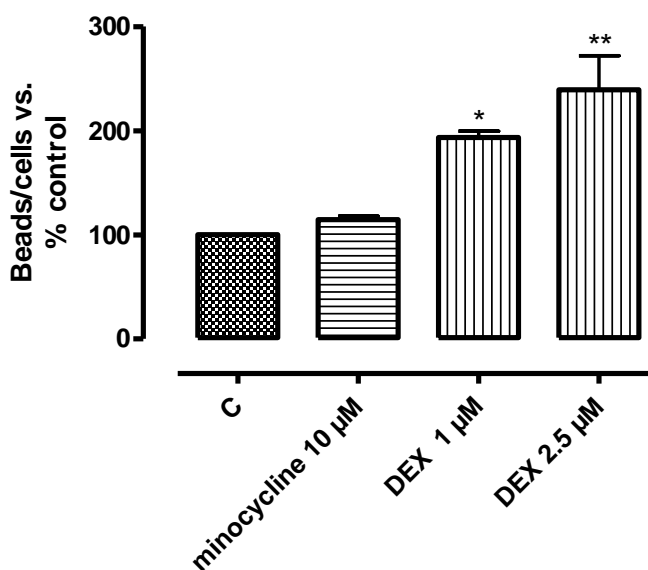


**Figure 3.15:** Histogram shows the effect of the microglial inhibitor minocycline and dexamethasone on phagocytosis in BV-2 cells. BV-2 ( $5 \times 10^5$  cells/well); were pre-treated with dexamethasone  $1 \mu\text{M}$  or  $2.5 \mu\text{M}$  for 24 hrs. Control wells (C, control) were incubated with culture medium alone. The cells were loaded with fluorescent latex beads ( $1 \mu\text{m}$ -size,  $0.5 \mu\text{l/ml}$ ) for 2 hours. The figure represents means  $\pm$  SEM of triplicates of three independent experiments. The data are shown as percentages of. The vertical Y axis represents the number of beads ingested /number of the cells. Data were analysed using one-way ANOVA followed by post-hoc Dunnett's test; \* $P < 0.05$  DEX  $1 \mu\text{M}$  compare with (C) control; \*\* $P < 0.01$ , DEX  $2.5 \mu\text{M}$  compare with (C) control.

#### 3.4.2.11 Effects of cannabinoids and endocannabinoids on microglial and macrophage phagocytosis

In this study we evaluated the effects of cannabinoids and endocannabinoids on phagocytosis in BV-2 cells; AM251 (a  $\text{CB}_1$  antagonist

and putative GPR55 agonist), the GPR55 agonist lysophosphatidylinositol (LPI), JWH133 (a CB<sub>2</sub> receptor selective agonist), CP55,940, a group of phytocannabinoids (CBDA, CBDV, THC, CBN and THC) and the endocannabinoids anandamide (AEA) and 2-AG (all at 10 $\mu$ M) failed to significantly affect phagocytosis. In contrast, the phytocannabinoid cannabidiol (CBD) produced a significant enhancement of phagocytosis at 10  $\mu$ M (Figure 3.16-3.18). Win55-212-2, a CB<sub>1</sub>/CB<sub>2</sub> agonist inhibited phagocytosis as shown in Figure 3.16.

We also measured phagocytosis of latex beads by primary microglia from C57BL/6 mice, RAW 264.7 and HAPI cells. Primary mouse microglia phagocytosed beads with a time course of uptake and concentration dependency similar to BV-2 cells (Figure 3.18). Pretreatment of the different cells with CBD enhanced the uptake of beads by similar amounts.

**(A) BV-2**

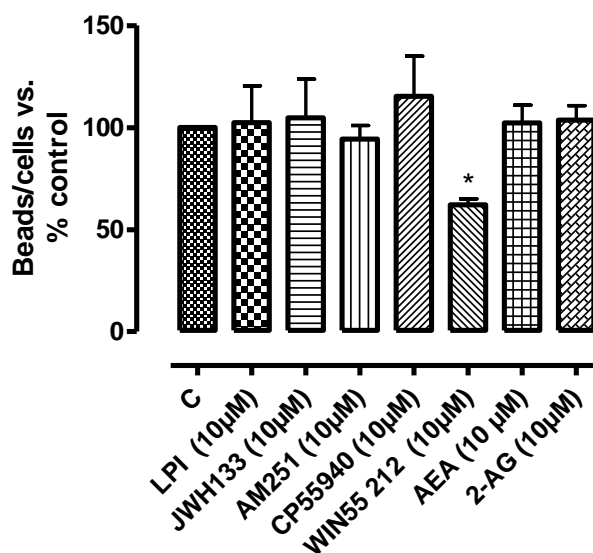


**Figure 3.16:** Histogram shows the effect of cannabinoids and endocannabinoids on phagocytosis in BV-2 cells. BV-2 cells (5x10<sup>5</sup>cells/well) were pre-treated with the indicated drugs (all 10  $\mu$ M) for 24 hours then incubated with fluorescent BSA latex beads (0.5  $\mu$ l/ml for 2 hours). The figure represents means  $\pm$ SEM of triplicate determinations of three independent experiments. The data are presented as a percentage of control. Data were analysed using one-way ANOVA followed by post-hoc Dunnett’s test; \*P<0.05 WIN55212-2 compare with (C) Control.

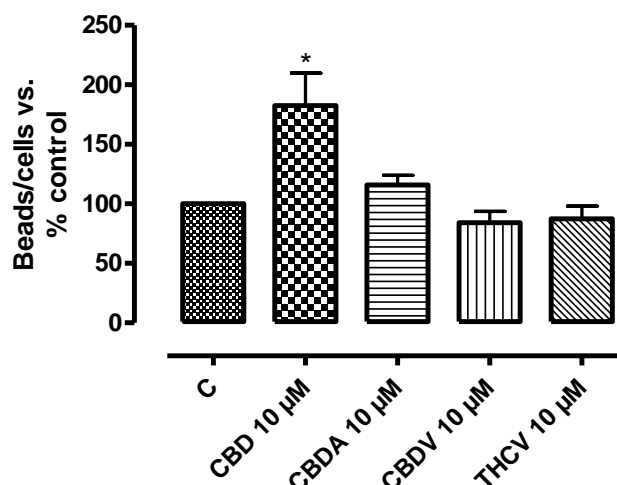


**Figure 3.17:** Histogram shows the effects of phytocannabinoids (10 μM) on phagocytosis in BV-2 cells. BV-2 cells were incubated with the indicated drugs for 24 hours then loaded with fluorescent BSA beads (1μm; 0.5 μl/ml) for 2 hours. The figure represents means ±SEM of triplicate determinations of three independent experiments. The data are presented as a percentage of control. Data were analysed using one-way ANOVA followed by post-hoc Dunnett’s test; \*P<0.05, CBD 10 μM compare with (C) control.

**(B) Primary mouse microglial cells**

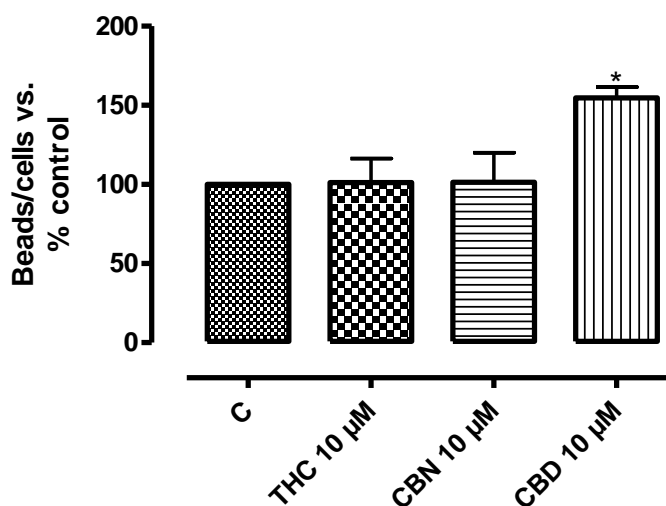


**Figure 3.18:** Histogram shows the effect of phytocannabinoids on phagocytosis in primary mouse microglial cells. Primary mouse microglial cells were pre-treated with the indicated drugs (all 10 μM) for 24 hours then incubated with fluorescent BSA latex beads (0.5 μl/ml for 2 hours). The figure represents means ±SEM of triplicate determinations of three independent experiments. The data are presented as a percentage of control. Data were analysed using one-way ANOVA followed by post-hoc Dunnett’s test; \*P<0.05 CBD 10 μM compare with (C) control.

**(C) RAW 264.7 cells:**

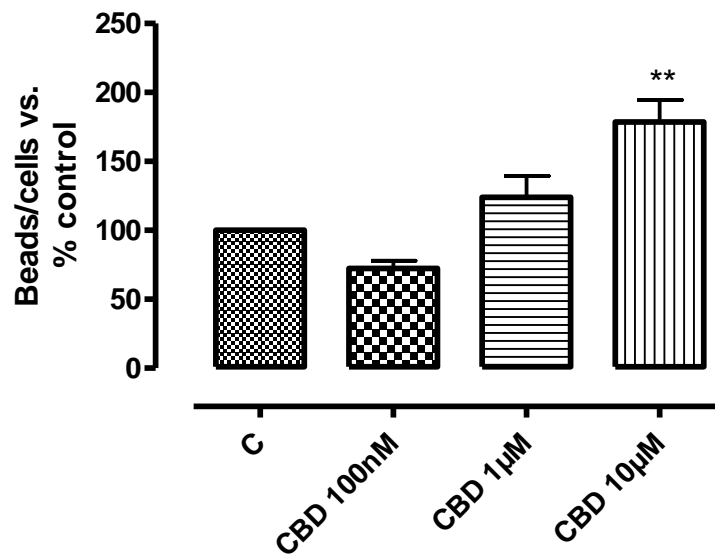


**Figure 3.19:** Histogram shows the effect of CBD on phagocytosis in RAW 264.7 cells. RAW 264.7 ( $5 \times 10^5$  cells/well) were treated with CBD at the indicated concentrations for 24 hours then incubated with ( $0.5 \mu\text{l/ml}$ ) fluorescent latex BSA beads for 2 hours. The figure represents means  $\pm$ SEM of triplicates of three independent experiments. The data are presented as a percentage of control. Data were analysed using one-way ANOVA followed by post-hoc Dunnett's test; \*\* $P < 0.01$ , CBD  $10 \mu\text{M}$  compare with (C) Control.

#### (D) HAPI

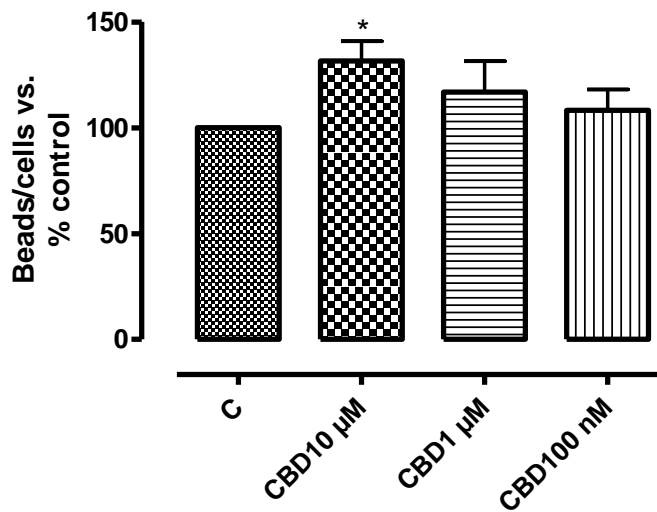


**Figure 3.20:** Histogram shows the effect of CBD on phagocytosis in HAPI cells. HAPI cells ( $5 \times 10^5$  cells/well) were treated with CBD at the indicated concentrations for 24 hours then incubated with (0.5  $\mu$ l/ml) fluorescent latex BSA beads for 2 hours. The figure represents means  $\pm$ SEM of triplicates of three independent experiments. The data are presented as a percentage of control. Data were analysed using one-way ANOVA followed by post-hoc Dunnett's test; \* $P < 0.05$  CBD 10  $\mu$ M compare with (C) control.

#### 3.4.2.12 Role of GPR18/Abn-CBD receptors in CBD induced phagocytosis

To examine whether GPR18 receptors were involved in phagocytosis previously reported its involvement in microglia migration (McHugh et al., 2010) and its enhancement by CBD, experiments were performed using N-arachidonylglycine (NAGLY) a putative endogenous GPR18 agonist.

NAGLY (10  $\mu$ M) did not significantly affect phagocytosis in BV-2 cells; neither was the effect of CBD reversed by pre-treatment with O-1918 (10  $\mu$ M) an Abn-CBD antagonist (Franklin and Stella 2003), (Figure 3.21); O-1918. These data rule out the involvement of GPR18 and Abn-CBD in CBD-augmentation of phagocytosis.

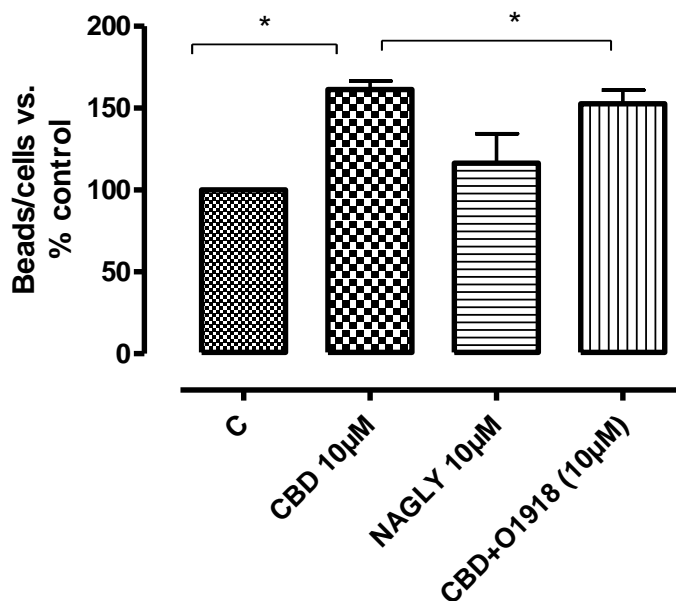


**Figure 3.21:** Histogram shows the effect of N-arachidonylglycine (NAGLY; GPR18 agonist) and O-1918 (an abn-CBD antagonist) on phagocytosis in BV-2 cells. BV-2 cells ( $5 \times 10^5$  cells/well) were pre-incubated with O-1918 for 1 hour then with CBD for 24 hours. Control wells (C) were incubated with culture medium alone or with NAGLY 10  $\mu$ M. The cells were loaded with (0.5  $\mu$ l/ml) fluorescent BSA beads for 2 hours. The figure represents means  $\pm$ SEM of triplicates of three independent experiments. The data are presented as a percentage of control. Data were analysed using one-way ANOVA followed by post-hoc Bonferroni multiple comparison test; \* $P < 0.05$ , CBD 10  $\mu$ M compare with (C) control; \* $P < 0.05$  CBD+O-1918 compare with CBD.

### 3.4.2.13 The effect of pertussis toxin on CBD-induced phagocytosis

Cannabinoid receptors are  $G_i$  protein-coupled and  $G_i$  signalling is suppressed by pertussis toxin. To examine if CBD-induced phagocytosis is mediated via a  $G_i$  protein-coupled mechanism, BV-2 cells were pretreated with 50 ng/ml of pertussis toxin for 18 hours followed by CBD (10  $\mu$ M) treatment for 24 hours, then incubated with latex beads for 2 hours. Pertussis toxin had no effect on the CBD-enhancement of phagocytosis (Figure 3.22). This finding suggests that  $G_i$  protein-coupled receptors are not involved in the CBD-induced phagocytosis.

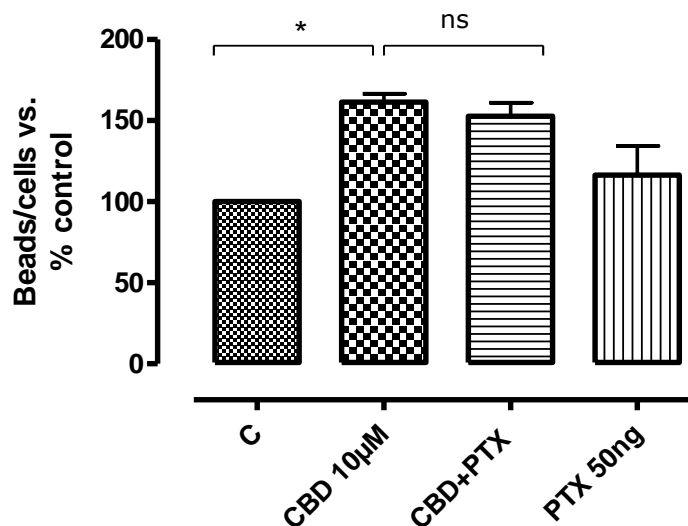


**Figure 3.22:** Histogram shows the effect of pertussis toxin (PTX) on CBD-induced phagocytosis in BV-2 cells. BV-2 cells ( $5 \times 10^5$  cells/well) were pre-incubated with or without 50 ng/ml PTX for 18 hours, then incubated in the presence or absence of CBD (10  $\mu$ M) for 24 hours. The cells were loaded with 0.5  $\mu$ l/ml fluorescent BSA latex beads for 2 hours. The figure represents means  $\pm$ SEM of triplicates of three independent experiments. The data are shown as percentages of control. Data were analysed using one-way ANOVA followed by post-hoc Bonferroni multiple comparison test; \* $P < 0.05$  CBD 10  $\mu$ M compare with (C) Control, ns (non-significant) CBD+PTX compare with CBD.

#### 3.4.2.14 The roles of PI3K, Rho/Rock kinase and p38 MAPK in CBD-enhancement of phagocytosis

We tested the effects of pre-incubation (1hr) with various inhibitors of PI3K, Rho kinases and p38 MAPK on phagocytosis in BV-2 and HAPI cells in the presence and absence of CBD. Cells were then incubated with (0.5  $\mu$ l/ml) fluorescent latex beads for 2 hours. Y27632 (a Rho/Rock inhibitor) decreased basal phagocytosis but did not affect CBD-enhanced phagocytosis; in fact the enhancement was somewhat more marked (Figure 3.23). SB203580 a P38 inhibitor had no effect on basal or CBD-enhanced phagocytosis (Figure 3.24).

The selective phosphoinositide 3-kinase (PI3K) inhibitor wortmannin (10  $\mu$ M) reversed basal phagocytosis but CBD still enhanced bead ingestion in the presence of wortmannin (Figure 3.25).

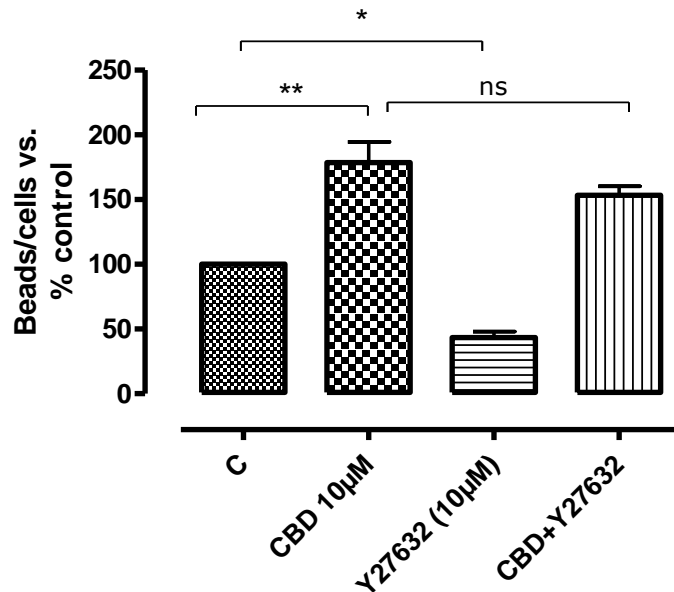


**Figure 3.23:** Histogram shows the effect of Y27632 (a Rho/ROCK signalling inhibitor) on phagocytosis in BV-2 cells. BV-2 ( $5 \times 10^5$  cells/well) were pre-incubated with Y27632 (10  $\mu$ M) for 1 hour, then treated with CBD for 24 hours. Control wells (C) were incubated with culture medium alone. The cells were loaded with (0.5  $\mu$ l/ml) fluorescent BSA latex beads for 2 hours. The figure represents means  $\pm$  SEM of triplicates of three independent experiments. The data are shown as percentages of control. Data were analysed using one-way ANOVA followed by post-hoc Bonferonni's multiple comparison; \*\* $P < 0.01$  CBD vs. control; \* $P < 0.05$  Y27632 compare with (C) control and \* $p < 0.05$  Y27632 compare with (C) Control; CBD+Y27632 compare with CBD ns (not significant).

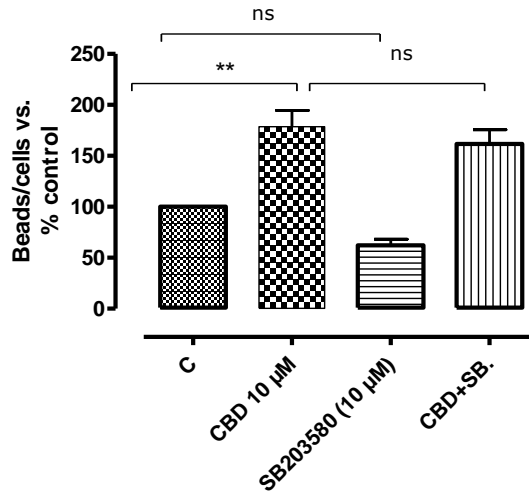


**Figure 3.24:** Histogram shows the effect of SB203580 (a P38 inhibitor) on CBD induced phagocytosis in BV-2. BV-2 ( $5 \times 10^5$  cells/well) were incubated with CBD (10  $\mu$ M) with or without SB203580 (10  $\mu$ M). The cells were loaded with fluorescent BSA latex beads (0.5  $\mu$ l/ml) for 2 hours. The figure represents means  $\pm$  SEM of triplicates in three independent experiments. Data were analysed using one-way ANOVA followed by post-hoc Bonferonni's multiple comparison; \*\* $P < 0.01$  CBD vs. (C) control. SB203580 compare with control; CBD+ SB203580 compare with CBD ns, (not significant).

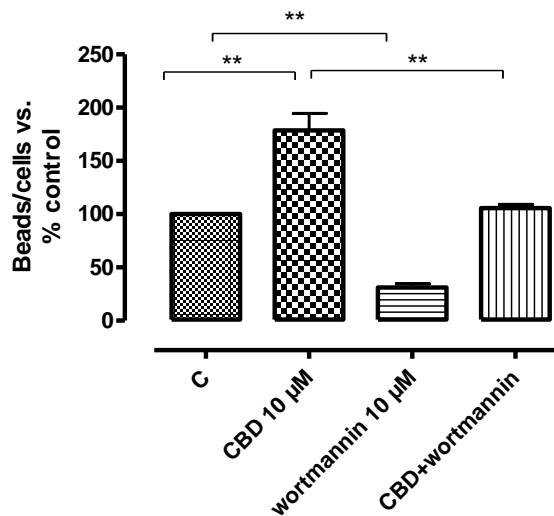


**Figure 3.25:** Histogram shows the effect of wortmannin on CBD induced phagocytosis in BV-2 cells. BV-2 ( $5 \times 10^5$  cells/well) were pre-incubated with wortmannin (10  $\mu$ M) for 1 hour, and then treated with CBD for 24 hours. (C) Control wells were incubated with culture medium alone. The cells were loaded with fluorescent BSA latex beads (0.5  $\mu$ l/ml) for 2 hours. The data are shown as percentages of control. Data were analysed using one-way ANOVA followed by post-hoc Bonferonni's multiple comparison; \*\* $P < 0.01$  CBD vs. control; \*\* $p < 0.01$  wortmannin compare with control and \*\* $p < 0.01$  CBD+ wortmannin compare with CBD.

### 3.4.2.15 The role of ROS in CBD induced phagocytosis

In order to investigate the role of reactive oxygen species (ROS) in CBD enhancement of microglial phagocytosis BV-2 cells were incubated with apocynin, a NADPH oxidase inhibitor (25  $\mu$ M) for 1 hour prior to CBD (10  $\mu$ M) exposure for 24 hours. The results show that apocynin inhibited basal phagocytosis but did not block the enhancement of phagocytosis in CBD-treated BV-2 (Figure 3.26).

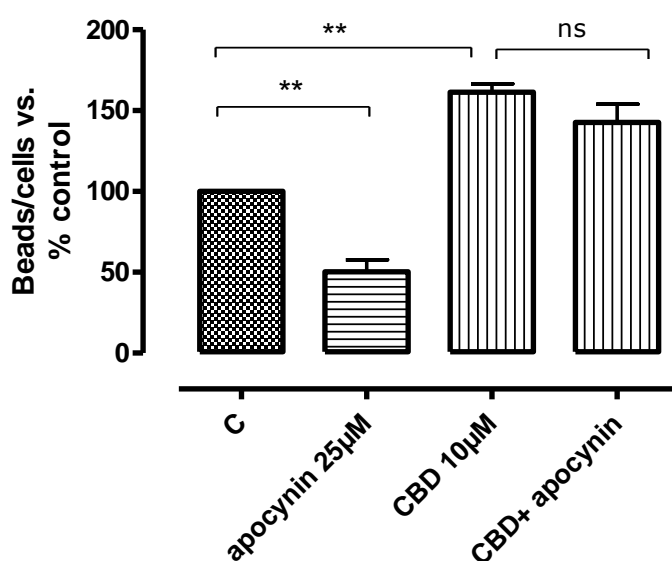


**Figure 3.26:** Histogram shows the effect of apocynin on CBD induced phagocytosis in BV-2 cells. BV-2 ( $5 \times 10^5$  cells/well) pre-incubated 1 hour with apocynin (25  $\mu$ M). Then treated with CBD 10  $\mu$ M for 24 hours and control wells (C) were incubated with culture medium alone. The cells were loaded with 1  $\mu$ M; 0.5  $\mu$ l/ml fluorescent BSA latex beads for 2 hours. The figure represents means  $\pm$  SEM of triplicates of three independent experiments. The data are shown as percentages of control. Data were analysed using one-way ANOVA followed by post-hoc Bonferonni's multiple comparison; \*\* $P < 0.01$  CBD compare with (C) control; \*\* $p < 0.01$  apocynin compare with (C) control and CBD+ apocynin compare with CBD (ns) not significant.

### 3.4.2.16 The role of intracellular calcium in microglial phagocytosis

BV-2 cells were exposed to the intracellular  $\text{Ca}^{2+}$  chelator BAPTA-AM (50  $\mu$ M) 1 hour prior to CBD (10  $\mu$ M). 24 hours later, BV-2 cells were incubated for 2 hours with fluorescent latex beads. BAPTA-AM did not significantly

affect either basal or CBD-enhanced phagocytosis. However, pre-incubation with EGTA (4 mM) despite having no effect on basal phagocytosis, abolished the CBD-enhancement (Figure 3.27).

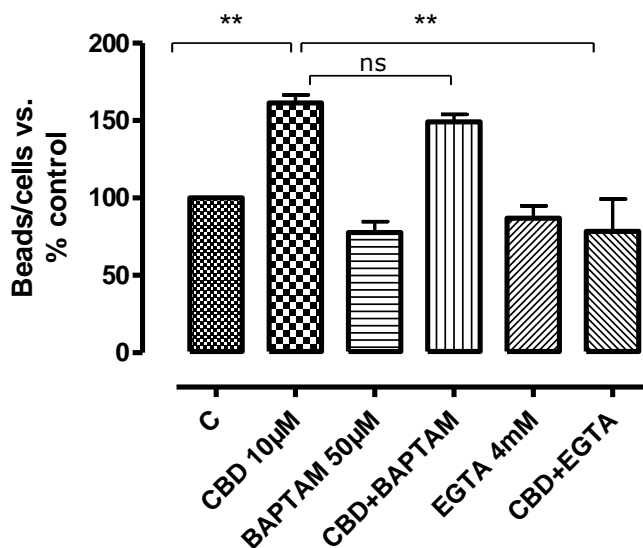


**Figure 3.27:** Histogram shows the effects of BAPTA-AM (an intracellular  $\text{Ca}^{2+}$  chelator) on CBD-induced phagocytosis in BV-2 cells. BV-2 cells were pre-treated with BAPTA-AM (50  $\mu\text{M}$ ) or with EGTA 4mM for 60 minutes prior to CBD (10 $\mu\text{M}$ ) for 24 hours. Control wells were incubated in culture medium alone. Cells were then loaded with fluorescent BSA latex beads (1 $\mu\text{m}$ ; 0.5ul/ml) for 2 hours. The figure represents means  $\pm$ SEM of triplicates of three independent experiments. The data are presented as percentage of control. Data were analysed using one-way ANOVA followed by post-hoc Bonferonni's multiple comparison; \*\* $P < 0.01$  CBD compare with control; (ns) not significant CBD+ BAPTA-AM compare with CBD; \*\* $p < 0.01$  CBD+EGTA compare with CBD.

#### 3.4.2.17 Effect of CBD and ATP on intracellular calcium in BV-2 cells

100  $\mu\text{M}$  ATP rapidly and transiently increased calcium nearly 2.5 fold from the basal levels. In contrast, CBD (10  $\mu\text{M}$ ) produced a sustained response, albeit of a similar peak height. Given the reports of CBD acting as a TRPV2 agonist (Qin et al., 2008), we examined the effects of a TRP channel blocker, ruthenium red (RR), which fully reversed CBD's effect (Figure 3.28; C).

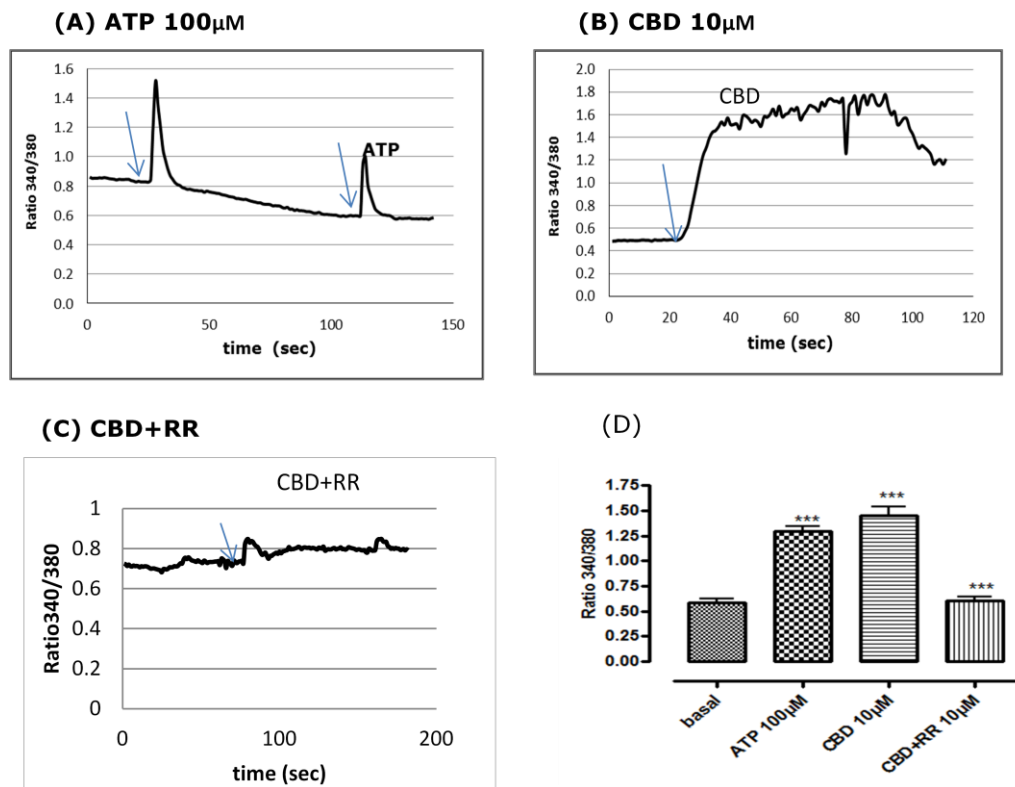


**Figure 3.28:** Histograms shows the effect of CBD on intracellular calcium in BV-2 by fura-2 ratiometric calcium imaging. In panels **(A)**, ATP was added to cells to show the induction of rapid and transient increase in  $[Ca^{2+}]_i$ . After a thorough wash with HBSS, buffer, second dose of ATP was added to the cells. **(B)** 10 $\mu$ M CBD was added after a thorough wash with HBSS, buffer and second dose was loaded **(C)** CBD was added with RR to cells. Changes in calcium were measured by converting the 340/380 ratio of Fura-2 fluorescence **(D)** A bar chart with pooled data and error bars (A, B and C), data obtained from at least three independent experiments ( $n = 40$  cells) were averaged and plotted.

### 3.4.2.18 The role of transient receptor potential channels in CBD-enhancement of phagocytosis

The concentration dependence of the TRP channel blocker ruthenium red (RR) was assessed by incubating BV2 cells at 100 nM, 1  $\mu$ M and 10  $\mu$ M for 1 hour which were then treated with or without CBD (10  $\mu$ M) for 24 hours. BV-2 cells were then incubated with fluorescent latex beads for 2 hours. RR, at the maximum concentration employed, had no effect on basal phagocytosis but blocked the enhancement due to CBD (Figure 3.29), while lower concentrations were less effective.

SKF-963651 (beta-[3-(4-methoxy-phenyl) mpropoxy]-4-methoxyphenethyl) 1H-imidazole hydrochloride), a blocker of TRPC, TRPV sub-family channels and of receptor-mediated and voltage-gated  $\text{Ca}^{2+}$  entry (Bomben and Sontheimer, 2008; Merritt et al., 1990; Kim et al., 2003), also completely prevented the enhancement of phagocytosis due to CBD (Figure 3.30) indicating that the effect of CBD is dependent on the influx of extracellular  $\text{Ca}^{2+}$ , probably via TRP channels.

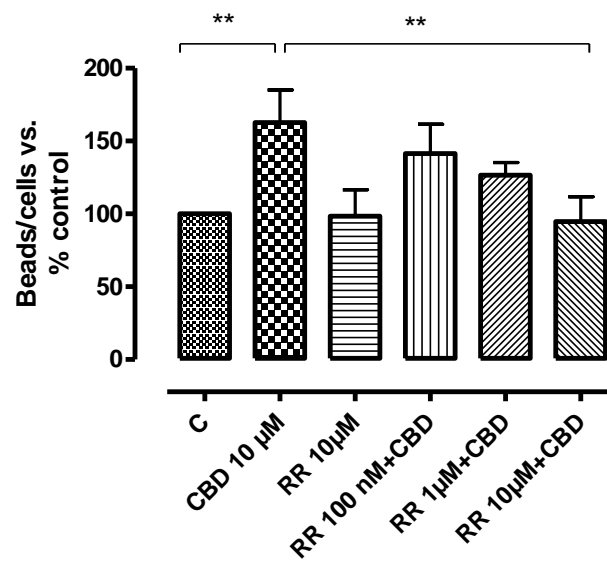


**Figure 3.29:** Histogram shows the effect of ruthenium red on CBD induced phagocytosis in BV-2 cells. BV-2 ( $5 \times 10^5$  cells/well) were pre-incubated with RR (100 nM, 1  $\mu\text{M}$  and 10  $\mu\text{M}$ ) for 1 hour, and then treated with CBD alone or in combination with RR for 24 hours. Control wells (C) were incubated with culture medium alone. The cells were loaded with 0.5  $\mu\text{l/ml}$  fluorescent BSA latex beads for 2 hours. The figure represents means  $\pm$ SEM of triplicates of three independent experiments. The data are shown as percentages of control. Data were analysed using one-way ANOVA followed by post-hoc Bonferonni's multiple comparison;  $**P < 0.01$  CBD compare with control;  $**p < 0.01$  CBD+ RR compare with CBD.

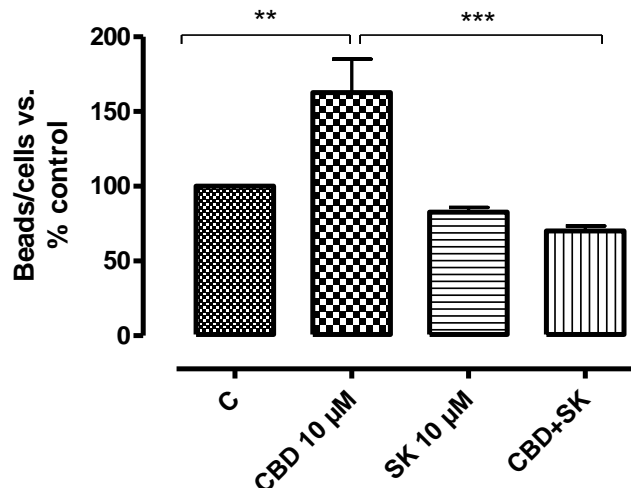


**Figure 3.30:** Histogram shows the effects of SKF96365 (SK) on CBD induced phagocytosis in BV-2 cells. BV-2 ( $5 \times 10^5$  cells/well) pre-incubated with SK at ( $10 \mu\text{M}$ ) for 1 hour, and then treated with CBD alone or with SK for 24 hours. Control wells (C) were incubated with culture medium alone. The cells were loaded with  $0.5 \mu\text{l/ml}$  fluorescent BSA latex beads for 2 hours. The figure represents means  $\pm$ SEM of triplicates of three independent experiments. The data are shown as percentages of control. Data were analysed using one-way ANOVA followed by post-hoc Bonferonni's multiple comparison;  $**P < 0.01$  CBD compare with control; not significant SK compare with control;  $***p < 0.001$  CBD+ SK compare with CBD.

#### 3.4.2.19 Expression of TRPV2 in BV-2 cells.

In BV-2 cells, intense TRPV2-like immunofluorescent staining was observed throughout control cells (Figure 3.31; A).

##### 3.4.2.19.1 Effect of CBD on TRPV2 expression.

To monitor the expression of TRPV2 and to evaluate the effect of CBD BV-2 cells were serum-starved 3 hours prior to treatment with CBD alone or in the presence of CBD plus the protein synthesis inhibitor cycloheximide or a PI3K inhibitor. In the cells treated with CBD for 1 hour, TRPV2 staining was clearly enhanced in the region of the cell membrane with apparently reduced staining in the cytoplasm, suggesting that CBD caused a translocation of TRPV2 to the membrane (Figure 3.30 ;B), this was

abolished in the presence of cycloheximide and with the PI3K inhibitor (Figure 3.31 ; C, E, F).

#### **3.4.2.19.2 The effect of latex bead phagocytosis on translocation of TRPV2**

In order to evaluate the significance of expression and translocation of TRPV2 to the cell membrane in phagocytosis, in BV-2 cells TRPV2 staining was present in the plasma membrane (Figure 3.31; D).

#### **3.4.2.19.3 Effect of serum on translocation of TRPV2 in BV-2**

To investigate other agents potentially causing changes of localization of TRPV2, BV-2 cells were incubated in 10% foetal bovine serum (FBS) at 5, 15, 30 and 60 minutes. In most of the un-stimulated cells, diffuse TRPV2-like immunofluorescence was observed in the cytoplasm. Addition of serum induced changes in the distribution of the TRPV2 towards the margin of the cells. The effect of serum was observed within 5 min (result not shown) and persisted for at least 60 minutes (data not shown).

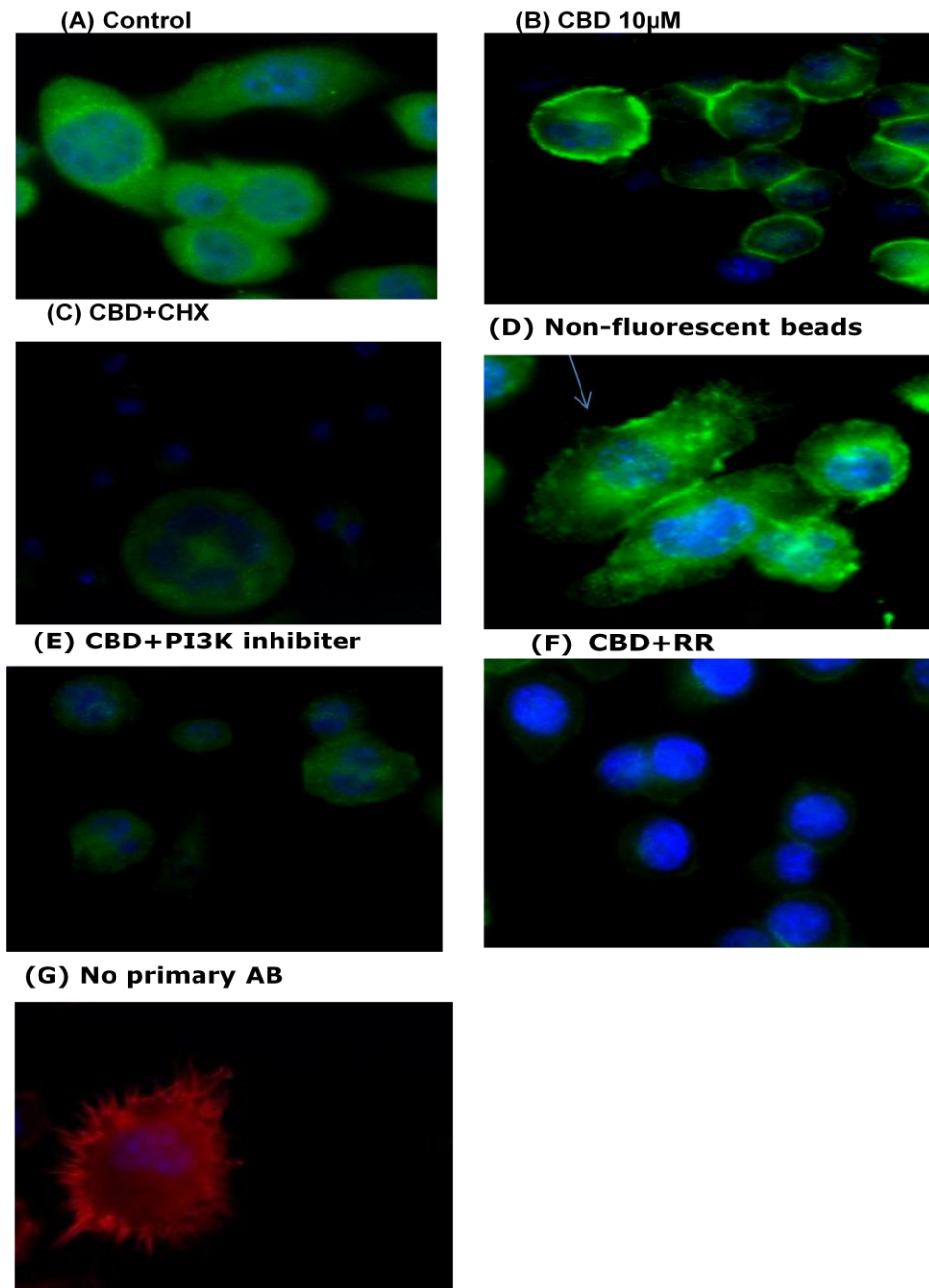


**Figure 3.31:** Images show the localization of TRPV2 in BV-2 by immunocytochemical analysis. **(A)** Control **(B)** CBD 10 $\mu$ M incubated for 1 hour **(C)** CHX 1 $\mu$ M incubated 1 hour prior to treatment with 10 $\mu$ M CBD for 1 hour **(D)** BV-2 incubated with non-fluorescent latex beads 0.5 $\mu$ l/ml for 2 hours **(E)** BV-2 incubated with wortmannin 10  $\mu$ M 1 hour before 10  $\mu$ M CBD for 1hour **(F)** RR 10 $\mu$ M incubated 1 hr prior to CBD for 1 hr **(G)** BV-2 cell without primary antibody stained with rhodamine phalloidin and secondary antibody. The cells were visualized by confocal microscopy under 63X magnification using a glycerin immersion objective lens.

#### 3.4.2.19.4 Expression of TRPV2 in primary murine microglial cells

To examine the expression of TRPV2 in murine brain microglia, double staining for TRPV2 and the microglial marker IB $\alpha$ -1 was assessed. We observed overlap of TRPV2 and IB $\alpha$ -1 staining. In IB $\alpha$ -1-positive microglia, TRPV2 translocation to the cell membrane was observed during activation with CBD (10 $\mu$ M) for 24 hours, confirming the results with BV-2 cells (Figure 3.32; B).

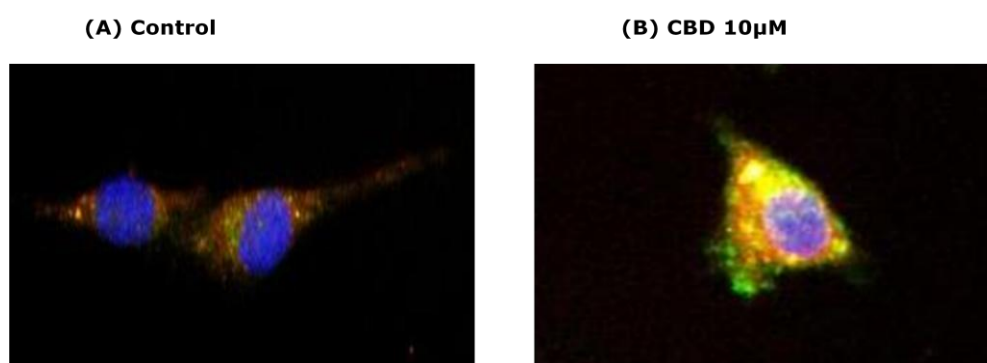


**Figure 3.32:** Images show the effect of CBD on colocalization of TRPV2 in primary mouse microglial cells by immunocytochemical analysis (A) control cell incubated with free serum media for 24 hours, (B) cell treated with CBD 10  $\mu$ M for 24 hours. Cells were fixed with formaldehyde, permeabilized with 0.1% Triton X-100, incubated overnight with the TRPV2 antibody (green), microglia marker (IB $\alpha$ -1) (red) and 60 min with a fluorescent secondary antibody and a nucleus is stained with DAPI (blue) yellow (red+green). The cells were visualized by confocal microscopy under 63X magnification using a glycerin immersion objective lens.

#### 3.4.2.20 Effect of CBD on TRPV2 protein expression in BV-2 cells

The expression of TRPV2 protein in BV-2 cells was investigated and found to be positive by Western blotting (Figure 3.33) in whole cells and membrane fractions; BV-2 cells were then incubated with CBD (10 $\mu$ M) at 5, 10, 15, 30, 60 minutes and 24 hours as shown in Figure 3.33. In addition, the effects of RR and wortmannin were examined.

BV-2 cells were incubated with RR or wortmannin 1 hour prior to CBD for 1 hour. CBD significantly enhanced whole cell TRPV2 expression after 30 and 60 minutes of incubation but this had returned to control levels by 24 hours at which time expression in the membrane fraction was much enhanced by CBD. Basal and CBD-enhanced TRPV2 expression were reduced in the presence of cycloheximide. Interestingly, TRP channel blockade (using ruthenium red) and PI3K inhibition somewhat reduced the enhanced expression due to CBD, while Rho/Rho kinase inhibition was ineffective (Figure 3.34).

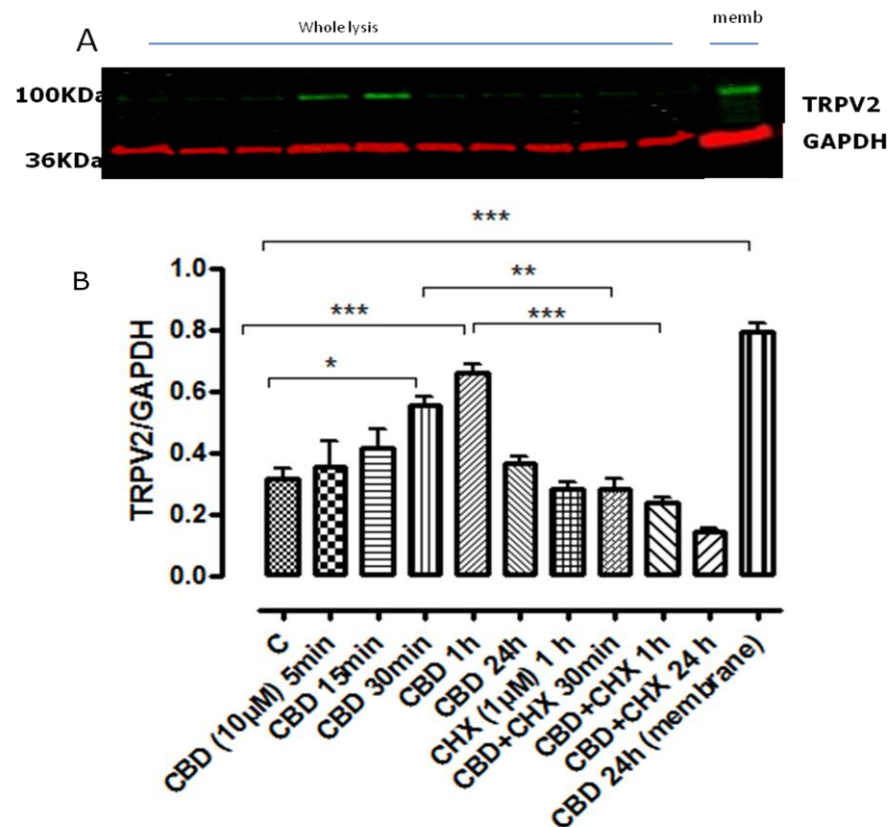


**Figure 3.33:** Western blot and histogram show increase of TRPV2 protein expression by CBD in whole lysis cells and membrane in BV-2. BV-2 were incubated with CBD (10 μM) for 5, 10, 15 and 60 minutes alone. Cycloheximide (CHX 1 μM) was incubated for 6 hours prior to CBD. Data shown are ratios of TRPV2: GAPDH expression and represent the means ± SEM of 3 independent experiments. Data were analysed using one-way ANOVA followed by post-hoc Bonferonni's multiple comparison; \*P<0.05 CBD 30" vs. control; \*\*\*P< 0.001 CBD 1h vs. control; \*\*\*P< CBD 24hrs (membrane) vs. control; \*\*p<0.01 CBD+ CHX 30" vs. CBD 30"; \*\*\*P<0.001 CBD+CHX 1h vs. CBD 1h.

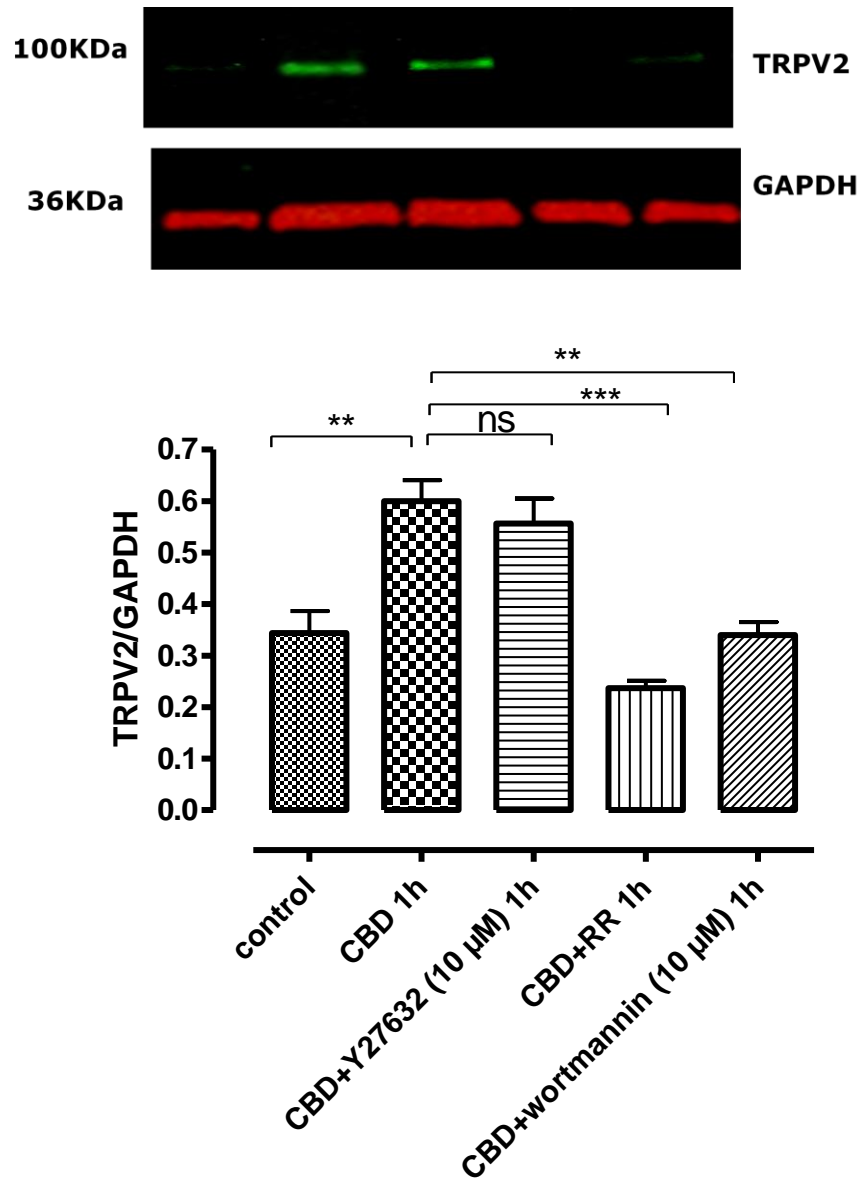


**Figure 3.34:** Western blot and histogram shows the effect of MAPK inhibitors (a Rho and PI3K) and non selective TRPVs inhibitor on CBD 10 μM caused TRPV2 activation at 1 hour in whole lysis of BV-2. RR (non selective TRPVs inhibitor) and wortmannin (a PI3K inhibitor) at 10 μM significantly inhibited TRPV2 stimulated by CBD after 1 hour, whereas Y27632 (a Rho inhibitor) did not block TRPV2 expression induced by CBD. Data were analysed using one-way ANOVA followed by post-hoc Bonferonni's multiple comparison; \*\*P<0.01 CBD 1hr vs. control; \*\*\*P< 0.001 CBD+ RR vs. CBD 1hr; \*\*P<0.01 CBD+ wortmannin vs. CBD 1h.

### 3.4.2.21 The role of a protein synthesis inhibitor (cycloheximide) on CBD-enhanced phagocytosis

To test the hypothesis that CBD was acting via up-regulation of TRPV2 receptor protein, we assessed the effect of cycloheximide, a protein synthesis inhibitor (CHX). BV2 cells were incubated with 1 $\mu$ M CHX for 6 hours then treated with or without CBD (10  $\mu$ M) for 24 hours before incubation with fluorescent latex beads for 2 hours. The results show that CHX reversed the CBD enhancement without affecting basal phagocytosis (Figure 3.35).

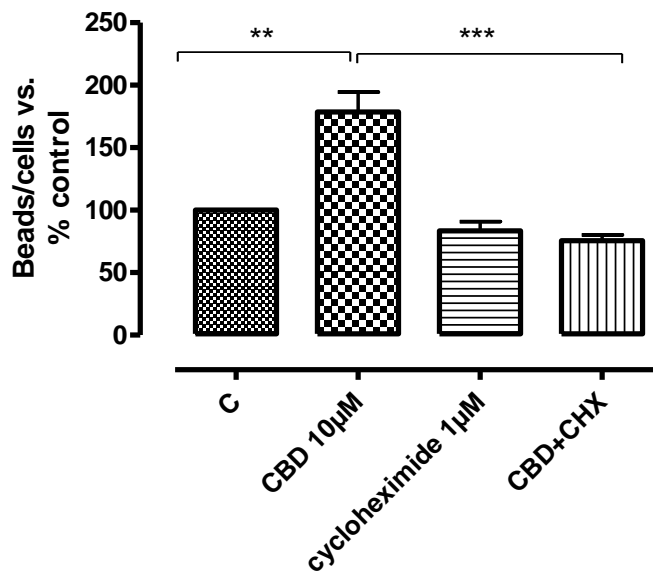


**Figure 3.35:** Histogram shows the effect of cycloheximide (CHX) on phagocytosis in BV-2 cells ( $5 \times 10^5$  cells/well); BV-2 cells were pre-incubated with CHX (1  $\mu$ M) for 6 hour, then treated with CBD for 24 hours. Control wells (C) were incubated with culture medium alone. The cells were loaded with fluorescent BSA latex beads (1  $\mu$ m; 0.5  $\mu$ l/ml) for 2 hours. The figure represents means  $\pm$ SEM of triplicates of three independent experiments. The data are shown as percentages of control. Data were analysed using one-way ANOVA followed by post-hoc Bonferonni's multiple comparison; \*\* $P < 0.01$  CBD vs. (C) control; \*\*\* $p < 0.001$  CBD+ CHX vs. CBD.

### 3.4.2.22 TRPV2 receptor message

Quantitative RT-PCR analysis indicated that TRPV2 mRNA was expressed at measurable levels in un-stimulated BV2 cells. There was a trend towards an increase, albeit non-significant, after 60 min incubation with CBD (10 $\mu$ M) and at 24 hours there was a considerable enhancement (Figure 3.36).

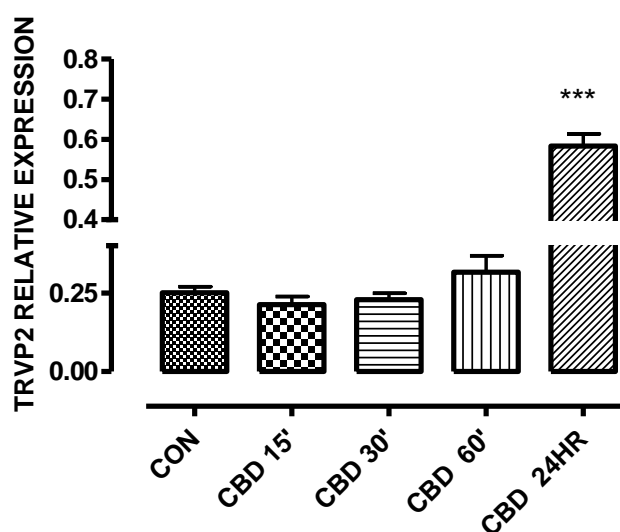


**Figure 3.36:** Histogram shows expression of TRPV2 in BV-2 cells and the effect of CBD on activation of TRPV2 by RT-PCR. RNA was extracted using Trizole reagent and RNA samples were reverse transcribed using the superscript reverse transcription, using mouse actin as a normalizing gene. Data are means  $\pm$  SEM of triplicate determinations of TRPV2/mouse actin ratio conducted in three separate experiments. Data were analysed using one-way ANOVA followed by post-hoc comparison; \*\*\*P<0.001, CBD 24hours compare with control.

### 3.4.2.23 Vanilloid receptor (TRPV1) protein expression in BV-2

We also investigated the expression of TRPV1 channels in BV-2 cells (Figure 3.38; A). CBD enhanced TRPV1 expression significantly at 60 minutes and this had returned approximately to control levels by 24hrs. TRPV1 (95-100 kDa) and GAPDH (36 kDa) was assessed in Western blots probed with specific antibodies. CBD enhancement of TRPV1 expression

was blocked by treatment with the channel blocker RR and by the PI3K inhibitor wortmannin (10  $\mu$ M at 1 hour) (Figure 3.37).

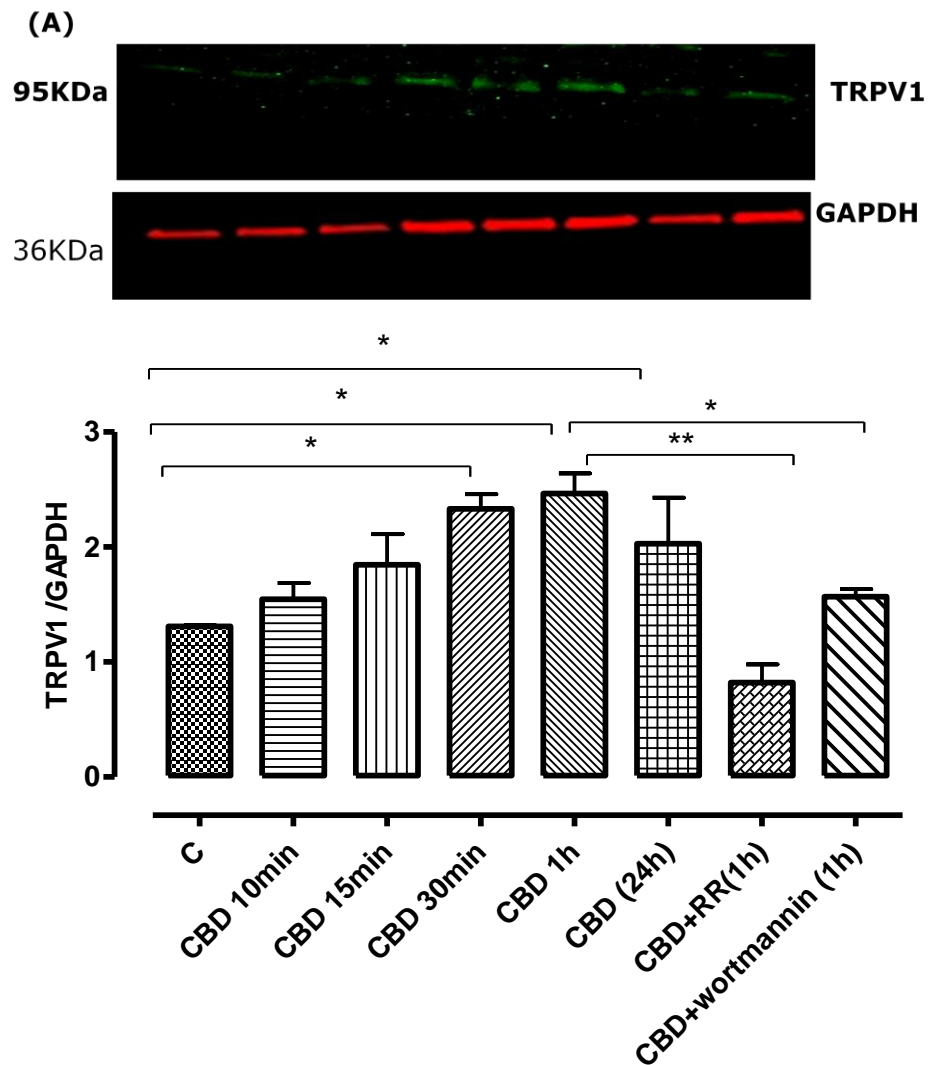


**Figure 3.37:** Western and histogram show the effect of CBD on TRPV1 protein expression of whole lysis cells in BV-2. BV-2 were incubated with CBD (10  $\mu$ M) for 10, 15, 30, 60 mins and 24 hrs alone. RR (non-selective TRPV channel blocker) and wortmannin (a PI3K inhibitor) at 10  $\mu$ M significantly inhibited TRPV1 stimulated by CBD after 1 hour, whereas Y27632 (a Rho inhibitor) did not block TRPV1 expression induced by CBD. The data represent the mean of 3 experiments  $\pm$  SEM. Normalized to GAPDH from three independent cultures. Data were analysed using one-way ANOVA followed by post-hoc comparison; \* $P$ <0.05 CBD 30 (mins) vs. (C) control, \* $P$ <0.05 CBD 1hrs vs. control; \* $P$ < CBD24hrs vs. control; \* $P$ <0.05 CBD+wortmannin 1hr compare with CBD 1hr; \*\* $P$ < 0.05 CBD+RR compare with CBD1hr.

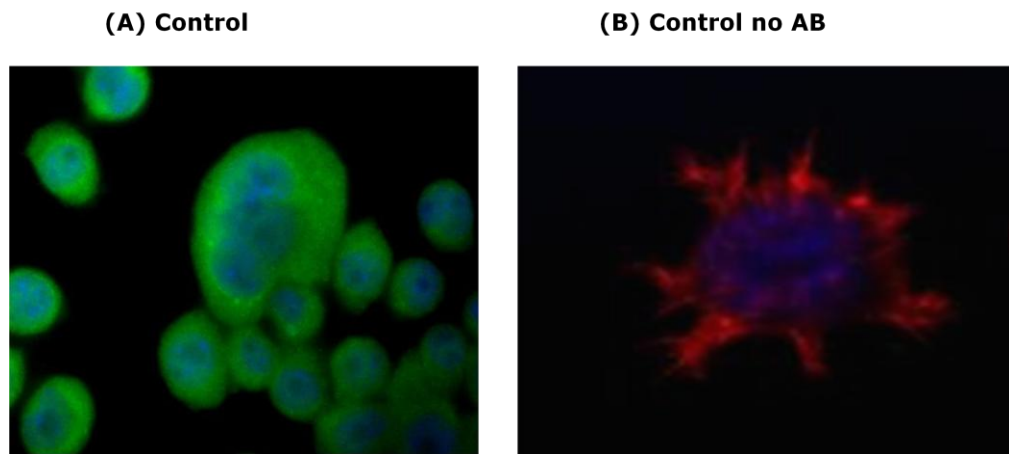


**Figure 3.38:** (A) Images show the expression of TRPV1 protein in control BV-2 cells by immunocytochemical analysis. (B) control cell without primary antibody stained with rhodamine phalloidin. BV-2 Cells were fixed with formaldehyde, permeabilized with 0.1% Triton X-100, incubated overnight with the TRPV1 antibody and 1h with a fluorescent secondary antibody. The cells visualized by confocal microscopy under 63X magnification.

#### **3.4.2.24 The role of AKT (protein kinase B) in CBD-mediated phagocytosis**

AKT is involved in several cellular processes such as cytoskeleton rearrangements and macrophage activation (Chan *et al.*, 1999). CBD was tested for its ability to activate (phosphorylate) AKT. Incubation of cultured BV-2 with CBD (10  $\mu$ M) failed to activate phosphorylation of AKT, whereas LPS stimulated phospho-AKT at 30 minutes and 24 hours (Figure 3.39). This result was confirmed by immunocytochemical analysis in which CBD also failed to alter AKT in BV-2 (Figure 3.40; B).

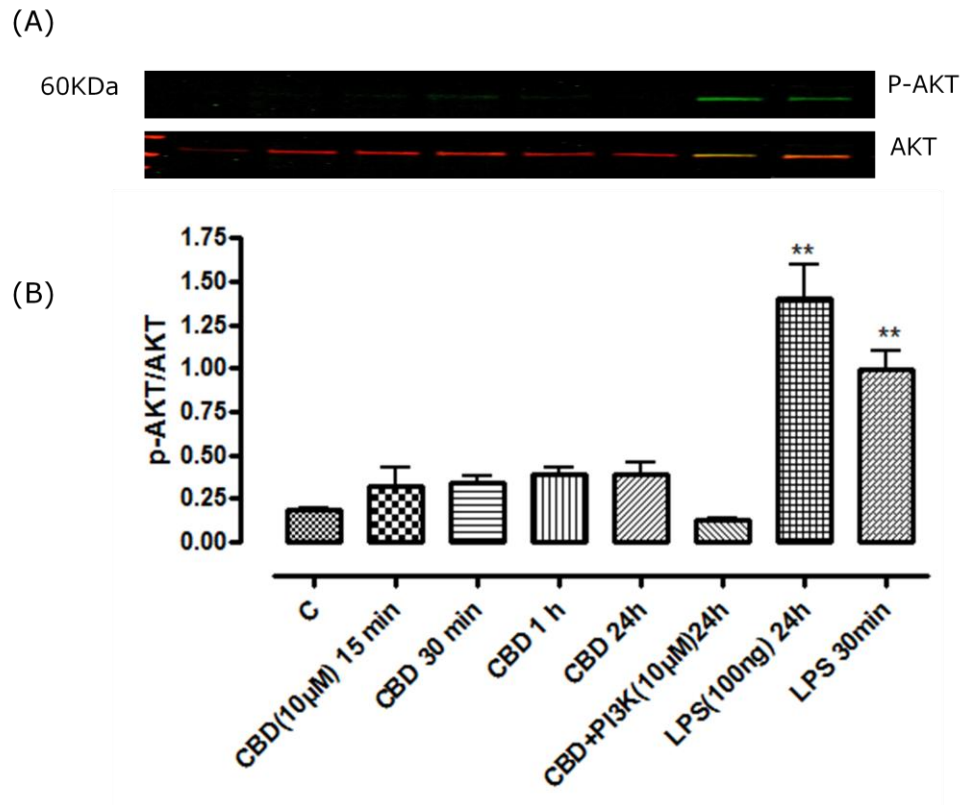


**Figure 3.39:** Western and histogram shows ratio of p-AKT and total AKT and the effect of CBD on AKT protein in BV-2 cells. BV-2 incubated with CBD 10  $\mu$ M at 15, 30, 60 minutes and 24 hours alone or with wortmannin (a PI3K inhibitor) at 10  $\mu$ M, which failed to activate of AKT activation at any time. LPS 100ng alone at time indicated significantly stimulated AKT. Data shown is the mean of 3 experiments  $\pm$  SEM. Data were analysed using one-way ANOVA followed by post-hoc comparison; \*\* $P < 0.01$  LPS (24hrs) vs. (C) control, \*\* $P < 0.01$  LPS (30mins) vs. (C) control.

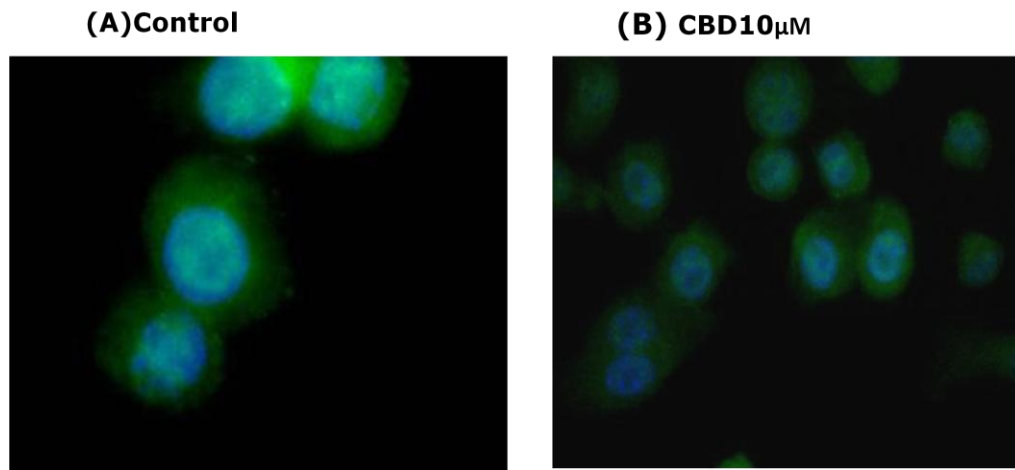


**Figure 3.40:** Images show the expression of P-AKT (A) Control and (B) the effect of CBD 10 $\mu$ M (at 1 hr) on P-AKT protein in BV-2 by immunocytochemical analysis. BV-2 Cells were fixed with formaldehyde, permeabilized with 0.1% Triton X-100, incubated overnight with the AKT antibody and 1hr with a fluorescent secondary antibody. The cells visualized by confocal microscopy under 63X magnification.

### 3.4.3 Migration

#### 3.4.3.1 Effect of UDP on cell migration in RAW 264.7 cells

Using the migratory device developed in the School of Biomedical Sciences, University of Nottingham (see method) we tested the effect of UDP (a selective P2Y<sub>6</sub> receptor agonist) on RAW 264.7 monocyte/macrophage cells migration as a positive control to validate the device. We found that UDP (10  $\mu$ M) stimulated migration significantly at 24 and 72 hrs.

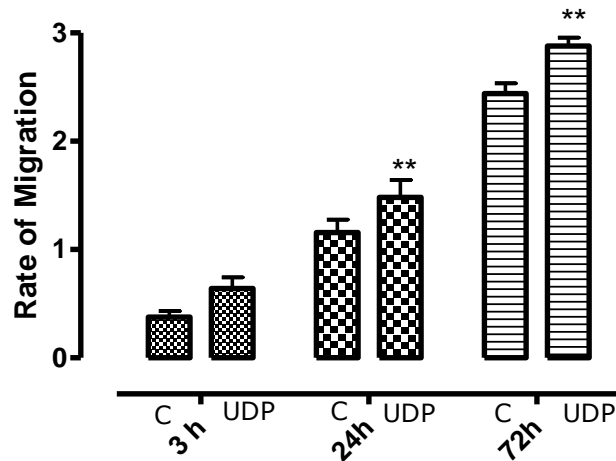


**Figure 3.41:** Histogram shows the effect of UDP (10 $\mu$ M) on RAW 264.7 cell migration at (3, 24 and 72 hs). RAW 264.7 were incubated with 10% FSA medium only (control) or with 10  $\mu$ M UDP. Data represent means $\pm$ S.E.M of three independent experiments. \*\*P<0.01, two way ANOVA compared with control.

### 3.4.3.2 Effect of CBD on BV2 cell migration

CBD (10 $\mu$ M) significantly enhanced BV-2 migration to a degree equivalent to that of UDP after 24 and 72 hrs of exposure (Figure 3.42 and 3.43).

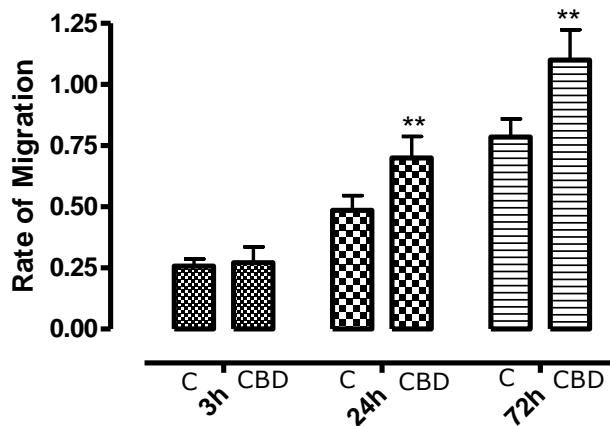
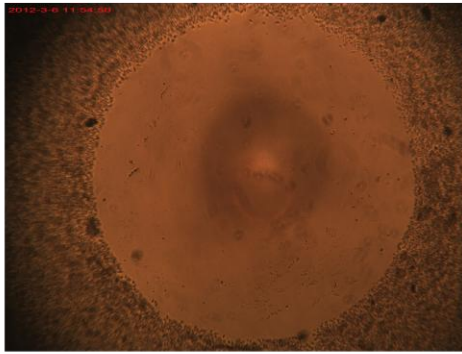
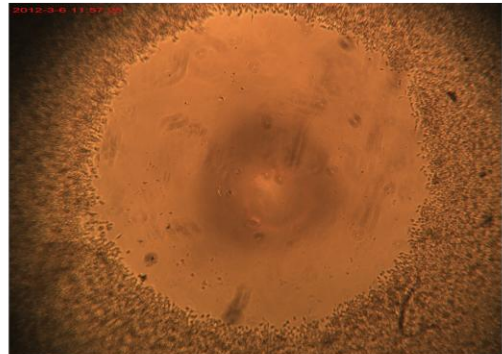


**Figure 3.42:** Histogram show the effect of CBD (10 $\mu$ M) on BV-2 cell migration (10  $\mu$ M) at 3, 24 and 72 hrs. BV-2 cell migration induced by CBD 10  $\mu$ M at the indicated times. BV-2 cells were incubated with 10% FSA medium only (control) or with 10  $\mu$ M CBD. Data represent means  $\pm$ S.E.M of three independent experiments. \*\*P<0.01 CBD vs. control, two way ANOVA. The rate of migration represents of difference between indicating migration with the basal using power point (see below).

**Control**  
**Basal**



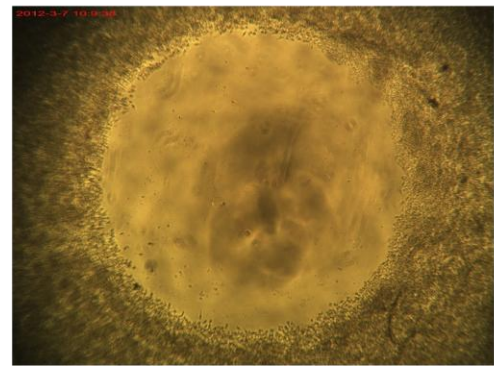
**CBD 10 $\mu$ M**  
**Basal**



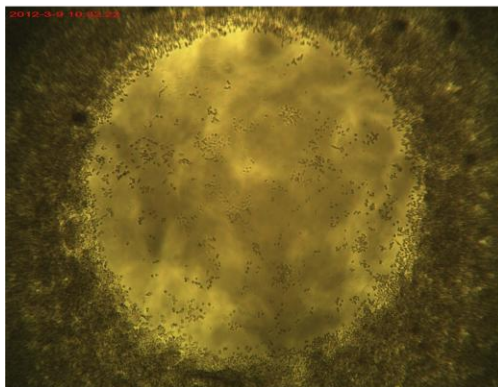
**24 hours**



**24 hours**



**72 hours**



**72 hours**

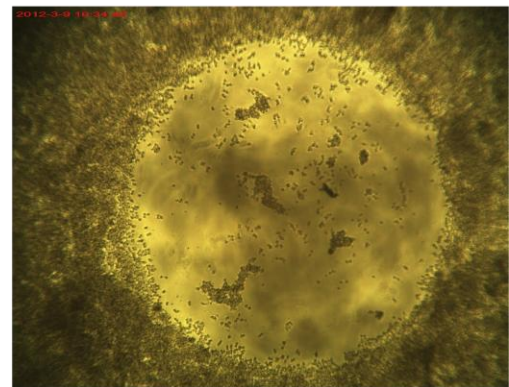


**Figure 3.43:** BV-2 cell migration induced by CBD (10  $\mu$ M) at 3, 24 and 72 hrs. Images showing BV-2 cell migration induced by CBD 10 $\mu$ M. BV-2 cells were incubated with 10% FSA medium only (control) or with 10  $\mu$ M CBD using inverted microscope attached with camera. The rate of migration represents of difference between indicating migration with the basal using power point.

### **3. 5 Discussion**

#### **3.5.1 Characterization of microglial phagocytosis**

Microglia, the brain's macrophages (Streit et al., 2004; Chew et al., 2006), play a critical role in remodeling and regenerating cells as well as providing the first line of defense against infection and brain insult (Liu et al., 2001; Perry, 2004). The ability of these cells to remove apoptotic cells by phagocytosis is essential for normal development, tissue homeostasis, and responses to injury or diseases (Hanisch and Kettenmann, 2007; Streit, 2001). The phagocyte removal of dying cells is generally believed to be a beneficial process and failure to clear apoptotic cells and/or cellular debris can itself lead to neuroinflammation and neurodegeneration (Napoli and Neumann, 2009). Furthermore, the phagocyte removal of apoptotic leukocytes by microglia has been shown to contribute to the resolution of autoimmune processes (Chan et al., 2003; Noda and Suzumura, 2012). Recognition and engulfment of tissue debris is a very complex process involving multiple ligand receptor interactions. Phagocytosis, therefore, represents a significant functional feature of microglial cells where the potential to influence the phenomenon by brain-penetrating ligands could result in therapeutic benefit.

Phagocytosis in the present study was assessed by measuring the ingestion of BSA latex particles, essentially as described by others. The first part of the chapter describes the characterization of phagocytosis in BV2 and other microglial cells as measured by this method. We found that at least 2 hours incubation with beads was required to be able to measure significant phagocytosis. It was clear that microglia at lower temperatures have a much lower ability to phagocytose beads in comparison to phagocytosis at

37 °C, consistent with previous studies which have reported that *in vitro* hypothermia suppresses microglial activation (Si *et al.*, 1997).

We assessed the functioning of the actin cytoskeleton in phagocytosis, using cytochalasin D. Cytochalasin D retards actin assembly by binding to actin filament ends (Brown and Spudich, 1981) and binds with high affinity to F-actin (Flanagan and Lin, 1980). In the present study, cytochalasin D completely blocked the phagocytosis of latex beads by BV-2, in agreement with the observation by Ting-Beall *et al.* (1992). In contrast, neither the mitochondrial uncoupler FCCP nor the mitochondrial ATPase inhibitor oligomycin had an effect on phagocytosis of latex beads, indicating that mitochondrial energy production is not important, at least not in the short term, for BV2 phagocytosis to proceed.

Myosin II plays an important role in the formation of phagosomes during FcR-mediated phagocytosis in macrophages and it has been shown to be localized around developing phagosomes (Diakonova *et al.*, 2002; de Lanerolle *et al.*, 1993). Previous reports indicated that myosin II was required for FcR-mediated phagocytosis but not actin recruitment (Olazabal *et al.*, 2002). Fc  $\gamma$  is the receptor for phagocytosis of immunoglobulin-opsonized cells and particles (Aderem and Underhill, 1999). In this study, myosin II light chain expression was activated during latex beads phagocytosis and appeared to become localized around the beads when compared to the control (bead-free) cells.

CD11b is widely expressed on both phagocytotically active cells and microglial cells in the CNS and is involved in the complement-mediated phagocytosis of pathogens (Stevens *et al.*, 2007). Our results suggested that CD11b failed to activate during latex-bead phagocytosis when compared with LPS-treated BV2 cells used as positive control. Phagocytosis

itself did not appear to activate microglia in the same way as an inflammatory challenge, as judged by CD11b expression, in contrast, to the widespread view that activation is a requirement for phagocytosis (Kettenmann, 2007).

Activated PLC- $\gamma$ , for example, following activation of Fc receptors, translocates to the inside surface of the cell membrane and catalyzes the hydrolysis of membrane-associated phosphatidylinositol 4,5-bisphosphate to form diacylglycerol and inositol 1,4,5-trisphosphate, which are capable of activating protein kinase C (PKC) and mobilizing intracellular calcium ( $[Ca^{2+}]_i$ ), respectively (Newton, 1997). We investigated the role of PLC $\gamma$ 2 in latex beads mediated phagocytosis in BV-2 microglia. PLC $\gamma$ 2 appeared to be translocated around the beads and cell membrane after ingestion. PLC $\gamma$  may influence actin rearrangement, and loss of function of PLC results in impaired membrane ruffling (Kurokawa et al, 2004).

Several studies indicate that PKC activity is required for Fc $\gamma$ R-mediated particle uptake. Phagocytosis of IgG-opsonized particles induces PKC activation and translocation to the membrane fraction. PKC $\alpha$  regulates the interaction of MARCKS with actin; its localization to the phagosome suggests a role in phagocytosis and phagosome maturation (Aderem and Underhill, 1999; Allen and Aderem, 1996). Consistent with these studies, we found that both PKC $\alpha$  and PKC $\epsilon$  translocated to the BV2 cell membrane indicating an involvement in phagocytosis of latex beads.

### **3.5.2 Regulation of phagocytosis**

It has been shown that pharmacological or immunological intervention can modulate the ability of microglia or macrophages to phagocytose and an aim of this chapter was to determine whether cannabinoids could act as

modulators of the process in BV2 and HAPI cells and mouse microglia in primary culture. JWH133, (a selective CB<sub>2</sub> agonist), AM251 (a CB<sub>1</sub> antagonist and putative GPR55 agonist), phytocannabinoid (THC, CBN, CBDA, CBDV, THCV), CP55, 940 (CB<sub>1</sub>/CB<sub>2</sub> agonist), endocannabinoids (AEA and 2-AG) and the GPR55 endogenous ligand LPI, all failed to alter the phagocytosis activity in microglia or macrophages. WIN55-212-2 (a CB<sub>1</sub>/CB<sub>2</sub> agonist), however, inhibited phagocytosis of latex beads, albeit at a concentration well above that required to activate cannabinoid receptors.

Given the lack of expression of cannabinoid receptors in the BV2 cells used in this study (discussed in Chapter 2) this is not surprising. However, the non-psychoactive phytocannabinoid cannabidiol did significantly enhance phagocytosis. Cannabinoids have been noted to interact with numerous 'off-target' sites other than CB<sub>1</sub>/CB<sub>2</sub> receptors and to affect fundamental processes involved in microglial cell activation, with one prominent recently-identified target being GPR18 (McHugh et al., 2010). However, NAGLY, an agonist of the orphan GPCR GPR18, did not inhibit or stimulate latex bead phagocytosis in BV-2 cells, and 0-1918 (abn-CBD antagonist) did not reverse CBD activation of phagocytosis. These findings rule out the involvement of GPR18 and abn-CBD receptors in phagocytosis and specifically in the enhancement due to CBD. Indeed, the finding that pertussis toxin had no effect either on basal or CBD-enhanced phagocytosis excludes the involvement of any G<sub>i/o</sub>-linked receptors in BV2 phagocytosis.

The roles of the purine receptors P2Y and P2X were evaluated in latex bead phagocytosis using UDP and ATP. Koizumi et al., (2007) have reported that microglia express the P2Y<sub>6</sub> receptor, where activation by the endogenous agonist UDP triggers microglia phagocytosis. The robust activation of phagocytosis by UDP in the BV2 cells is consistent with this. On the other hand, ATP failed to alter phagocytic activity. This does not agree with

recent findings reporting that extracellular ATP at millimolar (0.5-1 mM) concentrations inhibits phagocytosis in mouse macrophages (Fang *et al.*, 2009) and indicates that microglial and macrophage phagocytosis are differentially controlled.

We then investigated the potential roles of pro-inflammatory activators in latex bead phagocytosis in BV-2. Having previously assessed bacterial LPS (see Chapter 2), the effects of LPS and IFN- $\gamma$ , which reportedly activates phagocytosis through activation of Fc $\gamma$  receptors (Corradin *et al.*, 1991), were investigated. We found that both bacterial LPS and interferon stimulated latex bead phagocytosis. This observation is consistent with previous studies showing that microglia are stimulated by bacteria or bacterial products and can protect the brain by phagocytosis and killing of pathogens (Redlich *et al.*, 2012).

NO is reported to attenuate phagocytosis in microglia; the mechanism is not currently known, but modification of the cytoskeleton and inhibition of pseudopodia formation have been documented (Jun *et al.*, 1996). Kopec and Carroll, (2000) recently reported that the excessive formation of NO from cells within areas of brain inflammation may lead to the loss of microglial phagocytosis in these regions resulting in the inability of microglia to clear debris, resulting in neurodegenerative diseases. However, results presented here provide no support for the involvement of nitric oxide in bead phagocytosis in BV2 cells; for example, the iNOS inhibitor 1400W failed to alter latex bead phagocytosis.

Microglial activation may induce the rapid generation of ROS through NADPH oxidase (Sankarapandi *et al.*, 1998) and (Bergend *et al.*, 2003) suggested that ROS produced during phagocytosis are critical for the bactericidal action of phagocytes. We, therefore, investigated the role of

NADPH oxidase on phagocytosis using the NADPH oxidase inhibitor apocynin. Basal phagocytosis was attenuated by apocynin but CBD was still able to provide significant enhancement. It is interesting that even when ROS generation is compromised, the phagocytic action of microglia is still capable of amplification (in this case by CBD).

Next, we performed some experiments in order to investigate if another class of anti-inflammatory drugs could modulate the microglial phagocytic activity, using minocycline and dexamethasone. Minocycline (a tetracycline derivative) has anti-inflammatory effects and is neuroprotective in models of traumatic brain injury (Bye *et al.*, 2007), Parkinson's disease and Alzheimer's disease (Choi, *et al.*, 2007). However, minocycline failed to alter phagocytosis in BV-2 cells and did not reverse the CBD-mediated phagocytosis. This observation is supported by previous studies which showed minocycline inhibiting the production of pro-inflammatory cytokines by human microglia without affecting the phagocytosis of amyloid  $\beta$  fibrils (Familian *et al.*, 2007).

Dexamethasone, as expected, promoted phagocytosis in a concentration-dependent manner with the most prominent effect at 1  $\mu$ M. Liu *et al.* 1999 have reported that the steroid augmentation of phagocytosis in macrophage cells was mediated through the glucocorticoid receptor (GR) and blocked by the GR antagonist RU38486. Steroids such as dexamethasone, are recognized for their anti-inflammatory properties and their ability to inhibit production of pro-inflammatory cytokines such as TNF- $\alpha$  (Barnes, 1998). Furthermore, they are documented to increase phagocytosis of apoptotic cells (Heasman *et al.*, 2004). This observation may explain, at least in part, the powerful anti-inflammatory properties of steroids and their attenuation of chronic inflammatory conditions. These data are supported by a study by Giles *et al.*, (2001), which reported

dexamethasone activation of a phagocytic phenotype in macrophages with changes in adhesion-dependent loss of phosphorylation of adhesion mediators (paxillin and pyk2), reorganization of cytoskeletal elements and increased amounts of Rac GTPase.

Having ruled out the involvement of CBD's enhancement of phagocytosis by Gi-coupled receptors, including cannabinoid receptors, we evaluated potential signaling pathways associated with CBD-mediated latex-bead phagocytosis. First, we tested the role of phosphatidylinositol 3-kinase (PI-3K). The PI-3K pathway has been shown to be essential for pseudopod extension, a necessary step in phagocytosis. Furthermore, PI-3K was required for gene activation after FcγR engagement (Kanzaki *et al.*, 1991). However, we found that PI3K inhibition with wortmannin reduced basal phagocytosis but that CBD was still able to produce a marked enhancement in its presence.

We then investigated the role of Rho/ROCK signaling in latex bead phagocytosis. ROCK promotes actin-myosin-mediated contractile force generation through the direct phosphorylation of the regulatory myosin light chain (MLCII) and the myosin-binding subunit (MYPT1) of MLC phosphatase to inhibit catalytic activity. ROCK also plays a role in cell motility, adhesion, neurite retraction, and phagocytosis (Riento and Ridley, 2003).

Moreover, Rho/ROCK is involved in phagocytosis that is mediated by the complement receptor 3 (CR3), but not for phagocytosis through the Fcγ receptors (Caron and Hall, 1998; Olazabal *et al.*, 2002). In the present study using Y27632 (a Rho/ROCK inhibitor) we found, as with wortmannin, that Y27632 suppressed basal levels, but did not prevent CBD enhancement, of phagocytosis.

We then extended our analysis to P38, another MAPK regulator of microglial activation. Previous studies have suggested that the involvement of P38 kinase in phagocytosis might be due to the ability of P38 to phosphorylate the small heat shock protein HSP27 (Krump *et al.*, 1997). HSP27 plays an important role in modulation of actin microfilament (Lavoie *et al.*, 1993). Our data showed that P38 kinase was required for maximum basal phagocytic activity but it was not necessary for CBD enhancement.

Mobilization of intracellular calcium represents an important second messenger in cells and in microglia can be required for many inflammatory-mediated responses, affecting enzymes, ion channels, gene transcription and proliferation in all eukaryote cells. The actin cytoskeleton has been shown to play a role in the generation of calcium transients in some cells (May and Machesky, 2001). The involvement of intracellular calcium stores in CBD elevation of  $[Ca^{2+}]_i$  has also been demonstrated in hippocampal cells (neurons and glia) in culture (Drysdale *et al.*, 2006). Decreasing internal  $[Ca^{2+}]$  by an intracellular chelator of calcium ions (BAPTA-AM) did not inhibit phagocytosis of latex beads nor did it reverse CBD-enhanced phagocytosis.

This is perhaps conflicted with previous published data showing that BAPTA-AM had reduced Zymosan Phagocytosis in macrophages. However, these results and other studies suggest that the regulation of calcium mobilization and its role in phagocytosis differs depending on the receptors involved in mediating particle uptake (Girotti *et al.*, 2004).

Although depletion of intracellular stores can trigger a capacitative  $Ca^{2+}$  entry (Roderick and Cook, 2008). Furthermore, there is growing evidence reported that  $Ca^{2+}$  chelation does not attenuate particle binding by macrophages (Link *et al.*, 2010). However, when the transmembrane  $Ca^{2+}$

gradient was reduced in the presence of EGTA, the effect of CBD was abolished, suggesting that  $\text{Ca}^{2+}$  influx is required. Stimulation of phagocytosis by CBD was reversed by subsequent addition of 4 mM external  $\text{Ca}^{2+}$  (data not shown) so that the result could not be explained by a cytotoxic effect of EGTA.

Extracellular  $\text{Ca}^{2+}$  could represent a major source of mobilized  $[\text{Ca}^{2+}]_i$  as a result of binding to the FcR. Binding of the FcR results in a transient membrane depolarization of the intact macrophage (Roderick and Cook, 2008). This depolarization effect could activate opening of voltage-dependent  $\text{Ca}^{2+}$  channels on the plasma membrane of macrophages, increasing cytosolic  $\text{Ca}^{2+}$  levels.

That  $\text{Ca}^{2+}$  entry underpins the effect of CBD is supported by the finding that CBD produced an increase in  $[\text{Ca}^{2+}]_i$  equivalent to that of ATP in BV2 cells. A similar effect has been reported in a previous study in which CBD elevated intracellular  $\text{Ca}^{2+}$  ( $[\text{Ca}^{2+}]_i$ ) above the basal levels (Drysdale et al., 2006). Furthermore, this increase was blocked by the non-selective TRP channel blocker ruthenium red strongly suggesting the involvement of one of the TRP family members as the mediator of CBD enhancement of phagocytosis. A prime candidate is TRPV2 receptor as previous work has shown CBD elevation of calcium via this receptor channel (Qin *et al.*, 2008).

In support of this proposed mechanism, SKF96365, an inhibitor of receptor-mediated and voltage-gated  $\text{Ca}^{2+}$  entry also abolished the effect of CBD. Link et al. (2010) have reported TRPV2 involvement in early phagocytosis and it appears to be essential for innate immunity. TRPV2 channels play an important role in particle binding, the first step of phagocytosis (Link *et al.*, 2010). In addition to potentially activating TRPV2

channels, CBD appears to have an effect on TRPV2 protein expression and cell localization. CBD enhancement was reversed by the protein synthesis inhibitor cycloheximide (CHX) although this did not affect basal phagocytosis. This is further supported by recent reports that CBD increases TRPV2 expression, both at mRNA and protein levels in glioblastoma multiforme cells (Nabiss *et al.*, 2012).

In the present experiments, there was a rapid enhancement of TRPV2 protein expression due to CBD and this appeared to involve translocation of TRPV2 to the cell membrane with marked localization there by 24 hours. TRPV2 mRNA was also markedly increased by 24 hours although increases were difficult to detect over the first hour during which whole cell protein expression peaked. The reasons for this apparent disparity are unclear, but might be due to methodological or assay sensitivity differences. A further possibility exists that CBD influences protein translation without immediately altering gene transcription.

Interestingly, the enhanced expression was abolished in the presence of the TRP channel blocker and calcium-induced calcium release blocker from the ryanodine-sensitive intracellular calcium stores (Phillippe and Basa, 1996) ruthenium red, suggesting that the enhancement depends upon CBD activation of TRP channel activity with consequent  $\text{Ca}^{2+}$  entry and increases in gene transcription. TRPV2 channel activity is controlled by growth factors acting through a PI3-kinase-dependent signaling pathway (Kanzaki *et al.*, 1999). These data suggest the PI3-kinase pathway, may encourage a constitutive activity of TRPV2 channels.

TRPV2 translocation to the plasma membrane might be regulated by other mechanisms. It has been proposed that calcium could be involved in such a dynamic regulation of TRPV2 channels (Boels *et al.*, 2001) by stimulating

TRPV2 channel activity and, therefore, calcium influx, PI3-kinase could indirectly promote channel trafficking to the plasma membrane. Moreover, a TRPV2 associate known as the recombinase gene activator (RGA) protein has been reported. The RGA protein is localized at the endoplasmic reticulum/Golgi apparatus and interacts with intracellular TRPV2 (Barnhill *et al.*, 2004). Interaction of RGA with TRPV2 promotes the basal surface localization of TRPV2 and control of TRPV2 surface levels (Stokes *et al.*, 2005). (Barnhill *et al.* (2004) have demonstrated that RGA may play an important role for TRPV2 during the maturation of the ion channel protein.

Other TRP channels in addition to TRPV2 might be involved in the effect of CBD on microglial function and the cannabinoid also rapidly enhanced the expression of the vanilloid channel TRPV1. Interestingly this was inhibited by wortmannin and ruthenium red suggesting that enhancement of channel activity with activation of PI-3K underpins this effect. Previous studies have reported that CBD has very low affinity for CB<sub>1</sub> and CB<sub>2</sub> receptors, but that it activates TRPV1 channels (Bisogno *et al.*, 2001). Accumulating evidence indicates that TRPV1-receptor-mediated increases of [Ca<sup>2+</sup>]<sub>i</sub> by CBD occurs in a variety of cell types (Ligresti *et al.*, 2006), including hippocampal neurones (Drysdale *et al.*, 2006).

The cannabinoid ligands THC, CP55940, CBN and AEA all failed to alter phagocytosis either in microglia or macrophages. Anandamide is an endogenous activator of cannabinoid receptors, acting on CB<sub>1</sub> receptors with potency similar to that described for its action of TRPV1 (Marzo *et al.*, 2001; Ross, 2003). The functional relevance of the channel up-regulation is still to be investigated.

LPS activates both phagocytosis and AKT in a time dependent manner (Faisal *et al.*, 2005) so we next addressed whether or not the effect of CBD

was mediated by AKT signaling. The results show that CBD induced phagocytosis independently of Akt.

### **3.5.3 Migration of microglial cells**

Cannabinoids, whether phytocannabinoids or endocannabinoids, have been found to induce migration of BV-2 microglial cells (Walter *et al.*, 2003). In the present work, CBD promoted migration at 10 $\mu$ M concentrations in the BV-2 and macrophage cell lines using a novel "Compass" device. The positive control UDP also evoked a similar level of migration in BV2 cells. Although the cells do not express cannabinoid receptors, TRPV2 activation has been found to be involved in macrophage cell migration (Nagasawa *et al.*, 2007). The latter report documented that the chemotactic peptide fMetLeuPhe induces the migration of macrophages and that this migration is associated with the translocation of the TRPV2 channel through a PI3K pathway (Nagasawa *et al.*, 2007).

According to the report by Walter *et al.*, (2003), CBD increases migration of BV-2 cells in a Boyden chamber assay and the cannabinoids effects were mediated by CB<sub>2</sub> and abnormal cannabidiol receptors. However, CBD significantly inhibited migration of U87 glioma cells independently of cannabinoid and vanilloid receptors (Vaccani *et al.*, 2005).

### **3.6 Conclusion:**

Taken together the results in this chapter demonstrate that CBD, but not other cannabinoids, enhances microglial and monocyte/macrophages phagocytosis and migration. The effect appears to be mediated by TRPV2 channel activation leading to elevated [Ca<sup>2+</sup>]<sub>i</sub> and translocation of TRPV2 to the cell membrane.

TRPV2 has been documented as a potential pain target and is activated by noxious heat greater than 52°C (Caterina *et al.*, 1999), the non-selective agonists 2-APB, phenylborate, DPBA (Juvin *et al.*, 2007) and by probenecid. Recently it has been reported that CBD is an agonist for TRPV2 although, no selective endogenous activators or antagonists have been reported.

Translocation is an important mechanism for TRPV2 functional activation and it is up-regulated by growth factors which enhance its movement from intracellular pools into the plasma membrane (Iwata *et al.*, 2003). PI 3-kinase also activates TRPV2 translocation to plasma membrane (Penna *et al.*, 2006) but does not appear to be involved in the enhancement due to cannabidiol. Although the effects of cannabidiol were not potent, it is a possible chemical starting point for the development of more potent TRPV2 agonists which could have a beneficial effect on neuroinflammatory conditions via enhancement of microglial phagocytosis.

### 3.6.1 Summary of chapter 3

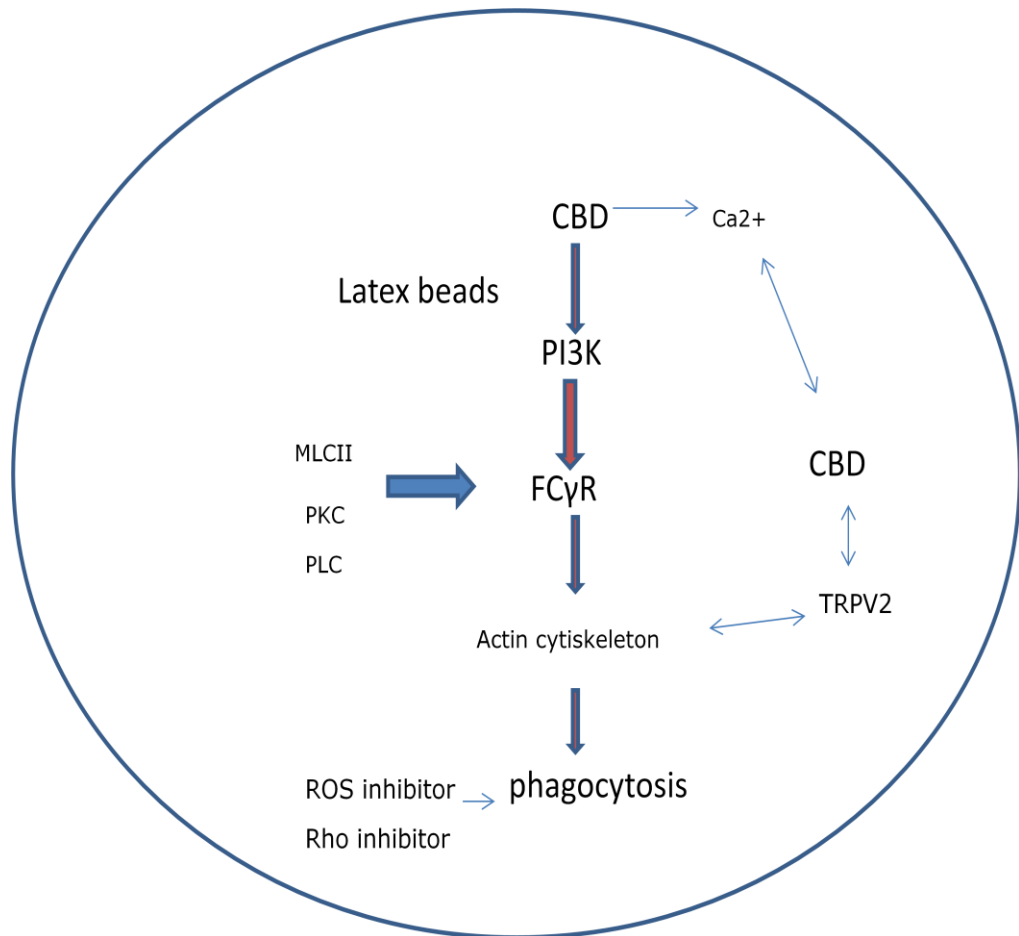


**Figure 3.44:** The graph represents the effect of CBD in enhancement of phagocytosis by increasing intracellular calcium and increases the expression of TRPV2. The involvement of MLCII, PKC, PLC, ROS in basal phagocytosis.

## 4. Overview

The work presented in this thesis focused upon an *in vitro* investigation of the effects of cannabinoid compounds on microglial function in order to explore their potential to modulate neuro-inflammatory conditions.

When viewed as a whole, microglial activation is beneficial to most acute CNS pathologies. The ultimate role of microglia is to create a barrier between the healthy cells in the CNS and damaged or infected cells (Garden and Möller, 2006; Block *et al.*, 2007) and they are the primary immune cells of the CNS, playing an important part in detecting and removing foreign bodies which invade the brain. This involves their transient activation involving the expression of receptors, the release of cytokines and phagocytosis of cell debris. Microglia cells are, therefore, an essential functional part of the CNS (Garden and Möller, 2006; Neumann *et al.*, 2009) and adapted to protect the more susceptible cells, particularly neurons from damage. Microglial dysfunction in the form of chronic activation may, however, be implicated in neuroinflammatory conditions.

The aim of studies reported here was to investigate the possibility of modulating microglial functions (NO release, phagocytosis, calcium mobilisation and migration) with cannabinoids. Cannabinoids have been suggested to be potentially useful therapeutic agents in the management of chronic pain with growing data supporting the CB receptors' role in immune cells, particularly microglia, in the CNS (Zhang *et al.*, 2003).

Nitric oxide (NO) is a key immune cell effector molecule and in the present study (Chapter 2), it was used as an indicator of microglial cell activation. The main activation stimulus used in the *in vitro* model was the bacterial exotoxin lipopolysaccharide (LPS) and it was demonstrated that LPS was

able to induce, in a concentration-dependant fashion, NO release in BV-2 cells, HAPI cells (a model of activated microglia) and in murine primary microglial cells. The BV-2 cell line, which was the most frequently used in the study, possesses functional and phenotypic properties common to primary microglia including phagocytic ability, secretion of pro-inflammatory cytokines and expression of surface receptors and antigens (Blasi *et al.*, 1990) and, as such, is a suitable *in vitro* model for investigation of microglial function. Moreover, these immortalized cells replicate readily and are easy to maintain in culture, allowing for convenient and cost-effective experimentation when compared with primary microglial cells for which such studies are time consuming; only a very limited quantity of purified microglia can be generated and there is no guarantee that even primary microglial cultures retain the same phenotype as the cells express *in situ*.

Cannabinoids have previously been reported to have effects in BV-2 cells, including effects on cell migration by CBD (Walter *et al.*, 2003). THC and CBD modulate the activities of BV-2 cells in different signalling pathway (Juknat *et al.*, 2012). On the basis of these prior reports, it was somewhat surprising that none of the cannabinoid receptor agonists in concentrations expected to activate CB<sub>1</sub> and/or CB<sub>2</sub> receptors affected LPS-stimulated NO formation, but it is clear that, under the culture conditions employed, the BV-2 cells failed to express either CB<sub>1</sub> or CB<sub>2</sub> receptors significantly. It does seem that BV-2 cell expression of cannabinoid receptors is not well maintained with increasing passage number (discussed in Chapter 2). The inhibitory effect of the CB<sub>1</sub>/CB<sub>2</sub> agonist CP55940 on NO formation, only in high concentration, may be explained by its acting through other potential cannabinoid-like receptors, for example, GPR55 (Chapter 2), which are

reported to be activated by CP55940 (Ryberg *et al.*, 2007, Kapur *et al.*, 2009) or some other, as yet unidentified, receptors.

However, one cannabinoid compound, cannabidiol (CBD) was found to significantly attenuate the effects of microglial cell activation by bacterial lipopolysaccharide (LPS). CBD is the major non-psychotropic constituent of marijuana and it has been shown to have both anti-inflammatory and anti-apoptotic actions on microglia (Iuvone *et al.*, 2004; Mechoulam *et al.*, 2007). The ability of CBD to decrease microglial activation has been proposed as a treatment for neurodegenerative diseases such as cerebral ischemia, Alzheimer's, and Parkinson's diseases and multiple sclerosis (Lastres-Becker *et al.*, 2005; Lakhan and Rowland, 2009). However, the mechanism(s) through which CBD alters microglia activation is not understood, and, in the present project, a deal of effort was spent in attempting to elucidate the molecular targets for CBD, using a variety of experimental techniques.

There are a number of reports suggesting the orphan receptor GPR55 as a potential member of the cannabinoid receptor family which may represent a novel pharmaceutical target (Johns *et al.*, 2007, Ryberg *et al.*, 2007) and, given that CBD has been identified as a GPR55 ligand, the potential roles of these receptors in modulating microglial functions were investigated. In the present study, GPR55 receptors appeared to be expressed in the BV-2 cells (as assessed by RT-PCR definition of measurable amounts of mRNA) and to be functional since the putative endogenous agonist LPI (Oka *et al.*, 2007) produced a concentration-dependent elevation of intracellular  $Ca^{2+}$  which was attenuated by CBD (Eldeeb *et al.*, 2009), in agreement with its designation as a GPR55 antagonist. However, CBD also reduced the  $Ca^{2+}$  response to ATP, calling into question its selectivity in this regard. Neither LPI nor O1602, another

GPR55 agonist (Johns *et al.*, 2007), affected LPS-stimulated NO formation lending little support to the possibility that the effect of CBD on NO formation is GPR55-mediated. Nevertheless, it is conceivable, given the effects of the novel GSK antagonist, that GPR55 receptors in the BV-2 cells are constitutively active and that CBD acts as a GPR55 antagonist/inverse agonist under the prevailing culture conditions. However, recently found that responses to activation of GPR55 are not seen in the presence of serum. Could this explain why there are no responses observed in the presence of serum in the microglia (oral discussion Dr Andy Irving (university of Dundee)).

Although the inhibitory effect of CBD on NO formation cannot be readily explained as being mediated by GPR55, it is interesting that the expression of GPR55 message and protein were reduced by CBD (Chapter 2). The functional significance of this is yet to be investigated, but since the receptor is implicated in the modulation of pro-inflammatory cytokine production, at least in peripheral cells, that promote neuropathic pain (Staton *et al.*, 2008), and CBD reduces neuropathic pain (Costa *et al.*, 2007) it is possible that reduced microglial GPR55 expression might play a part in CBD's analgesic mechanism, given the significance of the role of the microglia-neuronal interaction in neuropathic pain (Gao and Ji, 2010).

In this context, the inhibitory effect of CBD on microglial COX-2 generation (Chapter 2) with the expected reduction in pro-inflammatory eicosanoids could be of consequence. Also, there is evidence that reduction of COX-2 activity and PGE<sub>2</sub> synthesis depression can activate phagocytosis (Stachowska *et al.*, 2007), which might contribute towards the CBD activation of phagocytosis reported in Chapter 3.

Recently, CBD was shown to inhibit LPS-stimulated, NF $\kappa$ B-dependent pro-inflammatory cytokine release in BV-2 cells (Kozela *et al.*, 2010) although no cannabinoid nor cannabinoid-related receptor was implicated in the effect, indicating that control of NO release is not the only microglial effector mechanism impacted by CBD.

CBD is remarkable in the diversity of its actions on receptor and non-receptor targets when employed in the micromolar concentration range (Pertwee, 2004; 2008) and with regard to NO formation, whether CBD is initially recognized by a cell surface receptor or has its effects on a downstream component of a signalling cascade is uncertain. The lack of any effect of pertussis toxin on CBD's actions or of any CBD activation of GTP $\gamma$ S binding certainly appears to rule out the involvement of any Gi-protein coupled receptors. In Chapter 3, however, evidence for mediation of the effects of CBD on phagocytosis by the ligand-gated ion channel TRPV2 was gathered. CBD generated a sustained extracellular Ca<sup>2+</sup>-dependent increase in intracellular Ca<sup>2+</sup> concentration in BV-2 cells which was inhibited by the channel antagonists ruthenium red and SKF96365 and there was a marked enhancement of TRPV2-like immunoreactivity indicating TRPV2 up-regulation, particularly in the cell membrane. There was an accompanying increase in TRPV2 mRNA, at least after 24 hrs, although the lack of significant change in message at earlier time points needs further investigation.

It is somewhat counter-intuitive to see receptor activation resulting in up-regulation of that receptor; the opposite (i.e. down-regulation) response to a receptor agonist being the more common phenomenon, but activation accompanied by up-regulation of TRPV2 possibly indicates the functional importance of this amplified response to channel activation in the control of microglial phagocytosis.

In innate immune cells, TRPV2 is expressed in different types of phagocytic cells, including macrophages, in which it mediates fMet-Leu-Phe migration, zymosan-, immunoglobulin G-, and complement-mediated phagocytosis along with Ca<sup>2+</sup> influx and depolarisation (Nagasawa *et al.*, 2007; Santoni *et al.*, 2013). Link *et al.*, (2010) observed that activation of macrophage phagocytosis is accompanied by PI (3) kinase-dependent translocation of TRPV2 to the phagosomes and that this was impaired in TRPV2-KO macrophages.

Unfortunately, at the present time, there are no selective antagonists or agonists of the TRPV2 channel that could be used to unequivocally implicate it in the effects of CBD, although the phytocannabinoid could perhaps serve as a chemical template for future drug development.

In Chapter 3, evidence was produced that TRPV1 channels might also be involved in the effects of CBD since their expression was enhanced in BV-2. However, no evidence of functional modulation was produced and future experiments should include testing the effects of TRPV1 antagonists, such as capsazepine, on CBD-enhanced phagocytosis.

Effects of CBD on post- or non-receptor-mediated mechanisms are possible and results in Chapter 2 demonstrated that CBD alone enhanced generation of reactive oxygen species (ROS) (although it did appear to reduce the effects of LPS). This is interesting as ROS are reported to activate microglial phagocytosis (Zhang *et al.*, 2003) and they might have a mediating role in CBD-enhanced phagocytosis in BV-2 cells. CBD was found to have a remarkable protective effect against hydrogen peroxide-mediated microglial toxicity (Chapter 2), but whether this is related to its effects on ROS generation remains to be determined.

There is evidence demonstrating *in vitro* that the microglial triggering receptor expressed on myeloid cells-2 (TREM2) stimulates phagocytosis and down-regulates inflammatory signals in microglia via the signaling adaptor molecule DAP12 (Takahashi *et al.*, 2005). Microglial TREM2/DAP12-mediated phagocytosis appears to be an essential function for CNS tissue homeostasis (Neumann and Takahashi, 2007). Furthermore, in BV2 microglia, deletion of TREM2 led to reduced phagocytosis of apoptotic cells, but did not have an effect on phagocytosis of microbeads, indicating that TREM2 does not non-specifically promote phagocytosis (Hsieh *et al.*, 2009). It would be interesting, in future studies, to determine whether TREM2 is involved in CBD-enhancement of microglial phagocytosis.

It was stated earlier that NO generation was measured as an index of microglial activation, and it might appear to be a contradiction that CBD reduced NO formation but enhanced a clear functional end-point in phagocytosis. However, as stated in Chapters 2 and 3 it is probable that the *overproduction* of NO from microglial cells in areas of the brain (mimicked *in vitro* by LPS exposure) may reduce microglial phagocytosis in these regions resulting in the inability of microglia to clear debris and this could contribute to the neurodegenerative effects observed in chronic neuroinflammatory diseases such as Alzheimer's disease and it might, therefore, be the case that CBD inhibition of excessive NO production, as with LPS, actually contributes towards an enhanced phagocytotic effect.

It is important to consider, given the effects of CBD on microglial function, whether future developments should seek to enhance or inhibit such functions. Van Rossum and Hanisch (2004) suggest that modulation of excessive microglia activation should only be considered in three situations. First, it is only useful to inhibit microglial activation if the extracellular

signal that is activating the microglia has been eliminated from the CNS. Thus, therapies must be directly related to the channels and receptors that are involved in the disease, such as cannabinoid receptors in neurodegenerative disease. Second, the deactivation of microglia by cannabinoids needs to decrease all the products and signals of activation. The fine balance between various cytokines and chemokines highlights this situation because diminishing one harmful cytokine can increase the detrimental regulatory effects of other cytokines. Finally, the mechanisms of microglia activation in response to pathogenic stimuli can only be manipulated if they do not affect homeostatic functions of microglia. Inhibiting all microglial function in the brain during a disease would surely exacerbate other pathological processes. For example, decreasing the clearance of amyloid beta plaques during the initial phase of Alzheimer disease has been shown to have negative effects on disease morbidity (Martín-Moreno *et al.*, 2011). Therefore, the resolution of whether microglia is harmful or beneficial is contained in a better understanding of the intracellular interactions between microglia and disease components. Removing microglia cells from the CNS in healthy states would also necessarily have negative effects because of their beneficial role in synaptic control (Graeber *et al.*, 1993) The consequences of attempting to amplify microglial phagocytosis are unknown, given that, to date, no selective pharmacological enhancers of phagocytosis are available; CBD, or at least a more potent analogue, could provide the opportunity to test such a situation.

#### 4.1 Future directions and Points to Consider

In this PhD project a number of important observations have been made.

It was found that CBD can affect microglial cell function in the absence of cannabinoid receptors. The absence of CB1/2 receptors in our BV-2 cells allowed this unequivocal conclusion, but the effects of CBD in the presence of all of the naturally expressed microglial receptors (as *in situ*) should be tested. This is only truly possible by means of *in vivo* experimentation with CBD in animal models of neuroinflammatory conditions with measurement of microglial numbers and activity (using markers such as DAP12).

The protective effects of CBD against peroxide-mediated microglial cell death are intriguing and merit further mechanistic investigation by measuring the levels of glutathione and reduced glutathione.

TRPV2 was identified as a probable mediator of CBD-enhanced phagocytosis but the lack of appropriate pharmacological tools to investigate this further is a barrier. *In vitro* investigations using genetic knock-down of TRPV2 with siRNAs would be informative.

TRPV1 was also identified as a potential mediator of the effects of CBD and functional experiments using selective agonists such as capsaicin and antagonists such as AMG 9810 and capsazepine would be instructive. Investigation of the effects of CBD on the microglial expression of other members of the TRP channel family, particularly TRPV4 (given its proposed sensory role, activation by endocannabinoids, etc (Nilius *et al.*, 2007) would be interesting.

In relation to the methods employed, ingestion of latex beads is a widely employed protocol for measuring phagocytosis, but additionally employing

more physiologically appropriate paradigms, such as ingestion of apoptotic neurones (Takahashi *et al.*, 2005) for testing CBD effects would be interesting.

## **4.2 Conclusions**

In summary, it is worth considering that modulation of microglial functions with cannabinoids might be a possible therapeutic approach for neuroinflammatory conditions such as AD. Indeed it is accepted that regulation of CNS inflammation is essential to prevent irreversible cellular damage that can occur in neurodegenerative diseases such as multiple sclerosis (Baker *et al.*, 2007).

The results in this thesis are compatible with the proposal that CBD enhances the function of microglial cells, as demonstrated by increased motility and phagocytosis, albeit in the face of reduced NO production. The putative receptor(s) and signalling mechanisms mediating the effects of CBD are still uncertain although there is a clear role for TRPV2.

## Reffernces

- Abd-el-Basset E. and Fedoroff S. (1995) Effect of bacterial wall lipopolysaccharide (LPS) on morphology, motility, and cytoskeletal organization of microglia in cultures. *J Neurosci Res.* **41**: 222-37.
- Aderem A. and Underhill D.M. (1999) Mechanisms of phagocytosis in macrophages. *Annu Rev Immunol.* **17**: 593-623.
- Ahrens J, Demir R., Leuwer M., de la Roche J., Krampfl K., Foadi N., Karst M., Haesele G. (2009) The Nonpsychotropic Cannabinoid Cannabidiol Modulates and Directly Activates Alpha-1 and Alpha-1-Beta Glycine Receptor Functioninternational. *J. Experimental and clinical pharmacolog.* **83**: 4.
- Ahluwalia J., Urban L., Capogna M., Bevan S., Nagy I. (2000) Cannabinoid 1 receptors are expressed in nociceptive primary sensory neurons. *Neuroscience.* **100**: 685-688
- Akundi R.S., Candelario-Jalil E., Hess S., Hüll M., Lieb K., Gebicke-Haerter P.J., and Fiebich B.L. (2005) Signal transduction pathways regulating cyclooxygenase-2 in lipopolysaccharide-activated primary rat microglia. *Glia.* **51**: 3; 199-208.
- Alexander S.P.H. (2012) So what do we call GPR18 now?. *British Journal of Pharmacology.* **165**: 8; 2411-2413.
- Allen L.A. and Aderem A. (1996) Molecular definition of distinct cytoskeletal structures involved in complement- and Fc receptor-mediated phagocytosis in macrophages. *J. Exp. Med.* **184**: 627-637.
- Almeida A., Ciudad P., Delgado-Esteban M., Fernández E., García-Nogales P. and Bolaños J.P. (2005), Inhibition of mitochondrial respiration by nitric oxide: Its role in glucose metabolism and neuroprotection. *J. Neurosci. Res.* **79**: 166-171.
- Aloisi F. (2001) Immune function of microglia. *Glia.* **36**: 165-79.
- Ambrosini E. and Aloisi F. (2004) Chemokines and glial cells: a complex network in the central nervous system. *Neurochemical research.* **29**: 5: 1017-1038.
- Araki N., Hatae T., Furukawa A. and Swanson J.A. (2003) Phosphoinositide-3-kinase-independent contractile activities associated with Fcg-receptor-mediated phagocytosis and macropinocytosis in macrophages. *Journal of Cell Science.* **116**: 247-257.
- Arata S., Newton C., Klein T. and Friedman H. (1991) Tetrahydrocannabinol treatment suppresses growth restriction of *Legionella pneumophila* in murine macrophage cultures. *Life Sci.* **49**: 473-479.

- Ashton J., Friberg C., Darlington D., Smith P.F. (2006) Expression of the cannabinoid CB2 receptor in the rat cerebellum: an immunohistochemical study. *Neurosci Lett.* **396**: 113-6.
- Baker D., Pryce G., Davies WL. and Hiley CR. (2006) *In silico* patent searching reveals a new cannabinoid receptor. *Trends in Pharmacological Sciences.* **27**: 1; 1-4.
- Baker D., Jackson S.J. and Pryce G. (2007) Cannabinoid control of neuroinflammation related to multiple sclerosis. *Br J Pharmacol.* **152**:5: 649-654.
- Bal-Price A., Matthias A., Brown G.C. (2002) Stimulation of the NADPH oxidase in activated rat microglia removes nitric oxide but induces peroxynitrite production. *J Neurochem.* **80**: 1; 73-80.
- Banati R.B., Daniel SE. and Blunt SB. (1998) Glial pathology but absence of apoptotic nigral neurons in long-standing parkinson's disease. *Mov Disord.* **13**: 221-7.
- Banati R.B., Gehrman J., Schubert P. and Kreutzberg G.W. (1993) Cytotoxicity of microglia. *Glia.* **7**: 111-118.
- Banati R.B., Egensperger R., Maassen A., Hager G., Kreutzberg G.W. and Graeber M.B. (2004) Mitochondria in activated microglia in vitro. *J Neurocytol.* **33**: 535-41.
- Bard F., Cannon C., Barbour R., Burke R.L., Games D., Grajeda H., Guido T., Hu K., Huang J., Johnson-wood K., Khan K., Kholodenko D., Lee M., Lieberburg I., Motter R., Nguyen M., Soriano F., Vasquez N., Weiss K., Welch B., Seubert P., Schenk D. And Yednock T. (2000) Peripherally administered antibodies against amyloid beta-peptide enter the central nervous system and reduce pathology in a mouse model of Alzheimer disease. *Nat. Med.* **6**: 916-919
- Barger S.W., Goodwin M.E., Porter M.M., and Beggs M.L., (2007) Glutamate release from activated microglia requires the oxidative burst and lipid peroxidation. *J. Neurochem.* **101**: 1205-13.
- Barichello T. Ceretta R.A., Generoso J.S., Moreira A.P., Simões L.R., Comim C.M., Quevedo J., Vilela M.C., Zuardi A.W, Crippa J.A., Teixeira AL. (2012) Cannabidiol reduces host immune response and prevents cognitive impairments in Wistar rats submitted to pneumococcal meningitis. *European Journal of Pharmacology.* **697**: 15; 158-164.
- Bari M., Paradisi A., et al. (2005) Cholesterol-dependent modulation of type 1 cannabinoid receptors in nerve cells. *J Neurosci Res.* **81**: 2; 275-83.
- Barnhill J.C., Stokes A.J., Koblan-Huberson M., Shimoda L.M., Muraguchi A., Adra C.N., Turner H. (2004) RGA protein associates with a TRPV ion channel during biosynthesis and trafficking. *J. Cell Biochem.* **91**: 4; 808-20.
- Barnes P.J. (1998). Anti-inflammatory actions of glucocorticoids: molecular mechanisms. *Clin Sci (Lond).* **94**: 557-572. Barth F. and Rinaldi-Carmona M.

- (1999) The development of cannabinoid antagonists. *Curr Med Chem.* **6**: 8; 745-55.
- Battista N., Di Tommaso M., Bari M. and Maccarrone M. (2012). "The endocannabinoid system: an overview. *Front Behav Neurosci.* **6**: 9.
- Bauer M.K.A., Lieb K., Schulze-Osthoff K., Berger M, Gebicke-Haerter P.J., Bauer J., Fiebich B. (1997) Expression and Regulation of Cyclooxygenase-2 in Rat Microgli. *European Journal of Biochemistry.* **243**: 3; 726-731.
- Becher B., Prat A. and Antel J.P. (2000) Brain-immune connection: immunoregulatory properties of CNS-resident cells. *Glia.* **29**: 293-304.
- Berger J. and Moller D.E. (2002) The mechanisms of action of ppar $\alpha$ . *Annu Rev Med.* **53**: 409-435.
- Begg M., Pacher P., Batkai S., Osei-Hyiaman D., Offertaler L., Mo F.M., et al. (2005) Evidence for novel cannabinoid receptors. *Pharmacol Ther.* **106**: 133-145.
- Bergend L., Benes L., Durakova Z., Ferencik M (1999) Chemistry, Physiology and Pathology of free radicals. *Life Sci.* **65**: 1865-1874.
- Biber K., Sauter A., Brouwer N., Copray S.C.V.M. and Boddeke H.W.G.M. (2001) Ischemia-induced neuronal expression of the microglia attracting chemokine secondary lymphoid-tissue chemokine (SLC). *Glia.* **34**: 121-133.
- Bisogno T., Hanus L., De Petrocellis L., Tchilibon S., Ponde D.E., Brandi I., Moriello A.S., Davis J.B., Mechoulam R. and Di Marzo V. (2001) Molecular targets for cannabidiol and its synthetic analogues: effect on vanilloid VR1 receptors and on the cellular uptake and enzymatic hydrolysis of anandamide. *Br J Pharmacol.* **134**: 845-852.
- Blasi E.R., Barluzzi V., Bocchini R., Mazzolla F., Bistoni (1990) Immortalization of murine microglial cells by a *v-raf / v-myc* carrying retrovirus. *Journal of Neuroimmunology.* **27**: 2-3; 229-237.
- Block M.L. and Hong J.-S. (2005) Microglia and inflammation-mediated neurodegeneration: Multiple triggers with a common mechanism. *Progress in Neurobiology.* **76**: 77-98.
- Block M.L., Zecca L. and Hong J.-S. (2007) Microglia-mediated neurotoxicity: uncovering the molecular mechanisms. *Nat. Rev. Neurol.* **8**: 57-69.
- Boels K.G., Glassmeier D., Herrmann I.B., Hampe R.W., Kojima I., Schwarz R. and H.C. Schaller H.C. (2001) The neuropeptide head activator induces activation and translocation of the growth-factor-regulated Ca<sup>2+</sup>-permeable channel GRC, *J Cell Sci.* **114**: 3599-606.
- Bogdan (2001) Nitric oxide and the immune response. *Nat. Immunol.* **2**: 907-916.

- Boje KM, Prince K. Arora, Microglial-produced (1992) nitric oxide and reactive nitrogen oxides mediate neuronal cell death. *Brain Research*. **587**: 2; 250-256.
- Bolaños J.P., Almeida A., Stewart V., Peuchen S., Land J.M., Clark, Simon J. R. (1997) Nitric Oxide-Mediated Mitochondrial Damage in the Brain: Mechanisms and Implications for Neurodegenerative Diseases. *Journal of Neurochemistry*. **68**: 6; 2227–2240.
- Borsello T., Forloni G. (2007) JNK signalling: a possible target to prevent neurodegeneration. *Curr Pharm Des*. **13**: 18; 1875-86.
- Bosier B., Muccioli G.G, et al. (2010) Functionally selective cannabinoid receptor signalling: therapeutic implications and opportunities. *Biochem Pharmacol*. **80**: 1; 1-12.
- Botelho R.J. and Grinstein S. (2011) Phagocytosis. *Current Biology*. **21**: 14; R533–R538.
- Boucein C., Zacharias R., Farber K., Pavlovic S., Hanisch U.K. and Kettenmann H. (2003) Purinergic receptors on microglial cells: functional expression in acute brain slices and modulation of microglial activation in vitro. *Eur J. Neurosci*. **17**; 2267-76.
- Blanchetot C. and Boonstra J. (2008) Review: The ROS-NOX connection in cancer and angiogenesis. *Crit Rev Eukaryot Gene Expr*. **18**: 1; 35-45.
- Braida D., Pegorini S., Arcidiacono M.V., Consalez G.G., Croci L., Sala M. (2003) Post-ischemic treatment with cannabidiol prevents electroencephalographic flattening, hyperlocomotion and neuronal injury in gerbils. *Neurosci Lett*. **346**: 61–64.
- Breivogel G., Griffin V., Di Marzo V., Martin B.R. (2001) Evidence for a new G protein-coupled cannabinoid receptor in mouse brain. *Mol Pharmacol*. **60**: 1; pp. 155–163.
- Breivogel C.S., Walker J.M., Huang S.M., Roy M.B., Childers S.R., (2004) Cannabinoid signaling in rat cerebellar granule cells: G-protein activation, inhibition of glutamate release and endogenous cannabinoids. *Neuropharmacology*. **47**: 1; 81-91.
- Broderick C., Duncan L., Taylor N., Dick AD. (2000) IFN- $\gamma$  and LPS mediated IL-10-dependent suppression of retinal microglial activation. *Invest Ophthalmol Vis Sci*. **41**: 2613–2622.
- Brown G.C. (1997) Nitric oxide inhibition of cytochrome oxidase and mitochondrial respiration: Implications for inflammatory, neurodegenerative and ischaemic pathologies. *Molecular and Cellular Biochemistry*. **174**: 189–192.
- Brown A.J. (2007) Novel cannabinoid receptors. *BJP*. **152**: 567-575.
- Brown S.S. and Spudich J.A. (1981) Mechanism of Action of Cytochalasin: Evidence That it Binds to Actin Filament Ends. *The Journal of Cell Biology*. **88**: 487-491.

- Brown G.C. and Bal-Price (2003) A Inflammatory neurodegeneration mediated by nitric oxide, glutamate, and mitochondria. *Biomedical and Life Science*. **27**: 3; 325-355.
- Brown D. (2001) Microglia and prion disease. *Microscopy Research and Technique*. **54**: 2; 71-80.
- Brusco A., Tagliaferro P.A., et al. (2008) Ultrastructural localization of neuronal brain CB2 cannabinoid receptors. *Ann N Y Acad Sci*. **1139**: 450-7.
- Booz G.W. (2011).Cannabidiol as an emergent therapeutic strategy for lessening the impact ofinflammation on oxidative stress. *Free Radic Biol Med*. [Epub ahead of print].
- Burstein S.H. and Zurier R.B. (2009) Cannabinoids, Endocannabinoids, and Related Analogs in Inflammation. *The AAPS Journal*. **11**: 1; 109-119.
- Burkey T.H., Quock R.M., Consroe P., Roeske W.R., Yamamura H.I. (1997) D9-Tetrahydrocannabinol is a partial agonist of cannabinoid receptors in mouse brain. *European Journal of Pharmacology*. **323**: R3-R4.
- Bye N., Habgood M.D., Callaway J.K., Malakooti N., Potter A., Kossmann T., Morganti-Kossmann M.C. (2007) Transient neuroprotection by minocycline following traumatic brain injury is associated with attenuated microglial activation but no changes in cell apoptosis or neutrophil infiltration. *Exp Neurol*. **204**: 220-233.
- Cabral G.A. and Griffin-Thomas L. (2008) Cannabinoids as Therapeutic Agents for Ablating Neuroinflammatory Disease. *Endocr Metab Immune Disord Drug Targets*. **8**: 3; 159-172.
- Cabral G.A., Raborn E.S., Dennis J. And Marciano-Cabral C. (2008) CB2 receptors in the brain: role in central immune. *British Journal of Pharmacology*. **153**: 240-251.
- Cabral G.A., Harmon K.N. and Carlisle S.J. (2001) cannabinoid-mediated inhibition of inducible nitric oxide production by rat microglial cells: evidence for CB1 receptor participation. In K. T. F riedman H., *Advances in expermental medicine and biology neuroimmune circuits, drugs of abuse, and infectious diseases*. **493**: 207-214.
- Cabral G.A. and Staab A. (2005) Effects on the Immune System Cannabinoids *Handbook of Experimental Pharmacology*. **168**: 385-423.
- Cabral G.A. and Griffin-Thomas L. (2008) Cannabinoids as therapeutic agents forablating neuroinflammatory disease. *Endocrine, Metabolic & Immune Disorders .Drug Targets*. **8**: 159-172.
- Cabral G.A., Marciano-Cabral F. (2005) Cannabinoid receptors in microglia of the central nervous system: immune functional relevance. *J Leukoc Biol*. **78**:1192-1197.
- Cabral G.A. and Pettit D.A.D. (1998) Drugs and immunity: cannabinoids and their role in decreased resistance to infectious disease. *Journal of Neuroimmunology*. **83**: 1-2; 116-123.

- Callen L., Moreno E., et al. (2012) Cannabinoid receptors CB1 and CB2 form functional heteromers in brain. *J Biol Chem.* **287**: 25; 20851-65.
- Campbell V.A., Gowran A. (2007) Alzheimer's disease; taking the edge off with cannabinoids? *Br J Pharmacol.* **152**: 655-662.
- Carayon P., Marchand J., Dussosoy D., Dercocq J.M., Jbilo O., Bord A., Bouaboula M., Galiegue S., Mondiere P., Penarier G., Fur G.L., Defrance T. and Casellas P. (1998) Modulation and functional involvement of CB2 peripheral cannabinoid receptors during B-cell differentiation. *Blood.* **92**: 3605-15.
- Carlini E.A., Cunha J.M. (1981) Hypnotic and antiepileptic effects of cannabidiol. *J Clin Pharmacol.* **21**: 8-9; 417-427.
- Cartier L., Hartley O., Dubois-Dauphin M., and Krause KH. (2005) Chemokine receptors in the central nervous system: role in brain inflammation and neurodegenerative diseases. *Brain Research Reviews.* **48**: 1; 16-42.
- Carrier E.J., Kearn C.S., Barkmeier A.J., Breese N.M., Yang W., Nithipatikom K., Pfister S.L., Campbell W.B. and Hillard C.J. (2004) Cultured Rat Microglial Cells Synthesize the Endocannabinoid 2-Arachidonylglycerol, Which Increases Proliferation via a CB<sub>2</sub> Receptor-Dependent Mechanism. *Molecular Pharmacology.* **65**: 4; **999-1007**.
- Caron E. and Hall A. (1998) Identification of two distinct mechanisms of phagocytosis controlled by different Rho GTPases. *Science* **282**: 1717-1721.
- Caterina M.J., Rosen T.A, Tominaga M., Brake AJ., Julius D. (1999) A capsaicin-receptor homologue with a high threshold for noxious heat. *Nature.* **398**: 436-441.
- Chan A., Seguin R., Magnus T., Papadimitriou C., Toyka K.V., Antel J.P., Gold R. (2003) Phagocytosis of apoptotic inflammatory cells by microglia and its therapeutic implications: termination of CNS autoimmune inflammation and modulation by interferon-beta. *Glia.* **43**: 231-242.
- Chan W.J., Kohsaka S. and Rezaie P. (2007) The origin and cell lineage of microglia: new concepts. *Brain Res Rev.* **53**: 2; 344-54.
- Chao C.C., Hu S., Molitor T.W., Shaskan E.G., Peterson P.K. (1992) Activated microglia mediate neuronal cell injury via a nitric oxide mechanism. *J. Immunol.* **149**: 2736-2741.
- Chapman G.A., Moores K., Harrison D., Campbell C.A., Stewart B.R. and Strijbos P.J.L.M. (2000) Fractalkine cleavage from neuronal membranes represents an acute event in the inflammatory response to excitotoxic brain damage. *J Neurosci.* **20**: 1-5.
- Chaumont S., Jiang L.H., Penna A., North R.A., Rassendren F., (2004) Identification of a trafficking motif involved in the stabilization and polarization of P2X receptors. *J Biol Chem.* **279**: 29628-38.

Cheepsunthorn P., Radov L., Menzies S., Reid J., Connor J.R. (2001) Characterization of a novel brain-derived microglial cell line isolated from neonatal rat brain. *Glia*. **35**: 53-62.

Chen Z , Jalabi W., Shpargel K.B., Farabaugh K.T., Yin R.D., Kidd G.J., Bergmann C.C., Stohman S.A., and Bruce D. (2012) Trapp Lipopolysaccharide-Induced Microglial Activation and Neuroprotection against Experimental Brain Injury Is Independent of Hematogenous TLR4. *The Journal of Neuroscience*. **32**: 34; **11706-11715**.

Chen A., Kumar S.M., Sahley C.L. and Muller K.J. (2000) Nitric oxide influences injury-induced microglial migration and accumulation in the leech CNS. *J Neurosci*. **20**: 1036-1043.

Chew L.J., Takanohashi A. and Bell M. (2006) Microglia and inflammation: impact on developmental brain injuries. *Ment Retard Dev Disabil Res Rev*. **12**: 105-112.

Choi SH., Joe EH., Kim SU and Jin BK. (2003) Thrombin-induced microglial activation produces degeneration of nigral dopaminergic neurons in vivo. *J.Neurosci*. **23**: 5877-5886.

Choi Y., Kim H-S., Shin K.Y., Kim E-M., Kim, M., Kim, H-S., Park, C.H., Jeong, Y.H., Yoo J., Lee J-P., Chang K-A., Kim S., Suh Y-H (2007) Minocycline attenuates neuronal cell death and improves cognitive impairment in Alzheimer's disease models. *Neuropsychopharmacol*. **32**: 2393-2404.

Corradin S.B., Buchmüller-Rouiller Y., Mauël J. (1991) Phagocytosis enhances murine macrophage activation by interferon- $\gamma$  and tumor necrosis factor- $\alpha$ . *European Journal of Immunology*. **21**: 10; 2553–2558.

Costa B., Colleoni M., Conti S., Parolaro D., Franke C., Trovato A.E., Giagnoni G. (2004) Oral anti-inflammatory activity of cannabidiol, a non-psychoactive constituent of cannabis, in acute carrageenan-induced inflammation in the rat paw. *Naunyn Schmiedebergs Arch Pharmacol*. **369**: 74–79.

Covert M.W., Leung T.H., Gaston J.E., Baltimore D. (2005) Achieving stability of lipopolysaccharide-induced NF-kappaB activation. *Science*. **16**: 309; 1854-7.

Cox D. and Greenberg S. (2001). Phagocytic signaling strategies: Fc(gamma) receptor-mediated phagocytosis as a model system. *Semin. Immunol*. **13**: 339-345.

Cravatt B.F., Demarest K., Patricelli M.P., Bracey M.H., Giang D.K., Martin B.R., Lichtman A.H. (2001) Supersensitivity to anandamide and enhanced endogenous cannabinoid signaling in mice lacking fatty acid amide hydrolase. *Proc Natl Acad Sci USA*. **98**: 9371–9376.

Crippa Z.W., Hallak J.A., Moreira J.E. and Guimarães F.S. (2006) Cannabidiol, a *Cannabis sativa* constituent, as an antipsychotic drug. *Braz J Med Biol Res.* **39**: 4; 421-429.

Cristino L., de Petrocellis L., Pryce G., Baker D., Guglielmotti V., Di Marzo V. (2006) Immunohistochemical localization of cannabinoid type 1 and vanilloid transient receptor potential vanilloid type 1 receptors in the mouse brain. *Neuroscience.* **139**: 4; 1405-1415.

Croxford J.L. and Miller S.D. (2003) Immunoregulation of a viral model of multiple sclerosis using the synthetic cannabinoid R (+) WIN55,212. *J Clin Invest.* **111**: 1231-1240.

Cross D.K. and Woodroffe M.N. (1999) Chemokine modulation of matrix metalloproteinase and TIMP production in adult brain microglia and a human microglial cell line in vitro. *Glia.* **28**: 183-189.

Croxford J.L. and YAMAMURA T. (2005) Cannabinoids and the immune system: potential for the treatment of inflammatory diseases? *J Neuroimmunol.* **166**: 3-18.

Davalos D., Grutzendler J., Yang G., Kim J.V., Zuo Y., Jung S., Littman D.R., Dustin ML. and Gan W.B. (2005) ATP mediates rapid microglial response to local brain injury in vivo. *Nat Neurosci.* **8**: 752-8.

Davies SP., Reddy H., Caivano M., and Cohen P (2000) Specificity and mechanism of action of some commonly used protein kinase inhibitors. *Biochem. J.* **351**: 95-105.

David S. and Kroner A. (2011) Repertoire of microglial and macrophage responses after spinal cord injury. *Nat Rev Neurosci.* **12**: 388-399.

d'Avila J.C., Lam T.I., Bingham D., Shi J., Won S.J., Kauppinen T.M., Massa S., Liu J. and Swanson R.A. (2012) Microglial activation induced by brain trauma is suppressed by post-injury treatment with a PARP inhibitor *Journal of Neuroinflammation.* **9**: 31.

De Petrocellis L. and Di Marzo V. (2010). Non-CB1, non-CB2 receptors for endocannabinoids, plant cannabinoids, and synthetic cannabimimetics: focus on G-protein-coupled receptors and transient receptor potential channels. *J Neuroimmune Pharmacol.* **5**: 1; 103-21.

De Simone, R., Ambrosini E., Carnevale D., Ajmone-Cat M.A. and Minghetti L. (2007) NGF promotes microglial migration through the activation of its high affinity receptor: Modulation by TGF- $\beta$ . *J. Neuroimmunology.* **190**: 53-60.

Devane W.A., Hanus L., Breuer A., Pertwee R.G., Stevenson L.A., Griffin G, Gibson D., Mandelbaum A., Etinger A., Mechoulam R. (1992) Isolation and structure of a brain constituent that binds to the cannabinoids receptor. *Science.* **258**: 1946-1949.

Davalos D., Crutzendler J., Yang G., Kim J.V., Zuo Y., Jung S., Littman D.R., Dustin ML., Gan W.B. (2005) ATP mediates rapid microglial response to local brain injury in vivo. *Nature Neuroscience.* **8**: 6; 752-758.

- Diakonova M., Bokoch G., and Swanson J.A. (2002) Dynamics of cytoskeletal proteins during Fc $\gamma$  receptor-mediated phagocytosis in macrophages. *Mol. Biol. Cell.* **13**: 402-411.
- Demuth D. And Molleman A. (2006) Cannabinoid signalling. *LifeSci.* **78**: 6; 549-63.
- den Boon, F.S., Chameau P., Schaafsma-Zhao Q., Aken W.V., Bari M., Oddi S., Kruse C.G., Maccarrone M., Wadman W.J. and Werkman T.R. (2012). Excitability of prefrontal cortical pyramidal neurons is modulated by activation of intracellular type-2 cannabinoid receptors. *Proc Natl Acad Sci USA.* **109**: 9; 3534-9.
- De Petrocellis L., Ligresti A., Moriello A.S., Allara M., Bisogno T., Petrosino S. et al. (2011) Effects of cannabinoids and cannabinoid-enriched Cannabis extracts on TRP channels and endocannabinoid metabolic enzymes. *Br J Pharmacol.* **163**: 1479-1494.
- del Rio Hortega P. (1932) Microglia Cytology and cellular pathology of the nervous system. 483-534.
- de Lago E, Fernández-Ruiz J. (2007) Cannabinoids and neuroprotection in motor-related disorders. *CNS Neurol Disord Drug Targets.* **6**: 377-87.
- de Lanerolle P., Gorgas G., Li X. and Schluns K. (1993) Myosin light chain phosphorylation does not increase during yeast phagocytosis by macrophages. *J. Biol. Chem.* **268**: 16883-16886.
- Derocq J.M., Ségui M., Marchand J., Le Fur G. and Casellas P. (1995) Cannabinoids enhance human B-cell growth at low nanomolar concentrations. *FEBS Letter.* **369**: 177-182.
- Devane W.A., Dysarz F.A., Johnson M.R., Melvin L.S. and Howlett A.C. (1988) Determination and characterization of a cannabinoid receptor in rat brain. *Molecular Pharmacology.* **34**: 5; **605-613**.
- Devreotes P. and Janetopoulos C. (2003) Eukaryotic Chemotaxis: Distinctions between Directional Sensing and Polarization. *Journal of Biological Chemistry.* **278**: 20445-20448.
- Dib K., Melander F. and Andersson T. (2001) Role of p190RhoGAP in  $\beta_2$  Integrin Regulation of RhoA in Human Neutrophils. *The Journal of Immunology.* **166**: 10: **6311-6322**.
- Di Marzo V., Melck D., Bisogno T. and De Petrocellis L. (1998) Endocannabinoids: endogenous cannabinoid receptor ligands with neuromodulatory action. *Trends Neurosci.* **21**: 521-8.
- Dibaj P., Nadrigny F., Steffens H., Scheller A., Hirrlinger J., Schomburg E.D., Neusch C. and Kirchhoff F. (2010) NO mediates microglial response to acute spinal cord injury under ATP control in vivo. *Glia* **58**:1133-1144.
- Drysdale A.J., Ryan D., Pertwee R.G., and Platt B. (2006) Cannabidiol-induce intracellular Ca<sup>2+</sup> elevations in hippocampal cells. *Neuropharmacology.* **50**: 5; 621-631.

Duan Y., Sahley C.L. and Muller K.J. (2009) ATP and NO dually control migration of microglia to nerve lesions. *Developmental Neurobiology*. **69**: 60-72.

Eldeeb K., Alexander S., Pritchard D., Kendall D. (2009) LPI-evoked increases in intracellular calcium increases in microglial cells in culture, in. 19th Annual Symposium of the International Cannabinoid Research Society. *St. Charles, IL. ICRS*. 21.

El Manira A. and Kyriakatos A. (2010) The Role of Endocannabinoid Signaling in Motor Control. *Physiology*. **25**: 4; 230-238.

Esposito G., De Filippis D., Maiuri M.C., De Stefano D., Carnuccio R., and Iuvone T. (2006) Cannabidiol inhibits inducible nitric oxide synthase protein expression and nitric oxide production in beta-amyloid stimulated PC12 neurons through p38 MAP kinase and NF-kappaB involvement. *Neurosci Lett*. **399**: 91-95.

Fabrizi C., Silei V., Menegazzi M., Salmona M., Bugiani O., Tagliavini F., Suzuki H and Lauro G.M. (2001) The stimulation of inducible nitric-oxide synthase by the prion protein fragment 106-126 in human microglia is tumour necrosis factor-alpha-dependent and involves p38 mitogen-activated protein kinase. *J.Biol.Chem*. **276**: 25692-25696.

Facchinetti F., Del Giudice E., Furegato S., Passarotto M. and Leon A. (2003) Cannabinoids ablate release of TNFalpha in rat microglial cells stimulated with lipopolysaccharide. *Glia*. **41**: 161-8.

Familian A., Eikelenboom P., Robert Veerhuis R. (2007) Minocycline does not affect amyloid  $\beta$  phagocytosis by human microglial cells. *Neuroscience Letters*. **416**: 1; 87-91.

Fallman M., Gullberg M., Hellberg C., Andersson T. (1992) Complement receptor-mediated phagocytosis is associated with accumulation of phosphatidylcholine-derived diglyceride in human neutrophils. Involvement of phospholipase D and direct evidence for a positive feedback signal of protein kinase. *J. Biol. Chem*. **267**: 2656-2663.

Fang K-M, Yang C-S, Sun SH, Tzeng S-F (2009) Microglial phagocytosis attenuated by short-term exposure to exogenous ATP through P2X<sub>7</sub> receptor action. *Journal of Neurochemistry*. **111**: 5; 1225-1237.

Farber K., Pannasch U., Kettenmann H., (2005) Dopamine and noradrenaline control distinct functions in rodent microglial cells *Mol Cell Neurosci*. **29**: 128-138.

Ferreira R., Xapelli S., Santos T., Silva AP., Cristóvão A., Cortes L. and Malva J.O. (2010) Neuropeptide Y modulation of interleukin-1 beta (IL-1beta)- induced nitric oxide production in microglia. *Journal of Biological Chemistry*. **285**: 53; 41921-41934.

Fernandez-Ruiz J., Romero J., Velasco G., Tolon R. M., Ramos J. A. and Guzman M. (2007) Cannabinoid CB2 receptor: a new target for controlling neural cell survival?. *Trends Pharmacol Sci*. **28**: 39-45.

- Felder C.C., Joyce K.E., Briley E.M., Mansouri J., Mackie K., Blond O., Lai Y., Ma A.L., Mitchell R.L. (1995) Comparison of the pharmacology and signal transduction of the human cannabinoid CB1 and CB2 receptors. *Mol Pharmacol.* **4**: 443–450.
- Fiebich B.L., Biber K., Lieb K., Van Calker D., Berger M., Bauer J., Gebicke-Haerter P.J. (1996) Cyclooxygenase-2 expression in rat microglia is induced by adenosine A<sub>2a</sub>-receptors. *Glia.* **18**: 2; 152-160.
- Fiebich B.L., Butcher R.D., Gebicke-Haerter P.J. (1998) Protein kinase C-mediated regulation of inducible nitric oxide synthase expression in cultured microglial cells. **92**: 1–2; 170–178.
- Filipeanu C.M., de Zeeuw S.D., Nelemans A. (1997) Δ<sup>9</sup>-Tetrahydrocannabinol activates [Ca<sup>2+</sup>]<sub>i</sub> increases partly sensitive to capacitative store refilling. *European Journal of Pharmacology.* **336**: R1–R7.
- Finsen B.R., Sorensen T., Castellani B., Pedersen E.B. and Zimmer J. (1991) Leukocyte infiltration and glial reactions in xenografts of mouse brain tissue undergoing rejection in the adult rat brain. A light and electron microscopical immunocytochemical study. *J Neuroimmunol.* **32**: 159-83.
- Fontana A., Frei K., Bodmer S. and Hofer, E., (1987) Immunemediated encephalitis: on the role of antigen-presenting cells in brain tissue, *Immunol. Rev.* **100**: 185-201.
- Flanagan M.D. and Lin S. (1980) Cytochalasins block actin filament elongation by binding to high affinity sites associated with F-actin. *J. Biol. Chem.* **255**: 835-838.
- Franklin A., Parmentier-Batteur S., Walter L., Greenberg D.A., and Nephil Stella N. (2003) Palmitoylethanolamide Increases after Focal Cerebral Ischemia and Potentiates Microglial Cell Motility. *The Journal of Neuroscience.* **23**: 21; 7767–7775.
- Franklin A. and Stella N. (2003) Arachidonylcyclopropylamide increases microglial cell migration through cannabinoid CB2 and abnormal-cannabidiol-sensitive receptors. *European Journal of Pharmacology.* **474**: 2–3; 195-198.
- Frank-Cannon T., Alto L., McAlpine F. and Tansey M. (2009) Does neuroinflammation fan the flame in neurodegenerative diseases? *Molecular Neurodegeneration.* **4**: 47.
- Frederick J., Buck M.E., Matson D.J., Cortright D.N. (2007) Increased TRPA1, TRPM8, and TRPV2 expression in dorsal root ganglia by nerve injury. *Biochemical and Biophysical Research Communications.* **358**: 4; 1058-1064.
- Friedman M., Cepero M.L., Klein T., Friedman H. (1986) Suppressive effect of delta 9-tetrahydrocannabinol in vitro on phagocytosis by murine macrophages. *Proc Soc Exp Biol Med.* **182**: 225–22.

- Gallant M., Dufresne C., Gareau Y., Guay D., Prasit P.L., Rochette C., Sawyer N., Slipetz D.M., Tremblay N., Metters K.M. (1996) Labelle New class of potent ligands for the human peripheral cannabinoid receptor. *Bioorg Med Chem Lett.* **6**: 2263–2268.
- Gallily R., Breuer A. and Mechoulam R. (2000) 2-Arachidonylglycerol, an endogenous cannabinoid, inhibits tumor necrosis factor  $\alpha$ -production in murine macrophages, and in mice. *Eur J Pharmacol* **406**: R5–R7.
- Garcia-Garcia E. and Rosales C. (2002) Signal transduction during Fc receptor-mediated phagocytosis. *J. Leukoc. Biol.* **72**: 1092–1108.
- Garden G. and Möller T. (2006) Microglia biology in health and disease. *J. Neuroimmune Pharmacol.* **1**: 127–137.
- Ganesan L.P., Wei G., Pengal R.A., Moldovan L., Moldovan N., Ostrowski MC. And Tridandapani S. (2004) The Serine/Threonine Kinase Akt Promotes Fcy Receptor-mediated Phagocytosis in Murine Macrophages through the Activation of p70S6 Kinase. *J Biol Chem.* **279**: 52; 54416–54425.
- Gao Y-J. and Ji R-R. (2010) Chemokines, neuronal-glia interactions, and central processing of neuropathic pain. *Pharmacol Ther.* **126**: 1; 56–68.
- Gaoni Y. and Mechoulam R. (1966) Cannabichromene, a new active principle in hashish. *Chem Commun.* **1**: 20–21.
- Gebremedhin D., A.R. Lange A.R., Campbell W.B., Hillard W.B. and Harder D.R. (1999) Cannabinoid CB1 receptor of cat cerebral arterial muscle functions to inhibit L-type  $Ca^{2+}$  channel current. *American Journal of Physiology.* **276**: H2085-H2093.
- Gehrmann J., Matsumoto Y. and Kreutzberg G.W. (1995) Microglia: intrinsic immune effector cell of the brain. *Brain Res Rev.* **20**: 3; 269–87.
- Gehrmann J., Banati R.B. and Kreutzberg G.W. (1993) Microglia in the immune surveillance of the brain: Human microglia constitutively express HLA-DR molecules. *J Neuroimmunol.* **48**: 189–98.
- Gibbons H.M. and Dragunow M. (2006) Microglia induce neural cell death via a proximity-dependent mechanism involving nitric oxide. *Brain Res.* **1084**: 21; 1–15.
- Giles K.M., Ross K., Rossi A.G., Hotchin N.A., Haslett C., Dransfield I. (2001) Glucocorticoid augmentation of macrophage capacity for phagocytosis of apoptotic cells is associated with reduced p130Cas expression, loss of paxillin/pyk2 phosphorylation and high levels of active Rac. *J. Immunol.* **167**: 976–986.
- Gill E.W., Paton W.D., Pertwee R.G. (1970) Preliminary experiments on the chemistry and pharmacology of cannabis. *Nature.* **228**: 134–136.
- Gitik M., Reichert F. and Rotshenker S. (2010) Research Communication Cytoskeleton plays a dual role of activation and inhibition in myelin and zymosan phagocytosis by microglia. *The FASEB Journal.* **24**: 7; 2211–21.

Girotti M., Evans J.H., Burke D. and Leslie C.C. (2004) Cytosolic Phospholipase A<sub>2</sub> Translocates to Forming Phagosomes during Phagocytosis of Zymosan in Macrophages. *The Journal of Biological Chemistry*. **279**: 19113-19121.

Giulian D. and Baker T.J. (1986) Characterization of ameboid microglia isolated from developing mammalian brain. *J. Neurosci*. **6**: 2163-2178.

Giuffrida A., Rodríguez de Fonseca F, Piomelli D. (2000) Quantification of bioactive acylethanolamides in rat plasma by electrospray mass spectrometry. *Anal Biochem*. **280**: 87-93.

Green S.P., Cairns B., Rae J., Errett-Baroncini C., Hongo J.A., Erickson R.W., Curnutte J.T. (2001) Induction of gp91-phox, a component of the phagocyte NADPH oxidase, in microglial cells during central nervous system inflammation. *J Cereb Blood Flow Metab*. **21**: 374-384.

Green L.C., Wagner D.A., Glogowski J., Skipper P.L., Wishnok J.S. and Tannenbaum S.R. (1982) Analysis of nitrate, nitrite, and [15N] nitrate in biological fluids. *Anal Biochem*. **126**: 131-8.

Griffin G., Atkinson P., Showalter V.M., Martin B. and Abood M.E. (1998) Evaluation of Cannabinoid Receptor Agonists and Antagonists Using the Guanosine-5'-O-(3-[<sup>35</sup>S]thio)-triphosphate Binding Assay in Rat Cerebellar Membranes. *JPET*. **285**: 2; 553-560.

Golde S., Coles A., Lindquist J.A., Compston A. (2003) Decreased iNOS synthesis mediates dexamethasone-induced protection of neurons from inflammatory injury *in vitro*. *European Journal of Neuroscience*. **18**: 9; 2527-2537.

Gorina R., Font-Nieves M., Márquez-Kisinousky L., Santalucia T., Planas AM. Astrocyte (2011) TLR4 activation induces a proinflammatory environment through the interplay between MyD88-dependent NFκB signaling, MAPK, and Jak1/Stat1 pathways. *Glia*. **59**: 2; 242-255,

Graeber M.B., Bise K. and Mehraein P. (1993) Synaptic stripping in the human facial nucleus. *Acta Neuropathol*. **86**: 179 181.

Guasti L., Richardson D., Jhaveri M., Eldeeb K., Barrett D., Elphick M.R., Alexander S.P.H., Kendall D., J Michael G., and Victoria Chapman V. (2009) Minocycline treatment inhibits microglial activation and alters spinal levels of endocannabinoids in a rat model of neuropathic pain. *Molecular Pain*. **5**.

Gyoneva S., Orr A.G. and Traynelis S.F. (2009) Differential regulation of microglial motility by ATP/ADP and adenosine. *Parkinsonism & Related Disorders*. **15**: S195-S199.

Hacker H. and Karin M. (2006) Regulation and function of IKK and IKK-related kinases. *Sci STKE*. **357**: 13 9.

Hamalainen M., Lilja R., Kankaanranta H. and Moilanen E. (2008) Inhibition of iNOS expression and NO production by anti-inflammatory steroids. Reversal by histone deacetylase inhibitors. *Pulm Pharmacol Ther*. **21**: 331-9.

- Hampson A.J., Grimaldi M., Axelrod J., Wink D. (1998) Cannabidiol and (-) Delta9-tetrahydrocannabinol are neuroprotective antioxidants. *Proc Natl Acad Sci U S A*. **95**: 8268–8273.
- Han J., Lee J.-D., Bibbs L. and Ulevitch, R. J. (1994) A MAP kinase targeted by endotoxin and hyperosmolarity in mammalian cells. *Science* **265**: 808-811.
- Han I.O., Kim K.W., Ryu J.H. and Kim W.K. (2002) p38 mitogen-activated protein kinase mediates LPS not IFN- $\gamma$ -induced inducible nitric oxide synthase expression in mouse BV2 microglial cells. *Neurosci Letters*. **325**: 9-12.
- Hanisch U.K. (2002) Microglia as a source and target of cytokines. *Glia*. **40**: 140–155.
- Hanisch U.K. and Kettenmann H. (2007) Microglia: active sensor and versatile effector cells in the normal and pathologic. *Nat Neurosci*. **10**: 1387-94.
- Happe H.K., Bylund D.B., Charles L. (2001) Murrin Agonist-stimulated [<sup>35</sup>S]GTP $\gamma$ S autoradiography: optimization for high sensitivity. *European Journal of Pharmacology*. **422**: 22; 1–13.
- Harrison J.K., Jiang Y., Chen S., Xia Y., Maciejewski D., McNamara R.K., Streit W.J., Salafranca M.N., Adhikari S., Thompson D.A., Botti P., Bacon K.B. and Feng, L. (1998) Role for neuronally derived fractalkine in mediating interactions between neurons and CX3CR1-expressing microglia. *Proceedings of the National Academy of Sciences of the United States of America*. **95**:10896-10901.
- Hassan N.F., Campbell D.E., Rifat S., Douglas S.D., (1991) Isolation and characterization of human fetal brain-derived microglia in in vitro culture. *Neuroscience*. **41**: 149-158.
- Hayakawa N., Kato H. and Araki T. (2007) Age-related changes of astrocytes, oligodendrocytes and microglia in the mouse hippocampal CA1 sector. *Mechanisms of Ageing and Development*. **128**: 4; 311-316.
- Haynes S.E., Hollopeter G., Yang, G., Kurpius D., Dailey M.E., Gan W-B. and Julius D. (2006) The P2Y<sub>12</sub> receptor regulates microglial activation by extracellular nucleotides. *Nat Neurosci*. **9**: 1512-1519.
- Haziot A., Ferrero E., Kontgen F., Hijiya N., Yamamoto S., Silver J., Stewart CL., and Gyert SM. (1996) Resistance to endotoxin shock and reduced dissemination of gram-negative bacteria in CD14- deficient mice. *Immunity*. **4**; 407-414.
- Herkenham M., Lynn A.B., Little M.D., Johnson M.R., Melvin L.S., De Costa B.R., Rice K.C. (1990) Cannabinoid receptor localisation in brain. *Proceedings of the National Academy of Sciences of the United States of America*. **87**: 1932–1936.

- Hsieh CL., Koike M., Spusta S., Niemi E., Yenari M., Nakamura M.C. and Seaman W.E. (2009) A Role for TREM2 Ligands in the Phagocytosis of Apoptotic Neuronal Cells by Microglia. *J Neurochem.* **109**: 4; 1144–1156.
- Heasman S.J., Giles K.M., Rossi A.G., Allen J.E., Haslett C., and Dransfield I. (2004) Interferon gamma suppresses glucocorticoid augmentation of macrophage clearance of apoptotic cells. *Eur J Immunol.* **34**: 1752-1761.
- Henstridge C.M., Balenga N.A., Ford L.A., Ross R.A., Waldhoer M., Irving A.J. (2009) The GPR55 ligand L-alpha-lysophosphatidylinositol promotes RhoA-dependent Ca<sup>2+</sup> signaling and NFAT activation. *The FASEB Journal* . **23**: 1; 183–93.
- Hickey W.F., Hsu B.L. and Kimura H. (1991) T-lymphocyte entry into the central nervous system. *J Neurosci Res.* **28**; 254-60.
- Hill C.S. and Treisman R. (1995) Transcriptional regulation by extracellular signals: mechanisms and specificity. *Cell.* **27**: 80; 199-211.
- Hillard C.J., Manna S., Green berg M.J., Dicamelli R., Ross R.A., Stevenson L.A., Murphy V., Pertwee R.G. and Campbell W.B. (1999) synthesis and characterization of patent and selective agonist of neuronal cannabinoids receptor CB1. *JPh and Expermintal Therapeutic.* **289**: 3; 1427-1433.
- Hinkerohe D., Smikalla D., Schoebel A., Haghikia A., Zoidl G., Haase C.G., Schlegel U., Faustmann P.M. (2010) Dexamethasone prevents LPS-induced microglial activation and astroglial impairment in an experimental bacterial meningitis co-culture model. *Brain Research.* **1329**: 45–54.
- Hinojosa A.E., Garcia-Bueno B., C Leza J., and LM Madrigal J. (2011) CCL2/MCP-1 modulation of microglial activation and proliferation. *J Neuroinflammation.* **8**: 77.
- Hoek R.M., Ruuls S.R., Murphy C.A., Wright G.J., Goddard R., Zurawski S.M., Blom B., Homola M.E., Streit W.J., Brown M.H., Barclay A.N., Sedgwick J.D. (2000) Down-regulation of the macrophage lineage through interaction with OX2 (CD200). *Science.* **290**: 1768-71.
- Hodrea J., Majai G., Doró Z., Zahuczky G., Pap A., Rajnavölgyi É. and Fésüs L. (2012) programs human dendritic cells for enhanced phagocytosis of apoptotic neutrophils and inflammatory response. *Journal of Leukocyte Biology.* **91**:127-136.
- Hoffmann A., Hofmann F., Just I., Lehnardt S., Hanisch U-K., Brück W., Kettenmann H., Ahnert-Hilger G., Höltje M. (2008) Inhibition of Rho-dependent pathways by Clostridium botulinum C3 protein induces a proinflammatory profile in microglia. *Glia.* **56**: 11; 1162-1175.
- Hoffmann A., Kann O., Ohlemeyer C., Hanisch U-K., and Kettenmann H. (2003) Elevation of Basal Intracellular Calcium as a Central Element in the Activation of Brain Macrophages (Microglia): Suppression of Receptor-Evoked Calcium Signaling and Control of Release Function. *The Journal of Neuroscience.* **23**: 11; 4410-4419.

- Honda S. and Kohsaka S. (2001) Regulation of microglial cell function by ATP, *Nihon Shinkei Seishin Yakurigaku Zasshi*. **21**: 89-93.
- Honda S., Sasaki Y., Ohsawa K., Imai Y., Nakamura Y., Inoue K. and Kohsaka S. (2001) Extracellular ATP or ADP induce chemotaxis of cultured microglia through Gi/o-coupled P2Y receptors. *J Neurosci*. **21**: 1975-1982.
- Holm A., Tejle K., Gunnarsson T., Magnusson K-E., Descoteaux A., Rasmusson B. (2003) Role of protein kinase C  $\alpha$  for uptake of unopsonized prey and phagosomal maturation in macrophages. *Biochemical and Biophysical Research Communications*. **302**: 4; 653-658.
- Hooper C., Pinteaux-Jones F., Fry V.A., Sevastous., Baker D., Heales S.J., and Pocock J.M. (2009) Differential effects of albumin on microglia and macrophages; implications for neurodegeneration following blood-brain barrier damage. *J. Neurochem*. **109**: 694-705.
- Howlett A. (1995) Pharmacology of cannabinoid receptors. *Annu Rev Pharmacol Toxicol*. **35**: 607-634.
- Howlett A.C. (2002). The cannabinoid receptors. *Prostaglandins Other Lipid Mediat*. **68-69**: 619-631.
- Howlett A.C., Barth F., Bonner T.I., Cabral G., Casellas P., Devane W.A. et al. (2002) International Union of Pharmacology. XXVII. Classification Of cannabinoid receptors. *Pharmacol Rev*. **54**; 161-202.
- Hua X-Y., Svensson C.I., Matsui T., Fitzsimmons B., Yaksh T.L., Webb M. (2005) Intrathecal minocycline attenuates peripheral inflammation-induced hyperalgesia by inhibiting P38 MAPK in spinal microglia. *European Journal of Neuroscience*. **22**: 10; 2431-2440.
- Huffman J.W., Zengin G., Wu M-J., Lu J., Hynd G., Bushell K., Thompson A.L.S., Bushell S., Tartal C., Hurst D.P., Reggio P.H., Selley D.E., Cassidy M.P., Wiley J. and Martin B R. (2005) Structure-activity relationships for 1-alkyl-3-(1-naphthoyl)indoles at the cannabinoid CB<sub>1</sub> and CB<sub>2</sub> receptors: steric and electronic effects of naphthoyl substituents. New highly selective CB<sub>2</sub> receptor agonists. *Bioorganic & Medicinal Chemistry*. **13**: 1; 89-112.
- Huffman J.W. (2005) CB2 receptor ligands. *Mini RevMedChem*. **5**: 7; 641-9.
- Huestis M.A., Gorelick D.A., Heishman S.J., et al. (2001) Blockade of Effects of Smoked Marijuana by the CB1-Selective Cannabinoid Receptor Antagonist SR141716. *Arch Gen Psychiatry*. **1**: 58; 322-328.
- Hwang S.Y., Jung J.S., Lim S.J., Kim J.Y., Kim T.H., Cho K.H. and Han I.O. (2004) LY294002 inhibits IFN-gamma stimulated inducible nitric oxide synthase expression in BV2 microglial cells. *Biochem Biophys Res Comm*. **318**: 691-697.

Ichikawa H. and Sugimoto T. (2000) Vanilloid receptor 1-like receptor-immunoreactive primary sensory neurons in the rat trigeminal nervous system. *Neuroscience*. **101**: 719–725.

Imura T., Nakano I., Kornblum H.I., Sofroniew M.V. (2006) Phenotypic and functional heterogeneity of GFAP-expressing cells in vitro: differential expression of LeX/CD15 by GFAP-expressing multipotent neural stem cells and non-neurogenic astrocytes. *Glia*. **53**: 277–93.

Inoue K. (2002) Microglial activation by purines and pyrimidines. *Glia*. **40**: 2; 156–163.

Inoue K. (2008) Purinergic systems in microglia. *Cell Mol Life Sci*. **65**: 3074-80.

Inoue K. Nakajima K., Morimoto T., Kikuchi Y., Koizumi S., Illes P., Kohsaka S. (1998) ATP stimulation of Ca<sup>2+</sup>-dependent plasminogen release from cultured microglia. *Br.J.Pharmacol*. **123**: 1304–1310.

Isaksson J., Farooque M., Holtz A., Hillered L. and Olsson Y. (1999) Expression of ICAM-1 and CD11b After Experimental Spinal Cord Injury in Rats. *Journal of Neurotrauma*. **16**: 2; 165-173.

Iuvone T., Esposito G., Esposito R., Santamaria R., Di Rosa M., Izzo A.A. (2004) Neuroprotective effect of cannabidiol, a non-psychoactive component from Cannabis sativa, on beta-amyloid-induced toxicity in PC12 cells. *J. Neurochem*. **89**: 134-141.

Iuvone T., Esposito G., De Filippis D., Scuder C., Steardo L. (2009) Cannabidiol: A Promising Drug for Neurodegenerative Disorders?. *CNS Neuroscience & Therapeutics*. **15**: 1; 65–75.

Iuvone T., Gallily R.E., Even-Chen T., Katzavian G., Lehmann D., Dagan A., Mechoulam R. (2003)  $\gamma$ -Irradiation enhances apoptosis induced by cannabidiol, a non-psychotropic cannabinoid, in cultured HL-60 myeloblastic leukemia cells. *Leuk Lymphoma*. **44**: 1767–1773.

Iwata Y., Katanosaka Y., Arai Y., Komamura K., Miyatake K., Shigekawa M. (2003) A novel mechanism of myocyte degeneration involving the Ca<sup>2+</sup>-permeable growth factor-regulated channel. *J. Cell Biol*. **161**: 957–967

Izzo A.A., Borrelli F., Capasso R., Di Marzo V., Mechoulam R. (2009) Non-psychoactive plant cannabinoids: new therapeutic opportunities from an ancient herb. *Trend Pharmacol Sci*. **30**: 515-527.

Járai Z., Wagner J.A., Varga K., Lake K.D., Compton D.R., Martin B.R., Zimmer A.M., Bonner T.I., Buckley N.E., Mezey E., Razdan R.K., Zimmer A., Kunos G. (1999) Cannabinoid-induced mesenteric vasodilation through an endothelial site distinct from CB1 or CB2 receptors. *Proc Natl Acad Sci U S A*. **23**: 96; 14136-41.

Jang B.C., Paik J.H., Kim S.P., Bae J.H., Mun K.C., Song D.K., Cho C.H., Shin D.H., Kwon T.K., Park J.W., Park J.G., Baek W.K., Suh M.H., Lee S.H., Baek S.H., Lee I.S., Suh S.I. (2004) Catalase induces the expression of inducible nitric oxide synthase through activation of NF- $\kappa$ B and PI3K

signaling pathway in Raw 264.7 cells. *Biochem. Pharmacol.* **68**: 2167–2176.

Janeway C.A., Jr. (1992) The immune system evolved to discriminate infectious nonself from noninfectious self. *Immunol Today.* **13**:11-16.

Jeon Y.J., Yang K.H., Pulaski J.T., Kaminski N.E. (1996) Attenuation of inducible nitric oxide synthase gene expression by delta 9-tetrahydrocannabinol is mediated through the inhibition of nuclear factor-kappa B/Rel activation. *Mol Pharmacol.* **50**: 2; 334-41.

Johns D.G., Behm D.J., Walker D.J., Ao Z., Shapland E.M., Daniels D.A., Riddick M., Dowell S., Staton P.C., Green P., Shabon U., Bao W., Aiyar N., Yue T.L., Brown A.J., Morrison A.D. and Douglas S.A. (2007) The novel endocannabinoid receptor GPR55 is activated by atypical cannabinoids but does not mediate their vasodilator effects. *Br J Pharmacol.* **152**; 825-31.

Juknat A., Pietr M., Kozela E., Rimmerman N., Levy R., Coppola G., Geschwind D., Vogel Z. (2012) Differential transcriptional profiles mediated by exposure to the cannabinoids cannabidiol and  $\Delta$ 9-tetrahydrocannabinol in BV-2 microglial cells. *Br J Pharmacol.* **165**: 8; 2512-28.

Juknat A., Rimmerman N., Levy R., Vogel Z., Kozela E., (2012) Cannabidiol affects the expression of genes involved in zinc homeostasis in BV-2 microglial cells. *Neurochemistry International.* **61**: 6; 923-930,

Juel-Jensen B.E. (1972) Cannabis and recurrent herpes simplex. *Br Med J.* **4**: 296.

Jun C.D., Han M.K., Kim U.H. and Chung H.T. (1996). Nitric oxide induces ADP-ribosylation of actin in murine macrophages: association with the inhibition of pseudopodia formation, phagocytic activity, and adherence on a laminin substratum. *Cell Immunol.* **174**: 25–34.

Juvin V., Penna A., Chemin J., Lin Y-L., Rassendren F-A. (2007) Pharmacological characterization and molecular determinants of the activation of transient receptor potential V2 channel orthologs by 2-aminoethoxydiphenyl borate. *Mol Pharmacol.* **72**:1258–1268.

Kaczocha M., Glaser ST., and Deutsch DG (2009) Identification of intracellular carriers for the endocannabinoid anandamide. *PNAS.* **106**: 15; 6375–6380.

Kalis C., Kanzler B., Lembo A., Poltorak A., Galanos C., Freudenberg M.A. (2003) Toll-like receptor 4 expression levels determine the degree of LPS-susceptibility in mice. *Eur. J. Immunol.* **33**: 798–805.

Kaminska B., Gozdz A., Zawadzka M., Ellert-Miklaszewska A., Lipko M. (2009) MAPK Signal Transduction Underlying Brain Inflammation and Gliosis as Therapeutic Target. *Neurodegeneration and Neuroplasticity.* **292**: 12; 1902–1913.

Kaminski N.E. (1996) Immune regulation by cannabinoid compounds through the inhibition of the cyclic AMP signaling cascade and altered gene expression. *Biochem Pharmacol.* **52**: 1133-40.

Kaminski N.E., Abood M.E., Kessler F.K., Martin B.R. and Schatz A.R. (1992) Identification of a functionally relevant cannabinoid receptor on mouse spleen cells that is involved in cannabinoid-mediated immune modulation. *Mol Pharmacol.* **42**: 736-42.

Kaminski N.E., Koh W.S., Yang K.H., Lee M. and Kessler F.K. (1994) Suppression of the humoral immune response by cannabinoids is partially mediated through inhibition of adenylate cyclase by a pertussis toxin-sensitive G-protein coupled mechanism. *Biochem Pharmacol.* **48**: 1899-1908.

Kano M., Ohno-Shosaku T., Hashimotodani Y., Uchigashima M., Watanabe M. (2009) Endocannabinoid-mediated control of synaptic transmission. *Physiol. Rev.* **89**: 309-380.

Kanzaki M., Zhang Y.Q., Mashima H., Li L., Shibata H., Kojima I. (1999) Translocation of a calcium-permeable cation channel induced by insulin-like growth factor-1. *Cell Biol.* 165-170.

Kapur A., Zhao P., Sharir H., Bai Y., Caron M.G., Barak L.S. and Abood M.E. (2009) Atypical Responsiveness of the Orphan Receptor GPR55 to Cannabinoid Ligands. *The Journal of Biological Chemistry.* **284**: **29817-29827**.

Kawahara K., Yoshida A., Koga K., Yokoo S., Kuniyasu A., Gotoh T., Sawada M. And Nakayama H. (2009) Marked induction of inducible nitric oxide synthase and tumor necrosis factor- $\alpha$  in rat CD40+ microglia by comparison to CD40- microglia. *J Neuroimmunol.* **208**: 70-9.

Keston A.S. and Brandt R. (1965) The fluorometric analysis of ultramicro quantities of hydrogen peroxide. *Anal. Biochem.* **11**: 1-5.

Kettenmann H.R., Banati R. and Walz W. (1993) Electrophysiological behavior of microglia. *Glia.* **7**: 93-101.

Kettenmann H. (2007) Microglial cells, the immune elements of the brain, are activated in disease or following injury. New findings indicate how these cells are switched on to remove damaged cells and cellular debris. *Nature.* **446**: 987-989.

Kettenmann H., Hanisch U.K., Noda M. and Verkhratsky A. (2011) Physiology of microglia. *Physiol Rev.* **91**: 461-553.

Kigerl K.A., Gensel J.C., Ankeny D.P., Alexander J.K., Donnelly D.J., Popovich P.G. *et al.* (2009) Identification of two distinct macrophage subsets with divergent effects causing either neurotoxicity or regeneration in the injured mouse spinal cord. *J Neurosci.* **29**: 13435-13444.

Kim S.J., Kim Y.S., Yuan J.P., Petralia R.S., Worley P.F. and Linden D.J. (2003) Activation of the TRPC1 cation channel by metabotropic glutamate receptor mGluR1. *Nature.* **426**: 285-291.

- Kim W.K., Kan Y., Ganea D., Hart R.P., Gozes I., Jonakait G.M. (2000) Vasoactive intestinal peptide and pituitary adenylyl cyclaseM activating polypeptide inhibit tumor necrosis factor- $\alpha$  production in injured spinal cord and in activated microglia via a cAMP-dependent pathway. *J Neurosci.* **20**: 3622–3630.
- Kim S.U. and de Vellis J. (2005) Microglia in health and disease. *J Neurosci R.* **81**: 3; 302-13.
- Kim S.H., Smith C.J. and Eldik L.J. (2004) Importance of MAPK pathways for microglial pro-inflammatory cytokine IL-1 $\beta$  production, *Neurobiology of Aging*, **25**: 4; 431-439.
- Kim Y.S. and Joh T.H. (2006) Microglia, major player in the brain inflammation: their roles in the pathogenesis of Parkinson' disease. *Experimental and Molecular Medicine.* **38**:4; 333-347.
- Klein T.W., Newton C. and Friedman H. (1998) Cannabinoid receptors and immunity. *Immunol Today.* **19**: 373-381.
- Klein T.W. and Newton C.A. (2007) Therapeutic potential of cannabinoid-based drugs. *Adv Exp Med Biol.* **601**: 395–413
- Klein T., Newton C., Friedman H. (1998) Cannabinoid receptors and immunity. *Immunol Today.* **19**: 8; 373–381
- Kobayashi K., Hernandez L.D., Galán J.E., Janeway C.A.Jr, Medzhitov R., Flavell R.A. (2002) IRAK-M is a negative regulator of Toll-like receptor signaling. *Cell.* **26**: 110; 191-202.
- Kohno M., Hasegawa H., Inoue A., Muraoka M., Miyazaki T., Oka K Yasukawa M. (2006). Identification of N-arachidonylglycine as the endogenous ligand for orphan G-protein-coupled receptor GPR18. *Biochem Biophys Res Commun.* **347**: 827–832.
- Koizumi S., Shigemoto-Mogami Y., Nasu-Tada K., Shinozaki Y., Ohsawa K., Tsuda M., Joshi B.V, Jacobson K.A., Kohsaka S. and Inoue K. (2007) UDP acting at P2Y<sub>6</sub> receptors is a mediator of microglial phagocytosis. *Nature.* **446**: 1091-1095.
- Koistinaho M. and Koistinaho J. (2000) Role of p38 and p44/42 mitogen-activated protein kinases in microglia *Glia Special Issue: Microglia.* **40**: 2; 175–183.
- Koizumi S., Shigemoto-Mogami Y., Nasu-Tada K., Shinozaki Y., Ohsawa K., Tsuda M., Joshi B.V., Jacobson K.A., Kohsaka S. and Inoue K. (2007) UDP acting at P2Y<sub>6</sub> receptors is a mediator of microglial phagocytosis. *Nature.* **446**: 1091-1095.
- Kogan N.M., Rabinowitz R., Levi P., Gibson D., Sandor P., Schlesinger M. and Mechoulam R. (2004) Synthesis and antitumor activity of quinonoid derivatives of cannabinoids. *J Med. Chem.* **47**: 3800–3806.
- Kone B.C., Kunczewicz T., Zhang W. and Yu Z-Y. (2003) Protein interactions with nitric oxide synthases: controlling the right time, the right place, and

the right amount of nitric oxide. *Am J Physiol Renal Physiol.* **285**: F178–F190.

Kopec K.K. and Carroll R.T. (2000) Phagocytosis is Regulated by Nitric Oxide in Murine Microglia: *Biology and Chemistry. Departm Nitric Oxide.* **4**: 2; 103–111.

Kozak K.R., Gupta R.A., Moody J.S., Ji C., Boeglin W.E., Dubois R.N., Brash A.R. and Marnett L.J. (2002) 15-Lipoxygenase metabolism of 2-arachidonylglycerol. Generation of a peroxisome proliferator-activated receptor alpha agonist. *J Biol Chem.* **277**: 23278-86.

Kozela E., Pietr M., Juknat A., Rimmerman N., Levy R., Vogel Z. (2010) Cannabinoids Delta(9)-tetrahydrocannabinol and cannabidiol differentially inhibit the lipopolysaccharide-activated NF-kappaB and interferon-beta/STAT proinflammatory pathways in BV-2 microglial cells. *J Biol Chem.* **285**: 1616–26.

Kreitzer FR. and Stella N. (2009) The therapeutic potential of novel cannabinoid receptors. *Pharmacol Ther.* **122**: 2; 83-96.

Kremlev S.G., Roberts R.L. and Palmer C. (2004) Differential expression of chemokines and chemokine receptors during microglial activation and inhibition. *J. Neuroimmunol.* **149**: 1–9.

Krump E., Sanghera J.S., Pelech, S.L., Furuya W. (1997) Grinstein Chemotactic peptide N-formyl-Met-Leu-Phe activation of p38 mitogen-activated protein kinase (MAPK) and MAPK-activated protein kinase-2 in human neutrophils. *Journal of Biological Chemistry.* **272**: 2; 937-944.

Kuhn S.A., Frank K.H., van Landeghem, Zacharias R., Faerber K., Angelika Rappert A., Pavlovic S., Hoffmann A., Nolte C. and Kettenmann H. (2004) Microglia express GABAB receptors to modulate interleukin release. *Mol.Cell. Neurosci.* **25**; 312– 322.

Kurokawa K., Itoh R.E., Yoshizaki H., Nakamura Y.O., Matsuda M. (2004) Coactivation of Rac1 and Cdc42 at lamellipodia and membrane ruffles induced by epidermal growth factor. *Mol Biol Cell.* **15**: 1003–1010

Kwon J., Lee S.R., Yang K.S., Ahn Y., Kim Y.J., Stadtman E.R., Rhee S.G. (2004) Reversible oxidation and inactivation of the tumor suppressor PTEN in cells stimulated with peptide growth factors. *Proc Natl Acad Sci U S A.* **101**: **47**; 16419-24.

Lakhan S.E. and Rowland M. (2009). Whole plant cannabis extracts in the treatment of spasticity in multiple sclerosis: a systematic review. *BMC Neurology.* **9**: 59.

Lane J.R., Beukers M.W., Mulder-Krieger T., IJzerman A.P. (2010) The endocannabinoid 2-arachidonylglycerol is a negative allosteric modulator of the human A3 adenosine receptor. *Biochemical Pharmacology.* **79**: 1; 48-56.

Lastres-Becker I., Molina-Holgado F., A. Ramos J., Mechoulam R., Fernández-Ruiz J. (2005) Cannabinoids provide neuroprotection against 6-hydroxydopamine toxicity in vivo and in vitro: Relevance to Parkinson's disease. *Neurobiology of Disease*. **19**: 1–2; 96–107.

Lauckner J.E., Jensen J.B., Chen H.Y., Lu H.C., Hille B. and Mackie K. (2008) GPR55 is a cannabinoid receptor that increases intracellular calcium and inhibits M current. *Proc Natl Acad Sci U S A*. **105**; 2699-704.

Lavoie J.N., Hickey E., Weber L.A., Landry J. (1993) Modulation of actin-microfilament dynamics and fluid phase pinocytosis by phosphorylation of heat shock protein 27. *Journal of Biological Chemistry*. **268**: 32; 24210-24214.

Ledgerwood C.J., Greenwood S.M., Brett R.R., Pratt J.A., Bushell T.J. (2011) Cannabidiol inhibits synaptic transmission in rat hippocampal cultures and slices via multiple receptor pathways. *Br J Pharmacol*. **162**: 286–294.

Lee M., Schwab C., Mcgeer P.L. (2011) Astrocytes are GABAergic cells that modulate microglial activity. *Glia*. **59**: 1; 152–165.

Lee J.Y., Jhun B.S., Oh Y.T., Lee J.H., Choe W., Baik H.H., Ha J., Yoon K-S., Kim S.S., Kang I., (2006) Activation of adenosine A3 receptor suppresses lipopolysaccharide-induced TNF- $\alpha$  production through inhibition of PI 3-kinase/Akt and NF- $\kappa$ B activation in murine BV2 microglial cells. *Neuroscience Letters*. **396**: 1; 1-6.

Lee S.C., Liu W., Brosnan C.F., Dickson D.W. (1992) Characterization of primary human fetal dissociated central nervous system cultures with an emphasis on microglia. *Lab Invest*. **67**: 465-476.

Lewinter R.D., Skinner K., Julius D., Basbaum A.I. (2004) Immunoreactive TRPV-2 (VRL-1), a capsaicin receptor homolog, in the spinal cord of the rat. *Journal of Comparative Neurology*. **470**: 4; 400–408.

Liao B., Zhao W., Beers DR., Henkel J.S. and Appel S.H. (2012) Transformation from a neuroprotective to a neurotoxic microglial phenotype in a mouse model of ALS. *Exp Neurol*. **237**: 147–152.

Lieb K., Engels S., Fiebich B.L. (2003) Inhibition of LPS-induced iNOS and NO synthesis in primary rat microglial cells. *Neurochemistry International*. **42**: 2; 131-137.

Ligresti A., Moriello A.S., Starowicz K., et al. (2006) Antitumor activity of plant cannabinoids with emphasis on the effect of cannabidiol on human breast carcinoma. *J. Pharmacol. Exp. Ther*. **318**: 3; 1375–87.

Link T.M., Park U., Vonakis B.M., Raben D.M., Soloski M.J., Caterina M.J. (2010) TRPV2 has a pivotal role in macrophage particle binding and phagocytosis. *Nat. Immunol*. **11**: 232–239.

Liou G.I., Auchampach J.A., Hillard C.J., Zhu G., Yousufzai B., Salman Mian S., Khan S., and Khalifa Y. (2008) Mediation of Cannabidiol anti-

inflammation in the Retina by Equilibrative Nucleoside Transporter and A<sub>2A</sub> Adenosine Receptor. *Invest Ophthalmol Vis Sci.* **49**: 12; 5526–5531.

Litman G.W., Cannon J.P. and Dishaw L.J. (2005) Reconstructing immune phylogeny: new perspectives. *Nat Rev Immunol.* **5**; 866-79.

Liu G., Friggeri A., Yang Y., Park Y.J., Tsuruta Y. And Abraham R. (2009) miR-147, a microRNA that is induced upon Toll-like receptor stimulation, regulates murine macrophage inflammatory responses. *Proceeding of the National Academy of Sciences of the United State of America.* **106**: 37; 15819-15824.

Liu B., Wang K., Gao H.-M., Mandavilli B., Wang J.-Y. and Hong, J.-S. (2001) Molecular consequences of activated microglia in the brain: overactivation induces apoptosis. *Journal of Neurochemistry.* **77**: 182-189.

Lowry O.H., Rosebrough N.J., Farr A.L. and Randall R.J. (1951) Protein measurement with the Folin phenol reagent. *J Biol Chem.* **193**; 265-75.

Lu Y-C., Yeh W-C., Pamela S. and Ohashi (2008) LPS/TLR4 signal transduction pathway. *Cytokine.* **42**: 2; 145-151.

Ma D., Zerangue N., Lin Y.F., Collins A., Yu M., Jan Y.N., Jan L.Y. (2001) Role of ER export signals in controlling surface potassium channel numbers. *Science.* **291**; 316-9.

Maccarrone M., Bernardi G., Agrò A.F. (2011). Cannabinoid receptor signalling in neurodegenerative diseases: a potential role for membrane fluidity disturbance. *Br J Pharmacol.* **163**: 7; 1379-90.

Mackie K. and Stella N. (2006) Cannabinoids Receptors and Endocannabinoids: Evidence for New Players. *AAPS Journal.* **8**: 2; E298-E306.

Makranz C., Cohen G., Baron A., Levidor L., Kodama T., Reichert F., Rotshenker S. (2003) Phosphatidylinositol 3-kinase, phosphoinositide-specific phospholipase-C $\gamma$  and protein kinase-C signal myelin phagocytosis mediated by complement receptor-3 alone and combined with scavenger receptor-AI/II in macrophages. *Neurobiology of Disease.* **15**: 2; 279-286.

Makriyannis A., Yang D.P., Griffin R.G., Das Gupta S.K. (1990) The perturbation of model membranes by (-)-delta 9-tetrahydrocannabinol. Studies using solid-state <sup>2</sup>H- and <sup>13</sup>C-NMR. *Biochim Biophys Acta.* **1028**: 31-42.

Malfait A.M., Gallily R., Sumariwalla P.F., Malik A.S., Andreakos E., Mechoulam R. and Feldmann M. (2000) The nonpsychoactive cannabis constituent cannabidiol is an oral anti-arthritic therapeutic in murine collagen-induced arthritis. *Proc Natl Acad Sci USA.* **97**: 9561–9566.

Malin S.A. and Molliver D.C. (2010) Gi- and Gq-coupled ADP (P2Y) receptors act in opposition to modulate nociceptive signaling and inflammatory pain behaviour. *Molecular Pain.* **6**:21.

Mao H., Fang X., Floyd K.M., Polcz J.E., Zhang P., Liu B. (2007) Induction of microglial reactive oxygen species production by the organochlorinated pesticide dieldrin. *Brain Res.* **1186**: 267-74.

Maccarrone M., G. Bernardi et al. (2011) Cannabinoid receptor signalling in neurodegenerative diseases: a potential role for membrane fluidity disturbance. *Br J Pharmacol.* **163**: 7; 1379-90.

Maccarrone M., S. Rossi et al. (2008). Anandamide inhibits metabolism and physiological actions of 2-arachidonoylglycerol in the striatum. *Nat Neurosci* 11: **2**; 152-9.

Marciano-Cabral F., Ferguson T., Bradley S.G. and Cabral G. (2001) Delta-9-tetrahydrocannabinol (THC), the major psychoactive component of marijuana, exacerbates brain infection by *Acanthamoeba*. *J Euk Microbiol (Suppl)*: 4S-5S.

Martin W.J., Patrick S.L., Coffin P.O., Tsou K., Walker J.M (1995) An examination of the central sites of action of cannabinoid-induced antinociception in the rat. *Life Sci.* **56**: 2103-2110.

Martin B.R., Compton D.R., Thomas B.F, Prescott W.R., Little P.J., Razdan R.K., Johnson M.R., Melvin L.S., Mechoulam R., Ward S.J. (1991) Behavioral, biochemical, and molecular modeling evaluations of cannabinoid analogs. *Pharmacol Biochem Behav.* **40**: 471.

Martín-Moreno A.M., Reigada D., Ramírez B.G., Innamorato N., Cuadrado A. and de Ceballos M.L. (2011) Cannabidiol and other cannabinoids reduce microglial activation *in vitro* and *in vivo*: relevance to Alzheimer's disease. Neurodegeneration Group, Dept. of Cellular, Molecular and the American Society for *Pharmacology and Experimental Therapeutics Molecular Pharmacology Fast Forward.* **79**: 964-973.

Martinez-Orgado J., Fernandez-Lopez D., Moro M.A. and Lizasoain I. (2012) Nitric Oxide Synthase as a Target for the Prevention of Hypoxic-Ischemic Newborn Brain Damage. *Current Enzyme Inhibition.* **2**: 3; 219-229.

Marzo V. Di M.V, Bisogno T, De Petrocellis L (2001) Anandamide: some like it hot. *Trends Pharmacol. Sci.* **22**: 346-349

Mattiace L.A., Davies P., Yen S.H., Dickson D.W. (1990) Microglia in cerebellar plaques in Alzheimer's disease. *Acta Neuropathol. (Berl.)* **80**: 493-498.

May R.C., Caron E., Hall A. and Machesky L.M. (2000). Involvement of Arp 2/3 complex in phagocytosis mediated by FcγR or CR3. *Nat. Cell Biol.* **2**: 246-248.

May, R.C., and Machesky, L. M. (2001) Phagocytosis and the actin cytoskeleton. *J. Cell Sci.* **114**: 1061-1077.

Mayer A.M., Clifford J.A., Aldulescu M., Frenkel J.A., Holland M.A., Hall M.L., Glaser K.B., Berry J. (2011) Cyanobacterial *Microcystis aeruginosa* lipopolysaccharide elicits release of superoxide anion, thromboxane B<sub>2</sub>,

cytokines, chemokines, and matrix metalloproteinase-9 by rat microglia. *Toxicol Sci.* **121**: 63-72.

Merritt J.E., Armstrong W.P., Benham C.D., Hallam T.J., Jacob R., Jaxa-Chamiec A., Leigh B.K., McCarthy S.A., Moores K.E., Rink T.J. (1990) SK&F 96365, a novel inhibitor of receptor-mediated calcium entry. *Biochem J.* **271**: 515-522.

McAllister S.D., Christian R.T., Horowitz MP., Garcia A., Desprez P.Y. (2007) Cannabidiol as a novel inhibitor of Id-1 gene expression in aggressive breast cancer cells. *Mol. Cancer Ther.* **6**: 11; 2921-7.

McCoy K.L., Matveyeva M., Carlisle S.J. and Cabral G.A. (1999) Cannabinoid inhibition of the processing of intact lysozyme by macrophages: evidence for CB2 receptor participation. *J Pharmacol Exp Ther.* **289**: 1620-1625.

McHugh D., Page J., Dunn E., Bradshaw H.B. (2012)  $\Delta^9$ -Tetrahydrocannabinol and *N*-arachidonoyl glycine are full agonists at GPR18 receptors and induce migration in human endometrial HEC-1B cells. *British Journal of Pharmacology.* **165**: 8.

McHugh *et al.*, (2008) Inhibition of human neutrophil chemotaxis by endogenous cannabinoids and phytocannabinoids: evidence for a site distinct from CB1 and CB2 *Mol. Pharmacol.* **73**: 441-450.

McHugh D., Hu S.S.J., Rimmerman N., Juknat A., Vogel Z., Walker M. and Bradshaw H.B. (2010) *N*-arachidonoyl glycine, an abundant endogenous lipid, potently drives directed cellular migration through GPR18, the putative abnormal cannabidiol receptor. *BMC Neuroscience.* **11**: 44.

McGeer P.L., Itagaki S., Boyes B.E. and McGeer E.G., (1988) Reactive microglia are positive for HLA-DR in the substantia nigra of Parkinson's and Alzheimer's disease brains. *Neurology.* **38**: 1285-1291.

Mecha M., Torrao AS., Mestre L., Carrillo-Salinas FJ, Mechoulam R and Guaza C (2012) Cannabidiol protects oligodendrocyte progenitor cells from inflammation-induced apoptosis by attenuating endoplasmic reticulum stress. *Cell Death and Disease.* **3**: 71.

Mechoulam R., Parker L.A. and Gallily R. (2002) Cannabidiol: an overview of some pharmacological Aspects. *J. Clin. Pharmacol.* **42**; 11.

Mechoulam R., Peters M., Murillo-Rodriguez E., Hanus L.O. (2007) Cannabidiol-recent advances. *Chem Biodivers.* **4**: 1678-1692.

Mechoulam R., Ben-Shabat S., Hanus L., Ligumsky M., Kaminski N., Schatz A., Gopher A., Almog, S., Martin B. and Compton D. (1995) Identification of an endogenous 2 monoglyceride, present in canine gut, that binds to cannabinoid receptors. *Biochem. Pharmacol.* **50**: 83-90.

Mechoulam R. and Shohami E. (2007) Endocannabinoids and traumatic brain injury. *Mol Neurobiol.* **36**: 68-74.

Mechoulam R. and Parker L.A. (2012) The Endocannabinoid System and the Brain. *Annu Rev Psychol.* **64**: 21-47.

Meda L., Cassatella M.A., Szendrei G.I., Otvos L. Jr., Baron P., Villalba M., Ferrari D., Rossi F. (1995) Activation of microglial cells by  $\beta$ -amyloid protein and interferon- $\gamma$ . *Nature.* **374**: 647-650.

Medzhitov R. and Janeway C.A. Jr. (2000) Innate immunity. *N Engl J Med.* **343**: 338-344.

Meissner F., Molawi K. and Zychlinsky A. (2010) Mutant superoxide dismutase 1-induced IL-1 $\beta$  accelerates ALS pathogenesis. *Proc Natl Acad Sci USA.* **107**: 13046-1305.

Merrill J.E. (1992) Tumor necrosis factor- $\alpha$  interleukin-1 and related cytokines in brain development: normal and pathological. *Dev. Neuroscin.* **14**: 1-10.

Michelucci A., Heurtaux T., Grandbarbe L., Morga E., Heuschling P. (2009) Characterization of the microglial phenotype underspecific pro-inflammatory and anti-inflammatory conditions: Effects of oligomeric and fibrillar amyloid- $\beta$ . *Journal of neuroimmunology.* **210**: 1-2; 3-12.

Minghetti L. (2005) Role of inflammation in neurodegenerative diseases. *Curr Opin Neurol.* **18**: 315-321.

Michalik L., Auwerx J., Berger J.P., Chatterjee V.K., Glass C.K., Gonzalez F.J., Grimaldi P.A., Kadowaki T., Lazar M.A., O'Rahilly S., Plutzky C.N.A.P., Reddy J.K., Spiegelman B.M., Staels B. and Wahli W. (2006) International Union of Pharmacology. LXI. Peroxisome proliferator-activated receptors. *Pharmacol Rev.* **58**: 4; 726-41.

Miller A.M. and Stella N. (2009) Microglial cell migration stimulated by ATP and C5a involve distinct molecular mechanisms: quantification of migration by a novel near-infrared method. *Glia.* **57**: 875-883.

Minghetti L. and Pocchiari M. (2007) Cyclooxygenase-2, prostaglandin E<sub>2</sub>, and microglial activation in prion diseases. *International Review of Neurobiology* **82**: 265-75.

Mishima K., Hayakawa K., Abe K., Ikeda T., Egashira N., Iwasaki K., Fujiwara M. (2005). Cannabidiol prevents cerebral infarction via a serotonergic 5-hydroxytryptamine<sub>1A</sub> receptor-dependent mechanism. *Stroke; a Journal of Cerebral Circulation.* **36**: 5; 1077-82.

Mitrovic B., Ignarro L.J., Montestruque S., Smoll A and Merrill J.E. (1994) Nitric oxide as a potential pathological mechanism in demyelination: its differential effects on primary glial cells in vitro. *Neuroscience.* **61**: 575-585.

Molina-Holgado F., Molina-Holgado E., et al (2002) Role of CB1 and CB2 receptor in the inhibitory effects of cannabinoids on lipopolysaccharide-induced nitric oxide release in astrocyte cultures. *J Neurosci RES.* **67**: 6; 829-36.

Möller T., Kann O., Prinz F., Kirchhoff F., Verkhratsky A and Kettenmann H. (1997) Endothelin-induced calcium signalling in cultured mouse microglial cells is mediated through ETB receptors. *NeuroReport*. **8**: 2127-2131.

Morahan P.S., Klykken P.C., Smith S.H., Harris L.S. and Munson A.E. (1979) Effects of cannabinoids on host resistance to *Listeria monocytogenes* and herpes simplex virus. *Infect. Immun.* **23**: 3; **670-674**.

Muccioli G.G. and Stella N. (2008) Microglia produce and hydrolyze palmitoylethanolamide. *Neuropharmacology*. **54**: 16-22.

Munro S., Thomas k.I., Abu-Shaar M. (1993). Molecular characterization of a peripheral receptor for cannabinoids. *Nature*. **365**: 6441; 61-5.

Muraki K., Iwata Y., Katanosaka Y., Ito T., Ohya S., Shigekawa M., Imaizumi Y. (2003) TRPV2 is a component of osmotically sensitive cation channels in murine aortic myocytes. *Circ Res*. **93**: 829–838

Murray P.J. and Wynn T.A. (2011) Protective and pathogenic functions of macrophage subsets. *Nat Rev Immunol*. **11**: 11; 723-37.

Nabissi M., Morelli M.B., Santoni M. and Santoni G. (2013) Triggering of the TRPV2 channel by cannabidiol sensitizes glioblastoma cells to cytotoxic chemotherapeutic agents. *Carcinogenesis*. 34: **1**; 48-57.

Nagasawa M., Nakagawa Y., Tanaka S., Kojima I. (2007) Chemotactic peptide fMetLeuPhe induces translocation of the TRPV2 channel in macrophages. *J. Cell. Physiol*. **210**: 692–702.

Nakajima k. and Kohsaka S. (2004) Microglia: Neuroprotective and Neurotrophic Cells in the Central Nervous System. *Current Drug Targets - Cardiovascular & Haematological Disorders*. **4**; 65 -84.

Nakajima K., Honda S., Tohyama Y., Imai Y., Kohsaka S. and Kurihara, T. (2001) Neurotrophin secretion from cultured microglia. *Journal of Neuroscience Research*. **65**:322-331.

Nakamura Y. (2002) Regulating factors for microglial activation. *Biol Pharm Bull* **25**:945-953.

Napoli I. and Neumann H. (2009) Microglial clearance function in health and disease. *Neuroscience*. **158**: 1030–1038.

Neumann H., Kotter M.R. and Franklin R.J.M. (2009) Debris clearance by microglia: an essential link between degeneration and regeneration. *Oxford Journals Medicine Brain*. **132**: 2; **288-295**.

Neumann H. and Takahashi K. (2007) Essential role of the microglial triggering receptor expressed on myeloid cells-2 (TREM2) for central nervous tissue immune homeostasis. *Journal of Neuroimmunology*. **184**: 92-99.

Newton A.C. (1997) Regulation of protein kinase C. *Curr Opin Cell Biol.* **9**: 161-167.

Nilius B., Owsianik G., Voets T., and Peters J.A. (2007) Transient Receptor Potential Cation Channels in Disease. *Physiol Rev.* **87**: 1; **165-217**.

Noack H., Possel H., Rethfeldt C., Keilhoff G. and Wolf (1999) Peroxynitrite mediated damage and lowered superoxide tolerance in primary cortical glial cultures after induction of the inducible isoform of NOS. *Glia.* **28**: 13-24.

Noda M., Kettenmann H. and Wada K. (2006) Anti-inflammatory effects of kinins via microglia in the central nervous system. *Biol. Chem.* **51**: 167-171.

Noda M., Kariura Y., Amano T., Manago Y., Nishikawa K., Aoki S. and Wada K. (2003) Expression and function of bradykinin receptors in microglia. *Life Sci.* **72**: 1573-1581.

Noda M. and Suzumura (2012) sweepers in the CNS: microglial migration and phagocytosis in the Alzheimer disease pathogenesis. *International J. of Alzheimer' disease.* **89187**: 11.

Nolte C., Kirchhoff F. and Kettenmann H. (1997) Epidermal growth factor is a motility factor for microglial cells in vitro: Evidence for EGF receptor expression. *European Journal of Neuroscience.* **9**:1690-1698.

Obata T., Brown G.E., Yaffe M.B, (2000) MAP kinase pathways activated by stress: the p38 MAPK pathway. *Crit Care Med.* **6**: 7-77.

Ohtani Y., Minami M. and Satoh M. (2000) Expression of inducible nitric oxide synthase mRNA and production of nitric oxide are induced by adenosine triphosphate in cultured rat microglia. *Neuroscience Letters.* **293**: 1; 72-74.

Ohno-Shosaku T., Maejima T., Kano M. (2001). Endogenous cannabinoids mediate retrograde signals from depolarized postsynaptic neurons to presynaptic terminals. *Neuron.* **29**: 3; 729-38.

Ohsawa K., Irino Y., Sanagi T., Nakamura Y., Suzuki E., Inoue K. and Kohsaka S. (2010) P2Y12 receptor-mediated integrin- $\beta$  activation regulates microglial process extension induced by ATP. *Glia.* **58**: 790-801.

Ohsawa K., Irino Y., Nakamura Y., Akazawa C., Inoue K. and Kohsaka S. (2007) Involvement of P2X4 and P2Y12 receptors in ATP-induced microglial chemotaxis. *Glia.* **55**: 604-616.

Oka S., Nakajima K., Yamashita A., Kishimoto S. and Sugiura T. (2007) Identification of GPR55 as a lysophosphatidylinositol receptor. *Biochem Biophys Res Commun.* **362**; 928-34.

Oka S., Kimura S., Toshida T., Ota R., Yamahita A. and Sugiura T. (2010) Lysophatidlinositol induces rapid phosphorylation of p38 mitogen-activated protein kinase and activating transcription factor 2 in HEK293 cells

expressing GPR55 and IM-9 lymphoblastoid cells. *Journal of Biochemistry Advance access*. 1-24.

Oka S., Toshida T., Maruyama K., Nakajima A., Yamashita A., Sugiura T. (2009) 2-Arachidonoyl-sn-glycero-3-phosphoinositol: a possible natural ligand for GPR55. *Journal of Biochemistry*. **145**: 1; 13-20.

Olazabal I.M., Caron E., May R.C., Schilling K., Knecht D.A. and Machesky L.M. (2002) Rho-kinase and myosin-II control phagocytic cup formation during CR, but not FcγR, phagocytosis. *Curr. Biol.* **12**: 1413-1418.

O'Neill L.A.J, and Kaltschmidt C., NF-κB: (1997) crucial transcription factor for glial and neuronal cell function. *Trends in Neurosciences*. **20**: 6; 252-258.

O'Neill L.A.J., Fitzgerald K.A. and Bowie A.G. (2003) The Toll-IL-1 receptor adaptor family grows to five members. *TRENDS in Immunology*. **24**: 6; 286-89.

O'Sullivan SE. (2007) Cannabinoids go nuclear: Evidence for activation of peroxisome proliferator-activated receptors. *Br. J. Pharmacol.* **152**: 276-582.

O'Sullivan S.E. and Kendall D.A (2010) Cannabinoid activation of peroxisome proliferation-activated receptors: Potential for modulation of inflammatory disease. *Immunobiology*. **215**: 8; 611-616.

O'Sullivan S.E., Kendall D.A. and Randall M.D. (2006) Further characterization of the time-dependent vascular effects of delta9-tetrahydrocannabinol. *J Pharmacol Exp Ther.* **317**; 428-38.

O'Sullivan, S. E., Tarling E.J., BENNETT A.J., Kendall D.A. and Randall M.D. (2005) Novel time-dependent vascular actions of Delta9-tetrahydrocannabinol mediated by peroxisome proliferator-activated receptor gamma. *Biochem Biophys Res Commun.* **337**: 824-31.

Owens T. and Babcock A. (2002) Immune response induction in the central nervous system. *Front Biosci.* **7**: 427-38

Parkhurst C.N. and Gan W.-B. (2010) Microglia dynamics and function in the CNS. *Current Opinion in Neurobiology.* **20**: 595-600.

Patel S. and Hillard C.J. (2006) Pharmacological evaluation of cannabinoids receptor ligands in a mouse model of anxiety: further evidence for an anxiolytic role for endogenous cannabinoids signalling. *J.Pharmacol.ExpTher.* **318**: 1; 304-11.

Penna A., Juvin V., Chemin J., Compan V., Monet M., Rassendren F.A. (2006) PI3-kinase promotes TRPV2 activity independently of channel translocation to the plasma membrane. *Cell Calcium.* **39**: 495-507.

Perry V.H. (1998) A revised view of central nervous system microenvironment and major histocompatibility complex class II antigen presentation. *J Neuroimmunol.* **90**: 113-21.

- Perry and Gordon (1988) macrophages and microglia in the nervous system. *TINS*. **11**: 6.
- Perry V.H. and Gordon S. (1991) Macrophages and the nervous system. *Int Rev Cytol*. **125**: 203–244.
- Perry V.H. (2004) The influence of systemic inflammation on inflammation in the brain: implications for chronic neurodegenerative disease. *Brain Behav Immun*. **18**: 407–413.
- Petit P.X., Zamzami N., Vayssiere J.L., Mignotte B., Kroemer G., and Castedo M. (1997). Implication of mitochondria in apoptosis. *Molecular and Cellular Biochemistry*. **174**: 185–188.
- Petrosino S., Palazzo E., de Novellis V., Bisogno T., Rossi F., Maione S., Di Marzo V. (2007) Changes in spinal and supraspinal endocannabinoid levels in neuropathic rats. *Neuropharmacology*. **52**: 2; 415–422.
- Petrosino S L., Karsak C.M., Gaffal E., Ueda N., Tüting T., Bisogno T., De Filippis D., D'Amico A., Saturnino C., Orlando P., Zimmer A., Iuvone T., Di Marzo V. (2010) Protective role of palmitoylethanolamide in contact allergic dermatitis. *Allergy*. **65**: 6; 698–711.
- Pertwee R.G. (2008) The diverse CB<sub>1</sub> and CB<sub>2</sub> receptor pharmacology of three plant cannabinoids: delta -9-tetrahydrocannabinol, cannabidiol and delta-9-tetrahydrocannabivarin. *Br. J. Pharmacol*. **153**: 199–215.
- Pertwee R.G. (2004) The pharmacology and therapeutic potential of Cannibidiol. In: (ed.) DiMarzo, *Cannabinoids*. New York: Kluwer Academic/Plenum Publishers. 1–52.
- Pertwee R.G. (2007) GPR55: a new member of the cannabinoid receptor clan? *Br. J. Pharmacol*. **152**: 984–98
- Petrwee RG. (1997) Pharmacology of cannabinoids CB1 and CB2 receptors. *PharmacolTher*. **74**: 129–180.
- Pertwee R.G. (2006) The pharmacology of cannabinoid receptors and their ligands: an overview: *International Journal of Obesity*. **30**: S13–S18.
- Pertwee R.G., Howlett A.C., Abood M.E., Alexander S.P., Di Marzo V., Elphick M.R., Greasley P.J., Hansen H.S., Kunos G., Mackie K., Mechoulam R., Ross R.A. (2010). International Union of Basic and Clinical Pharmacology. LXXIX. Cannabinoid receptors and their ligands: beyond CB (1) and CB (2). *Pharmacol Rev*. **62**: 4; 588–631.
- Pertwee R.G. (2005) Inverse agonism and neutral antagonism at cannabinoid CB1 receptors. *Life Sci*. **76**: 1307–1324.
- Pertwee R.G. (2009) Emerging strategies for exploiting cannabinoid receptor agonists as medicines. *Br. J. Pharmacol*. **156**: 397–411.
- Pertwee R.G., Joeadigwe G., Hawksworth G.M. (1996) Further evidence for the presence of cannabinoid CB<sub>1</sub> receptors in mouse vas-deferens. *European Journal of Pharmacology*. **296**: 169–172.

Phillippe M. and Basa A. (1996) The Effects of Ruthenium Red, an Inhibitor of Calcium-Induced Calcium Release, on Phasic Myometrial Contractions. *Biochemical and Biophysical Research Communications*. **221**: 656–661.

Pietr M., Kozela E., Levy R., Rimmerman N., Lin Y.H., Stella N., Vogel Z., Juknat A. (2009) Differential changes in GPR55 during microglial cell activation. *FEBS Lett*. **18**: 583; 2071-6.

Piomelli D., Giuffrida A., Calignano A., de Fonseca, F.R. (2000). The endocannabinoid system as a target for therapeutic drugs. *Trends Pharmacol. Sci*. **21**: 218–224.

Pocock J.M. and Kettenmann H. (2007) Neurotransmitter receptors on microglia, *Trends in Neurosciences*. **30**: 10; 527-535.

Pocock J.M. and Liddle A.C. (2001) Microglial signalling cascades in neurodegenerative disease. *Prog. Brain Res*. **132**: 555-565.

Pollard T.D. and Borisy G.G. (2003) Cellular motility driven by assembly and disassembly of actin filaments. *Cell*. **112**: 453–465.

Ponomarev E.D., Maresz K., Tan Y., Dittel B.N. (2007) CNS-derived interleukin-4 is essential for the regulation of autoimmune inflammation and induces a state of alternative activation in microglial cells. *J Neurosci*. **27**: 10714–10721.

Price M.R., Baillie G.L., le Thomas A., Stevenson L.A., Easson M., Goodwin R., le McLean A., McIntosh L., Goodwin G., Walker G., Westwood P., Marrs J., Thomson F., Cowley., Christopoulos A., Pertwee R.G., and Ross R.A. (2005) Allosteric Modulation of the Cannabinoid CB1 Receptor. *Mol Pharmacol*. **68**: 1484–1495.

Prinz M., Häusler K.G., Kettenmann H., Hanisch U. (2001) Beta-adrenergic receptor stimulation selectively inhibits IL-12P40 release in microglia. *Brain Res*. **899**: 264-270.

Qiu L., Buie C., Reay A., Vaughn M.W., and Cheng K.H. (2011). Molecular dynamics simulations reveal the protective role of cholesterol in beta-amyloid protein-induced membrane disruptions in neuronal membrane mimics. *J Phys Chem B*. 115: **32**; 9795-812.

Qin L., Liu Y., Wang T., Wei S-J., Block M.L., Wilson B., Liu B. and Hong J-S. (2004) NADPH Oxidase Mediates Lipopolysaccharide-induced Neurotoxicity and Proinflammatory Gene Expression in Activated Microglia. *J. of Biological Chemistry*. **279**: 1415-1421.

Qin N., Neepner M.P., Liu Y., Hutchinson T.L., Lubin M.L. and Flores C.M. (2008) Cellular/Molecular; TRPV2 Is Activated by Cannabidiol and Mediates CGRP Release in Cultured Rat Dorsal Root Ganglion Neurons. *The Journal of Neuroscience*. 28: **24**; 6231– 6238.

Rajesh M., Mukhopadhyay P., Hasko G., Huffman J.W., Mackie K., Pacher P. (2008) CB2 cannabinoid receptor agonists attenuate TNF- $\alpha$ -induced human vascular smooth muscle cell proliferation and migration. *Br J Pharmacol*. **153**: 347-57.

Ramírez B.G, Blázquez C., del Pulgar T.G, Guzmán M., de Ceballos M.L. (2005): Prevention of Alzheimer's disease pathology by cannabinoids: neuroprotection mediated by blockade of microglial activation. *J.Neurosci.* **25**: 1904-1913.

Rappert A., Biber K., Nolte C., Lipp M., Schubel A., Lu B., Gerard N.P., Gerard C., Boddeke H.W.G.M. and Kettenmann H. (2002) Secondary lymphoid tissue chemokine (CCL21) activates CXCR3 to trigger a Cl<sup>-</sup> current and chemotaxis in murine microglia. *The Journal of Immunology.* **168**: 3221-3226.

Ryan D., Drysdale A.J., Lafourcade C., Pertwee R.G., and Platt B. (2009) Cannabidiol Targets Mitochondria to Regulate Intracellular Ca<sup>2+</sup> Levels. *The Journal of Neuroscience.* **29**: 7; 2053–2063.

Redlich S., Ribes S., Schütze S., Czesnik D. (2012) Palmitoylethanolamide stimulates phagocytosis of *Escherichia coli* K1 and *Streptococcus pneumoniae* R6 by microglial cells. *Journal of Neuroimmunology.* **244**: 1–2; 32–34.

Resstel L.B., Tavares R.F., Lisboa S.F., Joca S.R, Corrêa F.M., Guimarães F.S. (2009) 5-HT<sub>1A</sub> receptors are involved in the cannabidiol-induced attenuation of behavioural and cardiovascular responses to acute restraint stress in rats. *British Journal of Pharmacology.* **156**: **1**; 181–8.

Riento K., Ridley A.J. (2003) Rocks: multifunctional kinases in cell behaviour. *Nat Rev Mol Cell Biol.* **4**: 446–456.

Rieske E., Graeber M.B., Tetzlaff W., Czlonkowska A., Streit W.J., Kreutzberg G.W. (1989) Microglia and microglia-derived brain macrophages in culture: generation from axotomized rat facial nuclei, identification and characterization in vitro. *Brain Res.* **492**: 1-14.

Rietschel E.T., Kirikae T., Schade F.U., Mamat U., Schmidt G., Loppnow H., Ulmer A.J., Zahringer U., Seydel U., Di Padova F., *et al.* (1994) Bacterial endotoxin: molecular relationships of structure to activity and function. *FASEB J.* **8**: 217–225.

Rimmerman N., Bradshaw H.B., Kozela E., Levy R., Juknat A. and Vogel Z. (2012) Themed Section: Cannabinoids in Biology and Medicine, Part II RESEARCH Compartmentalization of endocannabinoids into lipid rafts in a microglial cell line devoid of caveolin-12438. *British Journal of Pharmacology* **165**; 2436–2449.

Rinaldi-Carmona M., Barth F, Heaulme M., Shire D., Calandra B., Congy C., Martinez S., Maruani J., Neliat G., Caput D., Ferrara P., Soubrie P., Breliere JC., Le Fur G. (1994) SR141716A, a potent and selective antagonist of the brain cannabinoid receptor. *FEBS Lett.* **350**: 240–244.

Rock R.B., Gekker G., Hu S., Sheng W.S., Cheeran M., Lokensgard J.R. and Peterson P.K. (2004) Role of microglia in central nervous system infections. *Clin Microbiol Rev.* **17**: 942-964.

Ross R. (2007a) Tuning the endocannabinoid system: allosteric modulators of the CB<sub>1</sub> receptor. *Br J Pharmacol.* **152**: 5; 565–566.

Ross R.A. (2007b) Allosterism and cannabinoid CB<sub>1</sub> receptors: the shape of things to come. *Trends in Pharmacological Sciences*. **28**: 11; 567-572.

Rock R.B., Gekker G., Hu S., Sheng W.S., Cheeran M., Lokensgard J.R. and Peterson P.K. (2004) Role of microglia in central nervous system infections. *Clin Microbiol Rev*. **17**: 942–964.

Rockwell C.E. and Kaminski N.E. (2004) A Cyclooxygenase Metabolite of Anandamide Causes Inhibition of Interleukin-2 Secretion in Murine Splenocytes. *JPET*. **311**: 2; 683-690.

Roderick H.L. and Cook S.J. (2008) Ca<sup>2+</sup> signalling checkpoints in cancer: remodelling Ca<sup>2+</sup> for cancer cell proliferation and survival. *Nat Rev Cancer*. **8**: 361–375.

Rothwarf D.M., Karin M. (1999) Review: The NF-kappa B activation pathway: a paradigm in information transfer from membrane to nucleus. *Sci STKE*. **5**: RE1.

Ross R.A. (2009) The enigmatic pharmacology of GPR55. *Trends Pharmacol Sci*. **30**: 3; 156-63.

Ross R.A., Brockie H.C. and Pertwee R.G. (2000) Inhibition of nitric oxide production in RAW264.7 macrophages by cannabinoids and palmitoylethanolamide. *Eur J Pharmacol*. **401**; 121-30.

Ross R. (2003) Anandamide and vanilloid TRPV1 receptors. *Br J Pharmacol* **140**: 5; 790–801.

Russo E.B., Burnett A., Hall B., Parker K.K. (2005) Agonistic properties of cannabidiol at 5-HT<sub>1a</sub> receptors. *Neurochem Res*. **30**: 8; 1037-43.

Russo E.B., Guy G.W., Robson P.J. (2007) Cannabis, Pain, and Sleep: Lessons from Therapeutic Clinical Trials of *Sativex*<sup>®</sup>, a Cannabis-Based Medicine. *Chemistry & Biodiversity*. **4**: 8; 1729–1743.

Ryberg E, Larsson N., Sjogren S., Hjorth S., Hermansson NO., Leonova J., Elebring T., Nilsson K., Drmota T. and Greasley PJ. (2007). The orphan receptor GPR55 is a novel cannabinoid receptor. *BrJPharmacol* .**152**: 1092-1101.

Ryu J., Pyo H., Jou I. & Joe E. (2000) Thrombin induces NO release from cultured rat microglia via protein kinase C, mitogen-activated protein kinase, and NF-kappa B. *J Biol Chem*. **275**: 29955-9.

Sacerdote P., Martucci C., Vaccani A., Bariselli A F., Panerai E., Colombo A., D. Parolaro D., Massi P. (2005) The nonpsychoactive component of marijuana cannabidiol modulates chemotaxis and IL-10 and IL-12 production of murine macrophages both in vivo and in vitro. *Journal of Neuroimmunology*. **159**: 1; 97-105.

Sagredo O, Pazos MR, Valdeolivas S, Fernandez-Ruiz J. (2012) Cannabinoids: novel medicines for the treatment of Huntington's disease. *Recent Pat CNS Drug Discov*. **1**: 1; 41-8.

Samuels S.E., Lipitz J.B., Dahl G. and Muller K.J. (2010) Neuroglial ATP release through innexin channels controls microglial cell movement to a nerve injury. *J Gen Physiol.* **136**: 425-442.

Santoni G., Farfariello V., Liberati S., Morelli M.B., Nabissi M., Santoni M., and Am C. (2013) The role of transient receptor potential vanilloid type-2 ion channels in innate and adaptive immune responses. *Front Immunol.* **4**: 34.

Sankarapandi S., Zweier J.L., Mukherjee G., Quinn M.T, Huso D.L. (1998) Measurement and characterization of superoxide generation in microglial cells: evidence for an NADPH oxidase-dependent pathway. *Arch Biochem Biophys.* **353**: 312-321.

Sarmad S., Alexander S.P.H., Barrett D.A., Marsden C.A., Kendall D.A. Depolarizing and calcium-mobilizing stimuli fail to enhance synthesis and release of endocannabinoids from rat brain cerebral cortex slices. *Journal of Neurochemistry.* **117**: 4; 665-677.

Sastre J., Pallardo F.V., Vina J. (2003) The role of mitochondrial oxidative stress in aging. *Free Radic Biol Med.* **35**: 1-8

Saura J. (2007) Review Microglial cells in astroglial cultures: a cautionary note *Journal of Neuroinflammation.* **4**: 26; 1742-2094.

Sawzdargo M., Nguyen T., Lee D.K., Lynch K.R., Cheng R., Heng H.H.Q., George S.R. and O'Dowd B.F. (1999) Identification and cloning of three novel human G protein-coupled receptor genes GPR52,  $\Upsilon$  GPR53 and GPR55: GPR55 is extensively expressed in human brain. *Molecular Brain Research.* **64**: 193-198.

Schumann R.R., Leong S.R., Flaggs G.W., Gray P.W., Wright S.D., Mathison J.C., Tobias P.S. and Ulevitch R.J. (1990) Structure and function of lipopolysaccharide binding protein. *Science.* **249**: 1429-1431.

Selley D.E., Stark S., Sim L.J., Childers S.R., (1996) Cannabinoid receptor stimulation of guanosine-5'-O-(3-[35S] thio)triphosphate binding in rat brain membranes. *Life Sciences.* **59**: 8; 659-668.

Scott C.C., Dobson W., Botelho R.J., Coady-Osberg N., Chavrier P., Knecht DA., Heath C., Stahl P. and Sergio Grinstein S. (2005) Phosphatidylinositol-4,5-bisphosphate hydrolysis directs actin remodeling during phagocytosis. *J. Cell Biol.* **169**: 139-149.

Sgeng W.S., S. H. (2005). Synthetic cannabinod WIN55,212-2 inhibits generation of inflammatory mediators by IL-1 $\beta$ -Stimulated human astrocytes. *Glia.* 211-219.

Sharir H. and Abood M.E. (2010) Pharmacological characterization of GPR55, a putative cannabinoid receptor. *Pharmacology & Therapeutics.* **126**: 3; 301-313.

Shimosato G., Amaya F., Ueda M., Tanaka Y., Decosterd I., Tanaka M. (2005) Peripheral inflammation induces up-regulation of TRPV2 expression in rat DRG. *Pain.* **119**: 225-232.

Showalter V.M., Compton D.R., Martin B.R., and Abood M.E. (1996) Evaluation of binding in a transfected cell line expressing a peripheral cannabinoid receptor (CB2): identification of cannabinoid receptor subtype selective ligands. *J Pharmacol Exp Ther.* **278**: 989–999.

Shrivastava A., Kuzontkoski P.M., Groopman J.E. and Prasad A. (2011) Therapeutic Discovery: Cannabidiol Induces Programmed Cell Death in Breast Cancer Cells by Coordinating the Cross-talk between Apoptosis and Autophagy. *Mol Cancer Ther.* **10**: 1161-1172.

Si Q-S., Nakamura Y., and Kataoka K. (1997) Hypothermic suppression of microglial activation in culture: inhibition of cell proliferation and production of nitric oxide and superoxide. *Neuroscience.* **81**: 1; 223–229.

Skaper S.D., Facci L., Culbert A.A., Evans N.A., Chessell I., Davis J.B. and Richardson J.C. (2006) P2X(7) receptors on microglial cells mediate injury to cortical neurons in vitro. *Glia.* **54**: 234-42.

Song X., Tanaka S., Cox D., and Lee S.C. (2004) Fcy receptor signaling in primary human microglia: differential roles of PI-3K and Ras/ERK MAPK pathways in phagocytosis and chemokine induction. *Journal of Leukocyte Biology.* **75**: 6; **1147-1155**.

Soontornniyomkij V., Wang G., Pittman C.A., Wiley C.A., Achim, C.L. (1998) Expression of brain-derived neurotrophic factor protein in activated microglia of human immunodeficiency virus type 1encephalitis. *Neuropathol. Appl. Neurobiol.* **24**: 453-460.

Srinivasan S., Wang F., Glavas S., Ott A., Hofmann F., Aktories K., Kalman D., and Bourne H.R. (2003). Rac and Cdc42 play distinct roles in regulating PI(3,4,5)P3 and polarity during neutrophil chemotaxis. *J. Cell Biol.* **160**: 375-385.

Stachowska E., Baśkiewicz-Masiuk M., Dziedziejko V., Adler G., Bober J., Machaliński B., Chlubek D. (2007) Conjugated Linoleic Acids Can Change Phagocytosis of Human Monocytes/Macrophages by Reduction in Cox-2 Expression. *Lipids.* **42**: 8; 707-716.

Staton P.C., Hatcher J.P., Walker D.J., Morrison A.D., Shapland E.M., Hughes J.P., Chong E., Mander P.K., Green P.J., Billinton A., Fulleylove M., Lancaster H.C., Smith J.C., Bailey L.T., Wise A., Brown A.J., Richardson J.C., Chessell I.P. (2008). The putative cannabinoid receptor GPR55 plays a role in mechanical hyperalgesia associated with inflammatory and neuropathic pain. *Pain.* **139**: 1; 225–36.

Stefano G.B., LIU Y. and Goligorsky M.S. (1996) Cannabinoid receptors are coupled to nitric oxide release in invertebrate immunocytes, microglia, and human monocytes. *J Biol Chem.* **271**: 19238-42.

Stefano G.B., Salzet B. and Salzet M. (1997) Identification and characterization of the leech CNS cannabinoid receptor: coupling to nitric oxide release. *Brain Res.* **753**; 219-24.

- Stella N., Schweitzer P. and Piomelli D., (1997) A second endogenous cannabinoid that modulates long-term potentiation. *Nature*. **388**: 773–778.
- Stella N. and Piomelli D. (2001) Receptor- dependent formation of endogenous cannabinoids in cortical neurons. *Eur J Pharmacol*. **425**: 189-196.
- Stella N. (2009) Endocannabinoid signaling in microglial cells. *Neuropharmacology*. **56**: 1; 244–253.
- Stella N. (2004) Cannabinoid signaling in glial cells. *Glia*. **48**: 267-277.
- Stevens B., Allen N.J., Vazquez L.E., Howell G.R., Christopherson K.S., Nouri N., Micheva K.D., Mehalow A.K., Huberman A.D., Stafford B., Sher A., Litke A.M., Lambris J.D., Smith S.J., John S.W., Barres B.A. (2007) The classical complement cascade mediates CNS synapse elimination. *Cell*. **131**; 1164–1178.
- Stokes A.J., Wakano C., Del Carmen K.A., Koblan-Huberson M., Turner H., (2005) Formation of a physiological complex between TRPV2 and RGA protein promotes cell surface expression of TRPV2. *J Cell Biochem Biochemistry*. 669–683.
- Storer P.D., Xu J., Chavis J. and Drew P.D. (2005) peroxisome proliferator-activated receptor-gamma agonist inhibit the activation of microglia and astrocytes: implications for multiple sclerosis. *J.Neuroimmunol*. **161**: 113-122.
- Streit W.J. (2005) Microglia and neuroprotection: implications for Alzheimer's disease. *Brain research. Brain research reviews*. **48**: 2; 234–239.
- Streit W.J., Walter S.A., Pennell N.A. (1999) Reactive microgliosis. *Prog. Neurobiol*. **57**: 563–581.
- Streit W., Mrak R. and Griffin W.S. (2004) Microglia and neuroinflammation: a pathological perspective. *Journal of Neuroinflammation*. **1**: 14.
- Streit W.J. (2001) Microglia and macrophages in the developing CNS. *Neurotoxicology*. **22**: 619-624.
- Sun H.N., Kim S.U., Lee M.S., Kim S.K., Kim J.M., Yim M., Yu D.Y., Lee D.S. (2008) Nicotinamide Adenine Dinucleotide Phosphate (NADPH) Oxidase-Dependent Activation of Phosphoinositide 3-Kinase and p38 Mitogen-Activated Protein Kinase Signal Pathways Is Required for Lipopolysaccharide-Induced Microglial Phagocytosis. *Biological & pharmaceutical bulletin*. **31**: 9; 1711-5.
- Sun Y., Alexander S.P.H., Garle M.J., Gibson C.L., Hewitt K., Murphy S.P., Kendall D.A., Bennet A.J (1990) Cannabinoid activation of ppar alpha; a novel neuroprotective mechanism. *Br. J. Pharmacol*. **152**: 734-743.

- Sugiura T., Kondo S., Sukagawa A., Tonegawa T., Nakane S., Yamashita A., Waku K. (1996) N-arachidonylethanolamine (anandamide), an endogenous cannabinoid receptorligand, and related lipid molecules in the nervous tissues. *J Lipid Mediat Cell Signal.* **14**: 51-6.
- Sweet M.J. and Hume D.A. (1996) Endotoxin signal transduction in macrophages. *J Leukoc Biol.* **60**: 8-26.
- Takahashi K., Rochford C.D.P., and Neumann H. (2005) Clearance of apoptotic neurons without inflammation by microglial triggering receptor expressed on myeloid cells-2. *JEM.* **201**: 4; 647-657.
- Tamashiro T.T., Dalgard C.L, Byrnes K.R. (2012) Primary microglia isolation from mixed glial cell cultures of neonatal rat brain tissue. *J Vis Exp.* **15**: 66.
- Tanaka J., Fujita H., Matsuda S., Toku K., Sakanaka M., Maeda N. (1997) Glucocorticoid- and mineralocorticoid receptors in microglial cells: the two receptors mediate differential effects of corticosteroids. *Glia.* **20**: 23-37.
- Tanveer R., McGuinness N., Daniel S., Gowran A., Campbell V.A. (2012) Cannabinoid receptors and neurodegenerative diseases Wiley Interdisciplinary Reviews: *Membrane Transport and Signaling.* **1**: 5; 633-639.
- Taylor D.L., Diemel L.T. Cuzner M.L., Pocock J.M. (2002) Activation of group 11 metabotropic glutamate receptors underlies microglial reactivity and neurotoxicity following stimulation with chromogranin A, a peptide up-regulated in Alzheimer's disease. *J Neurochem.* **82**: 1179-1191.
- Taylor D.L., Jones F., Kubota E.S. and Pocock J.M. (2005) Stimulation of microglial metabotropic glutamate receptor mGlu triggers tumor necrosis factor alpha-induced neurotoxicity in concert with microglial derived Fas ligand. *J. Neurosci.* **25**: 2952-2964.
- Taylor D.L., Diemel L.T. and Pocock JM. (2003) Activation of microglial group III metabotropic glutamate protects neurons against microglial neurotoxicity. *J. Neurosci.* **23**: 2150-2160.
- Tikka T.M. and Koistinaho J.E. (2001) Minocycline Provides Neuroprotection Against N-Methyl-D-aspartate Neurotoxicity by Inhibiting Microglia. *The Journal of Immunology.* **166**: 12; 7527-7533.
- Ting-Beall H.P., Lee A.S, and Hochmuth R.M., (1995) Effect of cytochalasin D on the mechanical properties and morphology of passive human neutrophils. *Annals of Biomedical Engineering.* **23**: 666-671.
- Toescu E.C., Moller T., Kettenmann H., Verkhratsky A. (1998) Long-term activation of capacitative Ca<sup>2+</sup> entry in mouse microglial cells. *Neuroscience* **86**: 925-935.

- Town T., Nikolic V. and Tan J. (2005) The microglial "activation" continuum: from innate to adaptive responses. *Journal of Neuroinflammation*. **2**: 24.
- Tsuboi K., Takezaki N., Ueda N. (2007) The N-Acylethanolamine-Hydrolyzing Acid Amidase (NAAA). *Chemistry & Biodiversity*. **4**: 8; 1914.
- Tubaro A., Giangaspero A., Sosa S., Negri R., Grassi G., Casano S., Loggia R.D., Appendino G. (2010) Comparative topical anti-inflammatory activity of cannabinoids and cannabivarins. *Fitoterapia*. **81**: 7; 816-819.
- Tymianski M., Wallace M.C., Spigelman I., Uno M., Carlen, P.L., Tator C.H., Charlton M.P. (1993) Cell-permeant Ca<sup>2+</sup> chelators reduces early excitotoxic and ischemic neuronal injury *in vitro* and *in vivo*. *Neuron*. **1**: 221-235.
- Vaccani A., Massi P., Colombo A., Rubino T., Parolaro D. (2005) Cannabidiol inhibits human glioma cell migration through a cannabinoid receptor-independent mechanism. *British Journal of Pharmacology*. **144**: 8; 1032–1036.
- Van Rossum U.K.D. and Hanisch (2004) Microglia Metab. *Brain Dis*. **19**: 393–411.
- Vilhardt F. (2005). Microglia: phagocyte and glia cell. *Int J Biochem Cell Biol*. **37**: 17-21.
- Viscomi M.T., Oddi S., Latini L., Pasquariello N., Florenzano F., Bernardi G., Molinari M., Maccarrone M. (2009) Selective CB2 receptor agonism protects central neurons from remote axotomy-induced apoptosis through the PI3K/Akt pathway. *J Neurosci*. **29**: 14; 4564-70.
- Vogel L.A. and Noelle R.J. (1998) CD40 and its role as a member of the TNFR family. *Semin Immunol*. **10**: 435-42.
- Volko M., Laibfritz D., Moncol J. (2007) Free Radical and Antioxidants in Normal Physiological Functions and Human Diseases. *International Journal Biochemistry Cell Biology*. **39**: 44-84.
- Vollner L., Bieniek D., Korte F. (1969) [Hashish. XX. Cannabidivarin, a new hashish constituent] *Tetrahedron Lett*. **3**:145–147.
- Waetzig V., Czeloth K., Hidding U., Mielke K., Kanzow M., Brecht S., Goetz M., Lucius R., Herdegen T., Hanisch U-K. (2005) c-Jun N-terminal kinases (JNKs) mediate pro-inflammatory actions of microglia. *Glia*. 50: 3; 235–246.
- Wahli W. and Michalik L. (2012) PPARs at the crossroads of lipid signaling and inflammation. *Trends Endocrinol Metab*. **23**: 7; 351-63.
- Waksman Y., Olson J.M., Carlisle S.J. and Cabral G.A. (1999) The central cannabinoid receptor (CB1) mediates inhibition of nitric oxide production by rat microglial cells. *J Pharmacol Exp Ther*. **288**: 3; 1357-66.

Walter L., Franklin A., Witting A., Wade C., Xie Y., Kunos G., Mackie K., Stella N. (2003) Nonpsychotropic cannabinoid receptors regulate microglial cell migration. *J Neurosci.* **23**: 1398-1405.

Walton K.M., DiRocco R., Bartlett B.A., Koury E., Marcy VR., Jarvis B., Schaefer E.M. (1998), Activation of p38<sup>MAPK</sup> in Microglia After Ischemia. *Journal of Neurochemistry.* **70**: 4; 1764-1767.

Wang P., Rothwell N.J., Pinteaux E. and Brough D. (2008) Neuronal injury induces the release of pro-interleukin-1beta from activated microglia in vitro. *Brain Res.* **1236**: 1-7.

Wang H. and Joseph J.A. (1999) Quantifying cellular oxidative stress by dichlorofluorescein assay using microplate reader. *Free Radic Biol Med.* 5-6; 612-6.

Wang M., Richards A.L., Friedman H. and Djeu J.Y. (1991) Selective inhibition of natural killer but not natural cytotoxic activity in a cloned cell line by delta-9-tetrahydrocannabinol. *Journal of Leukocyte Biology.* **50**: 2; **192-197**.

Watanabe H., Abe H., Takeuchi S., Tanaka R. (2000) Protective effect of microglial conditioning medium on neuronal damage induced by glutamate. *Neuroscience Letters.* Volume **289**; Issue 1; Pages 53-56.

Weinstein J.R., Swarts S., Bishop C., Hanisch U.K. and Moller T. (2008) Lipopolysaccharide is a frequent and significant contaminant in microglia-activating factors. *Glia.* **56**: 16-26.

Wilkinson B.L. and Landreth G.E. (2006) The microglial NADPH oxidase complex as a source of oxidative stress in Alzheimer's disease. *Journal of Neuroinflammation* *Journal of Neuroinflammation.* **3**: 30.

Williams K., Ulvestad E., Waage A., Antel J.P., McLaurin J. (1994) Activation of adult human derived microglia by myelin phagocytosis in vitro. *J. Neurosci. Res.* **38**: 433-443.

Wilms H., Rosenstiel P., Sievers J., Deuschl G., Zecca L. and Lucius R. (2003) Activation of microglia by human neuromelanin is NF-kappaB dependent and involves p38 mitogen-activated protein kinase: implications for Parkinson's disease. *FASEB J.* **17**: 500-502.

Wong L.F., Yip P.K., Battaglia A., Grist J., Corcoran J., Maden M., Azzouz M., Kingsman S.M., Kingsman A.J., Mazarakis N.D., McMahon S.B. (2006) Retinoic acid receptor beta2 pro-motes functional regeneration of sensory axons in the spinal cord. *Nat Neurosci.* **9**: 243-50.

Wright G.J., Puklavec M.J., Willis A.C., Hoek R.M., Sedgwick J.D., Brown M.H., Barclay A.N. (2000) Lymphoid/neuronal cell surface OX2 glycoprotein recognizes a novel receptor on macrophages implicated in the control of their function. *Immunity.* **13**: 233-242.

Wright S.D., Ramos R.A., Tobias P.S., Ulevitch R.J., Mathison J.C. (1990) CD14, a receptor for complexes of lipopolysaccharide (LPS) and binding protein. *Science.* **249**: 1431-3.

Wu D.U., Jackson-Lewis V., Vila M., Tieu K., Teismann P., Vadseth C., Choi D-K., Ischiropoulos H., and Przedborski S. (2002) Blockade of Microglial Activation Is Neuroprotective in the 1-Methyl-4-Phenyl-1,2,3,6-Tetrahydropyridine Mouse. *J Neurosci.* **22**: 5; 1763-71.

Xie G.W., Kashiwabara Y. and C Nathan C. (1994) Role of transcription factor NF-kappa B/Rel in induction of nitric oxide synthase. *The Journal of Biological Chemistry.* **269**: 4705-4708.

Xu H.E., Stanley T.B., Montana V.G., Lambert M.H., Shearer B.G., Cobb J.E., McKee D.D, Galardi C.M, Plunket K.D., Robert T. Nolte R.T., Parks D.J., Moore J.T., Kliwer S.A, Willson T.M. & Julie B. Stimmel J.B. (2002) Structural basis for antagonist-mediated recruitment of nuclear co-repressors by PPAR $\alpha$ . *Nature.* **415**: 813-817.

Yamamori T., Inanami O., Nagahata H., Cui Y-D., Kuwabara M. (2000) Roles of p38 MAPK, PKC and PI3-K in the signaling pathways of NADPH oxidase activation and phagocytosis in bovine polymorphonuclear leukocytes. *FEBS.* **467**: 2-3; 253-258.

Yano T., Matsumura T., Senokuchi T., Ishii N., Murata Y., Taketa K., Motoshima H., Taguchi T., Sonoda K., Kukidome D., Kawada T., Brownlee M., Nishikawa T., and Araki E. (2007) Statins activate peroxisome proliferator-activated receptor gamma through extracellular signal regulated kinase 1/2 and p38 mitogen-activated protein kinase-dependent cyclooxygenase-2 expression in macrophages. *Circulation Research.* 100: **1442-1451**.

Yao J., Harvath L., Gilbert D.L., and Colton C.A. (1990) Chemotaxis by a CNS macrophage, the microglia. *J.Neurosci. Res.* **27**: 36-42.

Yin H., Chu A., Li W., Wang B., Shelton F., Nguyen D.G., Caldwell JS., Chen YA., (2009) Lipid G protein-coupled receptor ligand identification using  $\beta$ -arrestin pathHunter assay. *J Biol Chem.* **284**: 12328-38.

Zanelati T., Biojone C., Moreira F., Guimarães F., Joca S. (2009) Antidepressant-like effects of cannabidiol in mice: possible involvement of 5-HT1A receptors. *British Journal of Pharmacology.* **159**: 1; 122-8.

Zhang J., Hoffert C., Vu H.K., Groblewski T., Ahmad S., O'Donnell D. (2003) Induction of CB2 receptor expression in the rat spinal cord of neuropathic but not inflammatory chronic pain models. *Eur J Neurosci.* **17**: 12; 2750-4.

Zheng L., Zomerdijk T.P., Aarnoudse C., van Furth R., and P. H. Nibbering P.H. (1995) Role of protein kinase C isozymes in Fc  $\gamma$  receptor-mediated intracellular killing of *Staphylococcus aureus* by human monocytes. *J. Immunol.* **155**: 776.

Zielasek J. and Hartung H.P. (1996) Molecular mechanisms of microglial activation. *Advances in Neuroimmunology.* **6**: 122-191.

Zhou M.J. and Brown E.J. (1994) CR3 (Mac-1, alpha M beta 2, CD11b/CD18) and Fc gamma RIII cooperate in generation of a neutrophil

respiratory burst: requirement for Fc gamma RIII and tyrosine phosphorylation. *J. Cell Biol.* **125**: 1407-1416.